

**Alternative Materials for Railcar Air-Brake Glad-Hand Gaskets**

**by**

**Rodrigo Arturo Hernandez Peralta**

**A thesis submitted in partial fulfillment of the requirements for the degree of**

**Master of Science  
in  
Engineering Management**

**Department of Mechanical Engineering  
University of Alberta**

**© Rodrigo Arturo Hernandez Peralta, 2018**

## **Abstract**

The objective of this research was to examine the cold temperature limitation of the elastomeric material currently used in railcar airbrake glad-hand gaskets. A test plan to assess gasket material performance was designed based on gasket operating conditions and material properties. Standards, specifications and test protocols from the International Organization for Standardization [ISO], the American Society for Testing and Materials [ASTM], and the Manual of Standards and Recommended Practices from the American Association of Railroads [AAR MSRP] were used as a base reference for generating a detailed test plan. Hardness, compression stress-strain properties, and chemical compatibility were measured under different loading conditions and temperatures. For the compressive tests, a custom Material Testing System [MTS] gasket fixture was designed and manufactured. Randomized tests were performed on 30 gaskets provided by Canadian Pacific. Two alternative elastomeric materials were selected through a decision analysis: EPDM and CR. Randomized tests were performed on 30 gaskets made of each alternative elastomeric material. The alternative material gaskets were produced by a third-party manufacturer. Gasket performance and features were evaluated with the same test plan in all cases. Statistical analysis of results showed that CR maintained good performance for sealing purposes in cold temperature. CR was more flexible when manipulating it, than both EPDM and the current material used in gaskets during all conditions. A protocol for testing airbrake glad-hand gaskets in-service was developed based on the hardness test. A group replacement policy simulated numerical example was examined.

## Preface

The research conducted for this thesis forms part of a research grant sponsored by the Canadian National Railway Company [CN], the Canadian Pacific Railway Company [CP] and the Western Grain Elevator Association [WGEA] in agreement with the Governors of the University of Alberta and was led by Dr. Michael Lipsett at the University of Alberta, with Roya Vaghar as the project lead collaborator. Contributions from Roya Vaghar include: The compression test fixtures design and the material decision matrix original idea mentioned in Chapter 3. Both contributions were made with the assistance of Dr. Lipsett. Also, the EPDM and Neoprene gasket samples mentioned in Chapter 3 were procured by Roya Vaghar with GEMMA Plastics Products Inc. The Literature Review in Chapter 2, the detailed test plan, data gathered, and procedures mentioned in the Methodology of Chapter 3, the Results and Discussions in Chapter 4, as well as the Industry Application considerations in Chapter 5 are my original work.

## Dedication

To my caring wife and my energetic daughter, Sara and Sammy, your support, tolerance, and smiles even in dire moments gave me the strength to push forward and accomplish this goal. You have my eternal gratitude and love.

To my parents, Rebeca and Alejandro, your calls, words of encouragement, and financial aid when needed, made this milestone possible. *Mamá, Papá, gracias, los quiero mucho.*

To my brother and sister, Tonatiuh and Mariana, hearing about your success and thrive gave me just enough stress and encouragement to push myself to excel as well.

To my friends, extended family, colleagues, and University staff, your continued support, opinions, and “when are you finishing that thesis?” \*cough\* Joaquin \*cough\*, heartened me to arrive to the finish line; I’ll never forget you as part of my Canadian international experience. Special thanks go to Dominika Juhaszova, a peer in Dr. Lipsett’s group, and Rita Neyer, graduate colleague, for your support, insight, and proof-reading of my thesis.



## Acknowledgments

First and foremost, I want to thank my master thesis supervisor, Dr. Michael Lipsett, who continuously supported and guided me. His patience with my progress gave me the necessary time and energy to gain momentum. On top of that, his professionalism and calmness when I did have some setbacks on my work are of outmost appreciation. It was a great learning experience to be under his wing; his broad knowhow and notable management skills are a statement of all the experience he has.

Secondly, I thank Roya Vaghar, who spearheaded the gasket research project and stayed on top of all the progress done, she always aimed to stay within the projected time-frame and pushed forward to exceed expectations. The basic idea for the alternative materials decision matrix algorithm, the compressive tests fixtures designs, and the procurement of the alternative materials gasket samples were essential contributions for the completion of my research.

Thirdly, the University of Alberta mechanical workshop technician, Bernie Faulkner, was vital to accomplishing this research. His help when configuring the Material Testing System machine and recommendations on what resources were available in the workshop were crucial to perform the gasket tests. I felt knowledgeable and safe when operating any equipment thanks to him.

This project was sponsored through a research grant from the Canadian National Railway Company [CN], the Canadian Pacific Railway Company [CP], and the Western Grain Elevator Association [WGEA] in agreement with the Governors of the University of Alberta; my most sincere thanks go to the sponsors for allowing me to finish my graduate studies.

# Table of Contents

Abstract.....	2
Preface.....	3
Dedication.....	4
Acknowledgments.....	5
Table of Contents.....	6
List of Tables.....	8
List of Figures.....	9
List of Symbols.....	12
1 Introduction.....	1
1.1 Background and Motivation.....	1
1.2 Problem Definition.....	5
1.3 Research Objectives.....	6
1.4 Thesis Outline.....	6
2 Literature Review.....	7
2.1 Elastomers.....	7
2.1.1 Elastomers deformation and behavior.....	9
2.1.2 Elastomer compounds and classifications.....	18
2.1.3 Elastomer properties and testing methods.....	22
2.2 Gasket failure modes.....	26
2.3 Gasket reliability and unit replacement.....	29
2.4 Hardness.....	32
2.4.1 Durometer measurements.....	34
2.4.2 Compression modulus correlation with hardness.....	36
2.5 Bulk modulus.....	38
3 Methodology.....	39
3.1 Detailed test plan.....	39
3.2 Elastomer selection.....	41
3.3 Material testing.....	46
3.3.1 General considerations.....	47
3.3.2 Hardness test.....	59
3.3.3 Compression tests.....	63

3.3.4	Chemical compatibility test .....	77
4	Results and Discussions .....	84
4.1	Hardness test .....	84
4.2	Compression tests .....	87
4.2.1	Stress-strain compression .....	88
4.2.2	Compression set at low temperature .....	93
4.2.3	Compression modulus .....	96
4.2.4	Bulk modulus .....	97
4.3	Chemical compatibility test .....	97
4.3.1	Hardness change .....	98
4.3.2	Mass change .....	105
5	Industry Application .....	112
5.1	In-service test protocol for gaskets .....	112
5.2	Gaskets group replacement policy numerical example .....	114
6	Conclusions and Future work .....	116
	References .....	120
	Appendices .....	127

## List of Tables

Table 1 List of terms, definitions, and equations or symbols related to mechanical testing .....	9
Table 2 General mechanical properties and information of different elastomeric compounds ....	21
Table 3 List of rubber properties and the corresponding ASTM or ISO testing method. ....	22
Table 4 Degradation factors and its effects in rubbers/elastomers .....	26
Table 5 Nominal values for a Shore A durometer with truncated-cone shape tip indenter .....	35
Table 6: List of Performance Tests done to the gasket samples and details for each one .....	40
Table 7 Elastomeric materials average price (Dick 2014). ASTM D1418 names were also included (ASTM 2017a) .....	42
Table 8 Elastomeric material options and their glass transition temperature (Brandrup et al. 1999; Gent 2012). ASTM D1418 names were also included (ASTM 2017a) .....	43
Table 9 Weight factors for 16 properties selected .....	45
Table 10 Weighted mean decision matrix for gasket alternative elastomeric material .....	45
Table 11: Properties of selected new gasket material .....	46
Table 12 Example of a random permutation for selecting gasket samples .....	47
Table 13 Variables of interest for the hardness test .....	49
Table 14 Variables of interest for the compression stress-strain properties and bulk modulus tests .....	50
Table 15 Variables of interest for the compression set at low temperature .....	50
Table 16 Variables of interest for the chemical compatibility [effect of liquids] test .....	51
Table 17 Random permutations for the room temperature hardness test .....	60
Table 18 Set of rubber samples with different known Shore A Hardness values .....	62
Table 19 One gasket compression test sample data .....	66
Table 20 Two gaskets compression test sample data .....	68
Table 21 Two gaskets pressurized compression test sample data .....	71
Table 22 Fire hazard properties of chemicals. Boiling point and flash point temperatures taken from MSDS .....	78
Table 23 Fire Hazard Risk Matrix for the chemicals used. Maximum allowed temperatures were highlighted in green .....	79
Table 24 Summary of Shore A hardness statistical test results .....	85
Table 25 Summary of stress-strain compression statistical test results .....	89
Table 26 Summary of compression set at low temperature statistical test results .....	94
Table 27 Chemical compatibility test results for Shore A hardness change in current material gaskets .....	98
Table 28 Chemical compatibility test results for Shore A hardness change in EPDM gaskets ..	100
Table 29 Chemical compatibility test results for Shore A hardness change in CR gaskets .....	101
Table 30 Chemical compatibility test results for mass change in Current material gaskets .....	105
Table 31 Chemical compatibility test results for mass change in CR gaskets .....	107
Table 32 Chemical compatibility test results for mass change in CR gaskets .....	109
Table 33: Sample table to gather gasket hardness data and replacement date .....	113
Table 34 Group replacement unit cost per unit time mock example for 50 railcar airbrake gaskets .....	115



## List of Figures

Figure 1 Glad-hand without gasket.....	2
Figure 2 Airbrake glad-hand gasket geometries (Left) Standard geometry (Right) Wide-lip geometry .....	3
Figure 3 (Left) Glad-hand and gasket front view (Right) Coupling.....	4
Figure 4 Line plot generated through MATLAB simulating a long polymer molecular chain.....	7
Figure 5 Stress-strain behavior of three polymer molecular structures: Glassy, Crystalline, and Rubbery [X represents failure] factors (Ashby and Jones 2013).....	8
Figure 6 Representation of the Arruda-Boyce eight-chain unit cell model in the a) undeformed state, and b) compressed state (Przbylo, P. A. and E. M. Arruda 1998, 730; Arruda and Boyce 1993, 389-412).....	9
Figure 7 Maxwell spring and dashpot in series model used to describe viscoelastic stress relaxation.....	13
Figure 8 Voigt-Kelvin spring and dashpot in parallel model used to describe viscoelastic creep behavior.....	13
Figure 9 Representation of time-dependent viscoelastic stress relaxation .....	14
Figure 10 Representation of time-dependent viscoelastic creep.....	14
Figure 11 Representation of a both molecular unions: a cross-link and an entanglement .....	14
Figure 12 Representation of mechanical hysteresis, set, and cyclic stress relaxation in an elastomer uniaxial compression test. Loading and unloading directions are shown for better understanding.....	16
Figure 13 Representation of stiffness change at glass temperature $T_g$ .....	18
Figure 14 ASTM D1418 general classification system for rubbers based on chemical composition of their polymer chain .....	19
Figure 15 Preventive group replacement policy representation .....	29
Figure 16 Hardness scale of rubbers, thermoplastic elastomers [TPE] and plastics (Dr Premamoy Ghosh 2011).....	32
Figure 17 General mechanics of a hardness test.....	33
Figure 18 Representation of a Shore A durometer presser foot and indenter with truncated-cone tip shape .....	35
Figure 19 Filtering process for selecting the gasket alternative elastomeric options .....	42
Figure 20 Procedure of material selection based on weighted mean.....	44
Figure 21 Gasket samples geometries cross-sections (a) Standard geometry (b) Simplified standard geometry.....	49
Figure 22 Dial micrometer with rigid metal base, stand, and flat presser foot used thickness measurements.....	51
Figure 23 Gnehm Härteprüfer Shore A Durometer with a scale of 0 to 100.....	52
Figure 24 Digital thermometer, thermocouple type K and surface probe .....	52
Figure 25 Thermal infrared camera picture of gasket fixture and gasket.....	53
Figure 26 Model 810 MTS machine with HMI panel for manual stroke/displacement control and Workstation with DAQ and TestWare® Software for automatic control and logging .....	54

Figure 27 One gasket stress-strain compression properties fixture (Left) Lateral view (Right) Front view .....	55
Figure 28 Two gaskets compression fixture for pressurized test (Bulk modulus and leakage) (Left) Lateral view (Right) Front view. Section A-A shows the air inlet port. ....	55
Figure 29 Air-brake solution with air pressure gage dials and high-precision air flowmeters for leakage assessment.....	56
Figure 30 Airbrake solution transducers (Left) Pressure dial gages (Right) Ball indicator flowmeters.....	56
Figure 31 Digital Caliper with LCD in inches scale.....	57
Figure 32 Beaker (200 ml graded) with rubber stopper and hook, immersion fluid, gasket hanger, and three gaskets, properly labeled.....	57
Figure 33 Borosilicate glass weighing bottle with lid. Dimensions were enough to fit the gaskets for weighing.....	57
Figure 34 Water bath with power switch and temperature control dial. The temperature was raised to 50°C.....	58
Figure 35 Support stand and clamp holding the reflux condenser. Polyvinyl hoses were attached to the condenser connecting the pump inside the 2L beaker creating the water flow circuit.....	58
Figure 36 High precision digital weighing scale used for jewellery mass measurement. Its own autocalibration process was done before each measurement.....	59
Figure 37 Five measurement points example sequence done in a gasket sample .....	59
Figure 38 Metallic compression test fixture and wooden base for cold temperature hardness test .....	61
Figure 39 Five measurement points were done in each gasket.....	61
Figure 40 Thermal picture of the metallic fixture, wooden base, and gasket before a hardness measurement .....	61
Figure 41 Cold temperature hardness measurement using nitrile gloves .....	62
Figure 42 Shore A hardness values check with rubber rings of nominal hardness .....	62
Figure 43 One gasket fixture automatic compression test.....	66
Figure 44 Stress-strain compression properties curve for a gasket made of the current material .....	67
Figure 45 Two gaskets compression test configuration.....	68
Figure 46 Force-displacement curve of the two gaskets compression test – with no air (Inverted values). The sign was inverted for better representation. ....	69
Figure 47 Test arrangement for the pressurized Two Gasket Compression Test .....	70
Figure 48 Time-force curve. The different phases of the automatic sequence are indicated .....	70
Figure 49 Time-displacement curve. The different phases of the automatic sequence are indicated.....	71
Figure 50 Force-displacement curve of the two gaskets compression test with air pressure (Inverted values). The sign was inverted for better representation.....	72
Figure 51 Hydrostatic pressure-volumetric strain curve with linear regression for apparent bulk modulus estimation.....	75
Figure 52 Separation-leakage behavior of three gasket materials. Zero force indicates major leakage .....	76
Figure 53 Original bottle presentation of the test fluids .....	77



Figure 54 Beaker and steel wire gasket hanger. (Left) Dimensions (Right) Three gaskets of the same material immersed in the test fluid and hanged from the rubber stopper .....	80
Figure 55 CRC and Kleen-flo gasket immersion test running for 70 hrs at room temperature ~76°F [~24°C]. Beakers were properly labeled and monitored every 12 hrs .....	81
Figure 56 After-immersion mass measurement setup at room temperature (From left to right) EPDM gaskets + CRC liquid, EPDM gaskets + Kleen-flo, beaker with acetone, and the tapered bottle. The analytical balance can be seen on the back.....	82
Figure 57 Laboratory setup for the increased temperature chemical compatibility test. The water bath was set to 50°C.....	83
Figure 58 Post-immersion gasket measurement after acetone clean-up. Mass was weighted with the tared tapered glass bottle.....	83
Figure 59 Histogram of the Shore A hardness at room (black color) and cold (blue color) temperatures for each type of gasket: Current, Ethylene-Propylene-Diene monomer [EPDM] and Chloroprene [CR]. The mean Shore A hardness per temperature ( $\mu_1$ : room, $\mu_2$ : cold), the coefficient of determination ( $R^2$ ), and the Shore A hardness mean difference between temperatures ( $\mu$ diff) are shown. ....	84
Figure 60 Probability plot of RT and CT Shore A hardness difference for Current gaskets.....	85
Figure 61 Probability plot of RT and CT Shore A hardness difference of EPDM gaskets .....	86
Figure 62 Probability plot of RT and CT Shore A hardness difference of CR gaskets .....	87
Figure 63 Force-strain plot of the stress-strain compression test up to 25% displacement for the three materials testes: EDPM, CR and current material. ....	88
Figure 64 Compressive stiffness ( $S_c$ ) median at 25% deformation of EPDM, CR and Current gaskets. Compression tests were performed at room temperature in an MTS machine model 810. ....	89
Figure 65 Probability plot of stiffness difference between EPDM-Current material .....	90
Figure 66 Probability plot of stiffness difference between EPDM-CR.....	91
Figure 67 Probability plot of stiffness difference between Current material-CR.....	92
Figure 68 Compression set [CS] median for the materials tested: EPDM, CR, and current. ....	93
Figure 69 Probability plot of compression set [CS] difference between EPDM-CR .....	94
Figure 70 Probability plot of compression set [CS] difference between Current-EPDM .....	95
Figure 71 Probability plot of compression set [CS] difference between Current-CR.....	96
Figure 72 Current material gaskets hardness change histograms for both chemicals at 23°C and 50°C .....	103
Figure 73 EPDM gaskets hardness change histograms for both chemicals at 23°C and 50°C ..	104
Figure 74 CR gaskets hardness change histograms for both chemicals at 23°C and 50°C .....	104
Figure 75 Current material gaskets mass change for both chemicals at 23°C and 50°C.....	111
Figure 76 EPDM gaskets mass change for both chemicals at 23°C and 50°C.....	111
Figure 77 EPDM gaskets mass change for both chemicals at 23°C and 50°C.....	112



## List of Symbols

• CP	Canadian Pacific Railway
• CN	Canadian National Railway
• WGEA	Western Grain Elevator Association
• TSB	Transportation Safety Board of Canada
• EOC	End-of-Car arrangement
• AAR	American Association of Railroads
• ASTM	American Society for Testing and Materials
• ISO	International Organization for Standardization
• MSRP	Manual of Standards and Recommended Practices
• RCM	Reliability Centered Maintenance
• EMU	Electronic Multiple Unit train
• ULD	Ultrasonic Leak Detection
• MTBF	Mean-Time-Before-Failure
• FMECA	Failure Mode, Effect and Criticality Analysis
• HALT	Highly Accelerated Life Testing
• SZGA	Successive Zooming Genetic Algorithm
• $t$	Time in seconds [sec]
• $T$	Temperature in degrees Celsius [ $^{\circ}\text{C}$ ]
• $F$	Force. Expressed in Newtons [N]
• $A$	Area. Expressed in $\text{m}^2$
• $\sigma = \frac{F}{A}$	Stress. Expressed in Pascals [Pa]
• $L_0 = h_0$	Initial gasket thickness in millimeters [mm].
• $L = h$	Final gasket thickness in millimeters [mm].
• $\Delta L = \Delta h$	Gasket thickness change during compression measured as the MTS machine stroke output in millimeters [mm]. For this research, deformation was negative i.e. compressive. The sign was inverted in Force-Deformation graphs for better presentation.

• $\varepsilon = \frac{\Delta L}{L_0} = \frac{\Delta h}{h_0}$	Strain. For this research, strain was negative i.e. compressive. The sign was inverted in Stress-Strain or Force-Strain graphs for better presentation.
• $F_N$	Normal Force measured by the MTS machine load cell expressed in Newtons [N]. For this research, normal force was negative i.e. compressive. The sign was inverted in Stress-Strain or Force-Strain graphs for better presentation.
• $A_0$	Original undeformed area expressed in squared meters [m <sup>2</sup> ]. For this research, the surface area of the gaskets was considered that of a ring with outer radius $R$ and inner radius $r$ , thus $A_0 = \pi(R^2 - r^2)$
• $\sigma_N = \frac{F_N}{A_0}$	Normal stress or Engineering stress expressed in megapascals [MPa]
• $E$	Young's modulus expressed in megapascals [MPa]
• $S_M$	Secant modulus expressed in megapascals [MPa]
• $S_C$	Stiffness at 25% compression strain expressed in Newtons [N]
• $B$	Bulk modulus expressed in megapascals [Pa]
• $P$	Hydrostatic pressure in megapascals [MPa]
• $\epsilon_V = \frac{\Delta V}{V_0} = \frac{\Delta h}{h_0}$	Dimensionless volumetric change or strain. Since the gasket are radially constrained, a change in thickness is equal to a change in volume.
• $H$	Hardness expressed in Shore A scale units, between 0 and 100.
• $CS$	Compression set expressed as percentage.
• $h_1$	Final gasket thickness after 30 min passed since release of compressive force in the compression set test expressed in millimeters [mm].
• $h_s$	Constant linear dimension of the spacers used (1/4" Dowell pins) in the compression set tests expressed in inches [in].
• $\nu$	Dimensionless Poisson ratio.
• $H$	Dimensionless hardness.
• $Y$	Dimensionless Young's modulus.
• $p_0$	Initial durometer indenter protrusion.
• $F_0$	Initial durometer compression spring force.
• $k$	Durometer spring constant.

- $\zeta$  Durometer spring sensitivity.
- $PF_{OD}$  Durometer presser foot Outer Diameter.
- $PF_{ID}$  Durometer presser foot Inner Diameter.
- $IN_{OD}$  Durometer indenter Outer Diameter.
- $IN_{ID}$  Durometer indenter Inner Diameter.
- $F_d$  Force resulting from the material rebound on the durometer's indenter expressed in Newtons [N].
- $d = \frac{F_d(1-\nu^2)}{2Er}$  Indentation displacement of a truncated cone inside an elastic material. This relationship is derived from Boussinesq's point load theory in millimeters [mm].
- $MI \equiv \frac{kp_0}{\zeta F_0}$  Mechanical indentability.
- $E_{c_1}$  Compression modulus derived from the calculated Young's modulus  $E_1$  and shape factor  $SF$  expressed in megapascals [MPa].
- $E_{c_2}$  Compression modulus derived from Shore A hardness values and shape factor  $SF$  expressed in megapascals [MPa].
- $E_1$  Young's modulus calculated from dimensionless Young's modulus  $Y$  and the Shore A durometer's nominal values expressed in megapascals [MPa]
- $\bar{w}$  Weighted mean calculated from the elastomeric materials selection matrix with ranked properties.
- $E_r(t)$  Viscoelastic relaxation modulus
- $E_c(t)$  Viscoelastic creep modulus
- $CI$  Confidence interval  $CI = 1 - \alpha$

# **1 Introduction**

## **1.1 Background and Motivation**

Canada has the third largest railway network in the world. Through it more than 70% of the country's goods and more than 70 million people are transported each year (Transportation Safety Board of Canada 2016). The Canadian rail network includes two national railways: the Canadian Pacific Railway [CP] and the Canadian National Railway [CN]. Together they transport more than 60 million tons of cargo each year through the Province of Alberta, Canada (Alberta Canada 2015). In 2016, there were 1305 rail occurrences reported to the Transportation Safety Board of Canada and 58% of the occurrences were non-main-track derailments and collisions (Transportation Safety Board of Canada 2016).

Airbrake leaks are a chronic reliability issue in the railroad industry as pressure must be kept in a train airline to operate the brakes when needed. High air pressure keeps the train brakes in an "off" position, but if pressure drops the brakes trigger and stay in an "on" position until the air pressure is reestablished (Jimenez, Munn, and Hua 2011). Research and operational experience have shown that some causes of large airbrake leaks during train travel can be undesired hose coupling separations, misalignment of airline couplings or gaskets, and cold temperature (Blaine 1980; Johnson 2001; Jimenez et al. 2010, 89-94). Any undesired brake engagement could have several detrimental consequences, including additional heat, wear and tear to the train wheels and axles, cargo delay, and even derailments. These consequences translate into an estimated cost of \$15 million dollars a year (Hua, Hixon, and Cobden 2006, 55-59; Jimenez et al. 2010, 89-94).

A train brake airline consists of interconnected flexible hoses under each railcar that stretch along the length of it. End hoses spread out from the front and back of each railcar to connect with adjacent railcars, by means of a special fitting known as a glad-hand. When two glad-hands are linked together they form a coupling, and when several couplings are formed, a train brake airline is formed. A coupling is comprised then of two joined glad-hands with elastomeric gaskets inside of each one. Couplings are a common point where leakage might occur (Jimenez, Munn, and Hua 2011). The coupling system configuration includes all the supports of the rubber hoses, which are: flexible hose-straps and the train castings, or brackets; this system is known as End-of-Car configuration [EOC]. In this system, the glad-hand fittings are designed for quick manual coupling and pull-apart decoupling. The gasket shape allows it to stay inside each glad-hand during coupling



and de-coupling (Hua, Hixon, and Cobden 2006, 55-59; Jimenez et al. 2010, 89-94). The EOC creates a stable and airtight seal connection when the train is moving, and it facilitates glad-hands decoupling when two railcars are pulled apart to separate. When a gasket inside a glad-hand is damaged, misaligned, or missing, a leak is prone to occur (Blaine 1980). An example of a glad-hand without a gasket can be seen in Figure 1.



Figure 1 Glad-hand without gasket

Research has been done to explain and resolve reliability issues with railcar airbrake leakage. In one study, researchers measured the load on hose-straps used to hold in place the railcars airbrake hoses that hang above the rail tracks. Researchers used a simulated system that mimicked two railcars airbrake lines coupled together, where one end of it was fixed, and the other one had a moving mechanism to separate the coupling. With this system, they controlled the coupling separation speed, the type of hose-strap used, and the End-of-Car [EOC] arrangement. Results showed that the reaction force on hose-straps could be minimized by selecting the proper combination of EOC arrangement and hose-straps, as the resultant load was decided by the rigidity of the EOC arrangement and the elasticity of the hose-straps, no matter which separation speed was used (Hua, Hixon, and Cobden 2006, 55-59).

Another study showed that the trolley arrangement in trains accounted for 52% of undesired hose separations, and that probably misaligned glad-hands combined with an incorrect type of End-of-Car arrangement could lead to these separations. The study mentioned that the force needed to move the end-hose of a trolley was sometimes greater than the force required to pull apart the glad-hands, and when this force overlap happened an undesired hose separation occurs. The hypothesis presented in this study was that if the force required to pull apart the end-hose connection was kept

greater than the force required to move the shackle on a trolley, the frequency of undesired hose separations would decrease. To test this hypothesis, new gasket designs were studied to find one that does not roll or twist when coupled. The results showed that the separation force needed to break apart the glad-hand coupling could be significantly increased by using a modified wide-lip airbrake gasket geometry (Jimenez et al. 2010, 89-94; Jimenez, Munn, and Hua 2011). This wide-lip gasket geometry (Figure 2) was also mentioned in US patent 6290238 B1 (Johnson 2001) and is currently used in the railroad industry (New York Air Brake 2017; Jimenez, Munn, and Hua 2011). Both gasket geometries, standard and wide-lip, are currently used in the railroad industry to create an airtight seal that complies with industry requirements and specifications.



Figure 2 Airbrake glad-hand gasket geometries (Left) Standard geometry (Right) Wide-lip geometry

In yet another study, researchers attempted to correlate the airbrake gasket stiffness to the separation force needed to pull apart a glad-hand coupling. In this study, a modified version of the fixture lower portion used in the Permanent set or Compression set test from Specification M-602 of the American Association of Railroads Manual of Standards and Recommended Practices [AAR MSRP] was manufactured. The design of the manufactured test jig in this study included different features to imitate real operational conditions of a gasket inside of a glad-hand, to mention a few: inlets to let air pressure in, a rim such as that of a glad-hand to hold a gasket, and threads to attach the fixture to a compression system (hydraulic press). All these features were needed to measure the gasket reaction forces while in simulated operation. Once the “in-operation stiffness” was measured, a separation test was performed on railcars with the same gaskets at a maintenance workshop. This study showed that no clear correlation was seen between the compression testing of the gaskets and the separation force, and that no linear behavior should be assumed when compressing gaskets. Also, the results showed that non-standard gaskets displayed higher stiffness during compression and significantly higher separation force when compared to standard ones. The increased separation force in non-standard gaskets was expected because they have a larger cross-sectional area than standard ones. This higher force was also seen in other separation test results (Sammon and Anderson 2015). Although not explicitly stated, it was assumed that the non-

standard gaskets referred in the study were wide-lip gaskets. Figure 3 shows an example of a glad-hand with a wide-lip gasket inside and two glad-hands coupled together:



Figure 3 (Left) Glad-hand and gasket front view (Right) Coupling

The AAR MSRP covers the minimum requirements for gaskets used in airbrake hose couplings for train service, including manufacture, physical requirements, dimensions and tolerances. Specification M-602 defines the material for air-brake gaskets and reads as follows: “*gaskets should be made of an elastomeric compound that shall be tough and have enough elasticity to conform to the requirements of strength and elongation such that the gaskets may be readily applied in the couplings under all service conditions and form an air-tight seat*” (AAR Publications 2002). This specification also mentions that “*gaskets shall attain a durometer reading of  $80\pm5$  or an AAR-approved alternate.*” In other industries, elastomeric seal standards and specifications have been created to assess sealability and performance, especially in the Automotive, Nuclear, and Oil and Gas sectors. The most common geometry used as an elastomeric seal is the O-ring, followed by thin-film and washer geometries. Consequently, many studies, protocols, and test methods, such as the published ones by the American Society for Testing Materials [ASTM] and the International Organization for Standardization [ISO], are focused on sealing performance of these geometries (Dick 2003; Gent 2012; Bauman 2008; Weise, Kowalewsky, and Wenz 1992, 555-557; Sommer 2009). Limited literature regarding airbrake glad-hand gaskets in specific was found, using as a base resource the AAR MSRP.

The research studies previously discussed focused on glad-hand coupling separation force or glad-hand gasket geometry but overlooked gasket material composition or just gave a general definition



about the compound used. Airbrake gaskets were generally defined as an elastomeric seal in the studies, which is the same description found in Specification M-602. The only documentation reviewed that suggested to use a specific compound for airbrake gaskets were US patents 6290238 B1 and 8061715 B2. Both documents recommended molding the gaskets from butadiene rubber, a thermoset elastomer. These patents also proposed the addition of an ozone inhibitor to the compound, and they encouraged the use of a material hardness in the range of 60 to 70 Shore A durometer scale. According to the patents, this hardness range could provide a softer and more flexible rubber for better sealing in cold weather (Jimenez, Munn, and Hua 2011; Johnson 2001).

## **1.2 Problem Definition**

One chronic reliability issue identified in the railroad industry is that airbrake leakages increase during cold weather (Blaine 1980). Along the railcar brake airline, the glad-hand and gasket link, or coupling, is a common location for leakages (Jimenez et al. 2010, 89-94). In cold weather, the main culprit for increased airbrake leakages is thought to be the elastomeric gasket inside a glad-hand, since temperature has a major impact on the elasticity of rubber type gaskets, and cold temperature makes them stiffer (Blaine 1980). Cold temperatures have caused reliability issues in other sealing applications, as in the Space Shuttle Challenger O-ring disaster (McDonald and Hansen 2009; National Aeronautics and Space Administration 1986).

Alternative elastomeric materials for the airbrake gaskets that are more resilient to low temperatures could improve airbrakes reliability by reducing leakage. These alternative elastomeric materials must comply with industry standards, provide ease of installation, have the necessary pliability to be manufactured in the required geometry, and stay in the current material price range. Additionally, to compare materials, the current one used and the alternatives require testing in short duration experimental trials to assess different features: performance, elastic response as a function of temperature, and durability (cracking, creep, chemical degradation, etc.). More detailed information on current railcars air-brake glad-hand gaskets is needed, including specific compound composition and their behavior in this specific application for cold-weather performance and durability. Moreover, data on their frequency of replacement, replacement policy, and records about their maintenance is necessary to ensure that the alternative is at least as reliable as the current generation of components.

### **1.3 Research Objectives**

The main purpose of this research is to examine the elastic response in cold temperature of railcar air-brake gasket materials and to develop a protocol for evaluating alternative materials. Additionally, durability is evaluated for different factors, such as gasket material response against the effect of certain liquids used during cold weather. The first step to achieve the objectives is to develop a preliminary test plan considering the key variables that could affect gaskets under service and design a simulated service operation system. The second step is to develop a detailed test plan defining the expected ranges of key variables to test and the measurement test methods, which is supported by revising standard and non-standard test methods for input on methodology and procedures. Once the detailed test plan is specified, alternative materials for the gaskets that could overcome the current one used are chosen using a decision analysis. The next step is to assess the gasket material currently used and the selected alternatives under laboratory conditions using the detailed test plan previously specified. Finally, a protocol for testing gaskets in service and a replacement policy is presented for industry application.

### **1.4 Thesis Outline**

Chapter 1 introduces the railroad industry importance for Canada and the relevance of the glad-hand gaskets for proper railcar brake operation. Chapter 1 also summarizes the current state of the art and mentions important results presented to date. Chapter 2 reviews relevant literature for concepts, definitions, and theory, with an overview of elastomers, and elastomeric material testing. Chapter 3 explains the methodology used in this research to select alternative elastomeric materials with better cold temperature performance than the current material used, as well as the detailed test plan used to assess both glad-hand gaskets made from the current material and from the alternative selections. Chapter 4 summarizes the results found and the comparisons made between conditions or materials. Chapter 5 presents an in-service protocol for recording gaskets maintenance, and a group replacement policy mock numerical example. Finally, Chapter 6 concludes the thesis work and recommends future work.

## 2 Literature Review

In this chapter, properties and behavior of elastomers are reviewed. Additionally, solids deformation concepts relevant to elastomeric material testing and durability are presented, with different compound features and testing methods.

### 2.1 Elastomers

The word elastomer comes from “elastic polymer”, that is, a polymer with high elastic or rubber-like properties. This “rubbery behavior” is one of the main reasons that the term “elastomer” is frequently interchanged with “rubber” in engineering and in standardized material testing methods. However, vulcanized natural rubber is just one of the many elastomeric compounds that can be used as an engineering material (Popa 2011; Bauman 2008).

Polymers, or macromolecules, are substances made up of many molecular units chained together by covalent bonds of atoms of carbon, hydrogen, oxygen, nitrogen, halogens, among other elements. They are typically grouped as organic compounds as they have backbone chains, or “element strips”, made up of either carbon or silicon atoms. Polymer chainlike molecules are made up of the same single unit, or monomer, repeated in sequence, generally achieved through polymerization (Strobl 2007; Gent 2012). Figure 4 shows an example of a schematic line-plot generated with MATLAB, which represents a polymer long molecular chain or wire model, which is frequently mentioned in literature (Treloar 2005; Callister and Rethwisch 2014):

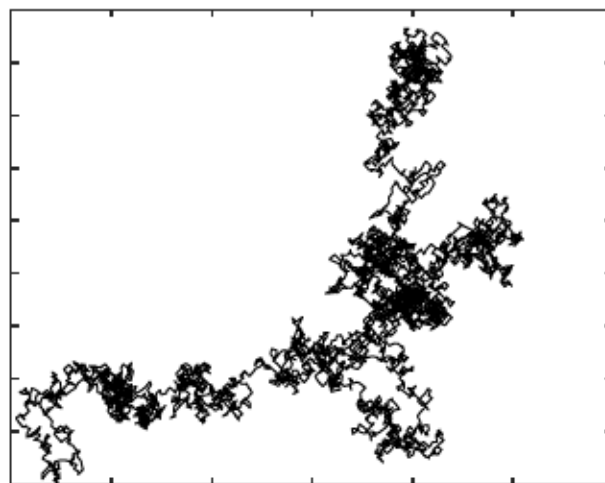


Figure 4 Line plot generated through MATLAB simulating a long polymer molecular chain



Solid materials can be grouped depending on the structure their atoms or ions are arranged, that is, depending on their crystal structure. A crystalline material has atoms ordered in a repeating or periodic array (a 3D repetitive pattern). All metals, many ceramics, and some polymers form crystalline structures. In contrast, non-crystalline or amorphous materials have no long-range atomic order. Polymers can have different and complex crystal structures, ranging from completely amorphous to semi-crystalline. Some properties of solid materials depend on crystal structure, for example mechanical behavior. Polymers can present three stress-strain behaviors: glassy, crystalline, or rubbery (Figure 5). Elastomers, being amorphous polymers, present rubbery behavior at room temperature (Gent 2012; Callister and Rethwisch 2014).

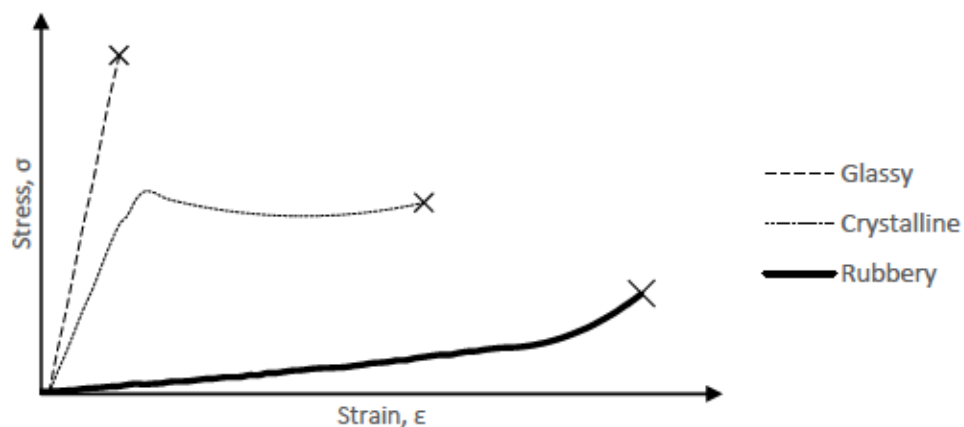


Figure 5 Stress-strain behavior of three polymer molecular structures: Glassy, Crystalline, and Rubbery [X represents failure] factors (Ashby and Jones 2013)

The mechanical behavior of elastomers can be further changed through cross-linking of their molecular chains. Amorphous polymers have molecules in random motion which can be vulcanized creating a defined cross-linked three-dimensional network (Strobl 2007). Vulcanization (cross-linking) is achieved by heating up an elastomeric liquid along with sulfur, peroxides, or metal oxides (Bauman 2008). This reaction creates strong covalent bonds between chains and transforms an elastomeric liquid into a proper elastomeric solid with the ability to withstand large elastic deformations due to its three-dimensional mesh of cross-linked macromolecules. A vulcanized elastomer mechanical properties depend on cross-link density, the functionality of its molecular units, and several other factors (Gent 2012; Strobl 2007; Ashby and Jones 2013). In a vulcanized elastomer, or vulcanizate, the long and twisted chainlike molecules between cross-links act as “springs” in response to external stresses, making the cross-links come

back to the original position they had before being disturbed. When these “molecular springs” recover, they return to the natural disordered coiled shape and position set before being stretched, this process is what gives an elastomer its hyper-elastic properties i.e. an elastomer can recover its original shape after being subjected to large strains of 300% or more (Treloar 2005; Mark, Erman, and Eirich 1994; Gent 2012).

A good example of an elastomer mesh is the Arruda-Boyce three-dimensional eight-chain network constitutive model used to explain the behavior of rubber elastic materials, or incompressible elastomers, which can be seen below:

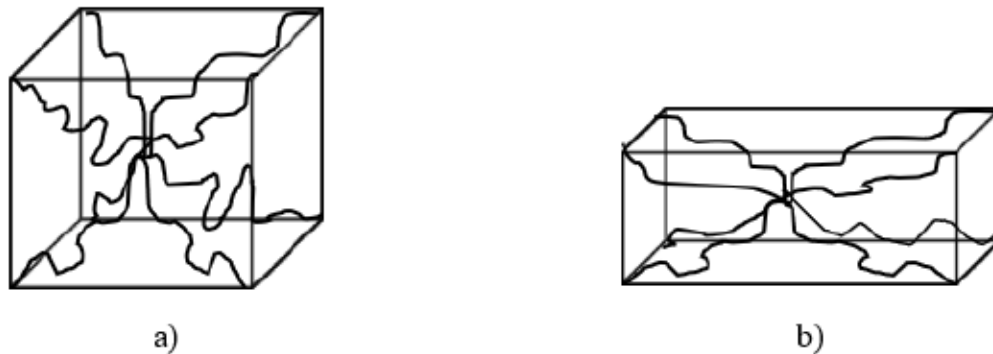


Figure 6 Representation of the Arruda-Boyce eight-chain unit cell model in the a) undeformed state, and b) compressed state (Przbylo, P. A. and E. M. Arruda 1998, 730; Arruda and Boyce 1993, 389-412)

### 2.1.1 Elastomers deformation and behavior

Elastomers present rubber-like elasticity, which is the ability to withstand large strains and elastically return to their original form. Elastomers moduli of elasticity are small and vary with strain. At small strains, elastomers present pseudo-linear behavior such as that of crystalline materials (Hooke’s law), but at large strains elastomers present complex mechanical behavior and a highly non-linear stress-strain curve (Callister and Rethwisch 2014; Bauman 2008).

Considering elastomers, or rubbers, as engineering materials, it is relevant to review fundamental terminology of mechanical testing of solids to make comparisons and to evaluate performance between options. Some terms used in this work are the following (ASTM 2017c; Hibbeler 2014; Hertzberg, Vinci, and Hertzberg 2012).

Table 1 List of terms, definitions, and equations or symbols related to mechanical testing

TERM	DEFINITION	EQUATION/ SYMBOL	EQ
Hardness	Physical resistance to indentation, scratching or permanent deformation. Its mechanics are complex and can be represented in several scales; thus, it is further explained in section 0.	$H$	
Normal force	Force applied parallel to the loading axis and perpendicular to the plane, or area, in which it is being applied, having units of Newtons [N]	$F_N$	
Stress	The intensity of forces, or components of force, $F$ exerted in a specific plane or area $A$ in a material, having units of Pascals [Pa], generally in the range of $10^6$ [Mega]	$\sigma = \frac{F}{A}$	(1)
Normal stress	Ratio of the normal force $F_N$ acting on the original area $A_0$ . If the normal force is “pulling”, $\sigma_N$ is called tensile stress; whereas if the force is “squeezing”, $\sigma_N$ is called compressive stress. $\sigma_N$ is also known as engineering stress.	$\sigma_N = \frac{F_N}{A_0}$	(2)
Strain	Dimensionless quantity defined as the ratio of length change $\Delta L$ (deformation) to original linear dimension $L_0$ , measured in line with the loading axis. It is generally expressed as a percentage in experiments or tests; also known as engineering strain.	$\varepsilon = \frac{\Delta L}{L_0}$	(3)
Stiffness	Defined as a material resistance to deformation from an applied force. It can be expressed as the ratio of force over a specified length, or just the resultant force at a certain strain. For this research, the compression stiffness $S_c$ is used, where $F_{N@25\%}$ is the normal force felt when a gasket	$S_{25} = F_{25}$	(4)

TERM	DEFINITION	EQUATION/ SYMBOL	EQ
	is depressed up to a strain of $\varepsilon=25\%$ , having units of Newtons [N].		
Poisson's ratio	Dimensionless ratio of lateral strain to the corresponding longitudinal, or axial strain. Elastomers, or rubbers, are considered incompressible solids, therefore $\nu \approx 0.5$ .	$\nu = -\frac{\varepsilon_{lat}}{\varepsilon_{long}}$	(5)
Young's modulus of elasticity	Ratio of stress to strain below the elastic limit, having the same units as stress. In an elastic object, this ratio is linear i.e. the deformation is directly proportional to force (Hooke's law) up to a certain elastic limit (strain). Rubbers at small strains follow a pseudo-linear behavior, but at large ones their mechanical behavior is non-linear, thus it is expressed rather as tangent, chord, or secant modulus.	$E = \frac{\sigma}{\varepsilon}$	(6)
Secant modulus of elasticity	Stress to strain ratio at a specific strain. It is the slope of the secant drawn from the origin to a specific point on a material stress-strain non-linear curve; hence, there are different secant moduli at different strains: $\varepsilon_{10\%}$ , $\varepsilon_{20\%}$ , and others. It has the same units as stress, Pascals [Pa]	Secant modulus at 25% strain: $S_M = \frac{\sigma_N}{\varepsilon_{25\%}}$	(7)
Set	Strain remaining after a load is released, when the force is compressive, it is called compression set [CS]. One way of measuring it, is depressing a test piece between two parallel plates limiting the compression up to the height of a spacer thinner than the test piece and measuring the final height after a set time. Thus, CS is the ratio of the differences of the initial height of the test piece $h_0$ and the	$CS = \frac{h_0 - h_1}{h_0 - h_s}$	(8)



TERM	DEFINITION	EQUATION/ SYMBOL	EQ
	final height $h_1$ , and the spacer height $h_s$ ; expressed as a percentage.		
Bulk modulus	Ratio of uniform hydrostatic pressure, $P$ , to volumetric change or strain, $\epsilon_V$ , having the same units as pressure or stress. Its importance to this research and a detailed explanation is on section 0.	$B$	

One property of polymers, and therefore of elastomers, is their range of mechanical behaviors at different temperatures, including brittle-elastic (glassy), rubbery, and viscous behaviors at low, mid, and high temperatures, respectively. Consequently, elastomer properties such as modulus of elasticity, hardness, and stiffness, change with temperature. Elastomers are made up of two types of bonds: strong covalent bonds that conform the backbone of their molecular chain, and soft secondary bonds created when chains are close to each other. The soft bonds are the one highly affected by temperature. Consequently, there is a transitional temperature region where their mechanical behavior changes due to melting of secondary bonds, shifting their mechanical behavior from brittle-elastic to rubbery. This transitional temperature is called the glass transition temperature, or glass temperature, and is denoted by  $T_G$ . Temperatures below  $T_G$  bring elastomers molecules close to each other, which increase their modulus of elasticity abruptly, making them hard and brittle (Ashby and Jones 2013; Callister and Rethwisch 2014).

Elastomers have a unique stress-strain behavior, where their Young's modulus is not a constant, but rather a range of values. The main difference of elastomers compared to other materials is that their strain is a function of time  $t$  (rate of deformation) and temperature  $T$  (Ashby and Jones 2013), having the expression:

$$E = \sigma/\varepsilon(t, T) \quad (9)$$

Hence, an elastomer modulus of elasticity is generally expressed as the secant modulus of elasticity, instead of Young's modulus of elasticity. The secant modulus of elasticity is used in the

standardized method ISO 7743 – Rubber, vulcanized or thermoplastic – Determination of compression stress-strain properties (ISO 2017).

Furthermore, at high-rates of straining and lower temperatures, elastomers behave as a viscoelastic material when observed in a long-term span, that is, depending on the rate of application of stress or strain, their modulus of elasticity also change. A viscoelastic material can be defined as one having mechanical characteristics of both an elastic solid, one that follows Hooke's law, and that of a viscous or liquid-like material (Callister and Rethwisch 2014). Maxwell and Voigt-Kelvin spring and dashpot models (Figure 7 and Figure 8) are used as a model to characterize these behaviors, as well as Mooney-Rivlin models (Grellmann and Seidler 2013, 73-231). Elastomers then also exhibit a viscoelastic relaxation modulus  $E_r(t)$ , and viscoelastic creep modulus  $E_c(t)$ , which are expressed as:

$$E_r(t) = \frac{\sigma(t)}{\varepsilon_0} \quad (10)$$

$$E_c(t) = \frac{\sigma_0}{\varepsilon(t)} \quad (11)$$

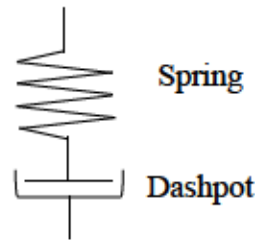


Figure 7 Maxwell spring and dashpot in series model used to describe viscoelastic stress relaxation

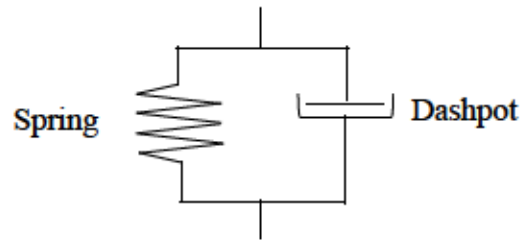


Figure 8 Voigt-Kelvin spring and dashpot in parallel model used to describe viscoelastic creep behavior

In Figure 9,  $\sigma(t)$  is the time-dependent viscoelastic stress relaxation curve experienced while a constant level of strain  $\varepsilon_0$  is maintained. In Figure 10,  $\sigma_0$  is a constant stress applied while the time-dependent strain  $\varepsilon(t)$  due to viscoelastic creep is being measured (Callister and Rethwisch 2014).



Figure 9 Representation of time-dependent viscoelastic stress relaxation

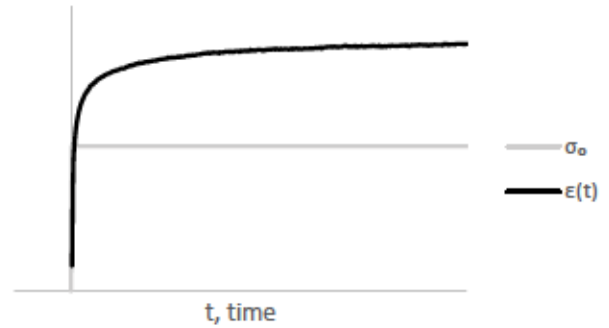


Figure 10 Representation of time-dependent viscoelastic creep

These behaviors can be explained by the elastomer molecular structure. In addition to the elastomer network crosslinks, entanglements or “knots” can also occur. These “knots” form due to the long elastomeric molecules intertwining between each other (Figure 11). Stress relaxation and creep happens when these entanglements migrate during deformation. At constant deformation,  $\epsilon_0$ , thermal vibrations move entanglements to lower energy configurations, loosening the elastomer network and lowering the stress; likewise, at constant load,  $\sigma_0$ , entanglements “slip” due to thermal vibrations making strain change with time, i.e. creep.

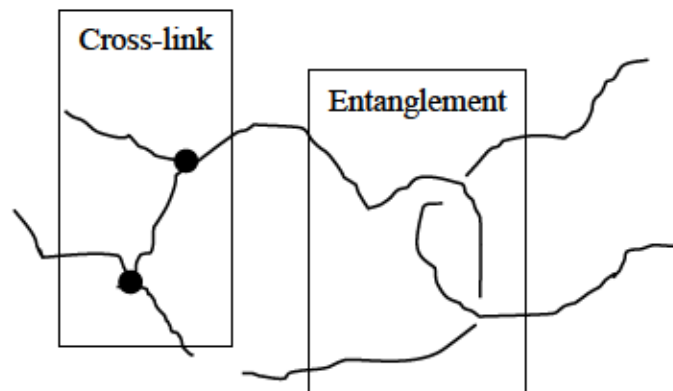


Figure 11 Representation of a both molecular unions: a cross-link and an entanglement

To improve these and other mechanical properties of elastomers, several additives can be used: curing agents, accelerators, activators or retarders, anti-degradants, reinforcing agents (fillers), plasticizers, and other property-specific additives. Carbon black or fumed silica are used as reinforcing agents or fillers to improve elastomer wear and tear resistance. Reinforced elastomers are known as “filled elastomers”, and if no reinforcing filler is added the materials are referred to as “unfilled elastomers” (Popa 2011; Dupont Dow Elastomers 2001). One direct effect of

reinforcers in elastomers is a hysteretic stress-strain behavior. Mechanical hysteresis is a result of energy loss due to heat dissipation during loading and unloading stress cycles (ASTM 2017c). In an elastomer, hysteresis is due to internal friction from splitting and restructuring contact points between the reinforcer and the elastomer, i.e. hysteresis increases with the quantity of reinforcing fillers or agents (Gent 2012; Bauman 2008; Dick 2014).

Additionally, elastomers can also exhibit set, cyclic stress relaxation, and recovery. Set in elastomers is the “offset deformation”, or strain, that stays after a force was applied and then removed. Its value increases with load and deformation rate. This mechanical set happens due to the elastomer molecular chains secondary-bonds fracturing during deformation, and then creating new connections while the deforming force is applied. When the force is removed, the chain segments that did not break will make the material return to its original shape, but the new connections made will resist this, thus “obstructing” full recovery. If the mechanical set does not change any further with time, it is called permanent set. If the force exerted is compressive, it is called compression set. A low compression set of an elastomeric seal is important to prevent leakage when there is movement of the confining metal or medium, i.e. a flange or a gland-hand (Gent 2012; Bauman 2008). Cyclic stress relaxation is observed when elastomers experience loading and unloading stress-strain cycles. During the first loading cycle, a small number of molecular chains get ruptured. On a second deformation cycle, up to the same strain level as the first one, the measured stress value is now lower than what was previously seen. If enough time without disturbances is given to the elastomer, part of the stress response will be restored. This phenomenon is known as recovery. The molecular chains reconnect to the original point where they were before strain rupture, or at least to a point near where they were (Bauman 2008). Quick recovery of an elastomeric seal shape is essential then to prevent leakage. When there is a decrease in temperature far below  $T_g$  and then it rises again, compression set can occur due to the thermal deformation of the elastomeric seal and the gland (Gent 2012). A representation of these phenomena can be seen in Figure 12.



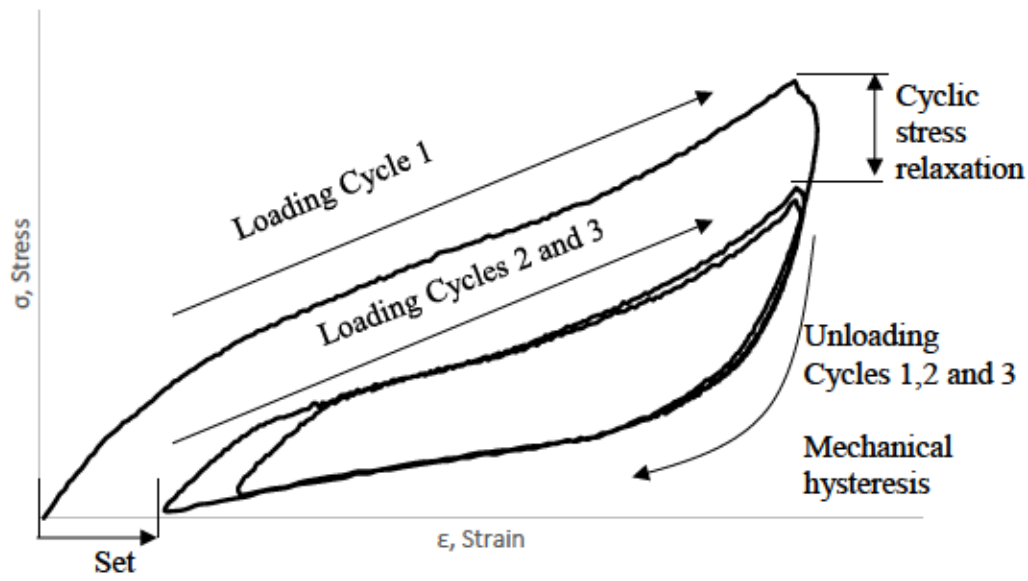


Figure 12 Representation of mechanical hysteresis, set, and cyclic stress relaxation in an elastomer uniaxial compression test. Loading and unloading directions are shown for better understanding.

Another concept related to elastomers is durability i.e. the resistance to changes, or degradation, in some property due to a certain service application or environment. Since the specific composition and microstructure of an elastomer depends on the compounding elements and the manufacturing process, the durability of elastomers varies widely (Gent 2012; Mark, Erman, and Eirich 1994). Elastomeric material durability has been studied in response to two detrimental factors: chemical degradation and low temperature.

Polymer degradation is defined as an alteration of a polymer physical properties due to reactions that rupture the bonds in the polymer backbone chains or in other locations throughout a polymer chain, as in side-chain sections. In linear polymers, for example, a break up reduces molecular chain length, which in turn reduces molecular weight. There are different modes of initiation for polymer degradation, including thermal, mechanical, photochemical, radiation, biological, and chemical (Schnabel 1981). Chemical degradation focuses in alterations made through acids, bases, solvents, and any other reactive agent that encounters the polymer. Depending on the kinetic energy, chemical degradation reactions can be divided in single-step or chain reactions. Single-step reactions are directly proportional to the rate of initiation, in contrast with chain reactions which are self-propagated once started and grow exponentially. One common type of chemical degradation reaction in polymers is solvolysis. This type of reaction involves the rupture of carbon

to non-carbon bonds found in a polymer backbone chain, some common solvolysis agents are water, alcohols, ammonia, and hydrazine (Schnabel 1981). Absorption and leaching are other common mechanisms of interaction with chemicals. Absorption is the intake of the chemical agent into the interstitial space of the polymer, which increases its weight and volume, thus swelling. Leaching happens when a component of the polymer dissolves out of it, for example, the dissolution of the plasticizer in PVC. The mechanism more prevalent in thermoset elastomers with fuels and solvents is absorption, which causes swelling but not dissolution of the material (Niesse 1995, 24-29; Mark, Erman, and Eirich 1994; Popa 2011).

An elastomer coefficient of thermal expansion can be ten times that of steel. Therefore, on cold temperature this discrepancy in coefficients could create an opening for leaks when an elastomeric seal shrinks away from a steel casing, or any other metallic casing (Bhowmick 2008). Some studies have shown that this process is reversible, and sealing can be restored upon heating (Weise, Kowalewsky, and Wenz 1992, 555-557). In addition to thermal contraction, there are two other phenomena elastomers suffer when temperature drops: glass transition and crystallization. These changes depend on cooling and crystallization rates and affect mechanical properties such as modulus of elasticity and hardness in addition to dimensional variation. Thus, low-temperature resilience of elastomeric seals depends on several factors that change properties in response to cooling rate, application, and environment (Bukhina and Kurlyand 2007; Bhowmick 2008).

Glass transition occurs in amorphous-glassy and semi-crystalline polymers because there is a decrease in movement of large portions of their molecular chains when temperature drops. This process can be seen in materials with low crystallization rates, or with no crystallization, since glass transition happens when the freezing rate exceeds that of crystallization. Elastomers have a low degree of crystallization and glass transition temperature is the predominant factor to focus on when analyzing their low temperature behavior. In contrast, materials with a high-rate of crystallization practically never go through the glassy state. Several factors can shift the glass transition temperature of an elastomer: spatial molecular structure, molecular mass, thermal history, and pressure/stress in application. Near the glass transition temperature, sudden changes in several physical properties happen, including change in their stress-strain response from rubbery to glassy, increase in stiffness and hardness, changes in both heat capacity and coefficient of thermal expansion; among others (Figure 13). There are many techniques to properly assess the

glass-transition temperature of an elastomer, such as dilatometry or differential scanning calorimetry [DSC] (Callister and Rethwisch 2014; Bukhina and Kurlyand 2007).

Although crystallization is not common on elastomers, it is worthy of mention. Crystallization is a process of primary nucleation and crystal growth. Primary nucleation can be homogenous (thermal) or heterogeneous (athermal). Homogeneous nucleation is the formation of primary nuclei from the own polymer crystallizing regions occurring in synchrony as they grow during temperature decrease. In contrast, the nucleation process is heterogenous if foreign impurities are the source of nuclei and crystal growth. Elastomer crystallization happens with a 2 to 2.5% volume decrease. Crystallization time may vary from minutes to days, depending on material molecular structure and external conditions (Bukhina and Kurlyand 2007).

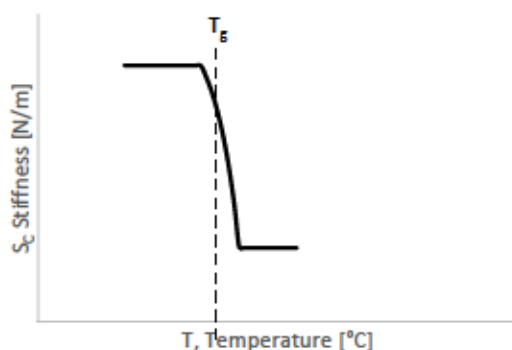


Figure 13 Representation of stiffness change at glass temperature  $T_g$

### 2.1.2 Elastomer compounds and classifications

Generally, elastomers can be classified in two groups: thermosets and thermoplastics. Vulcanized rubbers are in the thermoset group and are often called thermoset elastomers (Gent 2012; Dr Premamoy Ghosh 2011). Compared to thermoplastic seals, elastomeric seals have better resilience and recovery properties in broader ranges of temperature and pressure. Thermoplastics are also long-chain polymers but are not connected via cross-links. Instead, crystalline sectors, or aggregates, are created when their chains line-up and crystallize (Popa 2011; Dupont Dow Elastomers 2001). Thermoplastics aggregates do not have the same chemical strength as that of crosslinks. Thermoplastic elastomers tend to yield and flow under high stresses, having this factor intensified at high temperatures (Gent 2012).



A more detailed elastomer classification is by their molecular lattice or composition. ASTM standard practice D1418 presents a generic classification of rubber polymers based on their chemical composition and groups them in eight classes. Rubbers are named first with letters that represent the polymer monomer groups, and end with the corresponding class letter classification (ASTM 2017a). Some examples of this classification can be seen in Figure 14.

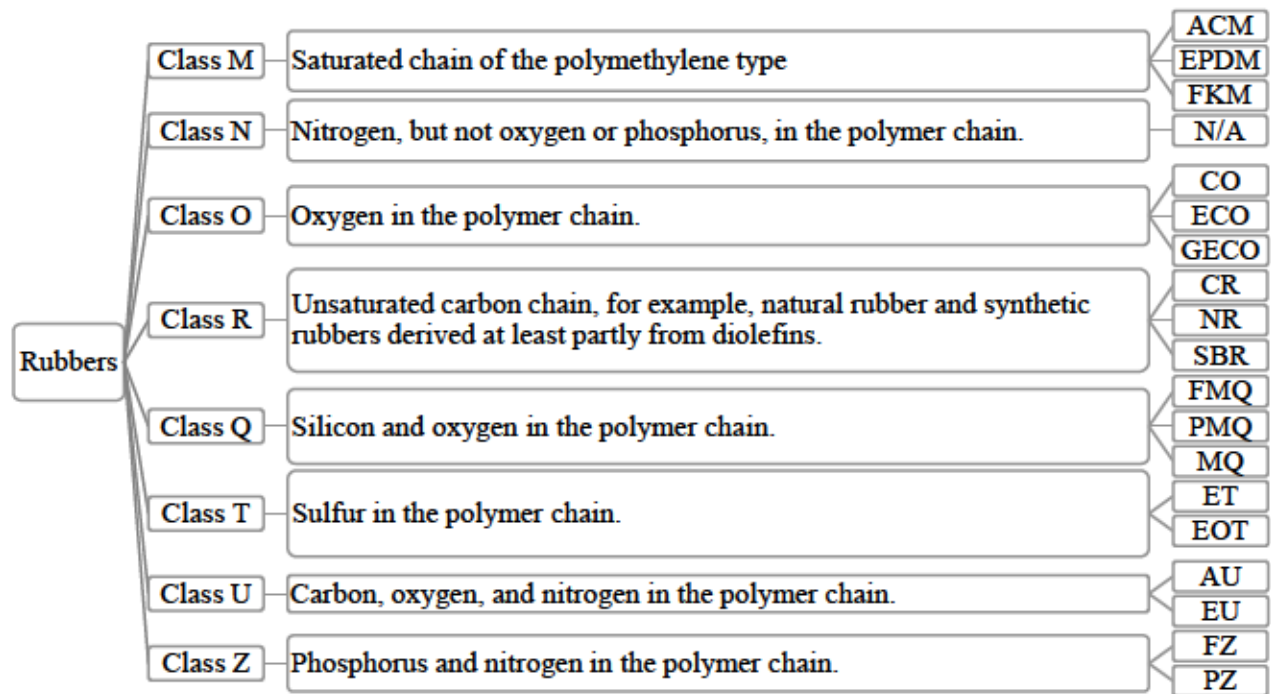


Figure 14 ASTM D1418 general classification system for rubbers based on chemical composition of their polymer chain

Another way of classifying elastomers is by their usage: general use and specialty. Specialty elastomers tend to be more expensive than general purpose elastomers. This group can be subdivided into high-volume use and low-volume use specialty elastomers. Styrene-Butadiene (SBR) and Polybutadiene (BR) are the most common type of elastomer as they are frequently used in vehicle tires. A partial list of both general use and specialty elastomers can be found below (Gent 2012).

- General use elastomers
  - Styrene-Butadiene (SBR)
  - Polyisoprene (NR, IR)
  - Polybutadiene (BR)

- Specialty elastomers
  - High-volume use
    - Polychloroprene (CR)
    - Acrylonitrile-Butadiene (NBR)
    - Ethylene-Propylene Diene (EPR, EPDM)
    - Butyl and halogenated butyl (IIR, BIIR, CIIR)
    - Chlorinated and Chlorosulfonated Polyethylene (CPE, CSM)
  - Low-volume use
    - Hydrogenated Nitrile (HNBR)
    - Silicone and fluorosilicone (MQ, VMQ, PMQ, PVMQ)
    - Polysulfide (T)
    - Chlorinated Polyethylene (CM)
    - Ethylene-Methyl Acrylate (AEM)
    - Polyacrylate Rubber (ACM)
    - Fluoroelastomers (FKM, FFKM, FEPDM)
    - Epichlorohydrin Rubber (CO, ECO)
    - Polyurethane (PUR, PU)

Some property values for a few elastomers mentioned before can be seen in Table 2 (Gent 2012; Brandrup et al. 1999; Dupont Dow Elastomers 2001).

Table 2 General mechanical properties and information of different elastomeric compounds

RUBBER PROPERTY	Engineering Stress, $\sigma_N$ @300% strain [MPa]	Shore A Durometer Hardness [Available Range]	Glass temp. $T_g$ [°C]	Bulk modulus [MPa]	General properties
CR	20.3	40 – 90	-45	2270	Mid cost. Better ozone and swelling resistance than NR. DuPont's commercial name is Neoprene™
EPDM	7.6 @200% strain	40 – 90	-55	1000	Mid-low cost. Superior ozone and weather/aging resistance. Slow cure and non-polar characteristics.
FKM	1.8 @100% strain	55 – 90	-20 to -10	2420	High cost. High-temp resistance. Diamine, bisphenol or peroxide cures are available.
NR	15.4	30 – 90	-72 to -61	1950	Lowest cost. Poor ozone resistance (weathering/aging). Extracted from the <i>Hevea</i> tree.
NBR	16.2 (35% ACN)	40 – 90	-40 to -10 (20 - 50% ACN)	1950	Mid-low cost. Copolymer of acrylonitrile-butadiene, with ratios between 18% to 40%. The acrylonitrile content affects $T_g$ (ACN: Acrylonitrile). Fast cure and polar characteristics.
SBR	17.9	40 – 90	-55	1960	Low cost. Copolymer of butadiene and styrene with ratios ranging between 23.5% to 25%.

Yet another classification is naming rubbers based on specific property requirements. ASTM D2000 suggests a classification system based on “line call-outs”, having the letter M [Indicating that requirements are in Si units], a grade number [1: Basic requirements, 2-8: Additional requirements per suffix letter], type and class material designation letters [A-K], hardness and tensile strength required values, and a suffix letter for additional requirements needed. At the end

of a “line call-out”, the suffix letters specify a property to be tested, with a testing method for each (ASTM 2017b; Gent 2012).

### 2.1.3 Elastomer properties and testing methods

There exist many different elastomeric compounds and product shapes, and each combination has its own properties. Standard grades hardly exist, and each product-compound combination must be evaluated individually. The structure of elastomers and their sensitivity to small compound or process changes translates to unintended variations in properties from batch to batch, presenting difficulties in quality control. Each elastomeric compound reacts differently to the way it is used and to any detrimental factor it encounters. An elastomer property response can change due to different factors, as if it were another material altogether in another environment. There is no universally accepted standardization for elastomeric compounds, and a formulation is often a company secret (Gent 2012; Dick 2014; Mark, Erman, and Eirich 1994). Nevertheless, there are different tests to measure and compare elastomer properties. Standardized methods for determining a specific property are published by standardization bodies including ASTM, ISO, or BS. Non-standardized test methods are presented in journals, digests, or papers by developers of technology, laboratories, universities, or companies (Brown 2006).

Depending on the property to assess, ASTM and ISO have different standardized testing methods to measure each one. The standards often describe several methods or focus on a specific application. ASTM D2000 divides specifications into tests required per each property. A partial list of properties and corresponding ASTM or ISO standard test method is presented in Table 3.

Table 3 List of rubber properties and the corresponding ASTM or ISO testing method.

PROPERTY	DOCUMENTS	COMMENTS
Dimensions	ASTM D3767, ISO 3302	Example apparatus used for these measurements include Vernier caliper or dial micrometer.
Density	ASTM D792, ISO 2781	Mass per volume ratio at a specified temperature. Can be determined using water displacement
Hardness	IRHD: ASTM D1415, ISO 48 Durometer: ASTM D2240, ISO 7619	Resistance to puncture, scratching or permanent damages.



PROPERTY	DOCUMENTS	COMMENTS
Adhesion	ASTM D429 Method A, B and C ISO 814, ISO 813, ISO 5600 ASTM D413, ISO 1827, ISO 36, ISO 6133 ASTM D2138, ASTM D2229, ISO 4647, ISO 5603, ISO 6505	This test is meant to determine the adhesive behavior of elastomers when they are joined with other materials, some examples of bonded pairs include rubber-textile, rubber-metals, rubber-plastic, among others. The peeling force is the variable to measure in both ASTM and ISO standards, with different methods depending on the bonded materials.
Stress-strain in Shear	ASTM D945, ISO 1827	These test methods correspond well to operation of elastomeric bearings or seismic pads. Two-point shear test is frequently used.
Stress-strain in Tension	ASTM D412, ISO 37	Deformation due to tensile stress. Elastomers withstand up to 300% tensile strain. Usually an MTS machine is used.
Stress-strain in Compression	ASTM D575, ISO 7743	Tests to determine the compression stress-strain properties often correspond better to actual seal products service conditions, in contrast to extension testing. Often hydraulic presses are used for this test.
Compression Set	ASTM D395, ISO 815-1, ASTM D1229, ISO 815-2	ASTM D395 and ISO 815-1 test compression set at high temperatures, and ASTM D1229 and ISO 815-2 at low temperature.
Free vibration	ASTM D945, ISO 4663	The ASTM method uses the Yertzley Oscillograph. The methods use a cantilever test piece in oscillation.
Dynamic response	ASTM D2231, ISO 2856, ASTM D5992, ISO 6721	Under dynamic conditions elastomers present a complex modulus $E = E_{real} + E_{imaginary}$ The real part is called storage modulus and the imaginary the loss modulus.
Time-dependent relaxation response	Stress-relaxation: ASTM D6147, ISO 3384 Creep: ASTM D2990 (plastics), ISO 8013	There is currently no ASTM standard for rubber creep, just plastics. Creep is measured with a relaxometer, whereas different fixtures, like the Shawbury-Wallace one, are used for stress-relaxation.

PROPERTY	DOCUMENTS	COMMENTS
Rebound	ASTM D1054, ASTM D2632, ISO 4662	Some rebound methods use a pendulum, like Goodyear-Healey Rebound Pendulum method, the falling weight method, the Lupke Pendulum, the Schob Pendulum, or the Zerbini Pendulum. These methods measure shock energy.
Low temperature response	Brittle Point: ASTM D2137, ISO 812 Retraction: ASTM D1329 Stiffening: ASTM D1053	Low temperature response depends on several factors, but general mechanical behavior changes can be assessed through these methods. Fracture after a shock in a specified low temperature determine brittle point, retraction is linear dimension reduction, and stiffening relates to stress-strain behavior under compression.
Gas permeability	ASTM D1434, ASTM D814, ISO 1399, ISO 2782, ISO 2528, ISO 6179	ASTM D1434 measures vapor permeability. ISO 1399 uses the constant volume method and ISO 2782 uses the constant pressure method. ISO 2528 uses water vapor and ISO 6179 volatile liquids.
Weathering resistance	ASTM D518, ASTM D750, ISO 4665	Weathering degradation is determined by leaving test pieces in the exterior, or in a setting with dry and moist cycles, UV rays, and warm temperature. Hardness and tensile properties differences are indicative of resistance.
Tear resistance	ASTM D624, ISO 6133	Tear strength is relevant to failure modes in products like engine mounts, albeit there is no relation to real application. The “splitting” force of a test piece when it is torn, usually through a mid-axis, is measured.
Flex fatigue	ASTM D430, ASTM D813, ASTM D1052, ASTM D3629, ASTM D4482, ISO 6943, ASTM D623, ISO 4666	Flex-cracking strain tests measure flexure. These tests are intended to assess rubber belts, tires, and footwear. Some types of flexing test include the De Mattia, “flipper”, Du Pont, and Ross.
Resistance to Liquids	ASTM D471, ISO 1817, ASTM D1460	To determine the resistance, elastomers are immersed in a specific way into the liquid. Immersing elastomers in reference fuels and oils often results in swelling.
Ozone resistance	ASTM D1149, ASTM D1171, ASTM D3395, ISO 1431	Ozone attack is determined by leaving test pieces in the exterior or in an ozone-rich environment. Resistance is determined by “crack grades” at a certain strain.

PROPERTY	DOCUMENTS	COMMENTS
Heat resistance	ASTM D573, ISO 188, ASTM D865, ASTM D454, ISO 6914, ASTM D572, ISO 188	Heat effects are determined by putting test pieces at a designated specific temperature and time. Air oven and oxygen bomb methods are used. Unaged and heat-aged pieces are compared for any property change sought.
Abrasion and wear resistance	ASTM D394, ASTM D1630, ASTM D2228, ASTM D3389, ISO 4649	Friction is the main force in action for wear and tear. Wear is the loss of material by any action, having abrasion wear, fatigue wear, and adhesive wear. Abrasion is wearing through friction of an abradant. Methods for abrasion and wear include linear tracks, rotating shafts or abrading wheels, inclined planes, and others.

Some elastomer properties without a standardized test method are bulk modulus or roughness. Nevertheless, there are documents that describe procedures to measure these properties (Shu, Takao, and Akbar 1994, 871-879; Fishman and Machmer 1994). Some documents also present simulated service tests performed by manufacturers, quality control laboratories, or research centers (Hua, Hixon, and Cobden 2006, 55-59; Sammon and Anderson 2015). Alternative or modified standard methods can be found in literature as well, such as a Standardized Polymer Durometry to correlate hardness with Young's modulus (Mix and Giacomini 2011), or new miniaturized test methods with shorter cooling or exposure times for elastomers compression set or dynamic analysis (Jaunich, Stark, and Wolff 2010, 815-823; Niesse 1994). In this thesis, a non-standard simulated service test for measuring bulk modulus and leakage was used.

Some applications where elastomers are used include seals, gaskets, vibration and shock absorption components, as well as load-bearing supports such as bridge or building pads (Gent 2012). Even though elastomers can withstand large deformations, components are designed to be used in the low-strain region of less than 50% strains in extension or compression, and less than 100% in shear strain (Bauman 2008). At low strains, an approximation of elastomer stress-strain behavior can be done using conventional elastic analysis, which is the approach taken in both ISO and ASTM standards to determine the compression stress-strain properties of rubber (ASTM 2012; ISO 2017; Bauman 2008).



## 2.2 Gasket failure modes

Limited literature on failure modes and lifetime prediction of railcar airbrake glad-hand gaskets was found; however, there are several studies for other elastomeric seal geometries. The most common geometries used for sealing purposes are O-rings and flat gaskets. Accordingly, several failure mode analysis and lifetime estimation studies on these common geometries have been done (Shao and Kang 2014, 16-21; Coveney and Rizk 2006, 141-151; Ghosh 2011; H. Li et al. 2012, 820-823). O-rings and flat gaskets are used in many systems to seal off liquids or gases, maintaining the pressure in the system and preventing leaks. Railcar airbrake glad-hand gaskets perform the same sealing action as that of O-rings and flat gaskets, and other similarities can be found as well. For example, railcar airbrake gaskets need to be made of an elastomeric material as per AAR regulations (AAR Publications 2002). In comparison, O-rings and flat gaskets are generally made of elastomeric materials as well (Gent 2012). Furthermore, the shape factor, geometry, and operational conditions are similar between O-rings, flat gaskets, and railcar gaskets (Gent 2012); therefore, knowledge from these common geometries can be extrapolated to railcar gaskets. Failure modes and lifetime estimation studies of O-rings and flat gaskets were consulted, and the information was used as basis to study railcar airbrake glad-hand gaskets reliability and performance. Additionally, the general factors that affect rubber components performance and the techniques used to estimate the lifetime of elastomeric seals were researched and are referenced in this section (Brown 2001; Albiñ 2006, 3-25; Daley 2006, 51-58; Sommer 2009).

The most common reasons for O-rings, flat gaskets, and elastomeric seals in general to fail are degradation factors and cold temperature. Frequently, an elastomeric seal will be exposed to one or more degradation factors during its useful lifetime. The individual contribution of each factor to the lifetime of a rubber seal and its degree of degradation is difficult to measure and discern, as some components might be exposed to all factors at the same time during operation. Even in laboratory conditions, it is difficult to isolate each degradation factor and analyze its individual effects, as sometimes these have a detrimental synergistic effect.

Table 4 lists the degradation factors for rubber or elastomeric components (Brown 2001).

Table 4 Degradation factors and its effects in rubbers/elastomers

<b>Factors</b>	<b>Effect</b>
Light	Photo-oxidation, cracking



Factors	Effect
Ozone	Oxidation, cracking
Humidity	Hydrolysis, cracking
Fluids	Chemical degradation, swelling, additive extraction, cracking
Mechanical stress	Fatigue, creep, stress relaxation, set, abrasion, adhesive failure, damage e.g. cuts, nibbles, extrusion, and flashes.
High Temperature	Thermo-oxidation, additive migration, further crosslinking, crosslinking loss (reversion)
Ionizing radiation	Radio-oxidation, crosslinking
Bio-organisms	Decomposition, mechanical attack
Electrical stress	Local rupture

Low temperature is a non-degrading factor, as it has temporary and reversible effects on the mechanical properties of rubber components. For example, cold temperature reduces rubber components recovery time after strain, and increases their stiffness, brittleness, and hardness. Although the effects of cold temperature can be reversed upon heating, it is an important reliability factor to consider as some studies show that a rubber seal function can be lost completely in sub-cooled temperatures (Jaunich, Stark, and Wolff 2010, 815-823; McKeen 2014; Weise, Kowalewsky, and Wenz 1992, 555-557; Grelle, Wolff, and Jaunich 2017, 219-226; Bukhina and Kurlyand 2007; National Aeronautics and Space Administration 1986).

Degradation factors and cold temperature influence the performance of elastomeric seals, either by making them more prone to fractures or by modifying their properties. When the properties of an elastomeric seal change, it might not be able to function as a seal anymore. Consequently, it is important that railcar airbrake gaskets maintain its properties, such as compressive strength and quick recovery after strain, at low temperatures and when they encounter degradation factors. Railcar airbrake gasket materials must be able to withstand common degradation factors such as light, ozone, humidity, fluids and mechanical stress, as they are used in an outdoor environment. Considering this, to evaluate a degradation factor effect on railcar airbrake gaskets, the variables associated with it can be manipulated under laboratory conditions, while isolating as many others as possible. The detailed test plan considers this for the assessing the selected degradation factors and when suitable alternative materials for railcar airbrake gaskets were selected.

Canada Rubber Group Inc. divides gasket failure modes in two: blowout and chronic leakage. Blowout is a sudden and violent release of the sealed medium due to a catastrophic failure of the gasket, whereas chronic leakage is a persistent leak of media caused due to progressive deterioration of the gasket that can lead to a blowout. Chronic leaks differ in size and severity, and

these factors will indicate whether a preventive or a corrective action needs to be done (Canada Rubber Group Inc 2015).

To assess the severity of a leak in a train airbrake system, Transport Canada applies inspection and safety rules. As per regulations, on conventional trains *the brake pipe pressure on the tail end of the train must be within fifteen (15) psi of the locomotive brake pipe pressure, and, air flow to the brake pipe must not exceed sixty (60) cubic feet per minute or CFM, as indicated by the flow indicator, or by a brake pipe leakage of no more than five (5) psi in sixty (60) seconds. Also, while on route, if the train brake pipe air flow exceeds sixty (60) CFM when the automatic brake handle is in the release position, other than during an intended brake application and/or release activity, corrective action must be taken if the flow does not return to sixty (60) CFM or below within a reasonable period of time, as determined by the locomotive engineer* (Transport Canada 2017). As can be inferred from these rules, railcar airbrake gaskets must be able to maintain the pressure in the system, otherwise the train will not comply with the minimum standards to safely operate the brakes. Additionally, as discussed in previous sections, a major leak in a train's airline would prematurely trigger the brakes and create additional issues to the train on route. To assess that the minimum conditions to safely operate the train brakes are met, there are three types of tests that can be performed according to Canada's transportation regulations: No. 1 brake test, No. 1A brake test, and a Continuity test (Transport Canada 2017). The simulated service operation tests in this study take as reference these three tests, as well as similar tests presented on other studies, along with ASTM and ISO standards.

Failure mode knowledge from glad-hand gaskets used in tractor-trailer airbrake systems can also be extrapolated to understand railcar airbrake gasket performance. Just as in a train, a tractor-trailer combination uses air to operate its brakes. The tractor is equipped with hoses ending in glad-hands to connect to the trailer's airline and brakes. Research has showed that the capacity of a glad-hand connection to stay joined during travel depends on how tight the rubber seal and detent hold the glad-hands and gaskets together, thus keeping them from rotating and separating. (Dilich, Goebelbecker, and Kopernik 2002). This information supports the idea that the railcar airbrake gaskets need sufficient compressive strength and hardness to stay in place and push one another to maintain the pressure in the air system.

### 2.3 Gasket reliability and unit replacement

Reliability is defined as the probability of a system, or a component, accomplishing the purpose it was designed for up to a threshold, in a determined period, and in specified operating conditions (Lipsett 2011, 1301-1358). Reliability estimation can be done based on probability of failure, determined through the frequency of failure or lifetime distribution of a system, with the final goal of finding the system reliability function, expressed in terms such as the Mean-Time-To-Failure (MTTF). The MTTF is the average period that a non-repairable component remains in operation, i.e. its average lifetime. One way of estimating the lifetime probability distribution is using the logged data of the frequency of failures of a component, or a group of components, and use these with an algorithm to find a model that generates a reliability function. Once the reliability function is established, this can be used as a decision-making parameter for maintenance policies, also known as reliability centered maintenance methodology (Poddar 2014; Vaghar Anzabi 2015; Lipsett 2011, 1301-1358; Marghoub Shadkar, Hendry, and Lipsett 2015).

Each system, or component, might follow a certain lifetime distribution function, which could be Normal, Weibull, Exponential, Hyper-exponential, or other type. When a nonrepairable component fails stochastically (unexpectedly) and is immediately replaced, failure following a normal distribution can be expected; which is the assumption made for railcar airbrake gaskets. Figure 15 illustrates a replacement policy where preventive group replacements happen at constant intervals  $t_p$  and replacements occur whenever a component fails, as many times as required, between  $t = 0$  and  $t = t_p$  in one cycle (Jardine and Tsang 2013):

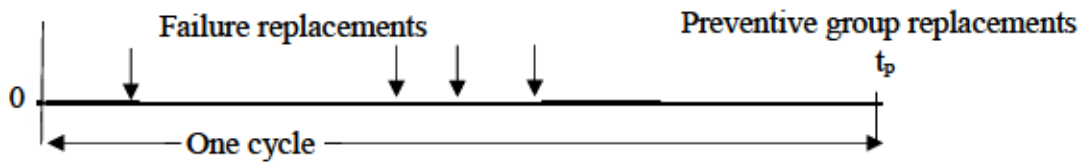


Figure 15 Preventive group replacement policy representation

Following this policy, the total expected cost per unit time  $C(t_p)$ , for group preventive replacements at time  $t_p$  is expressed as:

$$N C(t_p) = N \left( \frac{C_g + C_f H(t_p)}{t_p} \right), \quad (12)$$



where  $N$  is the number of components,  $C_g$  is the cost of replacing one item under group replacement conditions,  $C_f$  is the cost of a failure replacement, and  $H(T)$  is the expected number of failures in the interval  $(0, t_p)$ , also known as the failure rate, expressed as:

$$H(T) = \sum_{i=0}^{T-1} [1 + H(T - i - 1)] \int_i^{i+1} f(t) dt, T \geq 1. \quad (13)$$

Here,  $f(t)$  is the probability density function of a component failure rate. If this function follows a normal distribution with mean  $\mu$  and standard deviation  $\sigma$ , then:

$$f(t) = \frac{1}{\sigma\sqrt{2\pi}} e^{\left(\frac{-(t-\mu)^2}{2\sigma^2}\right)}, \text{ for } -\infty < t < \infty. \quad (14)$$

The cumulative distribution function of the standardized normal distribution with mean  $\mu = 0$ , and standard deviation  $\sigma = 1$  (Jardine and Tsang 2013), is expressed as:

$$\Phi(t) = \int_{-\infty}^t f(t) dt = \frac{1}{\sqrt{2\pi}} \int_{-\infty}^t e^{\left(\frac{-t^2}{2}\right)} dt. \quad (15)$$

Using equations (12), (13), (14), and (15), the minimum cost per unit time  $C(t_p)$  at the optimal maintenance interval  $t_p$  can be calculated.

In the railroad industry, reliability theory for maintenance or Reliability Centered Maintenance [RCM] has been studied to estimate the lifetime of some components. For example, wayside wheel temperature detectors data used with RCM was studied to detect wheels prone to failure (Marghoub Shadkar, Hendry, and Lipsett 2015; Marghoub Shadkar 2016), Ultrasonic Leak Detection [ULD] data used with RCM was studied to detect airbrake leakages (Poddar 2014), and Failure Mode, Effect and Criticality Analysis [FMECA] used along with RCM was studied as an assessment method for estimating the Electronic Multiple Unit train [EMU] brake system optimal maintenance interval (Kim et al. 2009, 1185-1188). No studies were found that use RCM to estimate the lifetime of railcar airbrake gaskets, in fact, there are few studies that use reliability theory to estimate the lifetime of other elastomer product geometries, such as O-rings or flat gaskets (Shao and Kang 2014, 16-21). Gathering replacement frequency data of railcar airbrake gaskets could be the first step to apply reliability theory to railcar airbrake gaskets.

To estimate the lifetime of elastomer products, several techniques have been researched. The Arrhenius equation is used in some studies to correlate a property change with the permanent effects of temperature, estimating elastomeric material life based on a threshold (Zeng, Chen, and



Kang 2013, 1004-1008; Woo et al. 2010, 11-17). In one study, the lifetime of an engine cover gasket was estimated using the Arrhenius equation. To specify the equation parameters, the successive zooming genetic algorithm [SZGA] was used along with experimental recovery rate curves. The SZGA method showed good agreement between theory and experiment. The experimental data was obtained through highly accelerated life testing [HALT]. This method is generally used for predicting the lifetime of rubber materials for long periods. The Arrhenius equation parameters were computed and life miles at different temperatures and compression rates were calculated and compared. The study showed that engine cover gasket lifetime is reduced when either compression rate or temperature are increased, with gasket lifetime values ranging from  $880 \times 10^3$  to  $72 \times 10^3$  miles (Young-Doo et al. 2014).

Other studies use fracture mechanics to estimate crack growth rate using the initial crack dimension and the material strain energy density, or a mechanical constitutive model, or a combination of all these; with the objective to estimate an elastomeric material lifetime and its performance. Some studies further validate these techniques using computerized Finite Element Analysis [FEA]. The main procedure is, first find the hyper-elastic constitutive model parameters for an elastomer compound through experimental data, and then estimate the fatigue life through software. Some hyper-elastic constitutive models included in FEA software like ABAQUS or ANSYS are Mooney-Rivlin, Ogden-Yeoh, Neo-Hookean, Arruda-Boyce, Gent, and Van der Waals (Plummer 2014, 35-70; Hertzberg, Vinci, and Hertzberg 2012; Yeoh 2006, 75-89; Nabil, Ismail, and Azura 2013, 385-393; Warren 2012, 1).

Elastomeric material properties, lifetime prediction, and performance assessment are important in the design procedure to ensure reliable components. Studies show that elastomers stiffness and hardness increase at high temperatures and after long aging periods. In contrast, mechanical fatigue creates a progressive weakening of physical properties during dynamic loads presenting a gradual reduction in stiffness, and prolonged static loads cause stress relaxation and may result in time-depending cracking (Abraham, Alshuth, and Jerrams 2006, 59-73; Bauman 2008). Thus, the service environment is a major factor in assessing elastomeric products durability. Because hardness-stiffness, bulk modulus, and compressive modulus are frequently used as a quality control measure and comparison thresholds to assess rubber products performance, it is pertinent to review these concepts more in depth.

## 2.4 Hardness

Hardness is the measure of the resistance of a material against deformation through scratching or indentation under specified conditions. There are different types of hardness measures, each one comparing the load applied to form a depression on a material with a tip or indenter and another physical response. Vickers, Brinell, and Koop hardness compares the area of the imprint left by an indenter tip; Rockwell hardness compares the depth of an indenter impression; Shore hardness measures the rebound of the indenter; and Mohs hardness measures the “scratching ability” of a material in contact with another (Smith 1998, 7/3). Hardness test methods are individually standardized for specific materials, and they use different indenter geometries, load magnitude, loading time, and mode of application (Grellmann and Seidler 2013, 73-231). Hardness testing on plastics is done considering their behavior, ranging from rubber-elastic (elastomers), viscoelastic-plastic (thermoplastics) or mostly plastic (Dr Premamoy Ghosh 2011). Hardness is also a measure of the wear resistance of a material (Smith 1998, 7/3). On rubbers, it corresponds to a measure of stiffness from the indentation test (ISO 2015). For measuring hardness on rubbers or elastomers, three scales of hardness have been used: Shore, International Rubber Hardness Degrees [IRHD] and the British Standard [BS] (Brown 2006). Figure 16 shows an example of a range of hardness values for rubbers, thermoplastic elastomers [TPE] and plastics between the Shore A and Shore D hardness scales.

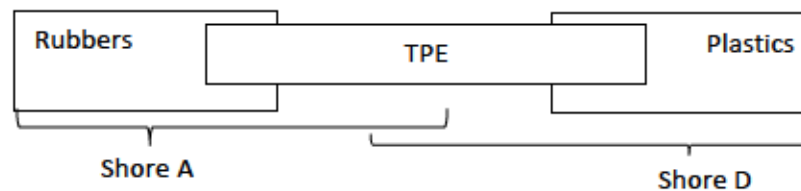


Figure 16 Hardness scale of rubbers, thermoplastic elastomers [TPE] and plastics (Dr Premamoy Ghosh 2011)

The mechanics behind the three types of hardness measurements for rubbers is based on the use of a load, either from a weight or a spring, pressing on a rigid indenter of defined geometry through the rubber and measuring the depth of the tip with a displacement transducer, usually a dial gauge. The indentation depth is taken relative to the top of the surface of the test piece or annular presser foot base, i.e. the annular foot is resting on top of the material (Brown 2006). A simplified explanation of the mechanics of a hardness test is shown on Figure 17.

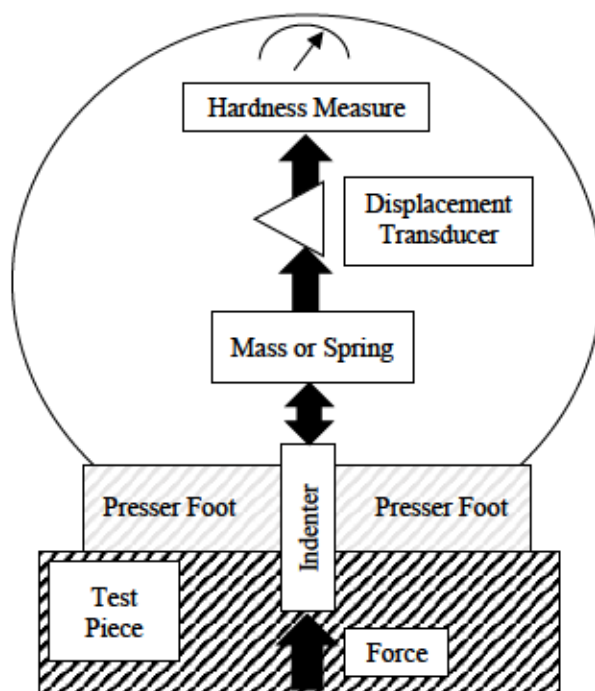


Figure 17 General mechanics of a hardness test

The most used standard testing methods for hardness measurement are from ASTM and ISO, with the following list of reference documents consulted for hardness measurement:

- ISO 18517 – Rubber, vulcanized or thermoplastic — Hardness testing — Introduction and guide (ISO 2015).
- ISO 48, Rubber, vulcanized or thermoplastic — Determination of hardness (hardness between 10 IRHD and 100 IRHD) (ISO 2010a).
- ISO 7619-1, Rubber, vulcanized or thermoplastic — Determination of indentation hardness — Part 1: Durometer method (Shore hardness) (ISO 2010b).
- ISO 7619-2, Rubber, vulcanized or thermoplastic — Determination of indentation hardness — Part 2: IRHD pocketmetremethod (ISO 2010c).
- ISO 18898, Rubber — Calibration and verification of hardness testers (ISO 2016).
- ASTM D2240 – Rubber Property—Durometer Hardness (ASTM 2015).

According to standard ISO 7619-1, the response to indentation on rubbers or elastomers is complex and depends on several factors (ISO 2010b):

- The elastic modulus of the rubber
- The viscoelastic features of the rubber
- The width of the test piece
- The form of the indenter tip
- The magnitude and rate of pressure applied
- The time at which hardness is logged

To measure hardness on elastomers, two distinct loading methods are used: a dead-load (weight) or a spring. The internationally accepted dead-load method is stated in ISO 48 and uses a ball indenter with hardness expressed in the IRHD scale, covering materials from 10 to 100 IRHD. The apparatus that uses a spring for hardness measurement is called a durometer (ISO 2015; Brown 2006).

#### 2.4.1 Durometer measurements

A durometer comprises an indenter connected to a preloaded spring that when compressed against a material surface yields a displacement along a standardized hardness scale from 0 to 100 (Brown 2006). The zero point on a durometer scale corresponds to no indenter displacement. Depending on how far the indenter depresses into the material, the reading increases. Soft elastomers give low hardness readings. The force resulting from the material rebound on the indenter,  $F_d$ , is given by the formula:

$$F_d = F_0 + kH \quad (16)$$

where  $F_0$  is the initial preload force on the spring,  $k$  is the spring constant, and  $H$  is the standardized hardness scale reading in units called degree of hardness. When the Shore scale is used, the letter of the type of durometer is indicated, i.e. A, D, AO, OO, etc.

The final indentation displacement  $d$  is given by:

$$d = p_0 - \zeta H \quad (17)$$

where,  $\zeta$  is the sensitivity of the spring in units of displacement per degree of hardness, and  $p_0$  is the initial indenter protruding position (Mix and Giacomini 2011).



The results of a durometer test can be expressed either in Shore or IRHD scales, having the ISO 7619 standard divided in two parts. Part 1 covers Shore scales A, D, AO and M, and Part 2 covers only the IRHD scale, but with four different methods; N for normal test, H for high-hardness test, L for low-hardness test, and M for microtest (ISO 2010b). Results expressed in the Shore scale have the letter of the type of durometer used and the hardness value; hence, there is Shore A 50 hardness, Shore D 50 hardness, and so on. It is worth noting that each Shore scale bears no direct relation to each other (Brown 2006). Standard ASTM D2240, lists twelve types of durometers: A, B, C, D, DO, E, M, O, OO, OOO, OOO-S, and R; with each type of durometer having a specific indenter tip geometry. ASTM D2240 methods apply to indentation hardness measurements of thermoplastic elastomers, vulcanized (thermoset) rubber, elastomeric materials, cellular materials, gel-like materials, and some plastics (ASTM 2015). Considering that the gaskets must be made of an elastomeric material with a Shore A hardness measure of  $80 \pm 5$ , in this work hardness measurements were done with a hand-held Shore A scale durometer, therefore ISO 7619-1 and ASTM D2240 are the most relevant reference documents. The Shore A durometer uses a truncated cone indenter tip geometry shown in Figure 18. Table 5 lists a Shore A durometer dimensions and characteristics (ASTM 2015; Mix and Giacomini 2011).

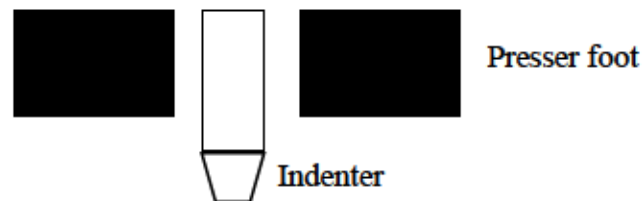


Figure 18 Representation of a Shore A durometer presser foot and indenter with truncated-cone tip shape

Table 5 Nominal values for a Shore A durometer with truncated-cone shape tip indenter

SYMBOL	DESCRIPTION	VALUE	UNIT
$p_0$	Initial indenter protrusion	$2.5 \pm 0.02$	mm
$F_0$	Initial compression spring force	0.55	N
$k$	Durometer spring constant	0.075	N/Degree-of-Hardness
$\zeta$	Spring sensitivity	0.0254	cm/Degree-of-Hardness

SYMBOL	DESCRIPTION	VALUE	UNIT
PF <sub>OD</sub>	Presser foot Outer Diameter	18 ±0.5	mm
PF <sub>ID</sub>	Presser foot Inner Diameter	3 ±0.1	mm
IN <sub>OD</sub>	Indenter Outer Diameter	1.25 ±0.15	mm
IN <sub>ID</sub>	Indenter Inner Diameter	0.79 ±0.01	mm
$\alpha$	Full angle of tip	35 ±0.25	Degrees
r	Radius of indenter, IN <sub>ID</sub> /2	0.395±0.1	mm

Standards ASTM D2240 and ISO 7619-1 indicate that durometer hardness measurements should be determined five times on the test pieces placed on a flat, hard, rigid surface such as tempered glass, and have all points of measurement 6.0 mm apart from each other (ASTM 2015; ISO 2010b). Also, if standard test pieces are used, the hardness readings are taken as “standard hardness”; otherwise if non-standard test pieces are used, they are taken as “apparent hardness”. This is due to the influence of test pieces thickness in hardness readings (Brown 2006; ISO 2015). Since the geometry tested in this work was that of finished gaskets, the results are expressed as “apparent hardness”. Finally, both standards indicate to report results with the date of the test, the relative humidity (when appropriate), ambient temperature; and durometer manufacturer, type, serial number, date of last calibration, and calibration due date (determined by the user based on frequency of use), as well as means of testing (hand-held or with a stand). Results should also include a description of the test specimen, its thickness, vulcanization date, hardness value obtained, and method of calculation (arithmetic mean or median) (ASTM 2015; ISO 2010b). In this work, Shore A hardness and hardness-compression modulus correlations were used.

#### 2.4.2 Compression modulus correlation with hardness

A number of models have been developed to relate hardness with modulus (Mix and Giacomini 2011; Oanea Fediuc et al. 2013, 157-166; Kunz and Studer 2006, 92-94). Mix and Giacomini Standardized Polymer Durometry relate the theory of Boussinesq of a defined boundary condition deformation, in this case, a Shore A durometer truncated-cone flat-tip (a circle), to basic linear elastic mechanics, having the following tip indentation correlation to modulus:

$$d = \frac{F_d(1-\nu^2)}{2Er} \quad (18)$$

Mix and Giacomini then present a new concept, called Mechanical Indentability, expressed as:

$$MI \equiv \frac{kp_0}{\zeta F_0} \quad (19)$$

Using the Shore A durometer values  $p_0=2.5\text{mm}$ ,  $F_0=0.55\text{N}$ ,  $k=0.075\frac{\text{N}}{\text{degree-of-hardness}}$ , and  $\zeta = 0.0254\frac{\text{mm}}{\text{degree-of-hardness}}$ ,  $MI = 13.64$ . Considering that a Shore A durometer has tip radius  $r=0.395\text{mm}$ , equations (16), (17), and (18) correlate dimensionless Young's modulus  $Y$ , with dimensionless hardness measurements  $H$ ,

$$Y = \frac{2rp_0E}{F_0(1-\nu^2)} = \frac{1+MIH}{1-H}, \quad (20)$$

where  $H$  is the durometer hardness measurement  $H$  divided by the full scale [0-100]. Considering elastomers as incompressible materials, Poisson ratio is  $\nu = 0.5$ . Young's modulus is thus calculated as:

$$E_1 \approx \frac{3F_0Y}{8p_0r} \quad (21)$$

Equation (22) is found in Fediuc's compression modulus study and in the ISO 7743 standard (Oanea Fediuc et al. 2013, 157-166; ISO 2017):

$$E_{C1} = E_1(1 + 2SF^2). \quad (22)$$

Putting dimensionless hardness values  $H$  and a  $MI = 13.64$  into equation (20) yields dimensionless Young's modulus values  $Y$ . Inputting these and the durometer nominal values into equation (21) yields Young's modulus  $E_1$ . Using Young's modulus  $E_1$  and shape factor  $SF$  values in equation (22) yields a correlation of compression modulus  $E_C$  with hardness  $H$ .

A second correlation is found using equation (23) directly with the Shore A hardness values  $H$  and each a component shape factor  $SF$ :

$$E_{C2} = \frac{H^{1.9}}{6700} \left( \frac{1+9SF^2}{1+4SF^2} + 2SF^2 \right), \quad (23)$$

where  $E_C$  is the compression modulus in ksi. The shape factor  $SF$  equation is:

$$SF = \frac{\text{loaded area}}{\text{force-free area}} = \frac{\pi(R^2-r^2)}{\pi(2R)h+\pi(2r)h} = \frac{(R^2-r^2)}{R2h}. \quad (24)$$

Standard ISO 7743 uses the force at 25% compression strain  $F_{25}$  for calculations. The experimental compression modulus for finished gaskets can be calculated using the ISO 7743 equation:

$$E_{Cexp} = \frac{F_{25}}{A\varepsilon_{25\%}} = \frac{F_{25}}{A_0(0.25)}. \quad (25)$$

## 2.5 Bulk modulus

Bulk modulus,  $B$ , of a material is a constant defined as the resistance to volume change when a compression load is applied, meaning, the ratio of uniform hydrostatic pressure,  $P$ , to volumetric change or strain,  $\epsilon_V = \Delta V/V_0$  (Shu, Takao, and Akbar 1994, 871-879; Halliday, Resnick, and Walker 2005). It is expressed as:

$$B = P/\epsilon_V = P(\Delta V/V_0) \quad (26)$$

Here,  $\Delta V$  is the absolute value in volume change, and  $V_0$  is the initial volume before compression. Volumetric strain is always positive in hydraulic compression. Since the final volume is lower than the initial one, the material shrinks. Elastomer seals are often under compressive loads, and so the bulk modulus of an elastomeric material is important for assessing mechanical performance.

No ASTM or ISO standard test method was found to obtain the bulk modulus of rubber or elastomers, but several papers suggest some compression techniques. Two studies, one by the Journal of Testing and Evaluation [JTEVA] (Fishman and Machmer 1994) and another from an elastomer seals manufacturer (Shu, Takao, and Akbar 1994, 871-879) include a simple confined compression test using a piston to determine a load-deflection curve and pressure-volume change, respectively.

To determine the bulk modulus at an infinitesimal strain, one technique plots the hydrostatic pressure against volumetric strain. Then, the pseudo-linear curve generated is extrapolated to a zero strain intersect (y-axis offset) and this hydrostatic pressure value is taken as the bulk modulus. In the present case, a change in thickness is assumed to be proportional to a change in volumetric strain, because glad-hand gaskets are constrained by the compression fixture in their outer radius and by the hydrostatic pressure of the air in their inner radius. Glad-hand gaskets only change in thickness while being compressed. Other linear dimensions (radii) remain constant.



### **3 Methodology**

In this section, the methodology used in this study to select and assess alternative materials for railcar airbrake glad-hand gaskets is presented. First, the considerations taken to design the test plan to assess gasket performance are described. Then, the process used to select the appropriate alternative materials is shown. Finally, the procedures followed to test the current and alternative materials selected as per the designed test plan are explained.

#### **3.1 Detailed test plan**

The railcar airbrake gasket environment, application, and industry specifications were considered for selecting the main variables to assess the gasket material performance. The main variables considered were:

- Geometry and linear dimensions
- Hardness low temperature response compared to room temperature one
- Compression stress-strain properties and stiffness
- Hardness and mass durability against the effect of liquids
- Leakage during separation

A set of tests to assess the gaskets material performance under laboratory conditions were selected based on input from standardized and non-standardized testing methods, as well as from the project sponsors. An alternative elastomeric material decision matrix was created based on weighted means for each material properties rank, assigning a higher weight to properties considered to be essential to outperform the current material used. Once the detailed test plan was decided, the tests selected were executed on gasket samples made of the current material. Afterwards, gaskets made from the alternative materials selected through the decision matrix were requested to be manufactured. Once the alternative material samples arrived, they were assessed with the same set of tests used for the current gasket material. Finally, a protocol for in-service hardness testing was designed, and a group replacement policy hypothetical numerical example was elaborated.

As per request of the project sponsors, the cold temperature to test the gaskets was  $-40^{\circ}\text{C}$ . This temperature was in the cryogenic range and was not easily reachable; therefore, there were few economical and safe options to achieve it. Some of the options researched included cooling baths with liquid nitrogen or dry ice, refrigerated rooms (laboratories or food storage) and specialty

freezers (i.e. healthcare freezers for vaccines or serum). The safer and economical option to achieve this temperature was a cool bath with isopropyl alcohol and water at 80% in volume, mixed with dry ice.

The measured properties and the equipment used are briefly described here and will be further explained in section □ Apparatus. Hardness was acquired with a handheld durometer. Compression stress and strain properties data was acquired with the data acquisition system of a Material Testing System machine equipped with specially designed gasket fixtures. Mass was measured with a high-precision analytical balance. Temperature was taken with a digital thermometer equipped with a thermocouple, and further verified with a thermal infrared camera. Linear dimensions were taken with a digital caliper and a dial micrometer. Leakage rate was measured with a third-party apparatus containing dial pressure gauges and flowmeters. All measurements were done at the University of Alberta Mechanical Engineering building, either at the mechanical shop or in an office-laboratory, where the temperature and humidity were controlled, and measured by the building gages or a generic portable one.

The following section lists the different tests selected. These tests are meant to assess the materials performance, as per the project objectives, as well as to verify the material compliance with industry standards and their use in service operation:

Table 6: List of Performance Tests done to the gasket samples and details for each one

TEST	TEMPERATURE	OBSERVATIONS
Hardness tests	Room temperature (20°C)	5-Shore A durometer measurement points and arithmetic mean
	Cold temperature (-40°C)	
Compression tests	Room temperature (20°C)	One gasket uniaxial compression. Compression stiffness at $\epsilon=25\%$
		Two gaskets uniaxial compression without air pressure (only current gaskets were tested) Compression stiffness at $\epsilon=25\%$
		Two gaskets uniaxial compression with air pressure. Bulk modulus and leakage.
	Cold temperature (-40°C)	One gasket compression set

Chemical compatibility tests	Room temperature (20°C)	CRC diesel airbrake antifreeze & conditioner
		Safe-t-brake airbrake antifreeze
	Increased temperature (50°C)	CRC diesel airbrake antifreeze & conditioner
		Safe-t-brake airbrake antifreeze

The ASTM and ISO standards, as well as other case studies, suggest the use of standard size and standard composition rubber samples (ASTM 2016; Fediuc Oanea et al. 2013, 157-166; ISO 2010b), but finished products, gaskets, were used instead. The procedures and guidelines presented in these documents were followed as closely as possible for each variable measured, but some deviations had to be taken. For example, since gaskets were used instead of standard samples, the minimum distance of 6.0 mm to take a hardness point measurement could not be followed as per ASTM D2240 and ISO 7619. Whenever deviations were taken in the tests, these were indicated in the results.

### 3.2 Elastomer selection

A crucial objective for this project, was to select alternative elastomeric materials candidates to study and test their durability in a laboratory setting. The tests result then would be used to compare and identify a suitable gasket material that would perform better in difficult operating conditions.

Several factors were considered when selecting the alternative materials. Low cost was one of them, since it was critical to stay in the price range of the elastomeric material options. Another consideration was environment temperature, as in winter, gaskets might freeze and lose their flexibility if the temperature was too low, thus, leading to a stiffer material behavior. In addition, during cold weather the gasket volume would decrease and a stiffer response might not be able to provide the required sealing; therefore, a soft rubber with low hardness value and high flexibility in cold weather would be the best option; the assumption was that selecting a compound with low glass transition temperature would have achieve these properties. Another important parameter was pressure, because gaskets would encounter around 90 psi of air pressure in their inner surfaces during operation. Moreover, as indicated by the project sponsors, gaskets would enter in contact with antifreeze products during cold weather. Then, the critical factors for selecting alternative materials were summarized as:



- Average low-price
- Material resilient to cold temperature ( $T_g \sim -40^\circ\text{C}$  or lower)
- Resistance to ozone and weathering (outdoor application)
- Resistance to chemical attack (antifreeze contact on winter)
- Resistance to air pressure (90 psi)

Figure 19 illustrates the set of rules followed to select material options:

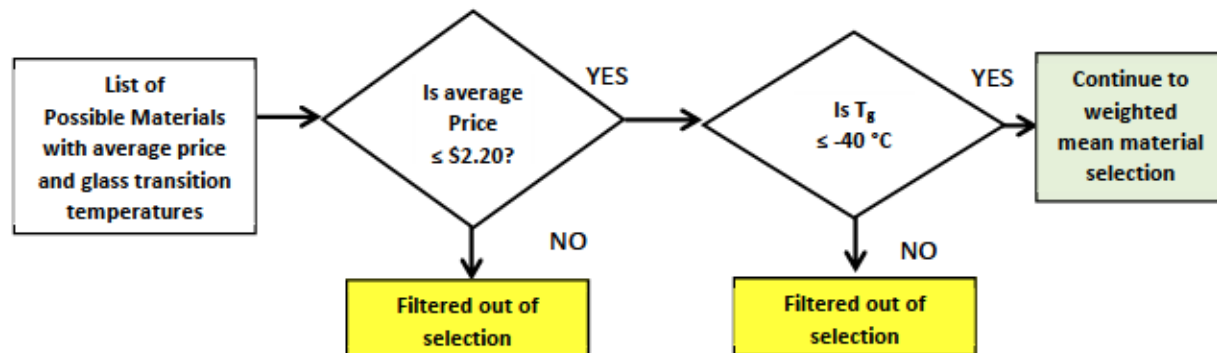


Figure 19 Filtering process for selecting the gasket alternative elastomeric options

Several elastomer options were selected from the information tables found in the literature review, having a list of 19 elastomer candidates. The first property used for filtering out candidates, was their average price (Table 7). From the 19 elastomer options selected, the median price was \$2.20, with Natural Rubber having the lowest price [\$0.45], and Silicone the highest one [\$19.00]. The low-price range of the elastomer options was selected due to economies of scale, since the gaskets are a component that is generally used in large quantities and selecting high-price materials would increase substantially the maintenance costs, even though they might have excellent performance on the required properties i.e. the elastomer price had to be less than or equal to \$2.20 for an elastomer option to continue in the selection process. Through this filtering, elastomer options 11 to 19 were taken out of the selection process.

Table 7 Elastomeric materials average price (Dick 2014). ASTM D1418 names were also included (ASTM 2017a)

No	ELASTOMER COMMON NAME	ASTM D1418 NAME	AVG. PRICE	≤ \$2.20
1	Natural rubber	NR	\$ 0.45	YES
2	Styrene butadiene	SBR	\$ 0.50	YES
3	Polybutadiene	BR	\$ 0.58	YES
4	Nitrile	NBR	\$ 1.00	YES



No	ELASTOMER COMMON NAME	ASTM D1418 NAME	AVG. PRICE	$\leq \$2.20$
5	Polyisoprene	IR	\$ 1.00	YES
6	Ethylene propylene diene	EPDM	\$ 1.10	YES
7	Isobutylene	IIR	\$ 1.26	YES
8	Chlorinated polyethylene	CM	\$ 1.80	YES
9	Polychloroprene	CR	\$ 1.95	YES
10	Chlorosulfonated polyethylene	CSM	\$ 2.20	YES
11	Polysulfide	T	\$ 2.50	NO
12	Polyester urethane	AU	\$ 3.50	NO
13	Polyether urethane	EU	\$ 3.50	NO
14	Ethylene acrylic	AEM	\$ 3.50	NO
15	Epichlorohydrin	ECO	\$ 6.00	NO
16	Polyacrylate	ACM	\$ 9.00	NO
17	Hydrogenated nitrile rubber	HNBR	\$ 10.00	NO
18	Fluorocarbon	FKM	\$ 13.00	NO
19	Silicone	MQ	\$ 19.00	NO

The next exclusion criterium was the glass transition temperature, where the minimum threshold was  $T_g \leq -40^\circ\text{C}$ ; this threshold was selected as per the project sponsors request, but it also relates to the lowest median ambient temperature recorded during winter in some areas of the railway routes throughout Canada (Government of Canada 2017).

Table 8 Elastomeric material options and their glass transition temperature (Brandrup et al. 1999; Gent 2012). ASTM D1418 names were also included (ASTM 2017a)

No	ELASTOMER COMMON NAME	ASTM D1418 NAME	GLASS TEMP $T_g$ [ $^\circ\text{C}$ ]	$T_g \leq -40^\circ\text{C}$
1	Natural rubber	NR	-72	YES
2	Styrene butadiene	SBR	-55	YES
3	Polybutadiene	BR	-100	YES
4	Nitrile	NBR	-29	NO
5	Polyisoprene	IR	-72	YES
6	Ethylene propylene diene	EPDM	-55	YES
7	Isobutylene	IIR	-72	YES
8	Chlorinated polyethylene	CM	-20	NO
9	Polychloroprene	CR	-45	YES
10	Chlorosulfonated polyethylene	CSM	-17	NO

With the glass transition temperature threshold, options 4, 8 and 10 were taken out of the selection process, having then 7 options of alternative elastomeric materials:

1. Polybutadiene	BR	5. Styrene butadiene	SBR
2. Isobutylene	IIR	6. Polychloroprene	CR
3. Polyisoprene	IR	7. Ethylene propylene diene	EPDM
4. Natural rubber	NR		

Some key properties considered for selecting a superior candidate material compared to the current one used were: Stress relaxation, compression set, alcohols and oils resistance, overall outdoor resistance, and resilience/rebound; hence, the corresponding properties have high weight factors. With the 7 options selected, a weighted mean decision matrix was then created, based on elastomer performance criteria found in the bibliography for each selected property. The performance criteria for each property were in the range of 1-5, where 1=poor, 2=fair, 3=good, 4=very good, 5=excellent, and can be seen in Table 10. To create the decision matrix, 16 properties were selected and a weight per each one was defined, the weight varies according to the level of importance, ranging from 4: critical, 3: mid-importance, 2: low-importance, and 1: non-important. The main factors were selected from the properties reviewed in section 2.1.3.

The weighted mean for each alternative material was calculated as:

$$\bar{w} = \frac{\frac{1}{n} \sum_{i=1}^n w_i x_i}{\frac{1}{n} \sum_{i=1}^n w_i} \quad (27)$$

Here, depending on the  $i$ th property,  $w_i$  and  $x_i$  were the corresponding weight factor and performance grade. Figure 20 summarizes the decision matrix selection procedure:

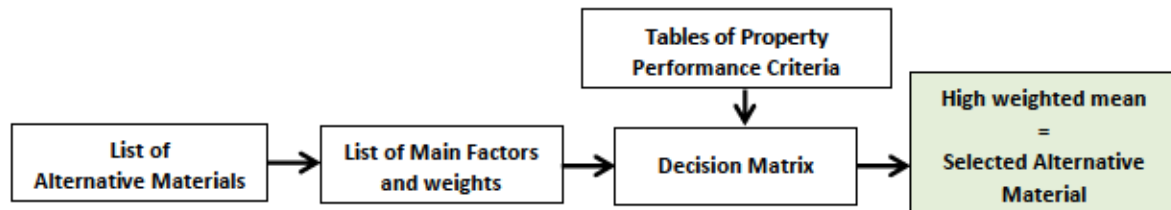


Figure 20 Procedure of material selection based on weighted mean

Table 9 Weight factors for 16 properties selected

No	MAIN FACTORS	$w$
1	Stress relaxation	4
2	Aging resistance	4
3	Weather resistance	4
4	Ozone resistance	4
5	Water resistance	4
6	Gas permeability	3
7	Tensile strength	1
8	Compression set	3

No	MAIN FACTORS	$w$
9	Resilience/Rebound	4
10	Tear resistance	2
11	Abrasion resistance	1
12	Electric properties	1
13	Adhesion to metals	3
14	Alcohols resistance	4
15	Oils resistance	4
16	Dynamic properties	1

Table 10 Weighted mean decision matrix for gasket alternative elastomeric material

Glass transition temp. $T_g$ [°C]		-100	-72	-72	-72	-55	-42	-55
Cost [\$]		0.58	1.26	1.00	0.45	0.50	1.95	1.10
Elastomer		BR	IIR	IR	NR	SBR	CR	EPDM
Main Factors – Weight								
Stress relaxation	4	4	2	4	5	4	3	2.5
Aging resistance	4	1	4	2	2	1	3	4
Weather resistance	4	2	5	1.5	1.5	2.5	4.5	5
Ozone resistance	4	1	5	1	1	1	5	4
Water resistance	4	5	4	5	5	4	2.5	5
Gas permeability	3	3	3	3	2.5	2	3	2.5
Compression set	3	2	4	5	5	3	2	2
Resilience/Rebound	4	3	2.5	5	4	3	3	3
Tear resistance	2	4	3	4	4	3.5	4	4
Abrasion resistance	1	5	2.5	5	5	5	5	4
Electric properties	1	0	5	5	4	5	4	4
Adhesion to metals	3	5	3	5	5	5	4.5	5
Alcohols resistance	4	3.5	4	3	3	3.5	3.5	4
Oils resistance	4	1	1	1	1	1	3	1
Dynamic properties	1	2.5	2	4	4	2.5	2	3.5
$\bar{w}$		2.77	3.38	3.28	3.23	2.82	3.42	3.52

If the property selected was considered important for the correct gasket performance, its weight factor value was bigger, in contrast to non-essential properties with low values; having the rank of properties as 1: non-essential, 2: low importance, 3: mid-importance, 4: important.

After the weighted mean calculations, the two alternative materials options were selected: Ethylene Propylene Diene elastomer (EPDM) and Chloroprene (CR). These two materials had the highest weighted mean according to the decision matrix, suggesting better performance than the current material used, considering the properties for the service application.

Table 11 summarizes some information about the selected elastomeric materials. Just considering weighted mean, price and  $T_g$ , EPDM appears to be a better option than CR.

Table 11: Properties of selected new gasket material

SELECTED ELASTOMERS	SUMMARY DESCRIPTION
Ethylene-propylene-diene rubber (EPDM)	Terpolymer of ethylene, propylene and diene monomers. It is a general-purpose material with excellent resistance to phosphate ester fluids, brake fluids, alcohols, weathering, aging, and ozone. Not suitable for petroleum-based fluids and fuels. It can be compounded for a wide range of temperature use (Mykin Inc 2017; Popa 2011; Gent 2012).
Chloroprene rubber (CR)	Monochlorinated butadiene polymer. Chloroprene commercial name is Neoprene®. It exhibits good resistance to oil, aging, refrigerants, and to chemical degradation. Excellent resistance to weather and ozone (oxidation). CR also has good mechanical properties over a wide temperature range, depending on the compound formula (Mykin Inc 2017; Popa 2011; Gent 2012).

### 3.3 Material testing

In this section, the tests performed on the gaskets are presented. First, general considerations that apply to all the tests performed are mentioned. After these general criteria, each test method is explained in detail. The tests include: Hardness test, compression tests, and chemical compatibility test.



### 3.3.1 General considerations

- Statistical principles

It was assumed that the experimental units, or test pieces (gaskets), were uniform, since each set of samples came from the same batch or provider. It was also assumed that each set of test pieces had the same vulcanization date, even if the precise date was unknown.

To estimate and control local experimental error variance, repeats were used. Measurement replications were performed as per each test method procedure (ASTM or ISO) for each corresponding property, and special care was taken to follow the techniques described as closely as possible to the descriptions depicted in each standardized test method. If deviations were taken, these were explicitly annotated in the corresponding test report. Additionally, local experimental error variance was further controlled through blocking and randomization. Blocking was done by dividing the three groups of samples in sets: current material, EPDM and Neoprene; and had all of them assessed with the exact same test plan. The sample size per each set was of  $N=30$ , and a label with the number 1 to 30 with the corresponding elastomer name was used where appropriate; the labels used were: “EPDM”, “Neo” and “Curr”. Random sample selection was done through MS Excel random function *rand()*, which pseudo-randomly generated 30 numbers. Afterwards, these were ranked from 1 to 30 with MS Excel function *rank()*; thus achieving true randomization. This process generates different permutations for testing (Kuehl 2000). Each permutation was followed to pick a sample. An example of a test unit selection permutation can be seen below:

Table 12 Example of a random permutation for selecting gasket samples

ID	RANDOM NUMBER	RANK	ID	RANDOM NUMBER	RANK	ID	RANDOM NUMBER	RANK
1	0.284	26	11	0.384	22	21	0.630	13
2	0.949	3	12	0.983	2	22	0.723	11
3	0.061	29	13	0.406	21	23	0.578	15
4	0.016	30	14	0.286	25	24	0.466	19
5	0.986	1	15	0.918	5	25	0.620	14
6	0.897	6	16	0.575	16	26	0.112	28
7	0.526	17	17	0.943	4	27	0.471	18
8	0.366	23	18	0.362	24	28	0.870	9
9	0.454	20	19	0.874	8	29	0.653	12
10	0.123	27	20	0.883	7	30	0.757	10

For this thesis, the arithmetic mean equation was used to express results,

$$\mu = \frac{1}{n} \sum_{i=1}^n x_i \quad (28)$$

as well as the Standard Deviation of a test piece set of measurements,

$$\sigma_s = \sqrt{\frac{1}{n-1} \sum_{i=1}^n (x_i - \mu)^2} \quad (29)$$

Both  $\mu$  and  $\sigma$  can have sub-indexes to indicate which corresponding measurement they refer to. For example,  $\mu_H$  was the mean of the  $H_i$  hardness measurements, having  $i = 1$  to 5 measurement points. Similarly, a test piece hardness measurement standard deviation was taken as  $\sigma_{SH}$

For hardness change and mass change mean comparisons, a paired t-test with a confidence interval of 95% was used. A paired t-test was used since the means were dependent i.e. before-and-after pair of measurements were done on the same unit. The data for the means was assumed to be continuous dependent and normally distributed. Normality was assessed through probability plots of the means difference. For compression set, stiffness and bulk modulus mean comparisons between different elastomeric materials, an independent t-test with a confidence interval of 95% was used. Statistical analysis was done through Minitab™ and MATLAB™ software.

- **Variables**

The following section enlists the variables of interest for every test performed. The variables being changed, or independent, are labeled as type *manipulated*. The dependent, or outcome, variables are named type *responding*. Finally, all variables that remain constant are specified as type *controlled*. For all tests, the gasket material was *controlled*. Three sets of 30 gasket samples per material were used: 30 Current material, 30 EPDM, and 30 CR. Gasket samples made of the current material were provided by CP through its Lambton mechanical shop in Edmonton. EPDM and CR gasket samples were requested to be manufactured by a third party, GEMMA Plastics Products Inc. The gasket dimensional geometry was also *controlled*, having two kinds: standard geometry (Current material) and simplified standard geometry (EPDM and CR). The standard geometry is a finished railroad airbrake gasket. The simplified standard geometry was designed

for this study and given to the third party for manufacturing purposes. The linear dimensions of the standard geometry gaskets provided by CP complied to the tolerances in specification M-602, AAR MSRP. It was requested to the third party that the alternative material gaskets simplified standard geometry dimensions were kept as close as possible to the AAR specifications, but due to the variability of the compression molding process and complexity of the standard geometry, discrepancies were found. A variation of 4.3% in thickness dimensions was found between the simplified geometry and the standard one, thus thickness in the simplified standard geometry samples did not comply with AAR specifications.



Figure 21 Gasket samples geometries cross-sections (a) Standard geometry (b) Simplified standard geometry

- Hardness Test

Table 13 Variables of interest for the hardness test

VARIABLE	TYPE	RANGE	COMMENTS
Temperature	Manipulated	Room Temperature $\sim 23 \pm 1^\circ\text{C}$	Room temperature provided by the university workshop facilities.
Humidity [50 %]		Cold temperature: $\sim -40 \pm 1^\circ\text{C}$	The gaskets were kept stored in an insulated container along with 15 lbs. of dry ice ( $-78^\circ\text{C}$ ) for 24 hours.
Load	Controlled	Manually	Following OEM indications, enough force was applied to make firm contact between the top surface and the presser foot to acquire a measurement
Gasket Hardness	Responding	Shore A 0 – 100	The apparatus used was a Shore A Härteprüfer Durometer (Gnehm Härtepruefe )

- Compression tests

- Stress-strain behavior, bulk modulus, and leakage

Table 14 Variables of interest for the compression stress-strain properties and bulk modulus tests

VARIABLE	TYPE	RANGE	COMMENTS
Temperature	Controlled	$\sim 23 \pm 1^\circ\text{C}$	Room temperature provided by the university workshop facilities.
Load	Responding	0 to $\sim 2000$ N	Load was applied with an MTS machine Model 810, then measured with a load cell Model 318, and logged with software.
Displacement [Stroke]	Manipulated	0 to $-3.00$ mm	Displacement was programmed as a controlled set-point of $-3.00$ mm to be reached by the MTS machine cross-head. The sign indicates compression direction.
Speed Rate	Controlled	10.00 mm/min and 0.01 mm/min	Speed was programmed as a RAMP of 10.00 mm/min for the stress-strain test, and of 0.01 mm/min for the Bulk/leak test
Sampling Frequency	Controlled	20 Hz	20 samples per second were programmed for the Data Acquisition (DAQ) software.
Pressure	Controlled	90 psi	Pressure was provided by the mechanical shop air supply

- Compression set at low temperature

Table 15 Variables of interest for the compression set at low temperature

VARIABLE	TYPE	RANGE	COMMENTS
Temperature	Manipulated	$\sim -40^\circ\text{C}$	The gaskets were compressed and stored in an insulated container along with a cool bath of dry ice and methanol for 2 hours.
Load	Controlled	Mechanical	Compression load applied with three C-clamps to depress and hold a test sample between two flat surfaces.
Displacement	Controlled	0.25 mm	Controlled through three 0.25 mm Dowell pins used as spacers.
Recovery period	Responding	30 sec and 30 min	Times when the test sample thickness was measured after the load release.
Thickness	Responding	0.345 in $\pm 5\%$	Thickness measurements were done using a dial micrometer with a flat presser foot. Current material gaskets were standard, whereas EPDM and CR were simplified.



- Chemical compatibility [effect of liquids]

Table 16 Variables of interest for the chemical compatibility [effect of liquids] test

VARIABLE	TYPE	RANGE	COMMENTS
Temperature	Manipulated	$\sim 23 \pm 1^\circ\text{C}$ $50 \pm 1^\circ\text{C}$	Room temperature provided by the university workshop facilities 50°C was maintained with a Water Bath.
Chemicals	Controlled	Methanol based [Boiling point: 64°C]	CRC® Diesel™ airbrake anti-freeze & conditioner (CRC Industries 2015) Kleen-flo airbrake antifreeze (Kleen-flo 2015)
Time	Responding	0 – 70 hrs	Immersion period option in ASTM D471 (ASTM 2016)
Mass	Responding	$\sim 8.000$ gr	Initial mass and its change was measured as per ASTM D471 (ASTM 2016)
Hardness	Responding	Shore A 0 – 100	Hardness was measured as per standard ASTM D2240 (ASTM 2015)

- Apparatus
  - Generic thermometer/hygrometer

Ambient temperature and humidity were measured through a generic brand digital thermometer and hygrometer during all tests.

- Dial micrometer

A dial micrometer was used to measure the thickness of the gaskets, as per indications in ASTM D3767 Standard practice for Rubber - Measurement of dimensions (ASTM 2014a). The Procedure followed was A, which encompasses thickness dimensions up to 30 mm using a dial micrometer with a flat circular presser foot, as shown below:



Figure 22 Dial micrometer with rigid metal base, stand, and flat presser foot used thickness measurements

- Durometer

The hardness measurements were done with a precision Shore A durometer, as shown below:



Figure 23 Gnehm Härteprüfer Shore A Durometer with a scale of 0 to 100.

Shore A durometers have a conical intender tip, and it is recommended for measuring hardness from soft rubbers, elastomers, natural rubber products, neoprene, resins, polyesters, soft PVC, leather, etc. (Gnehm Härteprüfe ). A set of rubber reference rings with known nominal Shore A Hardness values were used for calibration purposes.

- Digital Thermometer and Thermocouple.

Surface temperature was measured with an OMEGA HH506 digital thermometer, and a thermocouple type K enclosed in a surface probe case (Figure 24). The digital thermometer was previously calibrated by a technician following the Original Equipment Manufacturer [OEM] calibration manual. A thermocouple type K range is from  $-200^{\circ}\text{C}$  to  $1372^{\circ}\text{C}$  with a resolution of  $0.1^{\circ}\text{C}$ .



Figure 24 Digital thermometer, thermocouple type K and surface probe

- FLIR E60 Camera

Cold temperature was measured with a FLIR E50 infrared thermal imaging camera, to have a broader range of measurement points. With the camera, a temperature gradient along the surface of the gasket fixture, its surroundings, and the gasket itself were measured. Thermal imaging measurements were verified with the digital thermometer and thermocouple measurements.

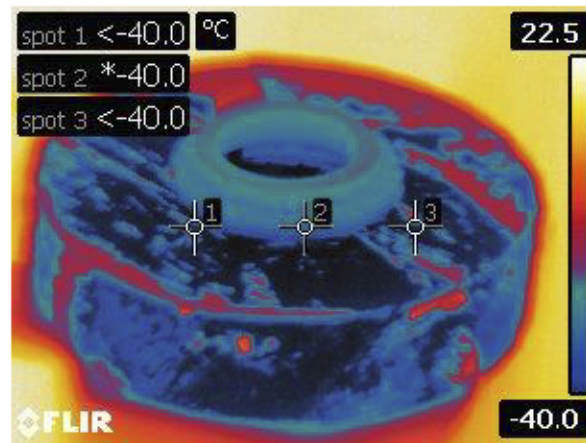


Figure 25 Thermal infrared camera picture of gasket fixture and gasket

- Material Testing System (MTS) machine

A model 810 MTS multipurpose servo hydraulic testing system for mechanical static and dynamic tests was used to perform the stress-strain compression properties and bulk modulus testing. The MTS crosshead was lowered with the hydraulic controls panel and stationed in the same position throughout all the tests sequence; this panel was also used to open and close the grips that held on the gasket fixtures. Manual control was performed to set the lower grip initial position before each automatic test using a cylindrical knob in the Human Machine Interface [HMI] panel, which can be seen in Figure 26. All automatic compression test sequences were programmed with the MTS proprietary software named TestWare®. The variables selected to be recorded in every test were: time in seconds [sec], load in Newtons [N], and crosshead displacement in millimeters [mm]; these were logged in a .txt file by the software at the end of each sequence. The variables were attained through a data acquisition (DAQ) card installed in the PC workstation and the appropriate transducers. The workstation internal clock monitored time, the load cell measured force, and the linear displacement transducer measured displacement.

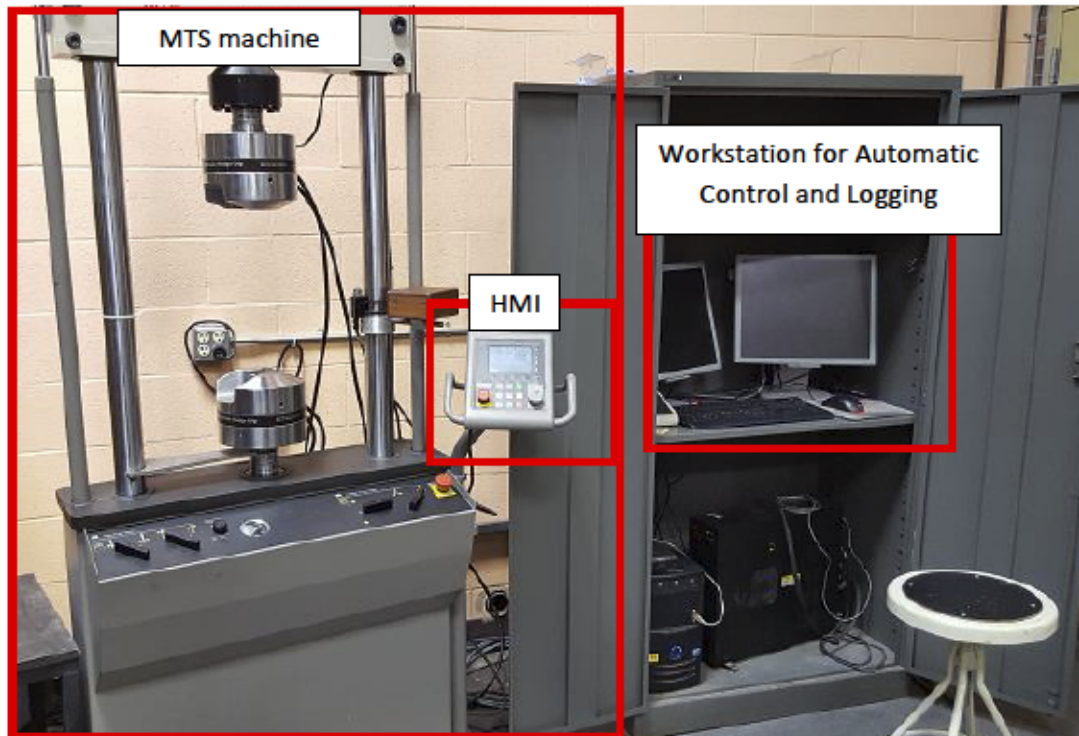


Figure 26 Model 810 MTS machine with HMI panel for manual stroke/displacement control and Workstation with DAQ and TestWare® Software for automatic control and logging

- Gasket Fixtures

Two sets of compression fixtures were designed and manufactured for the compression tests. The design in AutoCAD and the work requisition were done by Roya Vaghar. The first fixture was used to compress one gasket between two flat surfaces and the second fixture to compress two gaskets. The second set of fixtures has an inside a groove that mimics an Airbrake glad-hand. Also, one of the fixtures in the second set has a port for pressurizing the inside of the coupling, simulating a pressurized Airbrake. Both fixtures were designed to fit inside the MTS machine hydraulic grip system. Figure 27 shows the design draft for the first fixture and Figure 28 shows the second set:



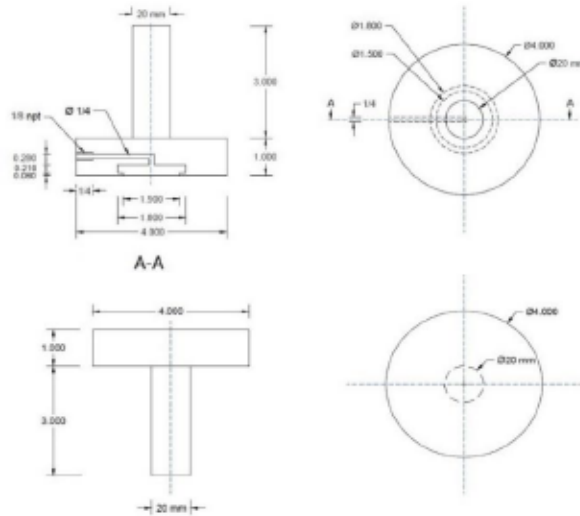


Figure 27 One gasket stress-strain compression properties fixture (Left) Lateral view (Right) Front view

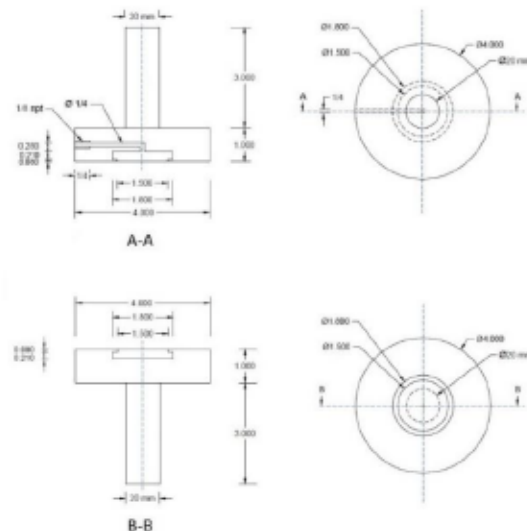


Figure 28 Two gaskets compression fixture for pressurized test (Bulk modulus and leakage) (Left) Lateral view (Right) Front view. Section A-A shows the air inlet port.

- Air-brake solution

Third-party proprietary equipment designed to provide leakage air flow readings within 0.2 liters-per-minute [LPM] in an air-pressurized system, allowing determination of the leak size and any remaining leakage if a repair was done. Air shop pressure must be connected on one side, and in the exit, it must be connected on the air system that wants to be evaluated for leakage i.e. airbrake. The equipment includes two pressure dial gages named TARGET and SYSTEM, as well as two flow meters marked as LO- FLOW & HI-FLOW; the TARGET pressure can be regulated with the front knob when air was connected to the equipment. When the lever was engaged in LOAD

position, the SYSTEM pressure will try to match the TARGET pressure. As the SYSTEM fills with air and the pressure reading gets close to the selected TARGET pressure, air flow will begin to slow down. When the SYSTEM pressure rises to approximately  $92 \pm 1$  psi, air flow was internally diverted to the air flow meters. When the air flow slows to 3LPM, the Hi-FlowmetreBall will begin to drop and a leakage measurement between 0 and 3LPM can be achieved. The LO-FLOWmetreranges from 0LPM to 0.2LPM, but a leak in this range was negligible.



Figure 29 Air-brake solution with air pressure gage dials and high-precision air flowmeters for leakage assessment



Figure 30 Airbrake solution transducers (Left) Pressure dial gages (Right) Ball indicator flowmeters

- Digital Caliper

The gaskets diameter dimensions were taken with a STM G711426 digital caliper (Figure 31). The caliper was factory calibrated and just needed zeroing at the beginning of each measurement.



Figure 31 Digital Caliper with LCD in inches scale

- Beakers

Two 200 ml and one 500 ml graded Pyrex™ glass beakers with rubber stoppers were used to store the chemicals and hang the gaskets for immersion (Figure 32). The stopper hook and gasket hanger were manually made from 316L stainless steel square wire, gauge 20.



Figure 32 Beaker (200 ml graded) with rubber stopper and hook, immersion fluid, gasket hanger, and three gaskets, properly labeled.

- Tapered weight bottle

A borosilicate glass weighing bottle for precision weighing was used for the post-immersion mass measurements, as per ASTM D471. Its dimensions were 60 mm in diameter and 30 mm in height.

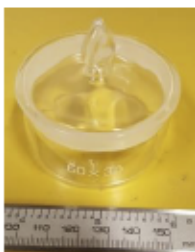


Figure 33 Borosilicate glass weighing bottle with lid. Dimensions were enough to fit the gaskets for weighing.

- Water Bath

PS (Precision Scientific Co) Thelco Model 81 water bath with temperature control dial capable of maintaining a stable water temperature up to 100°C. The power outlet was grounded, suitable for preventing fire hazards.



Figure 34 Water bath with power switch and temperature control dial. The temperature was raised to 50°C

- Water Cooled Reflux Condenser clamped to a rod and base

For immersion tests with volatile liquids at elevated temperature (50°C), a glass reflux condenser cooled down with water was used to condense and keep the evaporated volatile liquid inside of the beaker as per ASTM D471. The reflux condenser length was 500mm and its outside diameter 20mm, complying with ASTM D471. A 12V DC, submersible, brushless water pump was used to circulate water from a 2 L water container in and out the condenser. The water was replaced every 24 hrs with cold tap water (~18°C) to maintain condensation. The condenser was fixed to a support rod and stand with clamps.

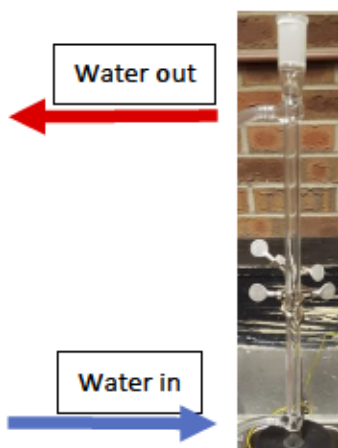


Figure 35 Support stand and clamp holding the reflux condenser. Polyvinyl hoses were attached to the condenser connecting the pump inside the 2L beaker creating the water flow circuit

- Analytical laboratory balance scale

A Sartorius 1207 MP2 high-precision scale was used to measure the gasket mass pre-immersion and post-immersion. The scale has a 0.0001 g resolution, complying with standard ASTM D471.





Figure 36 High precision digital weighing scale used for jewellery mass measurement. Its own autocalibration process was done before each measurement.

### 3.3.2 Hardness test

The objective of this test was to measure the hardness of a railcar airbrake gasket and to evaluate compliance with Specification M-602 of the American Association of Railroads Manual of Standards and Recommended Practices [AAR MSRP] at room temperature and when the gaskets were exposed to sub-zero temperatures. Specification M-602 states that gaskets shall attain a durometer reading of  $80 \pm 5$  and indicates that the gaskets shall be made of an elastomeric compound (AAR Publications 2002).

- **Room temperature**

Room temperature measurements were done in a clean, flat and stable work surface, positioning the gasket face with the protruding shoulder over the surface and its even face on top, as shown in Figure 37. The tip of the durometer was applied approximately 4 mm from the edge of the gasket, that is, the mid-point-radius between the outer radius and the inner radius. Five measurement points, 15.0 mm apart from each other, were defined clockwise along the gaskets mid-point-radius and performed as closely as possible the *manual (hand held) operation of durometer* procedure mentioned in ASTM D2240, ensuring consistent results.



Figure 37 Five measurement points example sequence done in a gasket sample

Table 17 Random permutations for the room temperature hardness test

ID	Points				
20	5	3	1	2	4
12	2	5	1	4	3
24	5	2	3	1	4
9	2	1	5	4	3
18	4	2	5	3	1
23	4	3	2	1	5
21	4	3	1	5	2
6	2	1	3	5	4

ID	Points				
22	3	5	4	1	2
2	2	5	4	1	3
25	4	3	5	2	1
14	4	1	5	3	2
27	4	5	2	3	1
1	1	5	3	2	4
7	2	1	4	3	5
16	3	1	2	5	4

ID	Points				
13	4	2	5	3	1
19	4	2	5	1	3
8	2	5	1	3	4
26	5	3	2	4	1
15	4	2	5	3	1
3	1	4	2	5	3
30	5	2	1	4	3
10	4	1	2	3	5

ID	Points				
5	2	1	4	3	5
28	5	1	3	4	2
11	3	4	1	5	2
4	1	2	3	4	5
29	4	5	2	1	3
17	3	5	4	1	2

Randomization was done to eliminate systematic error. Gasket sample and point measurement were randomly selected, having different permutations followed, shown in Table 17. The randomization process was the same as the one mentioned in section 3.3.1.

The hardness measurements were taken by pressing down with enough force the durometer against the gasket positioned over the work table and recording the dial measurement after 3 seconds; this delay gave enough time to attain a steady reading on the dial gage.

- **Cold temperature**

To reach the required cold temperature  $[-40^{\circ}\text{C}]$ , the 30 gasket samples and the compression test metallic gasket fixture were kept stored in an insulated container with 20 lbs of dry ice  $[-78^{\circ}\text{C}]$  up to 24 hours to perform this test; periodic checks of the temperature were done every 6 hours to verify if the desired temperature was achieved. When the desired cold temperature was attained  $[\sim -40^{\circ}\text{C}]$ , the frozen gasket fixture was pulled out, and the gasket samples hardness measurements were taken on the frozen, metallic compression test fixture surface, which was positioned between two wooden supports that worked as a base (Figure 38). The metallic fixture was also frozen to have the same surface temperature as the gasket, thus limiting the heat exchange and obtaining a cold work surface that would keep the gaskets at a low temperature for a longer time. After one point hardness measurement was performed, the sample selected was returned to the insulated enclosure, and another sample was then measures, allowing at least 15 minutes of “re-freezing” time between each sample hardness point measurements. For each measurement, a gasket was placed with its even face on top of the fixture, as shown in Figure 39. Then, the same procedure as with the room temperature hardness test was followed:

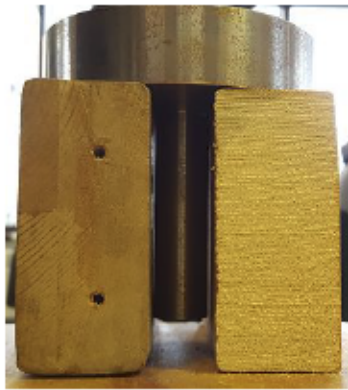


Figure 38 Metallic compression test fixture and wooden base for cold temperature hardness test

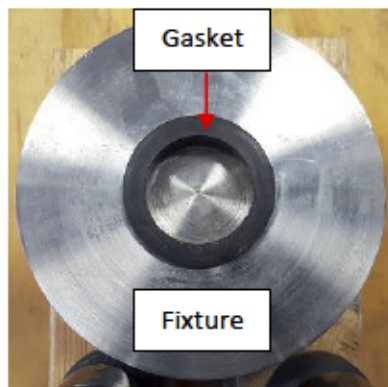


Figure 39 Five measurement points were done in each gasket

The measurements were taken pressing the durometer against the gasket over the metallic fixture, wooden base, and work table, with enough force, recording the dial gage value after 3 seconds; this delay gave enough time to attain a steady reading. Surface temperature was verified with the digital thermometer and surface thermocouple probe, and a triple point and gradient temperature were confirmed with the infrared thermal camera (Figure 25)

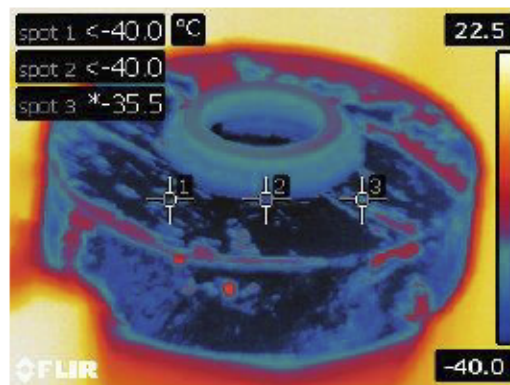


Figure 40 Thermal picture of the metallic fixture, wooden base, and gasket before a hardness measurement



Figure 41 Cold temperature hardness measurement using nitrile gloves

A verification of the durometer values was done with a set of rubber reference rings with known Shore A Hardness values, comparing the nominal and measured values. Measurements were taken before both room temperature and cold temperature tests were done.

A list of the rubber references rings and their Shore A Hardness nominal values can be seen in Table 18, as well as a perception scale created for better differentiation:

Table 18 Set of rubber samples with different known Shore A Hardness values

ID	Nominal Value [Shore A]	Hardness Perception	Shore A Hardness measurement					
			1	2	3	4	5	$\mu_H$
1	100	Hard	95	96	95	96	97	95.8
2	95	Hard	95	95	95	94	95	94.8
3	90	Mid-Hard	91	91	90	91	91	90.8
4	80	Mid-Hard	79	82	81	82	82	81.2
5	70	Medium-Soft	76	75	75	75	74	75.0
6	60	Medium-Soft	64	65	65	65	64	64.6
7	50	Soft	60	59	60	60	60	59.8
8	40	Soft	50	49	50	49	48	49.2
9	30	Soft	48	50	50	50	49	49.4

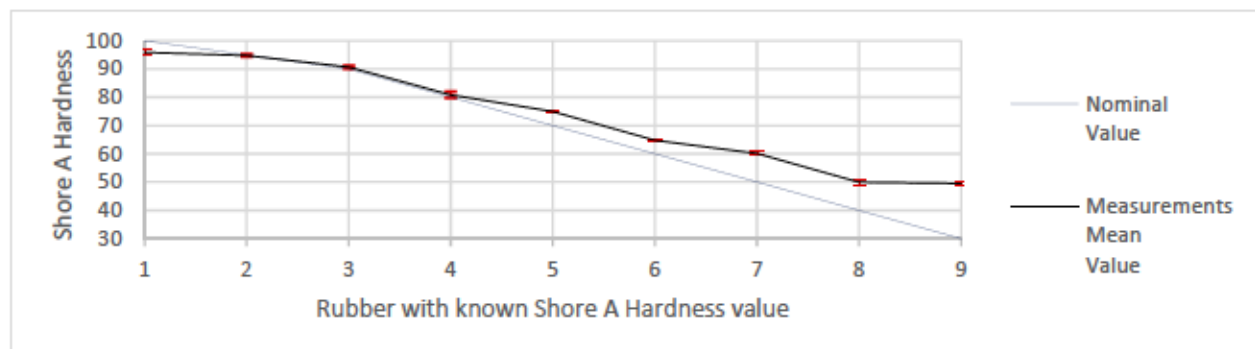


Figure 42 Shore A hardness values check with rubber rings of nominal hardness



Standard deviation and repeatability values were compared with the “within laboratory” or local domain values shown in standard ASTM D2240. Since all gaskets hardness standard deviations were within less than 1% error difference with the values from the standard, no outliers were found.

### **3.3.3 Compression tests**

The compression tests were done to evaluate stiffness, bulk modulus, and leakage of the airbrake gaskets at room temperature [ $\sim 20^{\circ}\text{C}$ ], as well as compression set at low temperature. Four different compression tests were performed: One gasket stress-strain compression properties test, two gaskets stress-strain compression properties test (only with the current material gasket), two gaskets pressurized with air and compressed; and one gasket compression set at low temperature.

To perform the pressurized tests, a modified version of the Compression Set [CS] test fixture shown in the American Association of Railroads Manual of Standards and Recommended Practices [AAR MSRP] Specification M-602 was used (AAR Publications 2002). The test procedure used, took as reference the techniques presented in the Technology Digest from the Transportation Technology Center [TTC] (Sammon and Anderson 2015). The leakage assessment in the pressurized test, took as reference the sealability determination test, method B, shown in ASTM F37 and Poddar’s thesis (Poddar 2014). For the one gasket compression test, method D from the ISO 7743 standard was followed.

The main objective of the compression tests was to assess the functionality of the gaskets, at room and cold temperature. With the stiffness values, a relationship between hardness could be done as well; in turn wear resistance of the gaskets material, allowing comparisons between the three materials: Current, EPDM, and CR. The overall aim was to assess a gasket durability, functionality and compliance with Specification M-602 (AAR Publications 2002).

- **Stress-strain compression properties**

To perform all the MTS machine compression tests, the following start-up sequence was followed:

1. Turn on the workstation and get the software ready (TestWare ®).
2. Turn on the hydraulic system through the software and check that the hydraulic pressure was under normal limits ( $\leq 15\text{ MPa}$ ).

3. Take the correct set of fixtures for the test to be done: flat fixtures for one gasket or grooved fixtures for two gaskets; and position the proper set inside the grips of the MTS machine and lock them in place with the hydraulic panel controls.
4. Depending on the type of test to be performed, the gasket or gaskets needed to be positioned in the following form:
  - a. One gasket: Lubricate with silicone oil the surface of the lower fixture and place one randomly selected gasket in the center of it. The upper fixture was the one with channels and threads to fit airline connections. These channels were left open to let air out when the gasket was being compressed.
  - b. Two gaskets: The test fixtures had grooves in them to hold in place one gasket each, mimicking the configuration seen in airbrake glad-hands. The fixture set to be the one in the upper grip was the one with channels and threads to fit airline connections, and on the lower grip, the fixture with only the groove for holding the gasket was used. A pair of gaskets were randomly selected, having the gasket with the highest identification number (the highest number possible was 30) placed on the upper fixture. The gaskets were pushed inside of the fixture grooves until properly set and then compressed. Pliers were used to change gaskets when done.
5. Lower the MTS crosshead to the lowest level possible with the hydraulic panel controls.
6. Activate the HMI panel and operate its knob for manual control of the lower grip vertical axial movement.
7. Bring the gasket-fixture or gasket-gasket surfaces to a pre-load of near 100 N.
8. Zero the load and displacement in the MTS software (TestWare®)
9. Set up the software with the Automatic Displacement sequence parameters. This only must be done once per test, as the same sequence was used for every gasket.

The first run of the MTS machine was a control run, where the flat fixtures faces were brought into contact and a load of -25000 N was applied; the negative sign indicates compression. While the compressive load was applied, the PID controls and resolution of the MTS machine were fine-tuned so that the measurements were as steady as possible; the data acquisition had a normal  $\pm 6$  N noise, as per OEM manual and experience. This first control run was programmed as follows:

- A. DAQ input check and setup (Sampling frequency: 20 Hz)
- B. Load phase (Type: Ramp, Rate: 10mm/min, Control: Load, End Level: -25000 N)
- C. Hold phase (Channel: Axial, Time to hold: 3.00 sec)
- D. Separation phase (Type: Ramp, Rate: 1mm/sec, End Level: 100.00 mm)

Upon having a steady load reading with the control run, the MTS machine was considered ready for performing the Compression tests.

- One Gasket

In this test, one gasket was compressed between the flat compression set fixtures. The MTS machine startup procedure was mentioned above. The automatic displacement sequence for this test consisted of the following phases:

- A. DAQ input check and setup (Sampling frequency: 20 Hz)
- B. Load phase (Rate: 10mm/min, Control: Stroke, End Level: -3.00 mm)
- C. Hold phase (Channel: Axial, Time to hold: 3.00 sec)
- D. Unload phase (Rate: 10mm/min, Control: Stroke, End Level: -3.00 mm)
- E. Repeat sequence points B, C, and D twice.
- F. Separation phase (Type: Ramp, Rate: 1mm/sec, End Level: 100.00 mm)

At the end of the sequence, the lower fixture and gasket were separated with the HMI manual knob control. Then, the current tested gasket was interchanged with another one and the process was repeated. Figure 43 depicts the one gasket compression test:



Figure 43 One gasket fixture automatic compression test

Table 19 shows a sample of the data taken for one gasket. The first two columns show the data points taken for both the Axial Load and the Axial Stroke, the third column shows the Time those measurements were taken. The last column shows the calculated stiffness for the corresponding values:

Table 19 One gasket compression test sample data

<b>Axial Load</b>	<b>Axial Stroke</b>	<b>Time</b>	<b>Stiffness</b>
<b>[N]</b>	<b>[mm]</b>	<b>[Sec]</b>	<b>[kN/m]</b>
-1.37	-0.16	2.04	8.33
-460.55	-1.25	15.03	369.58
-601.33	-1.73	20.83	347.65
-858.87	-3.00	36.12	285.90

Negative force and displacement values were changed to positive for better display the stress-strain curve. A compression stress-strain curve example (signs were inverted for better presentation) of one gasket made of the current material is shown below, the curve trend agrees with ISO 7743 examples and with other low-strain elastomer studies compression curves (Oanea Fediuc et al. 2013, 157-166; Yeoh 1987, 121-136). For the number of test pieces, three sets of three test pieces made from each different material (current material, EPDM, and CR) were tested, in compliance with ISO 7743 indications.



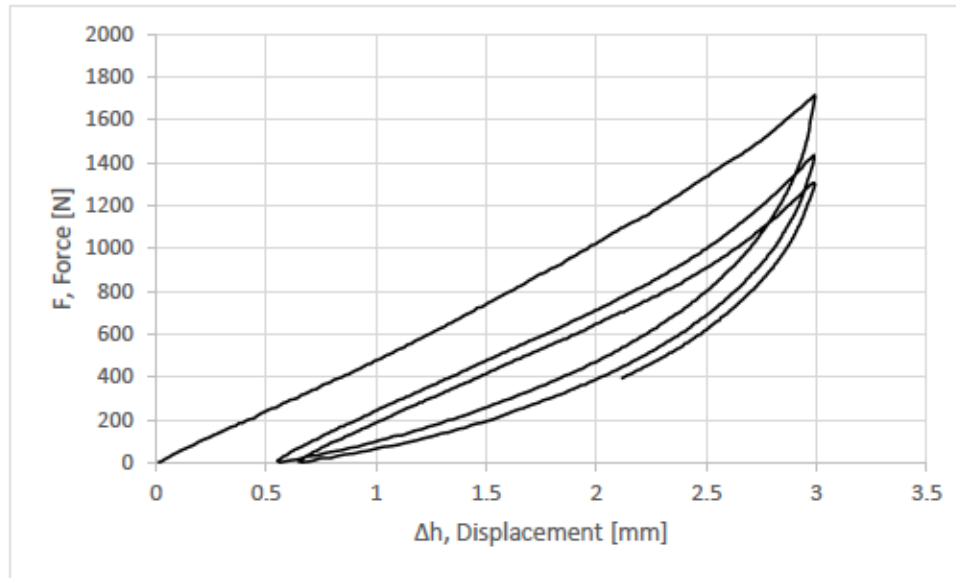


Figure 44 Stress-strain compression properties curve for a gasket made of the current material

- Two Gaskets – No air

For this test, a gasket was fitted into each of the two fixtures. The MTS start-up procedure was the same as mentioned above. This test did not show any substantial difference in comparison with the compression test done with one gasket; therefore, it was only performed with the current material gaskets and the general compression behavior was checked. This test did not reveal any relevant values, because adding a second gasket generates an apparent stiffness for both and having them in a radial constrained configuration the variables and setup were completely different; thus, not complying with standard ISO 7743 methods. The automatic sequence for this test was programmed as follows:

- DAQ input check and setup (Sampling frequency: 20 Hz)
- Load phase (Rate: 10mm/min, Control: Stroke, End Level: -2.00 mm)
- Hold phase (Channel: Axial, Time to hold: 3.00 sec)
- Unload phase (Rate: 10mm/min, Control: Stroke, End Level: -2.00 mm)
- Separation phase (Type: Ramp, Rate: 1mm/sec, End Level: 100.00 mm)

The compression displacement end level was changed to 2.00 mm, since the protruding height of the gaskets did not allow for any higher end level to be reached. After the sequence, the gaskets

were interchanged, and the same process was applied to other gasket pair, having three runs. Figure 45 shows an example of the two-gasket compression test:



Figure 45 Two gaskets compression test configuration

A test data sample can be seen on Table 20.

Table 20 Two gaskets compression test sample data

Axial Load	Axial Stroke	Time	Stiffness
[N]	[mm]	[Sec]	[kN/m]
-1.83	-0.02	0.14	101.47
-100.97	-0.42	4.93	242.96
-401.47	-1.42	16.92	283.68
-755.50	-2.01	24.07	376.16

Negative force and displacement values were changed to positive for better representation. Only three pairs of gaskets made from the current material were used as test pieces. One gasket pair Force-Displacement curve can be seen below:

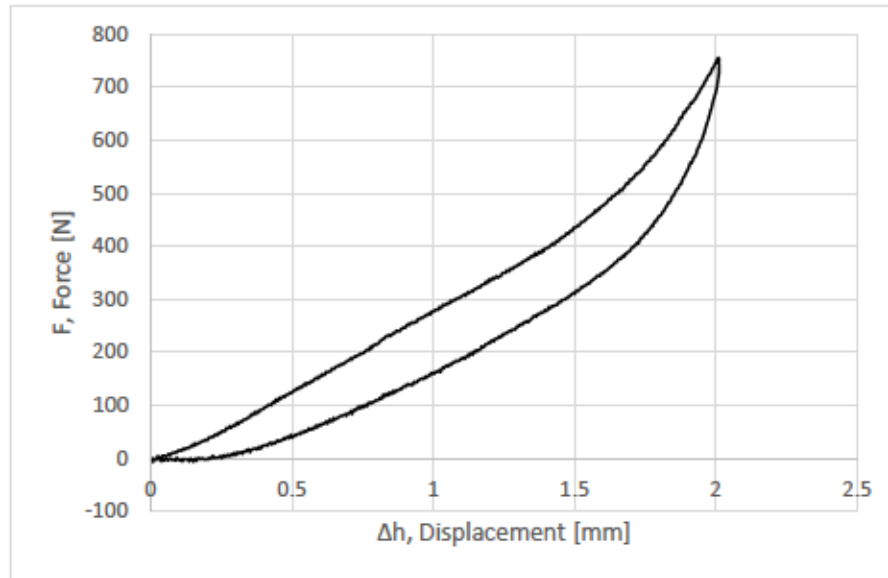


Figure 46 Force-displacement curve of the two gaskets compression test – with no air (Inverted values). The sign was inverted for better representation.

- Two Gaskets with Pressure

This test follows the same principle as the two-gasket test without pressure, the key variable was the pressurization of the system by means of the shop air supply up to 90 psi. A general schematic of the test arrangement can be seen below:

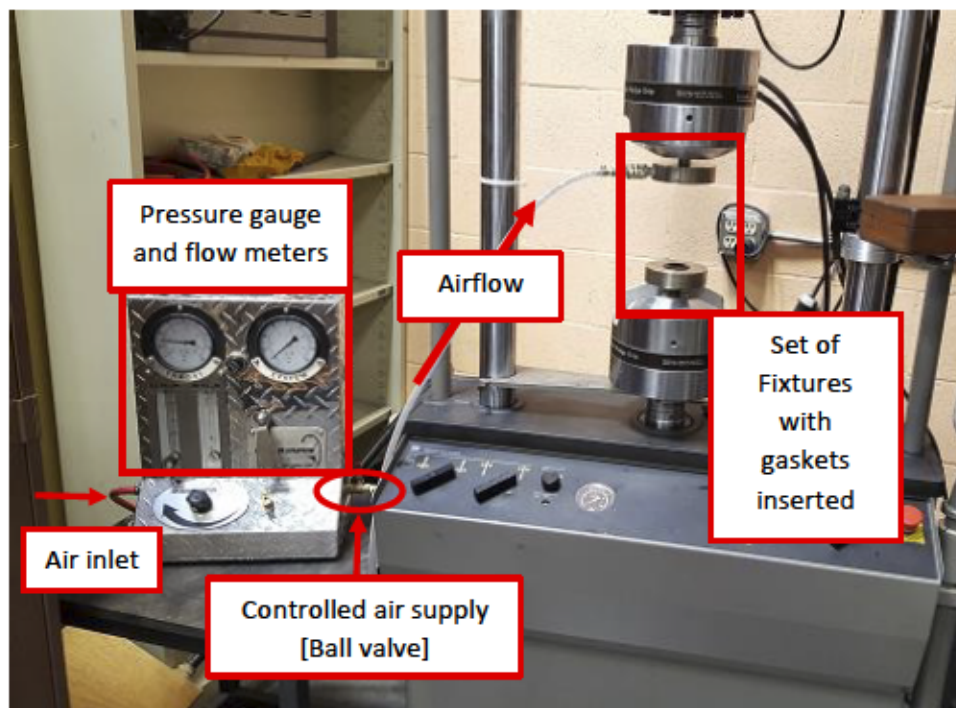


Figure 47 Test arrangement for the pressurized Two Gasket Compression Test

The automatic sequence for the first run of this test was as follows:

- A. DAQ input check and setup (Sampling frequency: 20 Hz)
- B. Preload (Time to reach value: 1 sec, Control: Load, End Level: -50.00 N)
- C. Set-up (Channel: Axial, Time to hold: 20.00 sec).
- D. Load phase (Rate: 10mm/min, Control: Stroke, End Level: -2.00 mm)
- E. Hold phase (Channel: Axial, Time to hold: 1.00 sec)
- F. Separation (Time to reach value: 5 sec, Control: Stroke, End Level: 100.00 mm)

The Preload phase was done to ensure a tight seal between the two gaskets before applying air. The “set-up” phase was a Hold stage of 20 seconds, which allowed time to open the ball valve and let the air go into the depressed fixture-gaskets arrangement.

The programmed time-force and time-displacement curves can be seen in Figure 48 and Figure 49 respectively:

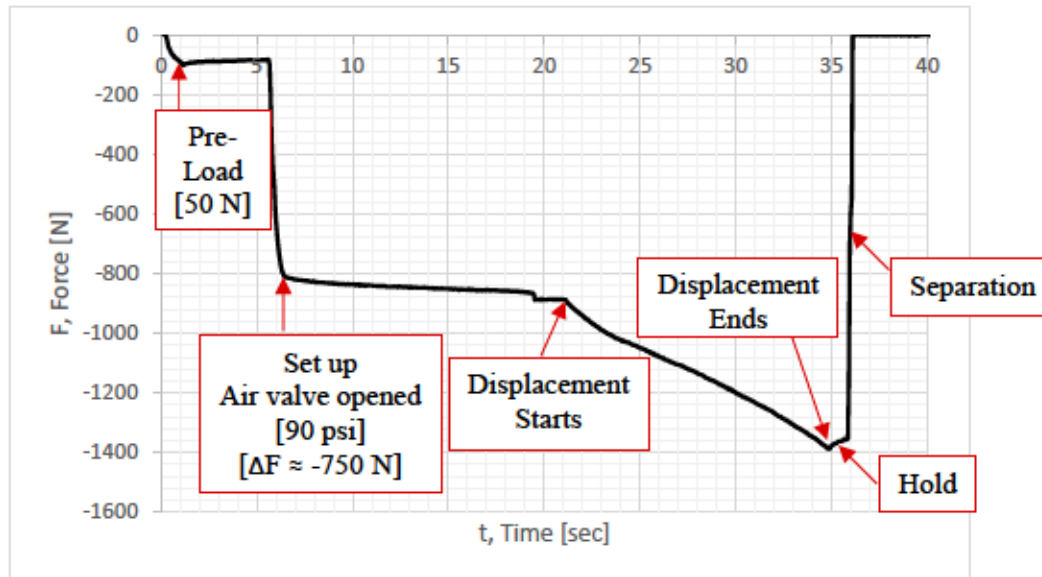


Figure 48 Time-force curve. The different phases of the automatic sequence are indicated



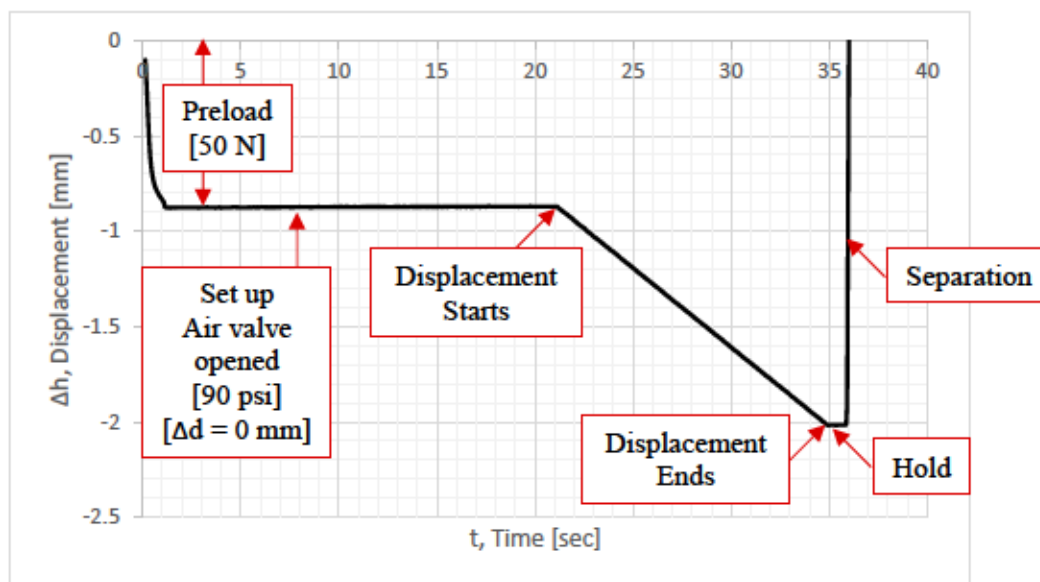


Figure 49 Time-displacement curve. The different phases of the automatic sequence are indicated

The test starts at zero force and displacement. Then, the Preload sequence was initiated, followed by the Set-up phase. During the Set-up phase, the air supply was opened and an additional compression force of -750 N was sensed by the load cell, but the displacement remains stable until the increased displacement ramp starts. After the displacement ends, there was a Hold phase, and at the end of the sequence, the fixture-gaskets arrangement was automatically separated.

Because there was no change in displacement when the air supply was engaged, this indicated that there was no relevant information provided for the stiffness calculation, all succeeding tests were performed only logging the displacement change after the air was engaged.

The air pressurized compression test data sample can be seen on Table 21. The stiffness was calculated by subtracting the -750 N offset of the air pressure to the Axial load. The stiffness value of 314.23 kN/m was similar to the one found in the other two tests (Table 19 and Table 20), having 376 kN/m at 2.00 mm for the two gaskets with no air test, and 347 kN/m at 1.73 mm for the one gasket test.

Table 21 Two gaskets pressurized compression test sample data

Axial Load	Axial Stroke	Time	Stiffness
[N]	[mm]	[Sec]	[kN/m]
-829.78	-0.68	0.10	117.57
-1100.01	-1.32	7.80	265.34

Axial Load	Axial Stroke	Time	Stiffness
-1304.98	-1.85	14.14	300.49
-1380.12	-2.01	16.04	314.23

Negative force and displacement values were changed to positive for better representation. Three test pieces were tested as per ISO 7743 indications on the number of test pieces. The Force-Displacement curve can be seen below:

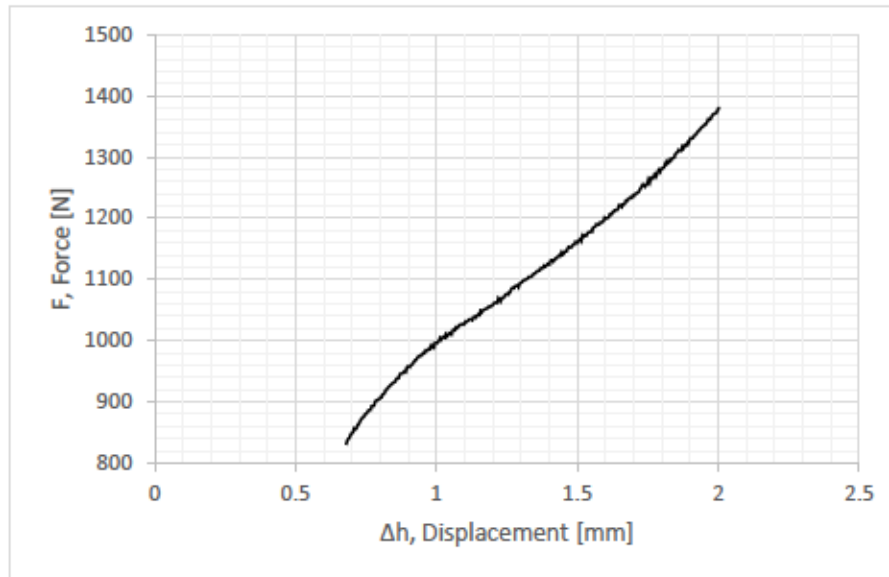


Figure 50 Force-displacement curve of the two gaskets compression test with air pressure (Inverted values). The sign was inverted for better representation.

The MTS machine had an error of  $\pm 10$  N, having a yearly calibration schedule performed by the Mechanical Engineering workshop technicians to ensure correct functionality and precision.

Standard deviation and repeatability values were compared with the “within laboratory” or local domain values shown in standard ISO 7743. Since all gaskets compressive stiffness at 25% strain standard deviations were within less than 1% error difference with the values from the standard, no outliers were found.

- **Compression set at low temperature**

This test was performed to verify the effects of cold temperature in the current and alternative materials, validating that this condition might prevent them to recover from their original shape after being held under a constant compressive load. When elastomers were compressed, physical or chemical changes can occur that modify the elastomers ability to return to its original shape

once the load was released, developing a set or offset from its original dimension. The degree of this set depends on the length of time, the load value and the temperature while compressed, as well as the same conditions once the load was released (recovery time). At low temperatures, changes resulting from glass hardening or crystallization become predominant in elastomers (ISO 2014); therefore, crystallization and material changes due to compression were thought to be the main reason of increased leakages in airbrake glad-hand gaskets during cold weather. The method to verify this, was standard ISO 815-2 *Rubber, vulcanized or thermoplastic — Determination of compression set — Part 2: At low temperatures* (ISO 2014)

The main considerations taken when using the apparatus for this test were:

- Three C-clamps spaced about 50 mm and 120° apart were used to keep the compression constant
- Three ¼" dowel pins were used as spacers between the two plates
- One sample instead of three was used per test run

The procedure followed for the compression set test was as follows:

1. First, the original thickness  $h_0$  of all specimens (current material, EDPM and Neoprene gaskets) were measured. Three specimens per each material were used, and three thickness measurements were done per each. The average thickness for the current material, EDPM and Neoprene were 0.381", 0.318" and 0.332" respectively. The specimens thickness was higher than the dowel pins average thickness of  $h_s=0.256"$ , allowing the gaskets to be compressed and the set to be measured.
2. After their original thickness was measured, one by one the specimens were tested following the same routine:
  - a. One gasket was positioned on the lower metallic plate center
  - b. Three dowel pins were positioned on the lower metallic plate about 20 mm away from the gasket, spaced around 50 mm and 120°C apart from each.
  - c. The upper plate was positioned on top of the gasket and the dowel pins, making sure to be concentric with the lower metallic plate.

- d. The three c-clamps were opened and placed as to compress both metallic plates. The c-clamps were loosely tightened around 50 mm and 120°C apart from each, trying to set them above the dowel pins.
- e. Once the configuration was stable, the c-clamps were hard tightened to compress the gasket until the upper and lower plates were touching the dowel pins. The load was thought stable when the dowel pins did not move or slip.
- f. The compression set device then was kept at -40°C in a dry ice and methanol cool bath for 3 hrs (This was a deviation to the 24 hrs noted on ISO 815-2 standard)
- g. 30 minutes before to the completion of the 3 hrs, the dial micrometer was kept at the same low temperature as the compression set device for conditioning. When the 3 hrs were completed, the compression set device and the dial micrometer were taken out. Then, the c-clamps were untightened, and the thickness of the gasket was measured around 10 minutes after release  $h_{t10}$  and then again after 30 minutes  $h_{t30}$ . The dial micrometer and the specimen were kept inside the low temperature cabinet between  $t_{10}$  and  $t_{30}$ .
- h. The compression set, expressed as a percentage of the initial compression, was given by equation (8) for  $t=10$  sec and  $t=30$  min:

$$\frac{h_0 - h_{t10}}{h_0 - h_s} \times 100 \qquad \frac{h_0 - h_{t30}}{h_0 - h_s} \times 100$$

- i.  $h_0$  was the initial thickness of the test piece, in millimetres.
- j.  $h_{t10}$  and  $h_{t30}$  were the thicknesses of the test piece after each recovery time, 10 seconds and 30 minutes respectively, in millimetres.
- k.  $h_s$  was the height of the dowel pins, in millimetres.
- l. The compression set measurement was repeated three times for averaging purposes.

- **Bulk modulus test**

The pressurized gasket test was also used to calculate an estimated bulk modulus, since the outer radius of the gaskets was constrained by the gasket fixtures and the inner radius was constrained by the air pressure; thus, a change in thickness was assumed to be proportional to a change in



volumetric strain i.e. the only dimensional change was in thickness while the gaskets were compressed and all other linear dimensions were assumed to remain constant.

Dividing the normal compressive force  $F_N$  and  $A_0$ , the hydrostatic pressure was assumed to be the same as the compressive stress,  $P = \sigma_N$ , having the normal force as the value acquired by the load cell and the area was assumed to be that of a ring geometry:

$$A_0 = \pi(R^2 - r^2) \quad (30)$$

Where  $R$  was the outer radius of the gaskets and  $r$  was the inner one; taken from the middle height of the gasket, corresponding to a cylindrical shape.

After calculating  $P$  and  $\epsilon_v$ , the pseudo-linear Pressure-volumetric strain curve was generated, and the extrapolation of the linear regression curve to a zero strain intersect i.e. y-axis offset value, was taken as the material bulk modulus. An example of this estimation can be seen below, having a bulk modulus of 2.275 MPa:

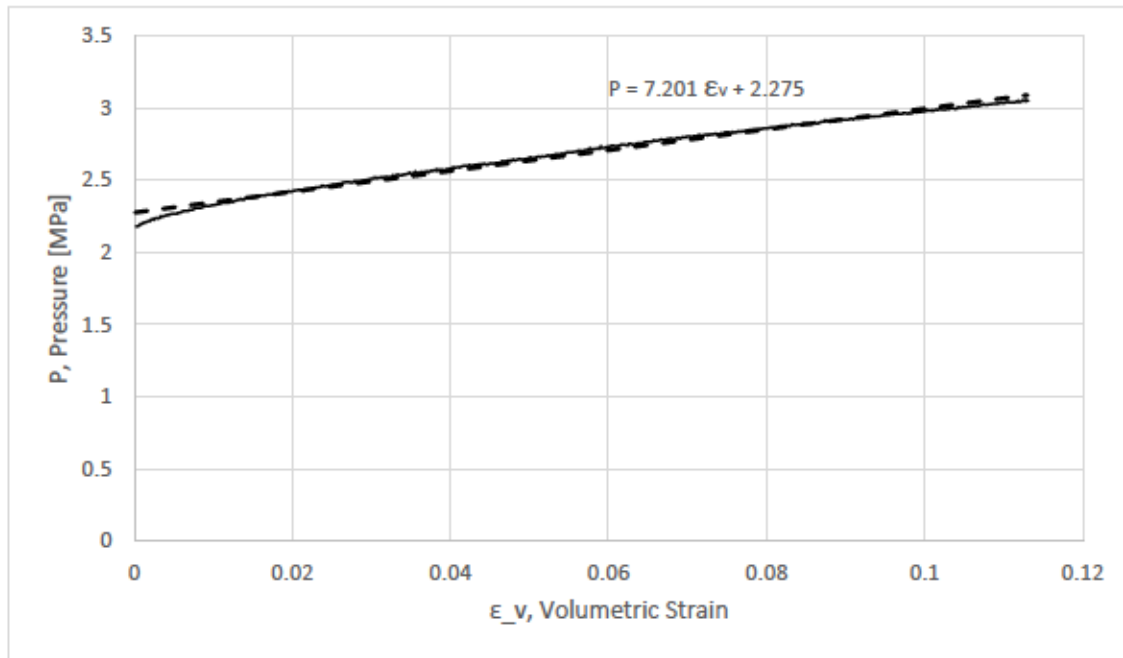


Figure 51 Hydrostatic pressure-volumetric strain curve with linear regression for apparent bulk modulus estimation

Estimating the bulk modulus with this method had a considerable difference (x1000) with the values found in the literature, therefore it was not further pursued as a comparison parameter between the elastomeric materials.

- **Leakage test**

The bulk modulus was calculated with the force-displacement data during the loading phase of the compression test with air, whereas in the leakage test, the focus turns to the unloading phase. Any abrupt change in the resultant force measured seen in the force-displacement curve during separation was taken as an indication of leakage; and major leakage was certain, when full separation (zero force) appeared. Thus, the time at which these changes in resultant force appeared was used to compare sealability of the three different material gaskets. During the unloading phase, an abrupt change in the resultant force was considered as an indication of leak, although in several occasions, the force was recovered after a short amount of time, even when the gasket fixtures kept on separating. When zero force happened, this event agreed with the Airbrake Solution flowmetre indication of a major leak ( $\geq 3.0$  LMP) i.e. the HI-FLOW flowmeter ball raised abruptly.

An example of the comparison between the separation behavior of the three gasket materials can be seen in Figure 52. In this comparison, CR was the first material to indicate leakage, but it then was restored after a brief period. In contrast, EPDM was the first material to present complete separation (major leakage) during the separation sequence:

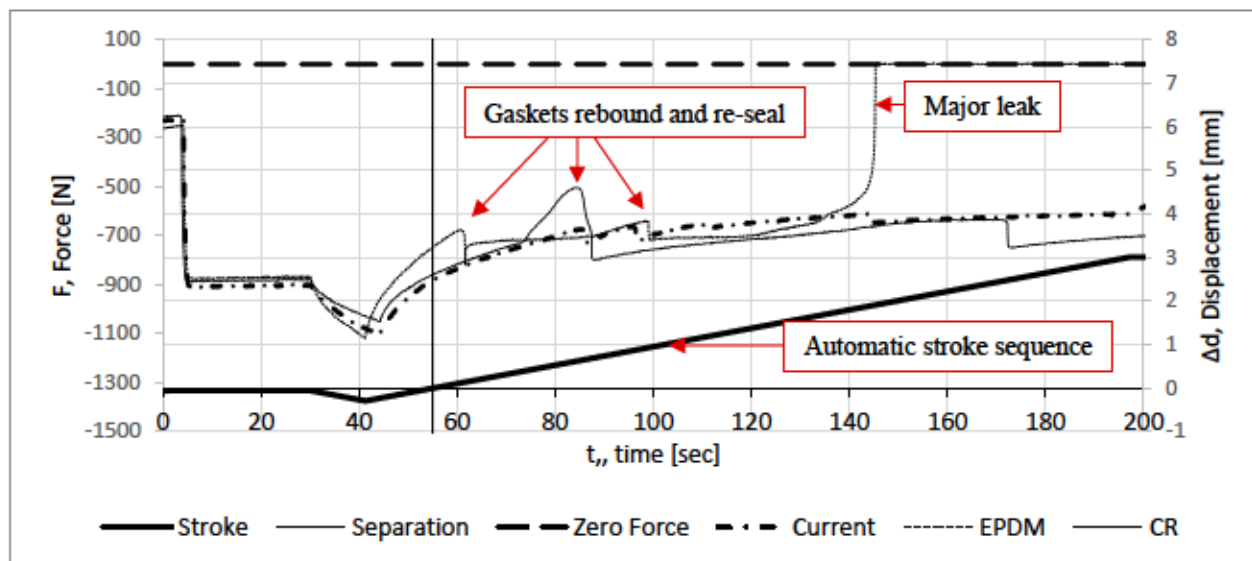


Figure 52 Separation-leakage behavior of three gasket materials. Zero force indicates major leakage

### 3.3.4 Chemical compatibility test

For this test, the standard test method ASTM D471 Standard Rubber Property—Effect of Liquids (ASTM 2016) was followed, with the main deviation that the test specimens were final products (gaskets), instead of standard test pieces (sheets, dumbbells, or product pieces). Two liquids were used in the tests: airbrake anti-freeze & conditioner manufactured by CRC® Diesel™ and kleen-flo safe-t-brake airbrake antifreeze. These chemicals were used as per the project sponsors recommendation, because of the high probability that they could get in contact with the gaskets during winter operational conditions, as these chemicals are occasionally used in winter time to remedy icing in the airbrake lines of railroad freight cars.

The objective of the Chemical Compatibility Test was to assess the durability in service of the gaskets when they encounter the before mentioned chemicals, measuring any change in mass and in hardness as per ASTM D471; hardness was evaluated post-immersion as per ASTM D2240 (ASTM 2016; ASTM 2015). Moreover, mass change and hardness change values before immersion were compared against the ones afterwards to evaluate the gasket compliance with AAR Specification M-602 and their chemical compatibility (AAR Publications 2002).

The commercial names of the fluids used in the test were Airbrake Anti-Freeze & Conditioner and safe-t-brake airbrake antifreeze (Figure 53). These fluids were Methanol based, with a boiling point of 64°C as indicated in their MSDS (CRC Industries 2015; Kleen-flo 2015).



Figure 53 Original bottle presentation of the test fluids

All MSDS considerations for safe handling, manipulation, and storage were followed. These considerations can be summarized as follows (CRC Industries 2015; Kleen-flo 2015):

- Safety Considerations
  - ignition under almost all normal temperature conditions.
  - Means of Extinguishing in the room: Carbon dioxide, Dry chemical media for small fire.
  - Hazardous combustion by-products: Fumes, smokes, oxides of carbon & formaldehyde.
  - Use of grounded equipment.
  - Use of mechanical means, such as a fume hood, if necessary to maintain vapor levels below the exposure guidelines.
- Personal Protective Equipment to be used for safe handling:
  - Gloves: Butyl Rubber, Nitrile, Chemical resistant gloves
  - Respiratory: Not needed

Because of these safety considerations, the test setup was performed in a well-ventilated area, with a CO2 extinguisher nearby, and the chemicals were handled with nitrile gloves and safety glasses..

Due to the volatility of the chemicals and the fire hazard considerations regarding them, a brief Risk Assessment was performed to decide on the maximum allowable temperature to test the chemicals with minimum additional equipment. A summary of the properties considered for selecting the test temperature are:

Table 22 Fire hazard properties of chemicals. Boiling point and flash point temperatures taken from MSDS

Liquids used	Base Component	Boiling Point [°C]	Flash Point [°C]
Kleen-flo	Methanol 60-100% by wt	64.5	11.5
CRC Airbrake conditioner	Methanol >99% by wt	64.5	12

Taken into consideration Methanol's boiling temperature, flash point, and the test temperature ranges suggested in ASTM D471, a risk matrix was developed (Table 23). Three test temperatures were selected from the ASTM D471 tables along the water bath temperature scale.



Table 23 Fire Hazard Risk Matrix for the chemicals used. Maximum allowed temperatures were highlighted in green

Temperature Range ASTM D471 [°C] $\pm 2$ °C	Note	Probability	Consequence*	Risk
23	< Boiling Point > Flash Point	30%	2	0.6
50	< Boiling Point > Flash Point	60%	2	1.2
100	> Boiling Point > Flash Point	80%	5	4

\*Consequence was related to fire, explosion, or another hazard being present, where 1=not present and 5=present.

All scenarios with a risk lower  $\leq 2$  do not need added precautions, just to follow regular MSDS recommendations for safe handling and fire prevention. Thus, temperatures of 100°C and above were best to be avoided, because of the elevated risk this condition presents. This assumption was made based on the test liquids boiling and flash point, as well as the boiling point of water [water bath equipment], which were below of or at 100°C (boiling point of water: 100°C). Additional safety controls and/or a different heating method would be needed for temperatures near of or above 100°C. Two temperatures were then selected to perform the test: At room temperature (~24°C) and at an elevated temperature of 50°C, achieved by water bath.

Beakers were used to allow for space to immerse whole gaskets (finished product). A finished gasket was used as the specimen geometry size for all tests. Using beakers and finished gaskets as specimens were slight deviations to standard ASTM D471 (ASTM 2016), instead of using test tubes and coupons or standard specimen size.

To immerse the specimens in the test fluid, 316L stainless steel wire with a square profile and a gauge size of 20 was used to make as a gasket hanger hook attached to the center of the beaker rubber stopper (Figure 54). Spacing of the samples was achieved with the hanger geometry instead of with glass beads, as mentioned on ASTM D471. The square part of the hanger for supporting the gaskets was 10mm wide (gasket thickness) and a 6mm separation was left between the 3 sections, leaving more than 6mm of separation between the hanger and the edges of the beaker; this spacing configuration complies with the indications mentioned in standard ASTM D471. Each hanger supported three specimens of a single material per each test. Every beaker used had a label

with the identification number of the three gaskets immersed, the initial date and time of the test, and the type of fluid being used.

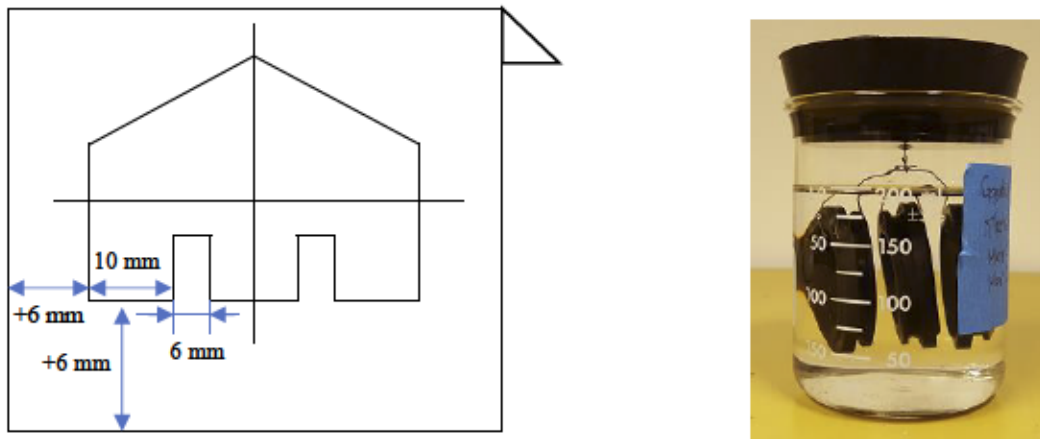


Figure 54 Beaker and steel wire gasket hanger. (Left) Dimensions (Right) Three gaskets of the same material immersed in the test fluid and hanged from the rubber stopper

- 24°C (76°F – Room Temperature) Test

Mass and hardness were measured before and after immersion. Gasket mass in air was measured with the sartorius analytical balance scale, following the technique described in standard ASTM D471, as well as the scale operation manual. First, the sliding glass door was opened, and one randomly selected gasket sample was then placed on the scale's platen. Then, the glass door was closed and the stable value after 10 seconds that the digital screen displayed was recorded. Three mass measurements were done. The procedure for mass change calculation mentioned on ASTM D471 was used (ASTM 2016), with the equation:

$$\Delta M = \frac{M_2 - M_1}{M_1} \quad (31)$$

Here,  $\Delta M$  was the mass change expressed as a percentage [%],  $M_1$  was the initial mass measured in air of the gasket before immersion, and  $M_2$  was the final mass measured in air after immersion. Both measurements were expressed in grams.

ASTM D471 refers to ASTM D2240 for hardness assessment (ASTM 2015); thus, the same technique used in the hardness test of section 3.3.2 was followed. The hardness change was then calculates as:

$$\Delta H = H_i - H_o \quad (32)$$

Having,  $\Delta H$  as the hardness change after immersion,  $H_i$  the final hardness value after immersion, and  $H_o$  the original hardness value before immersion. All hardness values were expressed in Shore A units i.e. hardness measured with Shore A durometer.

Although special care was taken to follow all indications and procedure in the ASTM D471 standard, some deviation in the test were done:

- ASTM D471 suggests the use of a reflux condenser for any volatile liquid at any temperature (ASTM 2016), but for the room temperature test (24°C), a simple beaker and rubber stopper configuration was used instead (Figure 55).
- The specimens were fully immersed into 200cm<sup>3</sup> of each of the test fluids, instead of 100cm<sup>3</sup>, the added volume was necessary to fully immerse the whole gaskets.

The environment test temperature was measured with the generic thermometer. On Figure 55, the configuration for both fluids tested at 24°C (76°F) with one type of material can be seen. Considering the project time constraint, a suitable immersion period was selected from the Table 3B on ASTM D471 (ASTM 2016); 70 hrs was selected as the test immersion period, which agrees with other studies minimum immersion time (Niese 1994).



Figure 55 CRC and Kleen-flo gasket immersion test running for 70 hrs at room temperature ~76°F [~24°C]. Beakers were properly labeled and monitored every 12 hrs

Every twelve hours, the beakers were verified for any change or abnormality. At room temperature, both test liquids did not volatilize, their volume did not reduce, and no fumes were generated. Once the minimum test immersion period was reached, mass and hardness measurements were done again. As indicated in ASTM D471, the tapered glass bottle was tared in the scale beforehand, and a quick acetone bath was performed before any after-immersion mass measurement was done.



Each gasket was cleaned of any test liquid residue by dipping it briefly in the acetone, and gently wiping it with absorbent paper. The gaskets were then stored in the tapered glass bottle, and both tapered bottle and gasket were introduced in the balance scale; then closing the glass door. Three weight measurements were performed. The setup before measuring the after-immersion mass can be seen below:



Figure 56 After-immersion mass measurement setup at room temperature (From left to right) EPDM gaskets + CRC liquid, EPDM gaskets + Kleen-flo, beaker with acetone, and the tapered bottle. The analytical balance can be seen on the back.

- 50°C Temperature Test

The test procedure with increased temperature was the same as with room temperature. The main difference was the addition of the reflux condenser to condensate the volatile liquid, so the volume wouldn't be reduced by evaporation. The reflux condenser was cooled down with tap water [ $\sim 18^{\circ}\text{C}$ ] stored in a 4L beaker used as heat sink, and having it re-circulated with a 12V water fountain pump. The temperature of the heat sink water and the test fluid was verified with the two thermocouples hooked up to the digital thermometer. The general setup for the increased temperature chemical compatibility can be seen below. In the image, the water bath was set to  $50^{\circ}\text{C}$ , and it can be observed that the beaker, with fluid and gaskets inside, was surrounded by the heated water, the reflux condenser was connected to the beaker rubber stopper and to hoses for water-cooled operation, and in the back, as well as the digital thermometer with its thermocouple inside of the beaker measuring the test fluid temperature:





Figure 57 Laboratory setup for the increased temperature chemical compatibility test. The water bath was set to 50°C

Mass and hardness were measured before and after immersion, just as with the room temperature test. The same technique and equations (31) and (32) were used for mass change and hardness change calculations, as well as recording.



Figure 58 Post-immersion gasket measurement after acetone clean-up. Mass was weighted with the tared tapered glass bottle

## 4 Results and Discussions

In this section, the results from each of the tests will be presented: Hardness test, compression tests, and chemical compatibility test.

### 4.1 Hardness test

Shore A hardness was evaluated for each type of elastomeric material, both at room and cold temperatures. The current elastomeric material used in railroad airbrake gaskets is labeled as “Current material”, and the alternative materials selected are identified with their acronyms, “EPDM” for Ethylene-Propylene-Diene monomer elastomer and “CR” for Chloroprene elastomer. Figure 59 shows the histograms of the data obtained for each material at both temperatures:

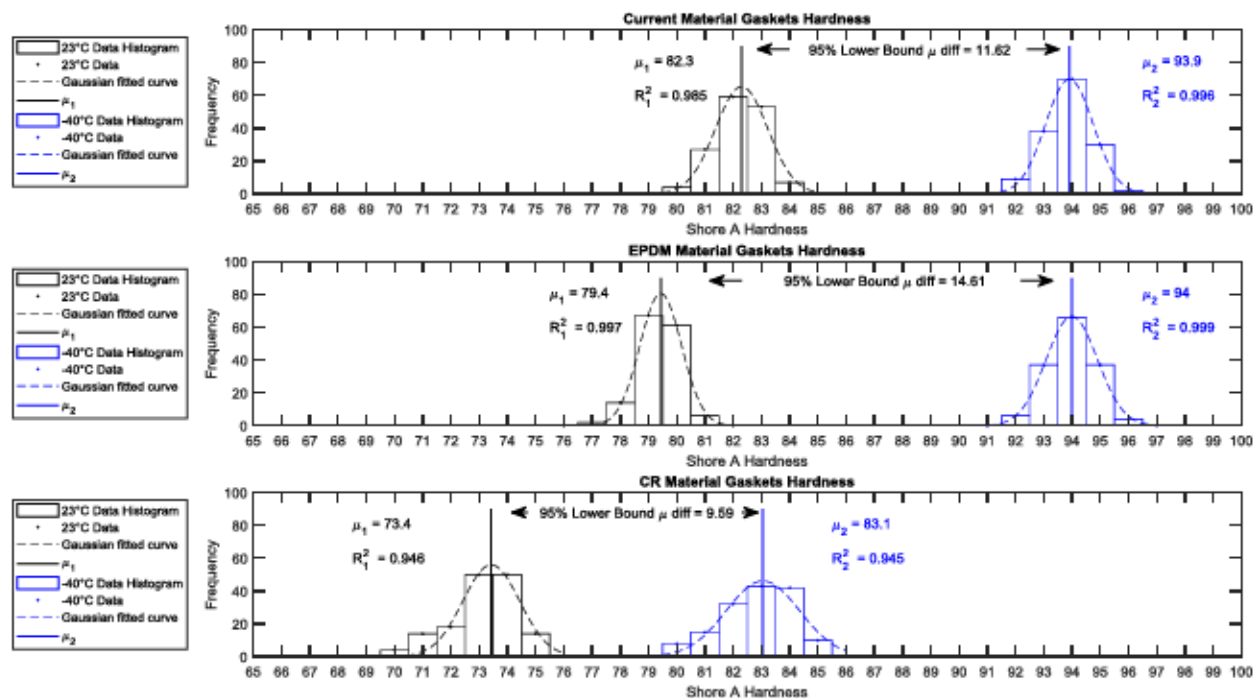


Figure 59 Histogram of the Shore A hardness at room (black color) and cold (blue color) temperatures for each type of gasket: Current, Ethylene-Propylene-Diene monomer [EPDM] and Chloroprene [CR]. The mean Shore A hardness per temperature ( $\mu_1$ : room,  $\mu_2$ : cold), the coefficient of determination ( $R^2$ ), and the Shore A hardness mean difference between temperatures ( $\mu$  diff) are shown.

A paired-samples t-test was run on the 30 gaskets of each material (Current, EPDM, and CR) to determine whether there was statistically significant mean difference between Shore A hardness at room temperature [RT] and cold temperature [CT]. Gasket hardness was higher in cold temperature for all three materials, and the results are summarized below:

Table 24 Summary of gaskets Shore A hardness statistical test results

MATERIAL	Mean at RT	Mean at CT	$\mu$ difference	CI	T-value	p-value
Current	82.213 $\pm$ 0.608	93.833 $\pm$ 0.576	11.620 $\pm$ 0.308	95%	206.76	0.000
EPDM	79.367 $\pm$ 0.587	93.973 $\pm$ 0.636	14.607 $\pm$ 0.238	95%	336.56	0.000
CR	73.253 $\pm$ 1.093	82.840 $\pm$ 1.081	9.587 $\pm$ 0.319	95%	164.50	0.000

The above results were expected, since low temperature near the glass transition point changes the stress-strain behavior of elastomers, increasing their hardness and making them less flexible and brittle. The material whose hardness values stayed within the AAR threshold of 75 – 85 Shore A hardness was Chloroprene [CR], both at room and cold temperatures. Chloroprene is commercially known as Neoprene™ (E.I. du Pont de Nemours & Company 1963)

The distribution of the differences of the Shore A Hardness between the two temperatures per each material were approximately normally distributed and were verified with probability plots (Figure 60, Figure 61, and Figure 62). The statistical test results using Minitab™ are shown below each probability plot graph:

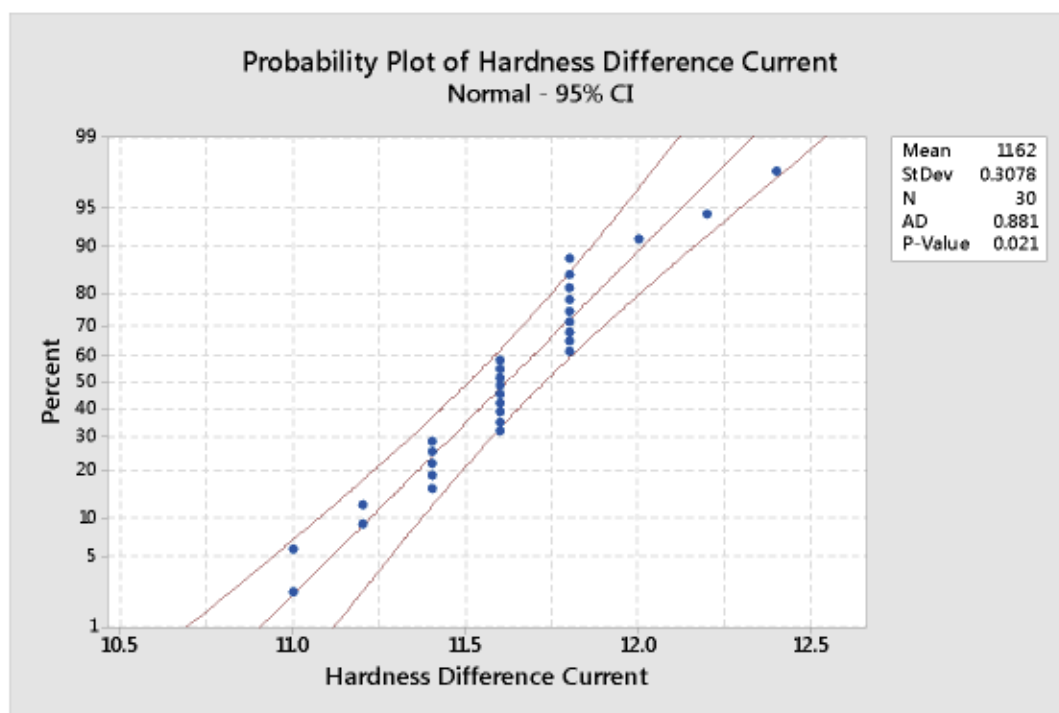


Figure 60 Probability plot of RT and CT Shore A hardness difference for Current gaskets

## Paired T-Test and CI: Hardness Current CT, Hardness Current RT

### Descriptive Statistics

Sample	N	Mean	StDev	SE Mean
Hardness Current CT	30	93.833	0.576	0.105
Hardness Current RT	30	82.213	0.608	0.111

### Estimation for Paired Difference

Mean	StDev	SE Mean	95% Lower Bound for $\mu_{\text{difference}}$
11.6200	0.3078	0.0562	11.5245

$\mu_{\text{difference}}$ : mean of (Hardness Current CT - Hardness Current RT)

### Test

Null hypothesis	$H_0: \mu_{\text{difference}} = 0$
Alternative hypothesis	$H_1: \mu_{\text{difference}} > 0$
T-Value	P-Value
206.76	0.000

Since p-value = 0.000 < 0.05, thus reject  $H_0$

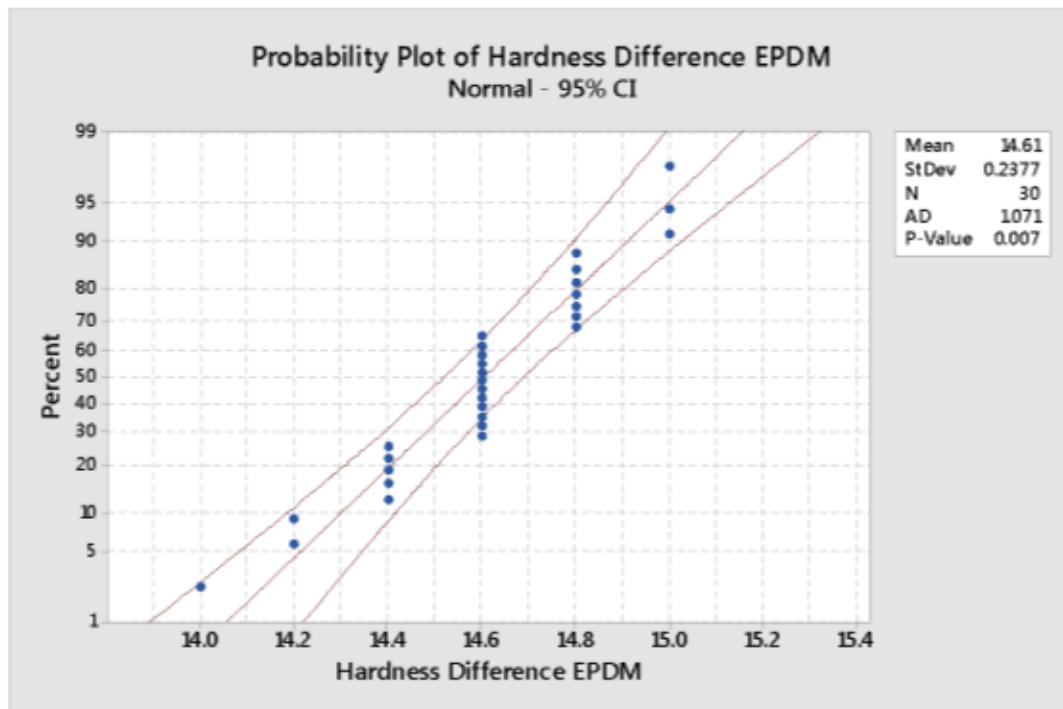


Figure 61 Probability plot of RT and CT Shore A hardness difference of EPDM gaskets

## Paired T-Test and CI: Hardness EPDM CT, Hardness EPDM RT

### Descriptive Statistics

Sample	N	Mean	StDev	SE Mean
Hardness EPDM CT	30	93.973	0.636	0.116
Hardness EPDM RT	30	79.367	0.587	0.107

### Estimation for Paired Difference

Mean	StDev	SE Mean	95% Lower Bound for $\mu_{\text{difference}}$
14.6067	0.2377	0.0434	14.5329

$\mu_{\text{difference}}$ : mean of (Hardness EPDM CT - Hardness EPDM RT)

### Test

Null hypothesis	$H_0: \mu_{\text{difference}} = 0$
Alternative hypothesis	$H_1: \mu_{\text{difference}} > 0$
T-Value	P-Value
336.56	0.000

Since p-value = 0.000 < 0.05, thus reject  $H_0$



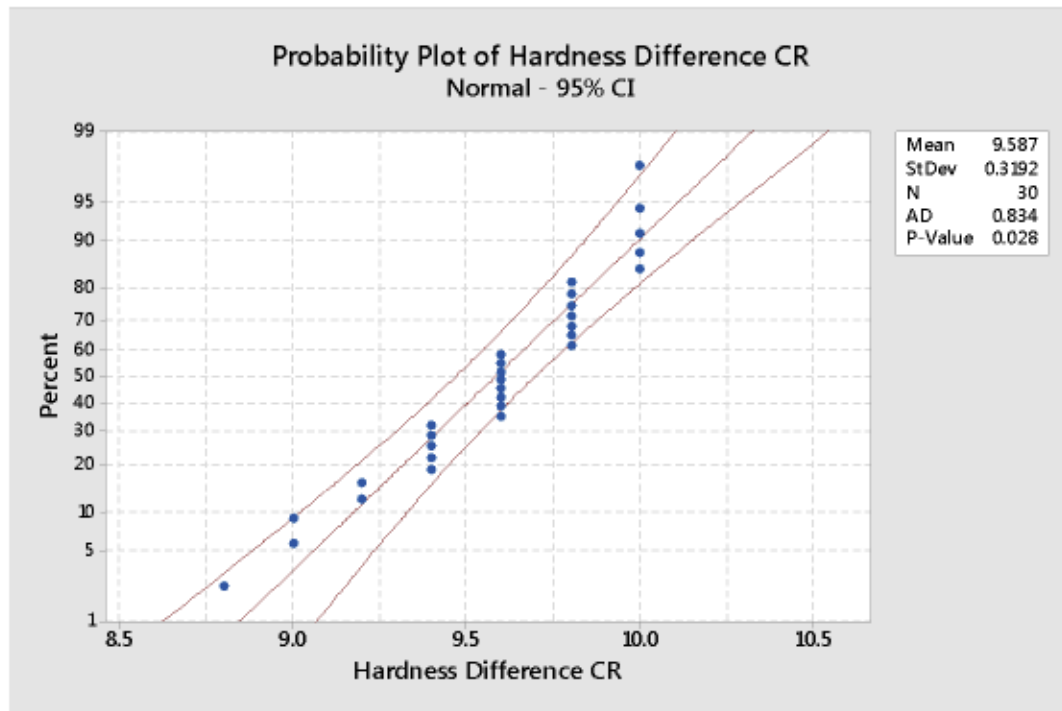


Figure 62 Probability plot of RT and CT Shore A hardness difference of CR gaskets

## Paired T-Test and CI: Hardness CR CT, Hardness CR RT

### Descriptive Statistics

Sample	N	Mean	StDev	SE Mean
Hardness CR CT	30	82.840	1.081	0.197
Hardness CR RT	30	73.253	1.093	0.200

### Estimation for Paired Difference

Mean	StDev	SE Mean	95% Lower Bound for $\mu_{\text{difference}}$
9.5867	0.3192	0.0583	9.4876

$\mu_{\text{difference}}$ : mean of (Hardness CR CT - Hardness CR RT)

### Test

Null hypothesis	$H_0: \mu_{\text{difference}} = 0$
Alternative hypothesis	$H_1: \mu_{\text{difference}} > 0$
T-Value	P-Value
164.50	0.000

Since p-value = 0.000 < 0.05, thus reject  $H_0$

## 4.2 Compression tests

In this section, the results of each one of the compression tests performed in the airbrake railroad gaskets made from the current material, EPDM, and CR are presented. The compression tests evaluated different dependent variables, including: Stiffness, compression set, compression modulus, and bulk modulus.

#### 4.2.1 Stress-strain compression

At 95% confidence level, it is concluded that, on average, the stiffness of the EPDM gasket samples was higher than that of the Current material gaskets. In the same manner, at 95% confidence level, on average, the stiffness of the EPDM gasket samples was higher than that of the CR gaskets. Finally, at 95% confidence level, on average, the stiffness of the Current material gaskets was equivalent to that of the CR gaskets. Based on these results, EPDM had the highest stiffness compared to the other two materials. This high stiffness was detrimental for handling samples during compression tests, because EPDM proved to be the most difficult material to manipulate while trying to insert gaskets inside of the fixtures. EPDM was also the material that more easily tore and nicked when using pliers to get a gasket out of the fixture. The easiest material to manipulate and push gaskets into, or out of, the fixtures was CR. These results show that stiffness is an important factor when considering ease-of-use and resilience for railroad airbrake gaskets. Another important factor to consider when adjusting mechanical properties in elastomers is filler content. Fillers, such as carbon black and fumed silica, must be properly controlled, since they increase hardness, stiffness, and mechanical hysteresis (Gent 2012).

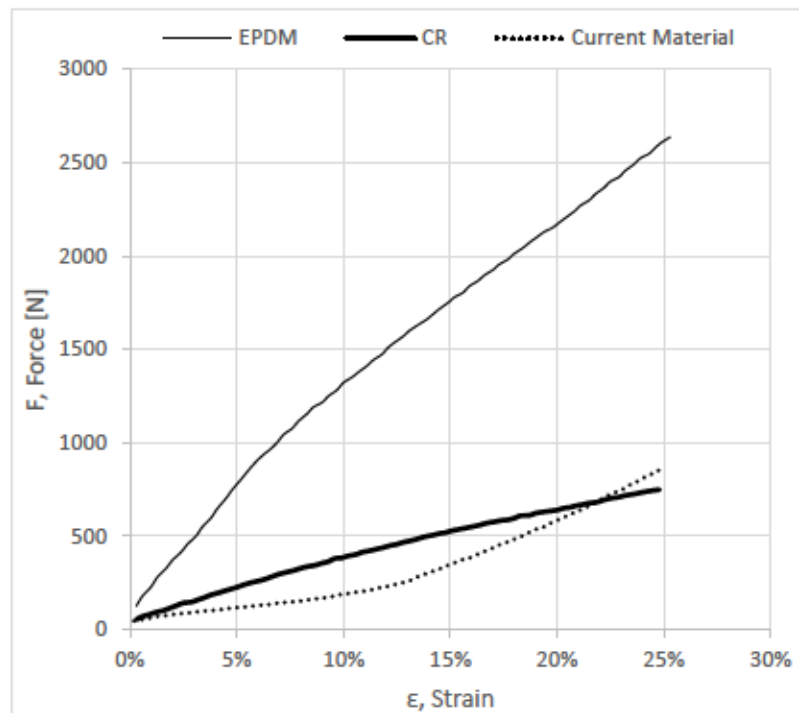


Figure 63 Force-strain plot of the stress-strain compression test up to 25% displacement for the three materials tests: EPDM, CR and current material.

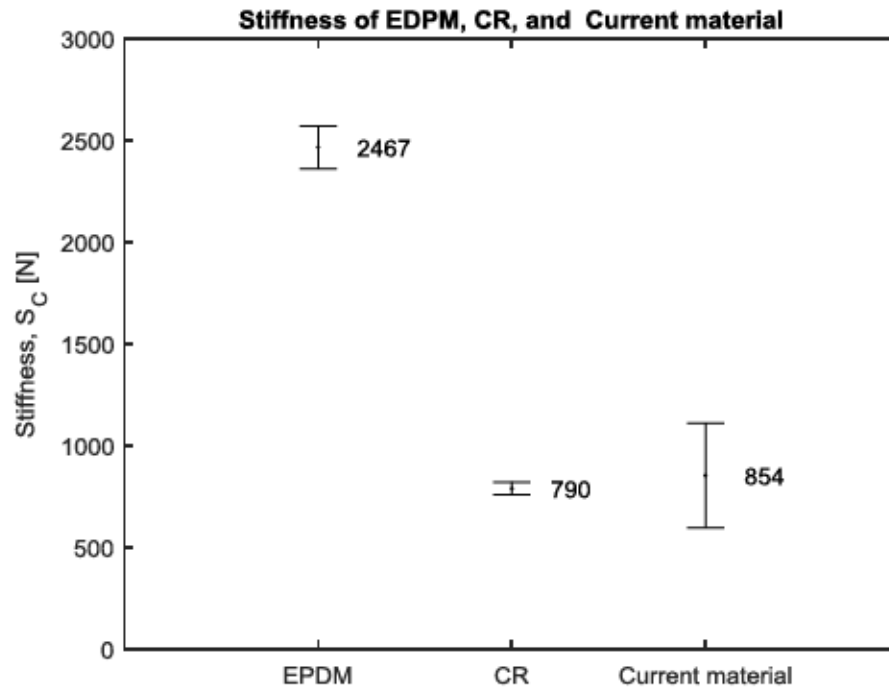


Figure 64 Compressive stiffness ( $S_c$ ) median at 25% deformation of EPDM, CR and Current gaskets. Compression tests were performed at room temperature in an MTS machine model 810.

A two-sample t-test was run on a sample of 3 gaskets made from each material (Current, EPDM, and CR) to determine whether there was statistically significant mean difference in the stiffness in three cases: EPDM-Current material, EPDM-CR, and Current material-CR. EPDM stiffness was the highest, whereas the stiffness of the current material and CR were lower than EPDM and comparable between each other. The stress-strain behavior test results are summarized below:

Table 25 Summary of stress-strain compression statistical test results

GASKETS STIFFNESS ( $S_c$ )						
MATERIAL	Mean [kN]	$\mu$ difference		CI	T-value	p-value
EPDM	$2.492 \pm 0.105$	EPDM-Current	$1.545 \pm 0.314$	95%	8.510	0.007
CR	$0.783 \pm 0.031$	EPDM-CR	$1.709 \pm 0.131$	95%	22.560	0.001
Current	$0.948 \pm 0.257$	Current-CR	$0.165 \pm 0.231$	95%	1.240	0.171

The distribution of the differences of the stiffness between two materials per each case were approximately normally distributed and were verified with probability plots (

Figure 65,

Figure 66, and Figure 67). The statistical test results using Minitab™ are shown below each probability plot graph:

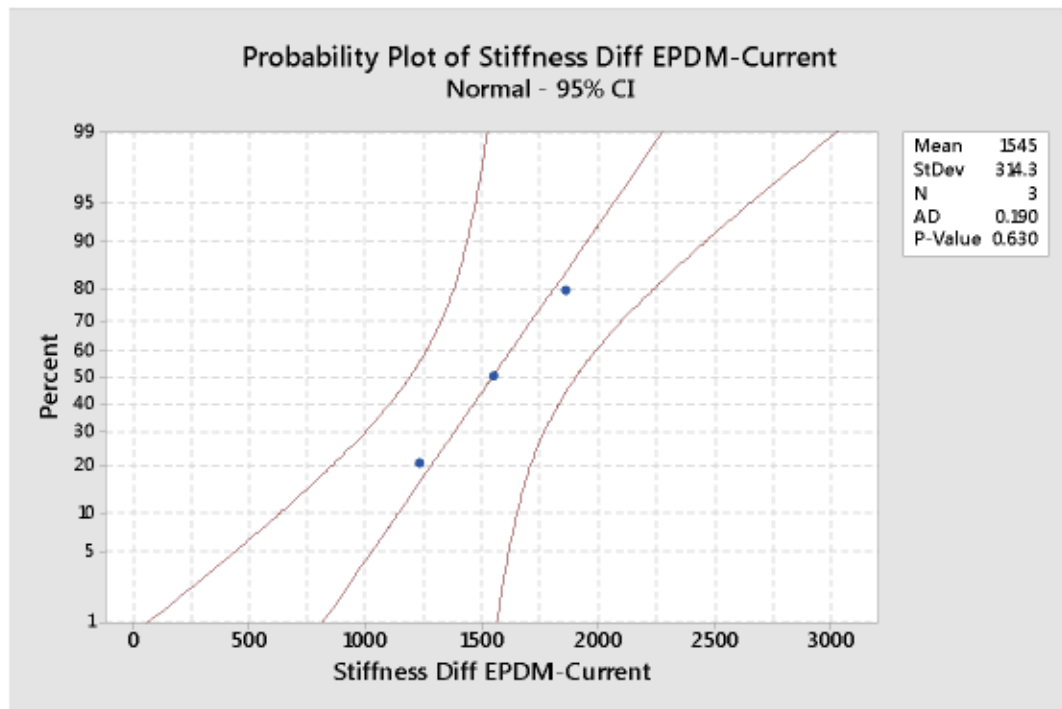


Figure 65 Probability plot of stiffness difference between EPDM-Current material

## Two-Sample T-Test and CI: EPDM Stiffness, Current Material Stiffness

### Method

$\mu_1$ : mean of EPDM Stiffness  
 $\mu_2$ : mean of Current Material Stiffness  
 Difference:  $\mu_1 - \mu_2$

*Equal variances are not assumed for this analysis.*

### Descriptive Statistics

Sample	N	Mean	StDev	SE Mean
EPDM Stiffness	3	2492	105	60
Current Material Stiffness	3	948	257	148

### Estimation for Difference

Difference	95% Lower Bound for Difference
1545	1077

### Test

Null hypothesis	$H_0: \mu_1 - \mu_2 = 0$	
Alternative hypothesis	$H_1: \mu_1 - \mu_2 > 0$	
T-Value	DF	P-Value
9.64	2	0.005

Since p-value = 0.005 < 0.05, thus reject  $H_0$



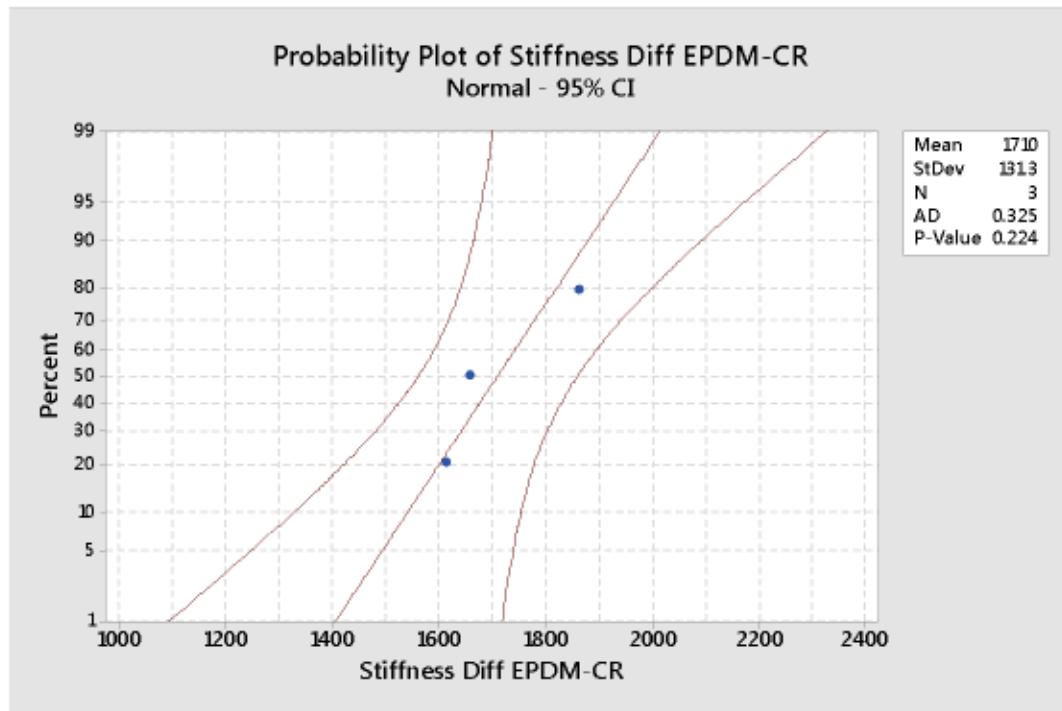


Figure 66 Probability plot of stiffness difference between EPDM-CR

## Two-Sample T-Test and CI: EPDM Stiffness, CR Stiffness

### Method

$\mu_1$ : mean of EPDM Stiffness

$\mu_2$ : mean of CR Stiffness

Difference:  $\mu_1 - \mu_2$

*Equal variances are not assumed for this analysis.*

### Descriptive Statistics

Sample	N	Mean	StDev	SE Mean
EPDM Stiffness	3	2492	105	60
CR Stiffness	3	782.5	31.1	18

### Estimation for Difference

Difference	95% Lower Bound for Difference
1709.7	1525.8

### Test

Null hypothesis  $H_0: \mu_1 - \mu_2 = 0$

Alternative hypothesis  $H_1: \mu_1 - \mu_2 > 0$

T-Value	DF	P-Value
27.15	2	0.001

Since p-value = 0.001 < 0.05, thus reject  $H_0$

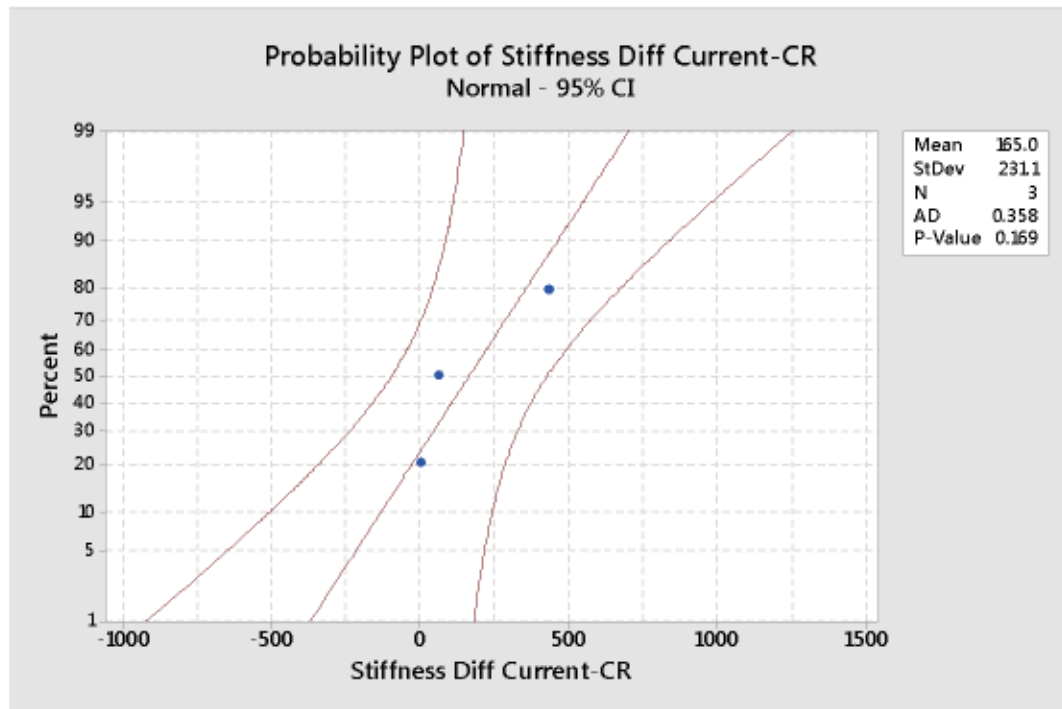


Figure 67 Probability plot of stiffness difference between Current material-CR

## Two-Sample T-Test and CI: Current Material Stiffness, CR Stiffness

### Method

$\mu_1$ : mean of Current Material Stiffness

$\mu_2$ : mean of CR Stiffness

Difference:  $\mu_1 - \mu_2$

*Equal variances are not assumed for this analysis.*

### Descriptive Statistics

Sample	N	Mean	StDev	SE Mean
Current Material Stiffness	3	948	257	148
CR Stiffness	3	782.5	31.1	18

### Estimation for Difference

Difference	95% Lower Bound for Difference
165	-272

### Test

Null hypothesis  $H_0: \mu_1 - \mu_2 = 0$

Alternative hypothesis  $H_1: \mu_1 - \mu_2 > 0$

T-Value	DF	P-Value
1.10	2	0.192

Since p-value = 0.192 > 0.05, thus accept  $H_0$

#### 4.2.2 Compression set at low temperature

At  $\alpha = 0.05$ , it is concluded that, on average, the Current material gasket samples compression set at low temperature was higher than the EPDM gasket samples compression set at the same temperature. In the same manner, at  $\alpha = 0.05$ , on average, the EPDM gasket samples compression set at low temperature was higher than the compression set at low temperature of the CR gasket samples at the same temperature. The Current material has the highest compression set value; thus, retuning the least to its original thickness in the same amount of time after the compressive load was released at low temperature. A high value of compression set at low temperature indicates that the Current material might not be the best option for cold temperature sealing. In comparison, the material that showed the lowest compression set at low temperature was CR, and almost fully returned to its original thickness after 30 mins passed since it was depressed i.e. near 5%. This result indicates that CR might be a good alternative material to use during winter time to reduce leakages. The only caution to take when using CR is that the ambient temperature must be much lower than  $0^{\circ}\text{C}$ , since some crystallizable types of CR have the highest crystallization rate near this temperature (E.I. du Pont de Nemours & Company 1963).

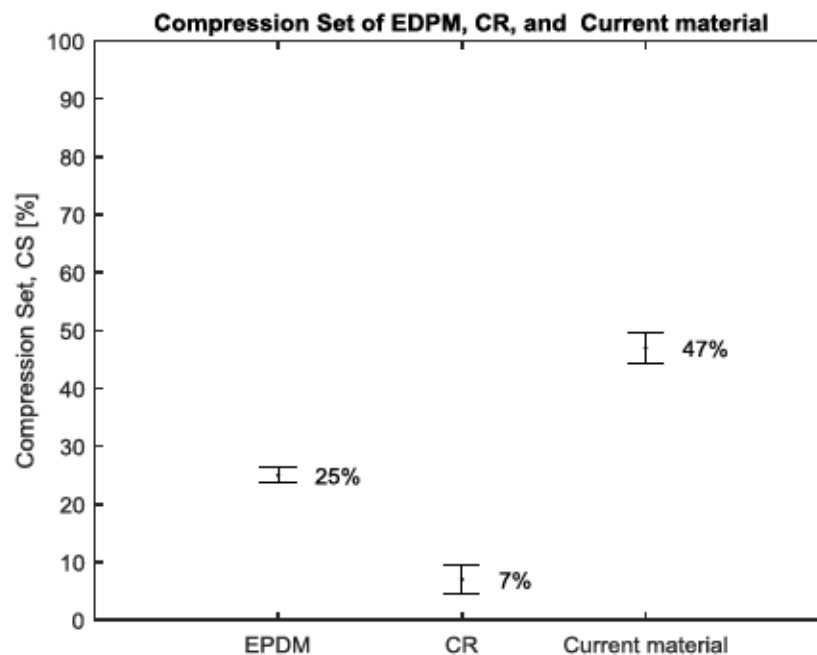


Figure 68 Compression set [CS] median for the materials tested: EPDM, CR, and current.

A two-sample t-test was run on a sample of 3 gaskets made from each material (Current, EPDM, and CR) to determine whether there was statistically significant mean difference in the compression set in three cases: EPDM-Current material, EPDM-CR, and Current material-CR. CR had the lowest compression set. The compression set at low temperature test results are summarized below:

Table 26 Summary of compression set at low temperature statistical test results

GASKETS COMPRESSION SET [CS] AT LOW TEMPERATURE						
MATERIAL	Mean	$\mu$ difference		CI	T-value	p-value
EPDM	24.67 $\pm$ 1.530	Current-EPDM	22.000 $\pm$ 4.000	95%	9.530	0.005
CR	6.00 $\pm$ 2.650	EPDM-CR	18.667 $\pm$ 1.155	95%	28.000	0.001
Current	46.67 $\pm$ 2.520	Current-CR	40.670 $\pm$ 5.030	95%	13.990	0.003

The distribution of the differences of the compression set at low temperature between two materials per each case were approximately normally distributed and were verified with probability plots (Figure 69). The statistical test results using Minitab™ are shown below each probability plot graph:

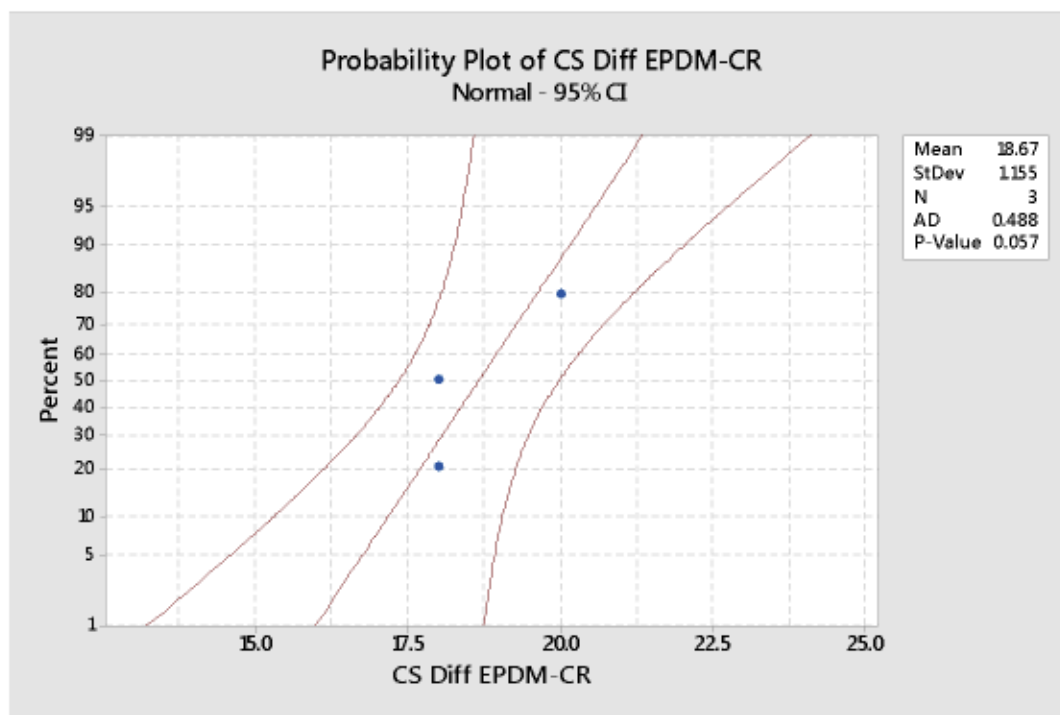


Figure 69 Probability plot of compression set [CS] difference between EPDM-CR



## Two-Sample T-Test and CI: Compression Set EPDM, Compression Set CR

### Method

$\mu_1$ : mean of Compression Set EPDM

$\mu_2$ : mean of Compression Set CR

Difference:  $\mu_1 - \mu_2$

*Equal variances are not assumed for this analysis.*

### Estimation for Difference

Difference	95% Lower Bound for Difference
18.67	14.52

### Test

Null hypothesis  $H_0: \mu_1 - \mu_2 = 0$

Alternative hypothesis  $H_1: \mu_1 - \mu_2 > 0$

T-Value	DF	P-Value
10.58	3	0.001

Since p-value = 0.001 < 0.05, thus reject  $H_0$

### Descriptive Statistics

Sample	N	Mean	StDev	SE Mean
Compression Set EPDM	3	24.67	1.53	0.88
Compression Set CR	3	6.00	2.65	1.5

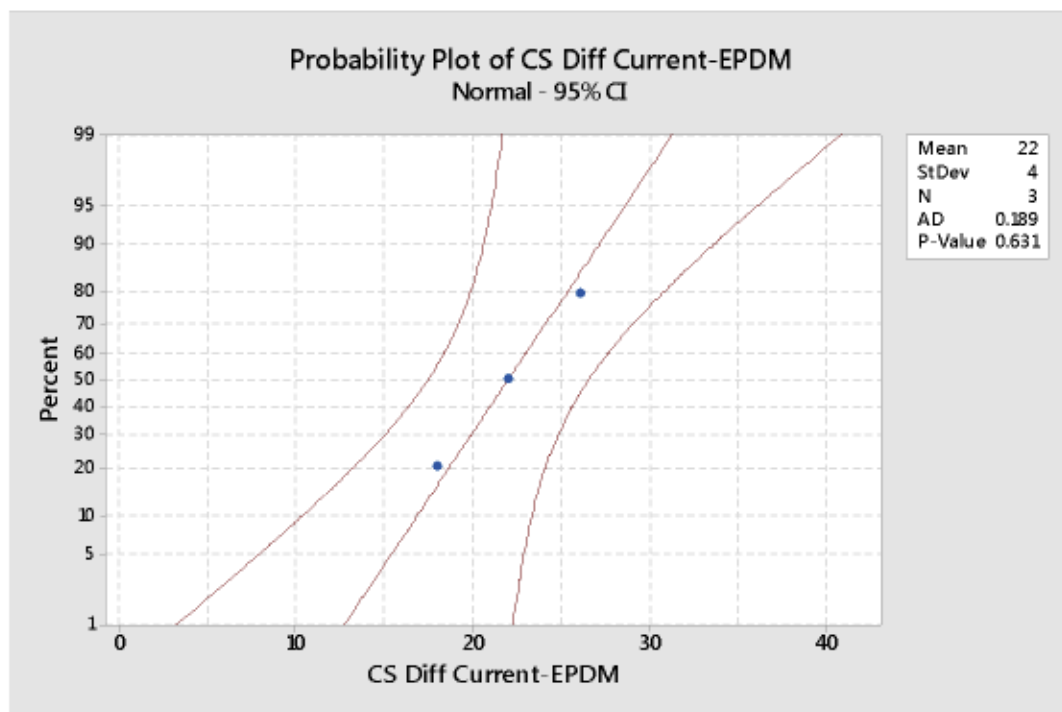


Figure 70 Probability plot of compression set [CS] difference between Current-EPDM

## Two-Sample T-Test and CI: Compression Set Current, Compression Set EPDM

### Method

$\mu_1$ : mean of Compression Set Current

$\mu_2$ : mean of Compression Set EPDM

Difference:  $\mu_1 - \mu_2$

*Equal variances are not assumed for this analysis.*

### Estimation for Difference

Difference	95% Lower Bound for Difference
22.00	18.00

### Test

Null hypothesis  $H_0: \mu_1 - \mu_2 = 0$

Alternative hypothesis  $H_1: \mu_1 - \mu_2 > 0$

T-Value	DF	P-Value
12.94	3	0.000

Since p-value = 0.000 < 0.05, thus reject  $H_0$

### Descriptive Statistics

Sample	N	Mean	StDev	SE Mean
Compression Set Current	3	46.67	2.52	1.5
Compression Set EPDM	3	24.67	1.53	0.88

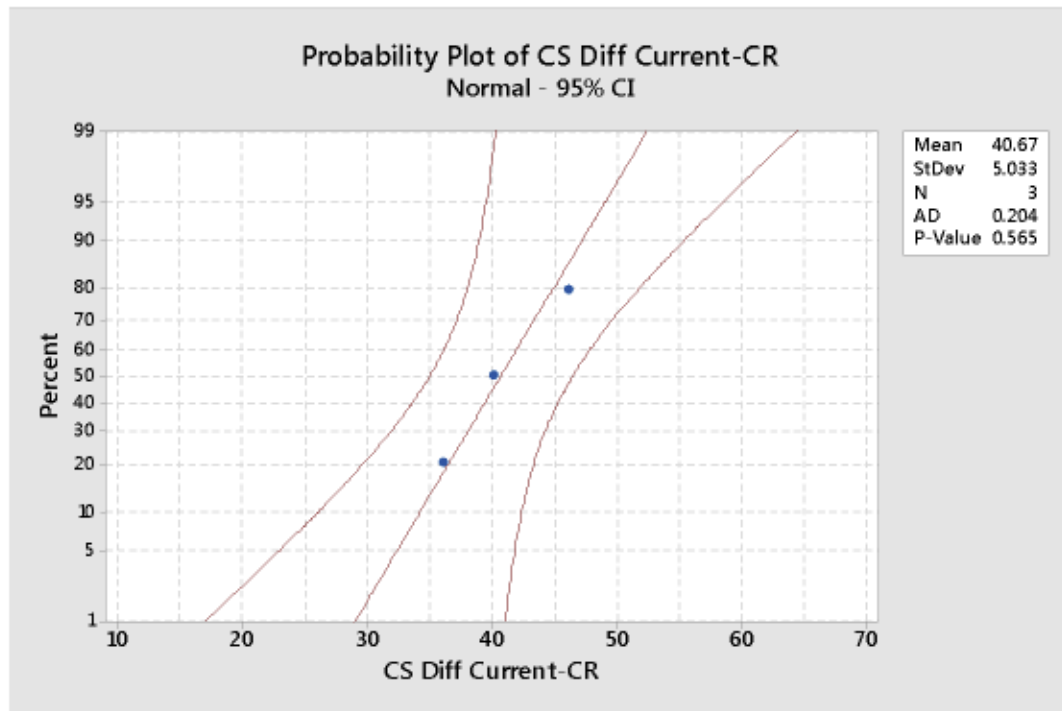


Figure 71 Probability plot of compression set [CS] difference between Current-CR

## Two-Sample T-Test and CI: Compression Set Current, Compression Set CR

### Method

$\mu_1$ : mean of Compression Set Current  
 $\mu_2$ : mean of Compression Set CR  
 Difference:  $\mu_1 - \mu_2$

*Equal variances are not assumed for this analysis.*

### Descriptive Statistics

Sample	N	Mean	StDev	SE Mean
Compression Set Current	3	46.67	2.52	1.5
Compression Set CR	3	6.00	2.65	1.5

### Estimation for Difference

Difference	95% Lower Bound for Difference
40.67	35.71

### Test

Null hypothesis	$H_0: \mu_1 - \mu_2 = 0$	
Alternative hypothesis	$H_1: \mu_1 - \mu_2 > 0$	
T-Value	DF	P-Value
19.29	3	0.000

**Since p-value = 0.000 < 0.05, thus reject  $H_0$**

### 4.2.3 Compression modulus

With a percent error difference of 30% between the experimental compression modulus obtained,  $E_{C_{exp}}$ , with both correlations used,  $E_{C_1}$  and  $E_{C_2}$ , these were found to be inconclusive and further investigation is needed; more experimentation to properly assess and calculate the shape factor in airbrake gaskets needs to be done. Moreover, the shape factor needs to be further investigated and defined in sealing applications, as there are several correlations that use this value to link hardness with compression modulus or Young's modulus, and no standardized shape factor values were

found. The methodology used in the study *Standardized Polymer Durometry* (Mix and Giacomini 2011) was found to be a straightforward method to estimate Young's modulus from hardness measurements and is encouraged to be used for comparisons.

#### **4.2.4 Bulk modulus**

The percent error for the bulk modulus measured with this test plan was considerable high (<1000%) when comparing experimental values with the ones from literature, thus, bulk modulus estimation was not successfully measured; however, gasket application performance and behavior comparisons were attained. When the EPDM gaskets went through the unloading phase of the compression cycle, the gaskets returned first to a zero force, indicating a much earlier total separation (major leakage) than what was observed with the Current material and CR gaskets. The CR gaskets were the first ones to show changes in the force measured during separation, but the force repeatedly recovered when the fixtures were still separating. In the end, the CR gaskets held up the pressure up to 3.00 mm of separation and had the highest compressive force when this displacement was reached.

### **4.3 Chemical compatibility test**

No significant changes, both in mass and hardness, were found with the interaction of the methanol-based fluids with all three materials: Current material, EPDM, and CR. The chemical compatibility test studied two methanol-based air brake anti-freeze additives that are used during winter time in trains airlines. The effect of these two chemicals was studied at room and at an elevated temperature of 50°C. After the gaskets were immersed in the chemicals at the specified conditions, on average, there was an increase of  $3.1 \pm 1.03$  Shore A hardness units and a decrease in mass of  $-0.059 \pm 0.045$  gr in mass. Although the change in hardness seems important, a change in less than 5 Shore A units wouldn't drive the gaskets out of compliance with AAR regulations; therefore, this change is considered negligible. These results confirm that all three elastomeric materials have high durability against methanol-based fluids. These low changes were expected, since literature mentions that thermoset elastomers have good performance against alcohols (Mykin Inc 2017). Although all materials experienced small changes, in comparison to CRC, Kleen-flo showed pronounced changes in both hardness and mass for all three materials, specially at 50°C. Hardness and mass changes appear to be intensified when the temperature is increased, having the highest change value of  $5.867 \pm 0.702$  Shore A hardness units with EPDM gaskets and

Kleen-flo @ 50°C. This could indicate that this product might damage EPDM gaskets if used for prolonged times.

#### 4.3.1 Hardness change

A paired-samples t-test was run on a sample of 3 gaskets made of the Current material to determine whether there was statistically significant mean difference between the Shore A hardness Pre and Post immersion in the chemicals at the specified conditions. Gasket hardness was higher after immersion in all cases. Below is a table with all the results and afterwards the paired-samples t-test Minitab™ output:

Table 27 Chemical compatibility test results for Shore A hardness change in current material gaskets

CONDITION	Pre-Immersion Mean	Post-Immersion Mean	$\mu$ difference	CI	T-value	p-value
CRC @ 23°C	83.000 ± 0.200	83.333 ± 0.231	0.333 ± 0.115	95%	5.000	0.019
CRC @ 50°C	82.400 ± 0.800	83.867 ± 0.416	1.467 ± 0.577	95%	4.400	0.024
Kleen-flo @ 23°C	81.733 ± 0.115	84.200 ± 0.200	2.467 ± 0.306	95%	13.98	0.003
Kleen-flo @ 50°C	82.200 ± 0.346	86.200 ± 0.346	4.000 ± 0.600	95%	11.550	0.004

#### Paired T-Test and CI: CURR Post H CRC @23°C, CURR Pre ... RC @23°C

##### Descriptive Statistics

Sample	N	Mean	StDev	SE Mean
CURR Post H CRC @23°C	3	83.333	0.231	0.133
CURR Pre H CRC @23°C	3	83.000	0.200	0.115

##### Estimation for Paired Difference

Mean	StDev	SE Mean	95% Lower Bound for $\mu$ difference
0.3333	0.1155	0.0667	0.1387

$\mu$  difference: mean of (CURR Post H CRC @23°C - CURR Pre H CRC @23°C)

##### Test

Null hypothesis	$H_0: \mu_{\text{difference}} = 0$
Alternative hypothesis	$H_1: \mu_{\text{difference}} > 0$
T-Value	5.00
P-Value	0.019



## Paired T-Test and CI: CURR Post H CRC @50°C, CURR Pre ... RC @50°C

### Descriptive Statistics

Sample	N	Mean	StDev	SE Mean
CURR Post H CRC @50°C	3	83.867	0.416	0.240
CURR Pre H CRC @50°C	3	82.400	0.800	0.462

### Estimation for Paired Difference

Mean	StDev	SE Mean	95% Lower Bound for $\mu_{\text{difference}}$
1.467	0.577	0.333	0.493

$\mu_{\text{difference}}$ : mean of (CURR Post H CRC @50°C - CURR Pre H CRC @50°C)

### Test

Null hypothesis	$H_0: \mu_{\text{difference}} = 0$
Alternative hypothesis	$H_1: \mu_{\text{difference}} > 0$
T-Value	P-Value
4.40	0.024

## Paired T-Test and CI: CURR Post H Kleen-flo @23°C, ... leen-flo @23°C

### Descriptive Statistics

Sample	N	Mean	StDev	SE Mean
CURR Post H Kleen-flo @23°C	3	84.200	0.200	0.115
CURR Pre H Kleen-flo @23°C	3	81.733	0.115	0.067

### Estimation for Paired Difference

Mean	StDev	SE Mean	95% Lower Bound for $\mu_{\text{difference}}$
2.467	0.306	0.176	1.952

$\mu_{\text{difference}}$ : mean of (CURR Post H Kleen-flo @23°C - CURR Pre H Kleen-flo @23°C)

### Test

Null hypothesis	$H_0: \mu_{\text{difference}} = 0$
Alternative hypothesis	$H_1: \mu_{\text{difference}} > 0$
T-Value	P-Value
13.98	0.003

## Paired T-Test and CI: CURR Post H Kleen-flo @50°C, ... leen-flo @50°C

### Descriptive Statistics

Sample	N	Mean	StDev	SE Mean
CURR Post H Kleen-flo @50°C	3	86.200	0.346	0.200
CURR Pre H Kleen-flo @50°C	3	82.200	0.346	0.200

### Estimation for Paired Difference

Mean	StDev	SE Mean	95% Lower Bound for $\mu_{\text{difference}}$
4.000	0.600	0.346	2.988

$\mu_{\text{difference}}$ : mean of (CURR Post H Kleen-flo @50°C - CURR Pre H Kleen-flo @50°C)

### Test

Null hypothesis	$H_0: \mu_{\text{difference}} = 0$
Alternative hypothesis	$H_1: \mu_{\text{difference}} > 0$
T-Value	P-Value
11.55	0.004

A paired-samples t-test was run on a sample of 3 gaskets made of EPDM to determine whether there was statistically significant mean difference between the Shore A hardness Pre and Post immersion in the chemicals at the specified conditions. Gasket hardness was higher after immersion in all cases. Below is a table with all the results and afterwards the paired-samples t-test Minitab™ output:

Table 28 Chemical compatibility test results for Shore A hardness change in EPDM gaskets

CONDITION	Pre-Immersion Mean	Post-Immersion Mean	$\mu$ difference	CI	T-value	p-value
CRC @ 23°C	78.867 ± 0.306	82.000 ± 0.346	3.133 ± 0.643	95%	8.440	0.007
CRC @ 50°C	79.867 ± 0.503	82.200 ± 0.200	2.333 ± 0.306	95%	13.230	0.003
Kleen-flo @ 23°C	79.067 ± 0.643	84.267 ± 0.416	5.200 ± 0.721	95%	12.490	0.003
Kleen-flo @ 50°C	79.867 ± 0.503	85.733 ± 0.231	5.867 ± 0.702	95%	14.470	0.002

### Paired T-Test and CI: EPDM Post H CRC @23°C, EPDM ... H CRC @23°C

#### Descriptive Statistics

Sample	N	Mean	StDev	SE Mean
EPDM Post H CRC @23°C	3	82.000	0.346	0.200
EPDM Pre H CRC @23°C	3	78.867	0.306	0.176

#### Estimation for Paired Difference

Mean	StDev	SE Mean	95% Lower Bound for $\mu$ difference
3.133	0.643	0.371	2.049

$\mu$  difference: mean of (EPDM Post H CRC @23°C - EPDM Pre H CRC @23°C)

#### Test

Null hypothesis	$H_0: \mu_{\text{difference}} = 0$
Alternative hypothesis	$H_1: \mu_{\text{difference}} > 0$
T-Value	P-Value
8.44	0.007

### Paired T-Test and CI: EPDM Post H CRC @50°C, EPDM ... H CRC @50°C

#### Descriptive Statistics

Sample	N	Mean	StDev	SE Mean
EPDM Post H CRC @50°C	3	82.200	0.200	0.115
EPDM Pre H CRC @50°C	3	79.867	0.503	0.291

#### Estimation for Paired Difference

Mean	StDev	SE Mean	95% Lower Bound for $\mu$ difference
2.333	0.306	0.176	1.818

$\mu$  difference: mean of (EPDM Post H CRC @50°C - EPDM Pre H CRC @50°C)

#### Test

Null hypothesis	$H_0: \mu_{\text{difference}} = 0$
Alternative hypothesis	$H_1: \mu_{\text{difference}} > 0$
T-Value	P-Value
13.23	0.003

## Paired T-Test and CI: EPDM Post H Kleen-flo @23°C, ... leen-flo @23°C

### Descriptive Statistics

Sample	N	Mean	StDev	SE Mean
EPDM Post H Kleen-flo @23°C	3	84.267	0.416	0.240
EPDM Pre H Kleen-flo @23°C	3	79.067	0.643	0.371

### Estimation for Paired Difference

Mean	StDev	SE Mean	95% Lower Bound for $\mu_{\text{difference}}$
5.200	0.721	0.416	3.984

$\mu_{\text{difference}}$ : mean of (EPDM Post H Kleen-flo @23°C - EPDM Pre H Kleen-flo @23°C)

### Test

Null hypothesis	$H_0: \mu_{\text{difference}} = 0$
Alternative hypothesis	$H_1: \mu_{\text{difference}} > 0$
T-Value	P-Value
12.49	0.003

## Paired T-Test and CI: EPDM Post H Kleen-flo @50°C, ... leen-flo @50°C

### Descriptive Statistics

Sample	N	Mean	StDev	SE Mean
EPDM Post H Kleen-flo @50°C	3	85.733	0.231	0.133
EPDM Pre H Kleen-flo @50°C	3	79.867	0.503	0.291

### Estimation for Paired Difference

Mean	StDev	SE Mean	95% Lower Bound for $\mu_{\text{difference}}$
5.867	0.702	0.406	4.683

$\mu_{\text{difference}}$ : mean of (EPDM Post H Kleen-flo @50°C - EPDM Pre H Kleen-flo @50°C)

### Test

Null hypothesis	$H_0: \mu_{\text{difference}} = 0$
Alternative hypothesis	$H_1: \mu_{\text{difference}} > 0$
T-Value	P-Value
14.47	0.002

A paired-samples t-test was run on a sample of 3 gaskets made of CR to determine whether there was statistically significant mean difference between the Shore A hardness Pre and Post immersion in the chemicals at the specified conditions. Gasket hardness was higher after immersion in all cases. Below is a table with all the results and afterwards the paired-samples t-test Minitab™ output:

Table 29 Chemical compatibility test results for Shore A hardness change in CR gaskets

CONDITION	Pre-Immersion Mean	Post-Immersion Mean	$\mu$ difference	CI	T-value	p-value
CRC @ 23°C	73.533 ± 0.416	75.333 ± 0.115	1.800 ± 0.346	95%	9.000	0.006
CRC @ 50°C	73.000 ± 0.529	76.400 ± 0.600	3.400 ± 1.058	95%	5.560	0.015
Kleen-flo @ 23°C	72.800 ± 1.000	76.533 ± 0.306	3.733 ± 1.222	95%	5.290	0.017

<b>Kleen-flo @ 50°C</b>	74.067 ± 0.115	77.533 ± 0.306	3.467 ± 0.231	95%	26.000	0.001
-----------------------------	----------------	----------------	---------------	-----	--------	-------

### Paired T-Test and CI: CR Post H CRC @23°C, CR Pre H CRC @23°C

#### Descriptive Statistics

Sample	N	Mean	StDev	SE Mean
CR Post H CRC @23°C	3	75.333	0.115	0.067
CR Pre H CRC @23°C	3	73.533	0.416	0.240

#### Estimation for Paired Difference

Mean	StDev	SE Mean	95% Lower Bound for $\mu_{\text{difference}}$
1.800	0.346	0.200	1.216

$\mu_{\text{difference}}$ : mean of (CR Post H CRC @23°C - CR Pre H CRC @23°C)

#### Test

Null hypothesis	$H_0: \mu_{\text{difference}} = 0$
Alternative hypothesis	$H_1: \mu_{\text{difference}} > 0$
T-Value	P-Value
9.00	0.006

### Paired T-Test and CI: CR Post H CRC @50°C, CR Pre H CRC @50°C

#### Descriptive Statistics

Sample	N	Mean	StDev	SE Mean
CR Post H CRC @50°C	3	76.400	0.600	0.346
CR Pre H CRC @50°C	3	73.000	0.529	0.306

#### Estimation for Paired Difference

Mean	StDev	SE Mean	95% Lower Bound for $\mu_{\text{difference}}$
3.400	1.058	0.611	1.616

$\mu_{\text{difference}}$ : mean of (CR Post H CRC @50°C - CR Pre H CRC @50°C)

#### Test

Null hypothesis	$H_0: \mu_{\text{difference}} = 0$
Alternative hypothesis	$H_1: \mu_{\text{difference}} > 0$
T-Value	P-Value
5.56	0.015

### Paired T-Test and CI: CR Post H Kleen-flo @23°C, CR Pre ... -flo @23°C

#### Descriptive Statistics

Sample	N	Mean	StDev	SE Mean
CR Post H Kleen-flo @23°C	3	76.533	0.306	0.176
CR Pre H Kleen-flo @23°C	3	72.800	1.000	0.577

#### Estimation for Paired Difference

Mean	StDev	SE Mean	95% Lower Bound for $\mu_{\text{difference}}$
3.733	1.222	0.706	1.673

$\mu_{\text{difference}}$ : mean of (CR Post H Kleen-flo @23°C - CR Pre H Kleen-flo @23°C)

#### Test

Null hypothesis	$H_0: \mu_{\text{difference}} = 0$
Alternative hypothesis	$H_1: \mu_{\text{difference}} > 0$
T-Value	P-Value
5.29	0.017



## Paired T-Test and CI: CR Post H Kleen-flo @50°C, CR Pre ... -flo @50°C

### Descriptive Statistics

Sample	N	Mean	StDev	SE Mean
CR Post H Kleen-flo @50°C	3	77.533	0.306	0.176
CR Pre H Kleen-flo @50°C	3	74.067	0.115	0.067

### Estimation for Paired Difference

Mean	StDev	SE Mean	95% Lower Bound for $\mu_{\text{difference}}$
3.467	0.231	0.133	3.077

$\mu_{\text{difference}}$ : mean of (CR Post H Kleen-flo @50°C - CR Pre H Kleen-flo @50°C)

### Test

Null hypothesis	$H_0: \mu_{\text{difference}} = 0$
Alternative hypothesis	$H_1: \mu_{\text{difference}} > 0$
T-Value	26.00
P-Value	0.001

Figure 73, Figure 74, and Figure 72 show the results for the hardness change comparisons for the current material, EPDM, and CR.

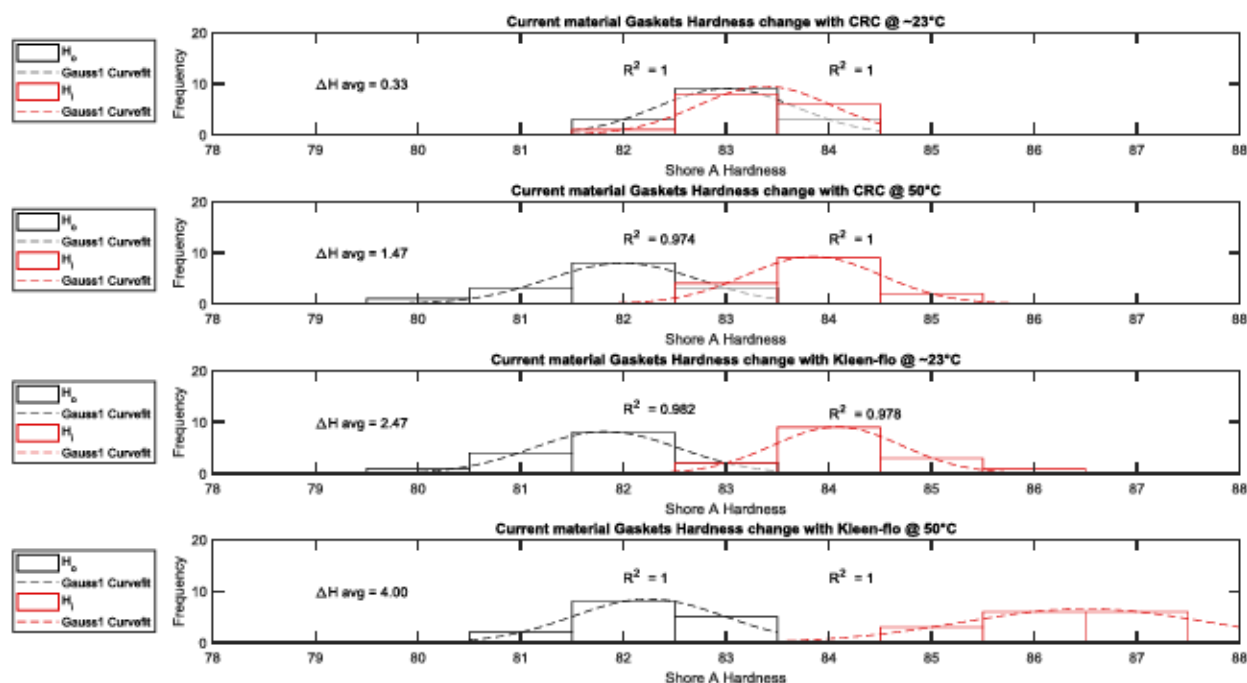


Figure 72 Current material gaskets hardness change histograms for both chemicals at 23°C and 50°C

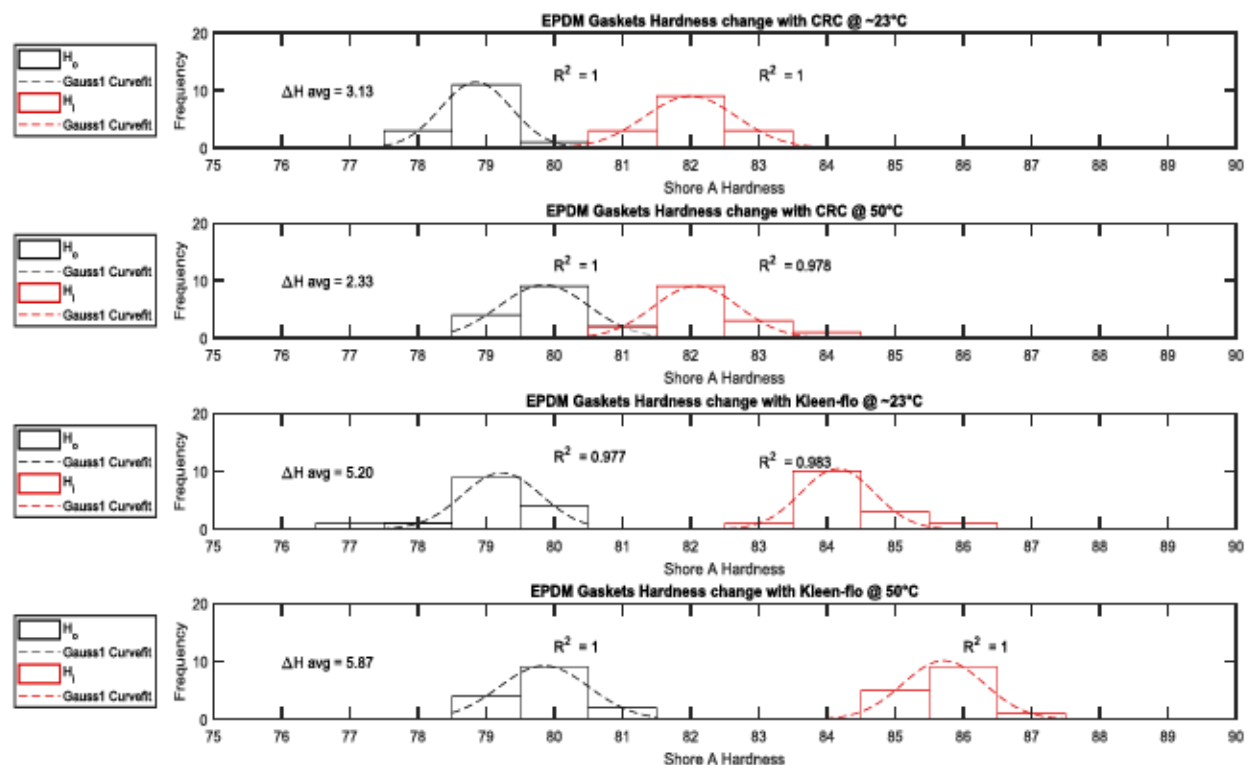


Figure 73 EPDM gaskets hardness change histograms for both chemicals at 23°C and 50°C

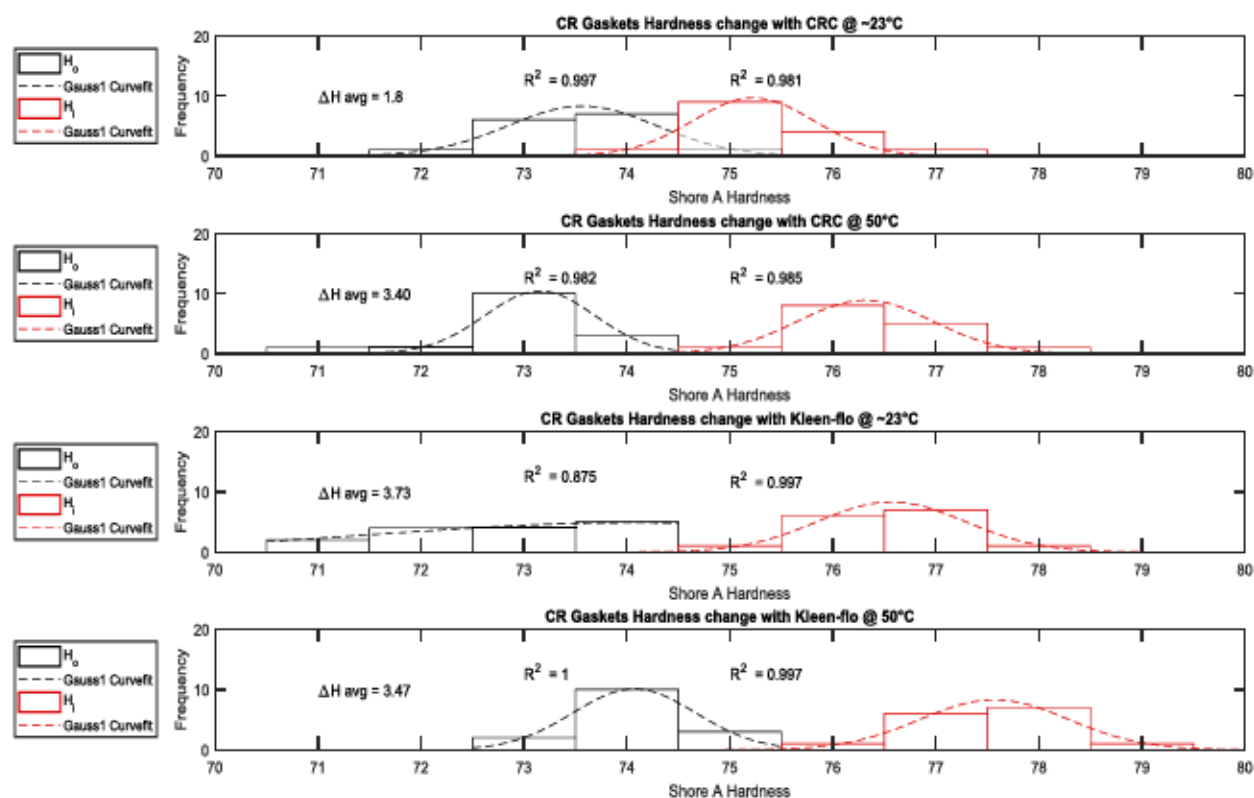


Figure 74 CR gaskets hardness change histograms for both chemicals at 23°C and 50°C

### 4.3.2 Mass change

A paired-samples t-test was run on a sample of 3 gaskets made of the current material to determine whether there was statistically significant mean difference between the mass Pre and Post immersion in the chemicals at the specified conditions. Gasket mass change was minimal after immersion and remained equivalent in all cases. Below is a table with all the results and afterwards the paired-samples t-test Minitab™ output:

Table 30 Chemical compatibility test results for mass change in Current material gaskets

CONDITION	Pre-Immersion Mean	Post-Immersion Mean	$\mu$ difference	CI	T-value	p-value
CRC @ 23°C	7.792 ± 0.044	7.787 ± 0.042	-0.004 ± 0.002	95%	-3.64	0.966
CRC @ 50°C	7.786 ± 0.005	7.776 ± 0.004	-0.010 ± 0.001	95%	-17.20	0.998
Kleen-flo @ 23°C	7.793 ± 0.065	7.781 ± 0.067	-0.012 ± 0.002	95%	-7.79	0.992
Kleen-flo @ 50°C	7.860 ± 0.027	7.811 ± 0.020	-0.049 ± 0.007	95%	-11.9	0.997

#### Paired T-Test and CI: CURR Post M CRC @23°C, CURR Pre ... RC @23°C

##### Descriptive Statistics

Sample	N	Mean	StDev	SE Mean
CURR Post M CRC @23°C	3	7.7879	0.0425	0.0245
CURR Pre M CRC @23°C	3	7.7921	0.0445	0.0257

##### Estimation for Paired Difference

Mean	StDev	SE Mean	95% Lower Bound for $\mu$ difference
-0.00422	0.00201	0.00116	-0.00761

$\mu$  difference: mean of (CURR Post M CRC @23°C - CURR Pre M CRC @23°C)

##### Test

Null hypothesis	$H_0: \mu_{\text{difference}} = 0$
Alternative hypothesis	$H_1: \mu_{\text{difference}} > 0$
T-Value	P-Value
-3.64	0.966

#### Paired T-Test and CI: CURR Post M CRC @50°C, CURR Pre ... RC @50°C

##### Descriptive Statistics

Sample	N	Mean	StDev	SE Mean
CURR Post M CRC @50°C	3	7.77611	0.00453	0.00261
CURR Pre M CRC @50°C	3	7.78622	0.00532	0.00307

##### Estimation for Paired Difference

Mean	StDev	SE Mean	95% Lower Bound for $\mu$ difference
-0.010111	0.001018	0.000588	-0.011828

$\mu$  difference: mean of (CURR Post M CRC @50°C - CURR Pre M CRC @50°C)

## Test

Null hypothesis	$H_0: \mu_{\text{difference}} = 0$
Alternative hypothesis	$H_1: \mu_{\text{difference}} > 0$
T-Value	P-Value
-17.20	0.998

## Paired T-Test and CI: CURR Post M Kleen-flo @23°C, ... leen-flo @23°C

### Descriptive Statistics

Sample	N	Mean	StDev	SE Mean
CURR Post M Kleen-flo @23°C	3	7.7812	0.0676	0.0390
CURR Pre M Kleen-flo @23°C	3	7.7932	0.0650	0.0375

### Estimation for Paired Difference

Mean	StDev	SE Mean	95% Lower Bound for $\mu_{\text{difference}}$
-0.01200	0.00267	0.00154	-0.01650

$\mu_{\text{difference}}$ : mean of (CURR Post M Kleen-flo @23°C - CURR Pre M Kleen-flo @23°C)

### Test

Null hypothesis	$H_0: \mu_{\text{difference}} = 0$
Alternative hypothesis	$H_1: \mu_{\text{difference}} > 0$
T-Value	P-Value
-7.79	0.992

## Paired T-Test and CI: CURR Post M Kleen-flo @50°C, ... leen-flo @50°C

### Descriptive Statistics

Sample	N	Mean	StDev	SE Mean
CURR Post M Kleen-flo @50°C	3	7.8113	0.0206	0.0119
CURR Pre M Kleen-flo @50°C	3	7.8606	0.0273	0.0157

### Estimation for Paired Difference

Mean	StDev	SE Mean	95% Lower Bound for $\mu_{\text{difference}}$
-0.04927	0.00717	0.00414	-0.06135

$\mu_{\text{difference}}$ : mean of (CURR Post M Kleen-flo @50°C - CURR Pre M Kleen-flo @50°C)

### Test

Null hypothesis	$H_0: \mu_{\text{difference}} = 0$
Alternative hypothesis	$H_1: \mu_{\text{difference}} > 0$
T-Value	P-Value
-11.90	0.997

A paired-samples t-test was run on a sample of 3 gaskets made of EPDM to determine whether there was statistically significant mean difference between the mass Pre and Post immersion in the chemicals at the specified conditions. Gasket mass change was minimal after immersion and remained equivalent in all cases. Below is a table with all the results and afterwards the paired-samples t-test Minitab™ output:



Table 31 Chemical compatibility test results for mass change in CR gaskets

CONDITION	Pre-Immersion Mean	Post-Immersion Mean	$\mu$ difference	CI	T-value	p-value
<b>CRC @ 23°C</b>	6.366 $\pm$ 0.006	6.354 $\pm$ 0.006	-0.012 $\pm$ 0.002	95%	-7.86	0.992
<b>CRC @ 50°C</b>	6.366 $\pm$ 0.051	6.302 $\pm$ 0.043	-0.064 $\pm$ 0.009	95%	-11.18	0.996
<b>Kleen-flo @ 23°C</b>	6.316 $\pm$ 0.032	6.284 $\pm$ 0.032	-0.032 $\pm$ 0.001	95%	-41.29	1.000
<b>Kleen-flo @ 50°C</b>	6.415 $\pm$ 0.061	6.300 $\pm$ 0.057	-0.115 $\pm$ 0.004	95%	-49.76	1.000

### Paired T-Test and CI: EPDM Post M CRC @23°C, EPDM ... CRC @23°C

#### Descriptive Statistics

Sample	N	Mean	StDev	SE Mean
EPDM Post M CRC @23°C	3	6.35433	0.00611	0.00353
EPDM Pre M CRC @23°C	3	6.36656	0.00619	0.00358

#### Estimation for Paired Difference

Mean	StDev	SE Mean	95% Lower Bound for $\mu$ difference
-0.01222	0.00269	0.00156	-0.01676

$\mu$  difference: mean of (EPDM Post M CRC @23°C - EPDM Pre M CRC @23°C)

#### Test

Null hypothesis	$H_0: \mu_{\text{difference}} = 0$
Alternative hypothesis	$H_1: \mu_{\text{difference}} > 0$
T-Value	P-Value
-7.86	0.992

### Paired T-Test and CI: EPDM Post M CRC @50°C, EPDM ... CRC @50°C

#### Descriptive Statistics

Sample	N	Mean	StDev	SE Mean
EPDM Post M CRC @50°C	3	6.3023	0.0438	0.0253
EPDM Pre M CRC @50°C	3	6.3666	0.0517	0.0298

#### Estimation for Paired Difference

Mean	StDev	SE Mean	95% Lower Bound for $\mu$ difference
-0.06422	0.00995	0.00574	-0.08099

$\mu$  difference: mean of (EPDM Post M CRC @50°C - EPDM Pre M CRC @50°C)

#### Test

Null hypothesis	$H_0: \mu_{\text{difference}} = 0$
Alternative hypothesis	$H_1: \mu_{\text{difference}} > 0$
T-Value	P-Value
-11.18	0.996

## Paired T-Test and CI: EPDM Post M Kleen-flo @23°C, ... leen-flo @23°C

### Descriptive Statistics

Sample	N	Mean	StDev	SE Mean
EPDM Post M Kleen-flo @23°C	3	6.2840	0.0329	0.0190
EPDM Pre M Kleen-flo @23°C	3	6.3161	0.0328	0.0189

### Estimation for Paired Difference

Mean	StDev	SE Mean	95% Lower Bound for $\mu_{\text{difference}}$
-0.032111	0.001347	0.000778	-0.034382

$\mu_{\text{difference}}$ : mean of (EPDM Post M Kleen-flo @23°C - EPDM Pre M Kleen-flo @23°C)

### Test

Null hypothesis	$H_0: \mu_{\text{difference}} = 0$
Alternative hypothesis	$H_1: \mu_{\text{difference}} > 0$
T-Value	P-Value
-41.29	1.000

## Paired T-Test and CI: EPDM Post M Kleen-flo @50°C, ... leen-flo @50°C

### Descriptive Statistics

Sample	N	Mean	StDev	SE Mean
EPDM Post M Kleen-flo @50°C	3	6.3003	0.0573	0.0331
EPDM Pre M Kleen-flo @50°C	3	6.4158	0.0611	0.0353

### Estimation for Paired Difference

Mean	StDev	SE Mean	95% Lower Bound for $\mu_{\text{difference}}$
-0.11544	0.00402	0.00232	-0.12222

$\mu_{\text{difference}}$ : mean of (EPDM Post M Kleen-flo @50°C - EPDM Pre M Kleen-flo @50°C)

### Test

Null hypothesis	$H_0: \mu_{\text{difference}} = 0$
Alternative hypothesis	$H_1: \mu_{\text{difference}} > 0$
T-Value	P-Value
-49.76	1.000

A paired-samples t-test was run on a sample of 3 gaskets made of CR to determine whether there was statistically significant mean difference between the mass Pre and Post immersion in the chemicals at the specified conditions. Gasket mass change was minimal after immersion and remained equivalent in all cases. Below is a table with all the results and afterwards the paired-samples t-test Minitab™ output:

Table 32 Chemical compatibility test results for mass change in CR gaskets

CONDITION	Pre-Immersion Mean	Post-Immersion Mean	$\mu$ difference	CI	T-value	p-value
CRC @ 23°C	6.137 $\pm$ 0.001	6.100 $\pm$ 0.002	-0.037 $\pm$ 0.001	95%	-63.12	1.000
CRC @ 50°C	6.152 $\pm$ 0.057	6.028 $\pm$ 0.052	-0.124 $\pm$ 0.005	95%	-38.57	1.000
Kleen-flo @ 23°C	6.143 $\pm$ 0.018	6.078 $\pm$ 0.017	-0.065 $\pm$ 0.001	95%	-89.97	1.000
Kleen-flo @ 50°C	6.110 $\pm$ 0.026	5.987 $\pm$ 0.024	-0.129 $\pm$ 0.002	95%	-97.00	1.000

### Paired T-Test and CI: CR Post M CRC @23°C, CR Pre M CRC @23°C

#### Descriptive Statistics

Sample	N	Mean	StDev	SE Mean
CR Post M CRC @23°C	3	6.10000	0.00200	0.00115
CR Pre M CRC @23°C	3	6.13711	0.00102	0.00059

#### Estimation for Paired Difference

Mean	StDev	SE Mean	95% Lower Bound for $\mu_{\text{difference}}$
-0.037111	0.001018	0.000588	-0.038828

$\mu_{\text{difference}}$ : mean of (CR Post M CRC @23°C - CR Pre M CRC @23°C)

#### Test

Null hypothesis	$H_0: \mu_{\text{difference}} = 0$
Alternative hypothesis	$H_1: \mu_{\text{difference}} > 0$
T-Value	P-Value
-63.12	1.000

### Paired T-Test and CI: CR Post M CRC @50°C, CR Pre M CRC @50°C

#### Descriptive Statistics

Sample	N	Mean	StDev	SE Mean
CR Post M CRC @50°C	3	6.0280	0.0527	0.0304
CR Pre M CRC @50°C	3	6.1520	0.0577	0.0333

#### Estimation for Paired Difference

Mean	StDev	SE Mean	95% Lower Bound for $\mu_{\text{difference}}$
-0.12400	0.00557	0.00321	-0.13339

$\mu_{\text{difference}}$ : mean of (CR Post M CRC @50°C - CR Pre M CRC @50°C)

#### Test

Null hypothesis	$H_0: \mu_{\text{difference}} = 0$
Alternative hypothesis	$H_1: \mu_{\text{difference}} > 0$
T-Value	P-Value
-38.57	1.000

## Paired T-Test and CI: CR Post M Kleen-flo @23°C, CR Pre ... -flo @23°C

### Descriptive Statistics

Sample	N	Mean	StDev	SE Mean
CR Post M Kleen-flo @23°C	3	6.0783	0.0171	0.0099
CR Pre M Kleen-flo @23°C	3	6.1439	0.0184	0.0106

### Estimation for Paired Difference

Mean	StDev	SE Mean	95% Lower Bound for $\mu_{\text{difference}}$
-0.065556	0.001262	0.000729	-0.067683

$\mu_{\text{difference}}$ : mean of (CR Post M Kleen-flo @23°C - CR Pre M Kleen-flo @23°C)

### Test

Null hypothesis  $H_0: \mu_{\text{difference}} = 0$   
 Alternative hypothesis  $H_1: \mu_{\text{difference}} > 0$

T-Value	P-Value
-89.97	1.000

## Paired T-Test and CI: CR Post M Kleen-flo @50°C, CR Pre ... -flo @50°C

### Descriptive Statistics

Sample	N	Mean	StDev	SE Mean
CR Post M Kleen-flo @50°C	3	5.9877	0.0242	0.0140
CR Pre M Kleen-flo @50°C	3	6.1170	0.0261	0.0150

### Estimation for Paired Difference

Mean	StDev	SE Mean	95% Lower Bound for $\mu_{\text{difference}}$
-0.12933	0.00231	0.00133	-0.13323

$\mu_{\text{difference}}$ : mean of (CR Post M Kleen-flo @50°C - CR Pre M Kleen-flo @50°C)

### Test

Null hypothesis  $H_0: \mu_{\text{difference}} = 0$   
 Alternative hypothesis  $H_1: \mu_{\text{difference}} > 0$

T-Value	P-Value
-97.00	1.000

Figure 75, Figure 76, and Figure 77 show the results for the mass change comparisons for the current material, EPDM, and CR.



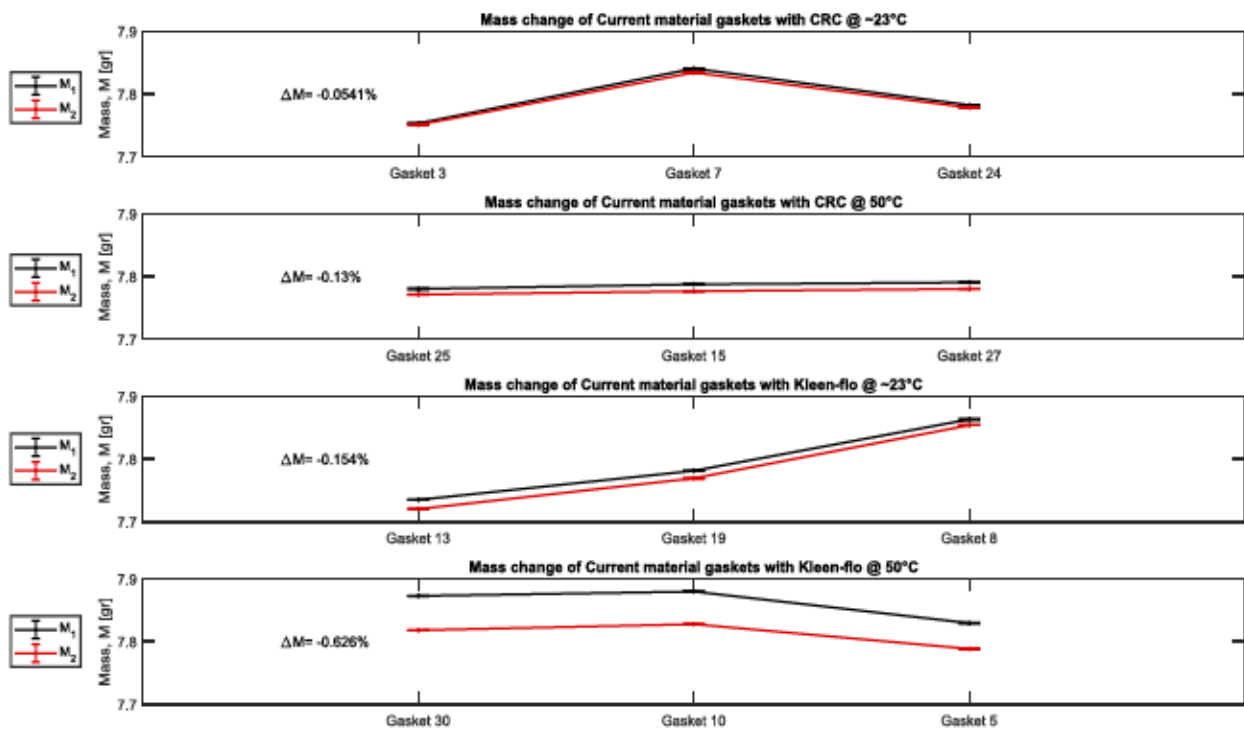


Figure 75 Current material gaskets mass change for both chemicals at 23°C and 50°C

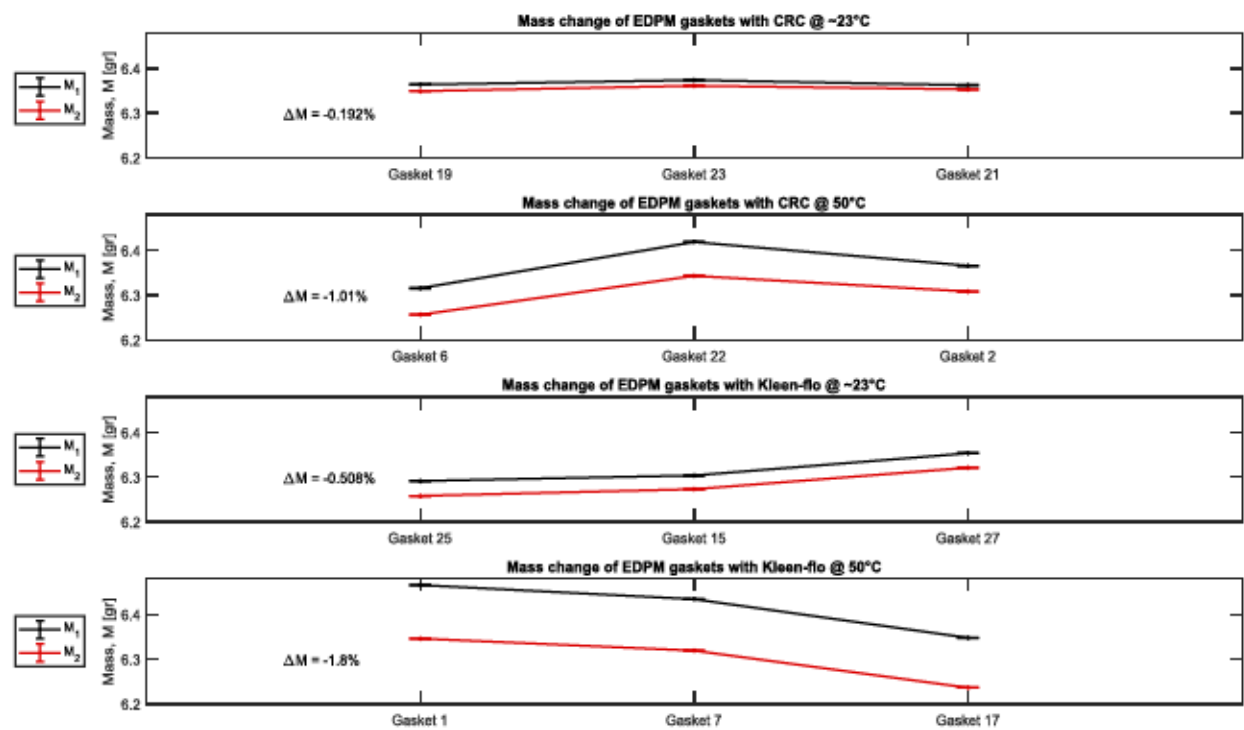


Figure 76 EPDM gaskets mass change for both chemicals at 23°C and 50°C

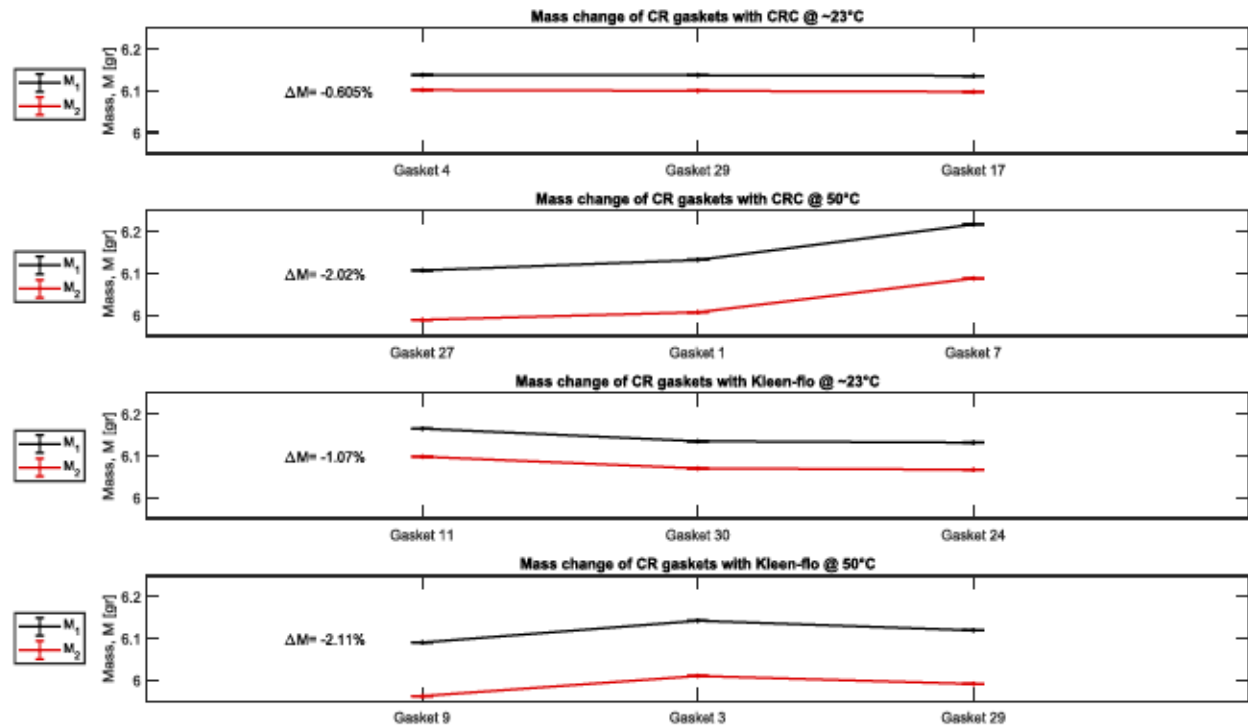


Figure 77 EPDM gaskets mass change for both chemicals at 23°C and 50°C

## 5 Industry Application

### 5.1 In-service test protocol for gaskets

To properly assess the performance and reliability of a component, in this case, railcar airbrake gaskets, records need to be maintained to assess component failure frequency and replacement. The recorded data can then later be used to estimate the lifetime of a component or to analyze and adjust the replacement policy used. To keep records of gasket failures and replacement frequency, a template to perform an in-service test protocol for railcar airbrake gaskets is proposed. The protocol for testing gaskets during operational service is based on the hardness test procedure performed in this study. This protocol could be used in railroad industry as the first step to perform predictive analytics for railroad airbrake gaskets. Predictive analytics uses statistical modelling techniques to provide insight and take strategic actions in maintenance (Kingsley 2012)

The procedure to perform the test protocol is the same as in the hardness test. Five hardness measurements will be taken with a handheld Shore A durometer, where the measurements points should be evenly spread throughout the gasket face, with at least 5.00 mm of separation. The

hardness points average and standard deviation must be recorded. The hardness measurements should be performed on a new gasket before it goes inside of a glad-hand and recorded; the date and ambient temperature prior to replacing the gasket should be recorded as well. The hardness measurements should be done on the gasket face that will create the air tight seal i.e. the gasket face that will get in contact with the other gasket. One key factor was to record hardness measurements in a random fashion to diminish systematic errors. The data can then be used to detect a faulty batch of gaskets and to create a database for further analysis, for example, it could be used to apply reliability centered maintenance theory on the gasket replacement cycle to optimize it, instead of using the current run-to-failure approach. Measurements should be done inside of the warehouse/mechanical shop, or where the testing conditions are optimal (Room Temperature 20 to 30°C and a relative humidity of  $50 \pm 10$  %RH) (ASTM 2014b). A proposed template to gather this information was presented below.

Table 33: Sample table to gather gasket hardness data and replacement date

ID	Date [YY/MM/DD]	Ambient Temp. [°C]	Hardness Measurements [Shore A 0 – 100]								Observations
			1	2	3	4	5	Sum (1-5)	Avg (1-5)	STD DEV	
1											
2											

In the *Observations* section, the maintenance staff can note down any failure condition or distinct problem encountered when servicing or replacing a gasket that was inside of the glad-hand i.e. some options to put in observations can be: nicked, cracked, or swollen.

Although the type of end hose arrangement, gasket batch number, supplier, among other factors were disregarded, this protocol keeps the procedure simple and straightforward for a swift execution. Moreover, this protocol gives the benefit of providing a record of compliance with AAR Specification M-602, as “*gaskets shall attain a durometer reading of  $80 \pm 5$  or an AAR approved alternative*”. Once the form is filled in, the hardness values provide proof that the gaskets being used comply with this specification and can also alert if there is any defect in the gasket quality.

The ambient temperature is also recorded in this form, since cold temperatures can affect elastomeric materials hardness, as well as their mechanical behavior. A proper record of the ambient temperature can be used later to find a correlation with failure frequency.

Date annotations in the template would aid in keeping track of the time of failure, as well as provide information to create a histogram of the gasket failure frequency, which would be the first step to start using predictive analytics.

In the next section, it is assumed that a correct set of information for gasket replacement frequency was recorded, therefore the gasket failure frequency distribution can be derived and then used to solve a numerical example of group replacement policy for railcar airbrake gaskets.

## 5.2 Gaskets group replacement policy numerical example

In this section, a hypothetical numerical example with group replacement policy was solved. A group replacement policy was believed to be the best preventive maintenance policy, considering economies of scale of the gaskets, and assuming that failure modes occur stochastically (lamp replacement approach).

It was estimated that 50 gaskets would need to be replaced each time. This comes from the assumption that 20% of the total number of gaskets used in a train with an average of 125 railcars (Deveau 2011), would be replaced during preventive group replacements. The calculation was then:

$$2 \frac{\text{gaskets}}{\text{railcar}} * 125 \frac{\text{railcars}}{\text{train}} = 250 \frac{\text{gaskets}}{\text{train}} * 20\% \text{ train} = 50 \text{ gaskets.}$$

In this exercise, the first assumption made for gasket replacement was that the gasket failures occur according to a normal distribution, with a mean of 8 weeks of average life expectancy and a standard deviation of 2 weeks; in other words, the probability density function of the failure times of the gaskets was  $f(t) = N(8,2)$ . Then, it was assumed that a cost of a failure replacement was  $C_f=\$15$ , and a cost of a replacement under conditions of group replacement was  $C_g=\$6$ , with 50 gaskets replaced in group. Using equation (12) the optimal interval  $t_p$  between group replacements was estimated.

With the above values, a table with the total replacement unit cost per unit time  $C(t_p)$  was created, having a total number of replacement units  $N=50$ :

$$N C(t_p) = N \left( \frac{C_g + C_f H(t_p)}{t_p} \right) = 50 \left( \frac{\$6 + \$15 H(t_p)}{t_p} \right)$$



Using the general failure rate equation (13), and solving for 8 iterations, the calculations were:

$$H(T) = \sum_{i=0}^{T-1} [1 + H(T - i - 1)] \int_i^{i+1} f(t)dt, T \geq 1$$

$$H(0) = 0$$

$$H(1) = [1 + H(0)] \int_0^1 f(t)dt = [1 + H(0)][\Phi(-3.5) - \Phi(-4.0)] = 0.00017$$

$$H(2) = [1 + H(1)] \int_0^1 f(t)dt + [1 + H(0)] \int_1^2 f(t)dt$$

... and so on...

The total replacement cost per unit time for all 50 gaskets,  $NC(t_p)$ , is shown on Table 34. The optimal period for preventive group replacements  $t_p$  was between 5 and 6 weeks.

Table 34 Group replacement unit cost per unit time mock example for 50 railcar airbrake gaskets

$t_p$	0	1	2	3	4	5	6	7	8
$\frac{(t_p - \mu)}{\sigma}$	-4	-3.5	-3.0	-2.5	-2.0	-1.5	-1.0	-0.5	0.0
$\Phi\left(\frac{(t_p - \mu)}{\sigma}\right)$	0.00003	0.00002	0.0014	0.0062	0.0228	0.0668	0.1587	0.3085	0.5000
$\int_i^{i+1} f(t)dt$	0.00003	0.00002	0.0011	0.0049	0.0165	0.0441	0.0919	0.1498	0.1915
$H(t_p)$	0	0.00017	0.0013	0.0062	0.0227	0.0668	0.1588	0.3089	0.5013
$C(t_p)$	N/A	\$6.00	\$3.01	\$2.03	\$1.59	\$1.40	\$1.40	\$1.52	\$1.69
$NC(t_p)$	N/A	\$300	\$150	100	\$80	\$70	\$70	\$75	\$85

Predictive analytics techniques, such as a group replacement policy, can help to reduce maintenance costs and to manage assets based on reliability. In summary, the benefit of applying the in-service protocol is twofold: First, it would create a record of compliance with AAR's specification 602. Secondly, once enough information is recorded, predictive analytics can be performed to optimize maintenance costs and manage assets more efficiently.

## 6 Conclusions and Future work

At the end of each of the tests, several conclusions could be made.

- In the hardness test, all materials increased their Shore A hardness when the temperature dropped to  $-40^{\circ}\text{C}$ . In this test, Chloroprene [CR] presented the lowest change in hardness, with a difference of 9.53 Shore A units between room and cold temperature hardness. In addition, even when frozen, CR still presented subtleness when manipulated. Although the Shore A mean hardness of CR (73) was below the AAR threshold (75), CR maintained a hardness lower than that of the AAR upper limit of 85 when frozen (83). These results indicate that CR is a good candidate for elaborating a “low-temperature” railcar airbrake gasket.
- In all compression tests, CR presented a better performance than the other materials. In the stress-strain compression test, CR stiffness was comparable to that of the current material used, indicating that it could be a viable replacement to the current material, since it would maintain the same compression response inside of a glad-hand as that of the current material. In the compression set at low temperature test, CR presented the lowest compression set of all materials, indicating a high recovery factor, which would translate in the ability to keep a proper seal even in cold conditions. Compression and bulk modulus were inconclusive, but CR still presented better performance by maintaining an air tight seal even when the zero-displacement point was surpassed. CR sealed off the air, even when the fixtures were separated by 3.00 mm.
- During the chemical compatibility test, one point to note, was that instead of swelling, like the literature mentions that happens with elastomers in contact with fuels, the response of the three materials tested with alcohols showed the opposite; a decrease in mass. This behavior indicates that some component “leach-out” of the gaskets compound. This was further verified, since at the end of all immersion tests the test fluid presented a change in color and “murkiness”. This could also indicate that some other reaction took place that made the gaskets to lose mass, probably elastomer molecular scission. Nevertheless, CR still withstood the effects of the methanol-based additives.

- Considering all the results given by CR, it can be concluded that CR the perfect candidate to use when fabricating railcar airbrake gaskets resilient to cold temperature. The next step would be to further verify this hypothesis on field testing.

Elastomer technology is a complex and broad subject, with many dependent variables involved and sometimes having synergistic effects between them. Because of this, elastomers encompass an extensive range of areas of expertise, including hyper-elastic and viscoelastic constitutive models, polymer technology, organic chemistry, continuum mechanics, among others. All these factors are only considering a static or pseudo-static condition, if a dynamic scenario is envisioned, additional knowledge would need to be covered, such as complex numbers, Fourier and Taylor series, etc.; this would be needed to fully understand their behavior.

Aside from the background knowledge needed to understand elastomers, other challenges were encountered during this research project, especially during testing. One of the major problems encountered during testing, were insulation and extreme low temperatures control. Commercial freezers have a range up to  $-35^{\circ}\text{C}$  and do not maintain that temperature constant. Temperatures below  $-35^{\circ}\text{C}$  enter in the realm of cryogenic temperatures, and specialized freezers or environmental chambers are needed. This type of equipment is expensive and if acquired, it would have offset the cost of the research project and surpassed the initial budget. In addition, elastomer fabrication through a third party is expensive and there are some variations in quality. All these factors proved to be challenges to overcome along the research project. The tests performed in this study were simple in practice but needed a detailed plan and proper allocation of resources to effectively achieve the objectives intended.

One future study that could be done in railcar airbrake gaskets, is to study the dynamic properties of elastomers. In a dynamic scenario, elastomer fatigue, crack propagation, and dynamic properties could be analyzed and tested, both at room and cold temperatures. The objective in dynamic conditions would be to estimate the airbrake gaskets average lifetime or MTTF. This data could be determined experimentally or by recording the frequency of gaskets failure using the proposed in-service test protocol. With a robust database of one or two years of recorded information on airbrake glad-hand gaskets frequency of failure, an estimation of the probability density function of the gaskets failure rate could be calculated. With enough information, an algorithm could be used to determine the reliability function of the gaskets, and then find out the cost of executing



reliability centered maintenance (Vaghar Anzabi 2015), this as an alternative of the current run-to-failure approach the gaskets have today. This study focused in pseudo-static conditions in compression, meaning that load and displacement was linearly applied and at very slow rates. Sine, cosine, or saw-tooth profiles for load and displacement in the MTS machine could be performed in future to analyze the dynamic behavior of the airbrake gaskets. Frequency and amplitude could be varied to verify the response of the elastomeric gaskets in different conditions. If dynamic testing would be performed, complex numbers theory would need to be studied, since the modulus in this scenario would be a complex number, having a real and imaginary part. This is known as the complex modulus; where the real part is known as the storage modulus and the imaginary part the loss modulus. Furthermore, viscoelastic material behavior would need to be studied in depth to properly understand and analyze these phenomena. Also, temperature manipulation would need to be considered, since it also affects the complex modulus of elastomers. Fatigue, as well as crack initiation and propagation, could be other subjects to study, since it is in dynamic conditions that any of these phenomena could appear.

Another approach to further develop airbrake gaskets, would be to modify even further their geometry, and correlate shape factor with durability and sealing properties in cold weather. It was found in the literature, that changing the thickness of the gaskets might allow for a better “cold seal”, with the caveat that the deformation would be larger ( $\geq 30\%$  strain) and the material response would enter in the realm of non-linear hyper-elastic deformation. With a thicker wide lip in the gasket, the compression factor could be increased, thus allowing for a better seal between the two gaskets. This new geometry would need to be studied with similar tests as in this study: stress-strain compression behavior, sealability, and hardness. Elastic response due to the shape factor variations would be an interesting point to study. In addition, improved sealability in cold temperature can also be studied with this modified gasket geometry. Also, in the same line of the gasket geometry, the angle of the wide lip gasket could be modified. Instead of having a slanted end, the new geometry could have a rounded bezel to increase the surface contact area between gaskets, thus increasing the separation force and ensuring a better seal.

One last future study option reviewed, would be to create a real options valuation to assess if the “expensive” elastomers are worth reviewing and see if those could be a viable option to ensure sealability. To develop this approach, first a price list of specialty elastomers and railcars maintenance costs would be needed. API standards and compounds used in the Oil and Gas



industry, such as fluorocarbon-based synthetic rubbers, should be reviewed. Once an estimated price and availability are obtained, a hypothetical initial project capital would be estimated, and a forecast analyzed. Options to expand, contract, or abandon the project would then be analyzed alongside the forecast. Also, considering material price and production resources, a cost-benefit study could be made, relating the economies of the compound, its market price, and evaluate the benefits that the improvement would make, if any. Cost issues with respect to current base cost of existing glad-hand gaskets include cost of elastomeric material and additives (e.g., ozone inhibitors, fillers, and plastifiers), fixed cost for the molds, variable costs of manufacturing method, inventory control, and shipping. Alternatives should be assessed not only for unit cost, but also for use in service, for example, not falling out of the glad hand when inserted.

With all above considered, elastomer research, and railcar airbrake gasket research in specific, still has several areas of opportunity that can be further explored.

## References

- AAR Publications. 2002. *Specification M-602 Gaskets, Air Hose*. Vol. Section E.
- Abraham, F., T. Alshuth, and S. Jerrams. 2006. "Chapter 5 - Parameter Dependence of the Fatigue Life of Elastomers." In *Elastomers and Components*, edited by V. A. Coveney, 59-73: Woodhead Publishing.
- Alberta Canada. "Business in Alberta/Alberta Industries/Logistics and Market Access/about the Industry ." About the industry., last modified Mon, 29 Jun 2015 03:20:18, accessed 08/01, 2017, <http://www.albertacanada.com/business/industries/lma-about-the-industry.aspx>.
- Albiñ, P. 2006. *Chapter 1 - the 5-Year Accelerated Ageing Project for Thermoset and Thermoplastic Elastomeric Materials: A Service Life Prediction Tool*. Elastomers and Components., edited by V. A. Coveney Woodhead Publishing.
- Arruda, Ellen M. and Mary C. Boyce. 1993. *A Three-Dimensional Constitutive Model for the Large Stretch Behavior of Rubber Elastic Materials*. Vol. 41.
- Ashby, Michael F. and David R. H. Jones. 2013. *Engineering Materials 2 - an Introduction to Microstructures and Processing (4th Edition)*. 4th ed ed. Elsevier.
- ASTM. 2015. *ASTM D2240 - Standard Test Method for Rubber Property—Durometer Hardness* ASTM International.
- . 2014a. *Astm D3767. Standard Practice for Rubber—Measurement of Dimensions*. ASTM International.
- . 2016. *ASTM D471 - Standard Test Method for Rubber Property—Effect of Liquids*.
- . 2012. *ASTM D575 - Standard Test Methods for Rubber Properties in Compression*.
- . 2017a. *D1418 Standard Practice for Rubber and Rubber Latices—Nomenclature*.
- . 2017b. *D2000 Standard Classification System for Rubber Products*.
- . 2017c. *Designation E6 - 15 Standard Terminology Relating to Methods of Mechanical Testing. Standard Terminology Relating to Methods of Mechanical Testing*.
- . 2014b. *Standard Practice for Rubber—Standard Conditions for Testing* ASTM International.
- Bauman, Judson T. 2008. *Fatigue, Stress, and Strain of Rubber Components - A Guide for Design Engineers* Hanser Publishers.
- Bhowmick, Anil K. 2008. *Current Topics in Elastomers Research*. Boca Raton, FL: CRC Press.
- Blaine, David G. 1980. *Modern Freight Car Air Brakes*. New York: Simmons-Boardman.

- Brandrup, J., Edmund H. Immergut, Eric A. Grulke, Akihiro Abe, and Daniel R. Bloch. 1999. *Polymer Handbook (4th Edition)* John Wiley & Sons.
- Brown, Roger. 2006. *Physical Testing of Rubber*. 4th ed. New York: Springer.
- . 2001. *Practical Guide to the Assessment of the Useful Life of Rubbers* Shrewsbury, U.K. : Rapra Technology, 2001.
- Bukhina, M. F. and S. K. Kurlyand. 2007. *Low-Temperature Behaviour of Elastomers*. New Concepts in Polymer Science. [Morozostoikost' elastomero. English]. Vol. 31. Leiden ;Boston: Vsp.
- Callister, William D. and David G. Rethwisch. 2014. *Materials Science and Engineering : An Introduction*. 9th ed. Hoboken, NJ; Ic©2014: Wiley.
- Canada Rubber Group Inc. "Preventive Maintenance: Gasket Failures." Canada Rubber Group Inc., last modified January 21, 2015, accessed June/2017, 2017, <http://www.canadarubbergroup.com/preventive-maintenance-gasket-failures/>.
- Coveney, V. A. and R. Rizk. 2006. "Chapter 9 - Life Prediction of O-Rings used to Seal Gases." In *Elastomers and Components*, edited by V. A. Coveney, 141-151: Woodhead Publishing.
- CRC Industries. "Air Brake Anti Freeze - CRC Industries.", last modified 03-24-2015, accessed 05/10, 2017, <http://www.crcindustries.com/products/air-brake-anti-freeze-32-fl-oz-05532.html>.
- Daley, J. R. 2006. "Chapter 4 - Assessment of Life Prediction Methods for Elastomeric Seals – A Review." In *Elastomers and Components*, edited by V. A. Coveney, 51-58: Woodhead Publishing.
- Deveau, Scott. "How Long can Trains Go?" National Post, last modified Feb 26, 2011 1:51 PM, accessed 12/20, 2017, <http://www.nationalpost.com/long+trains/4348592/story.html>.
- Dick, John S. 2003. *Basic Rubber Testing - Selecting Methods for A Rubber Test Program: (MNL 39)* ASTM International.
- . 2014. *Rubber Technology - Compounding and Testing for Performance (2nd Edition)* Hanser Publishers.
- Dilich, M., J. Goebelbecker, and D. Kopernik. 2002. "Gladhands - an Achilles Heel in Truck Air Brakes." *Safety Brief - Triodyne Inc* 22 (2).
- Dr Premamoy Ghosh, Ph D. 2011. *Polymer Science and Technology: Plastics, Rubbers, Blends and Composites, Third Edition*. 2011 McGraw Hill Education (India) Private Limited ed. McGraw-Hill Education: New York, Chicago, San Francisco, Athens, London, Madrid, Mexico City, Milan, New Delhi, Singapore, Sydney, Toronto.
- Dupont Dow Elastomers. 2001. *Selecting the Best Elastomer : New Applications , Process Changes, Failure Analysis a Methodology for Chemical and Hydrocarbon Process Engineers*. S. 1:.
- E.I. du Pont de Nemours & Company. 1963. *The Language of Rubber*. Rev ed. Wilmington, Del.: E.I. du Pont de Nemours & Co.

- Fediuc Oanea, Daniela, Mihai Budescu, Vlad Fediuc, and Vasile-Mircea Venghiac. 2013. "Compression Modulus of Elastomers." *Fascicle: 2 LIX (LXIII)*: 157-166.
- Fishman, K. and D. Machmer. 1994. "Testing Techniques for Measurement of Bulk Modulus." .
- Gent, Alan N. 2012. *Engineering with Rubber - how to Design Rubber Components (3rd Edition)* Hanser Publishers.
- Ghosh, Premamoy. 2011. *Polymer Science and Technology*. New York, N.Y.: McGraw-Hill Education LLC.
- Gnehm Haertepruefe. "Gnehm Haertepruefe Products. Shore.", last modified 2014, accessed 07/2017, 2017, <http://www.gnehm-haertepruefer.ch/#screen3>.
- Government of Canada. "Canadian Climate Normals 1981-2010 Station Data.", last modified 2017-06-01, accessed 09/30, 2017, [http://climate.weather.gc.ca/climate\\_normals/results\\_1981\\_2010\\_e.html?stnID=5415&lang=e&StationName=Montreal&SearchType=Contains&stnNameSubmit=go&dCode=1](http://climate.weather.gc.ca/climate_normals/results_1981_2010_e.html?stnID=5415&lang=e&StationName=Montreal&SearchType=Contains&stnNameSubmit=go&dCode=1).
- Grelle, Tobias, Dietmar Wolff, and Matthias Jaunich. 2017. *Leakage Behaviour of Elastomer Seals Under Dynamic Unloading Conditions at Low Temperatures*. Vol. 58.
- Grellmann, Wolfgang and Sabine Seidler. 2013. "Mechanical Properties of Polymers." In *Polymer Testing (Second Edition)*, edited by Wolfgang Grellmann, , and Sabine Seidler, 73-231: Hanser.
- H. Li, W. Cui, W. Guo, and T. Yu. 2012. "The Failure Mode Analysis for a Hydraulic System and Sealing Gasket Design." .
- Halliday, David, Robert Resnick, and Jearl Walker. 2005. *Fundamentals of Physics*. 12-7 Elasticity. 7th ed ed. Hoboken, NJ : Wiley, 2005].
- Hertzberg, Richard W., Richard Paul Vinci, and Jason L. Hertzberg. 2012. *Deformation and Fracture Mechanics of Engineering Materials*. Fifth ed. Hoboken, NJ: John Wiley & Sons, Inc.
- Hibbeler, R. C. 2014. *Mechanics of Materials*. 9th ed. Upper Saddle River, N.J.: Prentice Hall.
- Hua, L., L. Hixon, and G. Cobden. 2006. "Hose Strap Reaction Forces in Railroad Freight Cars." Web Portal ASME (American Society of Mechanical Engineers), 2006.
- ISO. 2015. *ISO 18517 - Rubber, vulcanized or thermoplastic - Hardness testing - Introduction and guide - Second Edition*.
- . 2016. *ISO 18898 Rubber — Calibration and Verification of Hardness Testers*.
- . 2010a. *ISO 48, Rubber, Vulcanized Or Thermoplastic — Determination of Hardness (Hardness between 10 IRHD and 100 IRHD)*.
- . 2010b. *ISO 7619-1 - Rubber, Vulcanized Or Thermoplastic — Determination of Indentation Hardness — Part 1: Durometer Method (Shore Hardness) - Second Edition*.



- . 2010c. *ISO 7619-2 Rubber, Vulcanized Or Thermoplastic — Determination of Indentation Hardness — Part 2: IRHD Pocket Meter Method* ISO - International Organization for Standardization.
- . 2017. *ISO 7743 Rubber, Vulcanized Or Thermoplastic — Determination of Compression Stress-Strain Properties*.
- . 2014. *Iso 815-2. Rubber, Vulcanized Or Thermoplastic -- Determination of Compression Set -- Part 2: At Low Temperatures*.
- Jardine, A. K. S. and Albert H. C. Tsang. 2013. *Maintenance, Replacement, and Reliability : Theory and Applications*. Dekker Mechanical Engineering. Second ed. Boca Raton: CRC Press, Taylor & Francis.
- Jaunich, Matthias, Wolfgang Stark, and Dietmar Wolff. 2010. *A New Method to Evaluate the Low Temperature Function of Rubber Sealing Materials*. Vol. 29.
- Jimenez, E., Munn, C. and Hua, L. "Glad Hand Fitting and Gasket for Railroad Car Brake Hose." Google Patents, last modified 11/22, accessed 04/17, 2017, <https://www.google.com/patents/US20100237569>.
- Jimenez, Edgardo, Lin Hua, Michelle Monear, and Kevin Nilson. 2010. "Root Cause of Undesired Hose Separations and a Solution." American Society of Mechanical Engineers, 2009.
- Johnson, T. C. "Gasket for use with an Air Brake Hose Coupling Member." Google Patents, last modified 09/18, accessed 04/23, 2017, <https://www.google.ca/patents/US6290238>.
- Kim, Jaehoon, Hyun-Yong Jeong, Jun-Seo Park, and Dong-Wook Cha. 2009. "The Study on the Evaluation of Failure Consequence and the Adequacy Ofmaintenance Task for the Air Brake System of a Railroad Vehicle." IEEE Computer Society, 2009.
- Kingsley, Eliot. 2012. *Predictive Asset Management* Society of Petroleum Engineers.
- Kleen-flo. "Safe-T-Brake™ Air Brake Anti-Freeze.", last modified January 2, 2015, accessed 05/20, 2016, <http://www.kleenflo.com/products/509-510-511-513.html>.
- Kuehl, R. O. 2000. *Design of Experiments : Statistical Principles of Research Design and Analysis*. Pacific Grove, CA: Duxbury/Thomson Learning.
- Kunz, J. and M. Studer. 2006. "Determining the Modulus of Elasticity in Compression Via Shore-a Hardness." *Kunststoffe International* 96 (6): 92-94.
- Lipsett, M. G. 2011. "Reliability and Maintenance of Bitumen Production Operations." Chap. 13, In *Handbook on Theory and Practice of Bitumen Recovery from Athabasca Oil Sands*, edited by Jacob H. Masliyah, Z. Xu, Jan A. Czarnecki and Marta Dabros, 1301-1358: Cochrane, Alta. : Kingsley Knowledge Pub., c2011-2013.

- Marghoub Shadkar, A., M. T. Hendry, and M. G. Lipsett. 2015. "Wayside Wheel Temperature Detector Data Mining to Predict Potential Sensor and Railcar Component Failures." Society for Machinery Failure Prevention Technology, 2015.
- Marghoub Shadkar, Azadeh. 2016. "Reliability Study and Maintenance Decision Making of Wheel Temperature Detectors." University of Alberta.
- Mark, James E., Burak Erman, and F. R. Eirich. 1994. *Science and Technology of Rubber*. San Diego: Academic Press.
- McDonald, Allan J. and James R. Hansen. 2009. *Truth, Lies, and O-Rings : Inside the Space Shuttle Challenger Disaster*. Gainesville: University Press of Florida.
- McKeen, Laurence W. 2014. *Effect of Temperature and Other Factors on Plastics and Elastomers (3rd Edition)* Elsevier.
- Mix, A. W. and A. J. Giacomini. 2011. "Standardized Polymer Durometry." *Journal of Testing and Evaluation* 39 (4).
- Mykin Inc. "Rubber Properties.", last modified 2017, accessed 09/30, 2017, <http://mykin.com/rubber-properties>.
- Nabil, H., H. Ismail, and A. R. Azura. 2013. *Compounding, Mechanical and Morphological Properties of Carbon-Black-Filled Natural Rubber/Recycled Ethylene-Propylene-Diene-Monomer (NR/R-EPDM) Blends*. Vol. 32.
- National Aeronautics and Space Administration. "Report of the PRESIDENTIAL COMMISSION on the Space Shuttle Challenger Accident.", last modified 2010-12-08.
- New York Air Brake. "TG-020 Cold Loc Wide Lip Glad-Hand Gasket Technical Guide.", last modified 2017/2017.
- Niesse, J. E. 1994. *A New Chemical Test Method for Plastics and Elastomers*; . United States: NACE International, Houston, TX (United States).
- Niesse, John E. 1995. "New Chemical Test Method for Plastics and Elastomers." *Materials Performance* 34 (3): 24-29.
- Oanea Fediuc, Daniela, Mihai Budescu, Vlad Fediuc, and Vasile-Mircea Venghiac. 2013. "Compression Modulus of Elastomers." *Bulletin of the Polytechnic Institute of Iasi - Construction & Architecture Section* 63 (2): 157-166.
- Plummer, C. J. G. 2014. "1.03 - Testing of Polymeric Materials." In *Comprehensive Materials Processing*, edited by Saleem Hashmi, Gilmar Ferreira Batalha, Chester J. Van Tyne and Bekir Yilbas, 35-70. Oxford: Elsevier.
- Poddar, V. 2014. "Reliability Centered Maintenance (RCM) and Ultrasonic Leakage Detection (ULD) as a Maintenance and Condition Monitoring Technique for Freight Rail Airbrakes in Cold Weather Conditions." University of Alberta.

- Popa, Gabriel A. 2011. *Rubber : Types, Properties, and Uses*. New York: Nova Science Publishers, Inc.
- Przybylo, P. A. and E. M. Arruda. 1998. "Experimental Investigations and Numerical Modeling of Incompressible Elastomers during Non-Homogeneous Deformations." *Rubber Chemistry and Technology* 71 (4): 730.
- Sammon, Devin and Gerald Anderson. 2015. "Testing to Correlate Gasket Stiffness and Separation Force." *Transportation Technology Center, Inc. Technology Digest* 15 (TD-15-016).
- Schnabel, W. 1981. *Polymer Degradation : Principles and Practical Applications*. Munich, West Germany: Hanser ;New York, N.Y.
- Shao, Y. and R. Kang. 2014. "A Life Prediction Method for O-Ring Static Seal Structure Based on Physics of Failure." doi:10.1109/PHM.2014.6988124.
- Shu, H. P., C. Takao, and N. Akbar. 1994. "Measurement of Elastomers Bulk Modulus by Means of a Confined Compression Test." *Rubber Chemistry and Technology* 67 (5): 871-879.
- Smith, Edward H. 1998. "7. Materials, Properties and Selection." Chap. 7, In *Mechanical Engineer's Reference Book (12th Edition)*, 7/3: Elsevier.
- Sommer, John G. 2009. *Engineered Rubber Products : Introduction to Design, Manufacture and Testing*. Munich ;Cincinnati: Hanser.
- Strobl, Gert R. 2007. *The Physics of Polymers : Concepts for Understanding their Structures and Behavior*. rev and expand ed. Berlin ;New York: Springer.
- Transport Canada. "Railway Freight and Passenger Train Brake Inspection and Safety Rules.", last modified 2017-12-05, accessed 12-10, 2017, <https://www.tc.gc.ca/eng/railsafety/rules-tco0184-137.htm>.
- Transportation Safety Board of Canada. "Transportation Safety Board of Canada - Rail.", last modified 2016-09-09, accessed 07/10, 2017, <http://www.tsb.gc.ca/eng/rail/index.asp>.
- Treloar, L. R. G. 2005. *The Physics of Rubber Elasticity*. Oxford Classic Texts in the Physical Sciences.
- Vaghar Anzabi, Roya. 2015. "Haul Truck Tire Reliability and Condition Monitoring." University of Alberta.
- Warren, P. 2012. "Extrusion Resistance of Elastomers: A Study of Factors that Affect Performance." Copthorne Hotel Aberdeen, UL, Smithers Rapra, 17-18 April.
- Weise, H-P, H. Kowalewsky, and R. Wenz. 1992. *Behaviour of Elastomeric Seals at Low Temperature*. Vol. 43.
- Woo, C. S., S. S. Choi, S. B. Lee, and H. S. Kim. 2010. "Useful Lifetime Prediction of Rubber Components using Accelerated Testing." *IEEE Transactions on Reliability* 59 (1): 11-17. doi:10.1109/TR.2010.2042103.

- Yeoh, O. H. 2006. "Chapter 6 - Strain Energy Release Rates for some Classical Rubber Test Pieces by Finite Element Analysis." In *Elastomers and Components*, edited by V. A. Coveney, 75-89: Woodhead Publishing.
- . 1987. *A Method for the Routine Determination of Compression Modulus of Rubber Vulcanizates*. Vol. 7.
- Young-Doo, Kwon, Roh Kwon-Taek, Kim Sung-Soo, and Doh Jae-Hyeok. 2014. "Regression of the Recovery Rate of ACM Rubber Gasket for Long-Term Performances." *Journal of Testing and Evaluation* 42 (3).
- Zeng, Z. G., Y. X. Chen, and R. Kang. 2013. *The Effects of Material Degradation on Sealing Performances of O-Rings*. Applied Mechanics and Materials. Vol. 328.



## Appendices

Here is include the curve fit and goodness-of-fit results in MATLAB for Gaussian 1 curve (Normal distribution). The mean (b1), standard deviation (c1), and the coefficient of determination (rsquare) were the results of interest.

### **MATLAB Current material, EPDM, and CR Hardness data goodness-of-fit test for a Gaussian 1 (Normal Distribution) fitted curve results**

#### Current material Hardness @ Room Temperature

General model Gauss1:

$$\text{curvefit1}(x) = a1 * \exp(-((x-b1)/c1)^2)$$

Coefficients (with 95% confidence bounds):

$$a1 = 65.25 \quad (43.04, 87.46)$$

$$b1 = 82.3 \quad (81.93, 82.66)$$

$$c1 = 1.317 \quad (0.794, 1.84)$$

gof1 =

struct with fields:

sse: 58.0511

rsquare: 0.9775

dfe: 2

adjrsquare: 0.9551

rmse: 5.3875

#### Current material Hardness @ Cold Temperature

General model Gauss1:

$$\text{curvefit2}(x) = a1 * \exp(-((x-b1)/c1)^2)$$

Coefficients (with 95% confidence bounds):

$$a1 = 69.77 \quad (62.44, 77.09)$$

$$b1 = 93.91 \quad (93.8, 94.01)$$

$$c1 = 1.197 \quad (1.056, 1.339)$$

gof2 =

struct with fields:

sse: 16.6288

rsquare: 0.9954

dfe: 3

adjrsquare: 0.9923

rmse: 2.3543

#### EPDM Hardness @ Room Temperature

General model Gauss1:

$$\text{curvefit3}(x) = a1 * \exp(-((x-b1)/c1)^2)$$

Coefficients (with 95% confidence bounds):

a1 = 80.5 (67.08, 93.91)  
b1 = 79.43 (79.31, 79.55)  
c1 = 1.047 (0.8288, 1.265)

gof3 =

struct with fields:

sse: 13.5681  
rsquare: 0.9966  
dfe: 2  
adjrsquare: 0.9931  
rmse: 2.6046

#### EPDM Hardness @ Cold Temperature

General model Gauss1:

$$\text{curvefit4}(x) = a1 * \exp(-((x-b1)/c1)^2)$$

Coefficients (with 95% confidence bounds):

a1 = 66.51 (60.25, 72.76)  
b1 = 93.99 (93.89, 94.09)  
c1 = 1.287 (1.15, 1.425)

gof4 =

struct with fields:

sse: 4.6546  
rsquare: 0.9982  
dfe: 2  
adjrsquare: 0.9965  
rmse: 1.5256

#### CR Hardness @ Room Temperature

General model Gauss1:

$$\text{curvefit5}(x) = a1 * \exp(-((x-b1)/c1)^2)$$

Coefficients (with 95% confidence bounds):

a1 = 55.58 (34.61, 76.54)  
b1 = 73.43 (72.99, 73.87)  
c1 = 1.443 (0.795, 2.09)

gof5 =

struct with fields:

sse: 153.5586  
rsquare: 0.9225

dfc: 3  
adjrsquare: 0.8709  
rmse: 7.1545


### CR Hardness @ Cold Temperature

General model Gauss1:  
 $\text{curvefit6}(x) = a1 * \exp(-((x-b1)/c1)^2)$   
Coefficients (with 95% confidence bounds):  
a1 = 45.62 (30.24, 61)  
b1 = 83.06 (82.54, 83.58)  
c1 = 1.892 (1.108, 2.677)


gof6 =


struct with fields:

sse: 107.0088  
rsquare: 0.9161  
dfc: 3  
adjrsquare: 0.8602  
rmse: 5.9724


Airbrake Elastomeric Gasket - Durometer Hardness Report																
Test Details		Test results														
Date of Test:	20-Jun-17	Sample	Thickness [in] - ASTM D3767					Hardness [Shore A]								Time [s]
Relative Humidity [%]:	50	ID No	h <sub>1</sub>	h <sub>2</sub>	h <sub>3</sub>	σ <sub>s</sub>	MEDIAN	H <sub>1</sub>	H <sub>2</sub>	H <sub>3</sub>	H <sub>4</sub>	H <sub>5</sub>	σ <sub>s</sub>	μ <sub>s</sub>	t	Reading
Test Temperature [°C]:	23	1	0.348	0.348	0.347	0.0006	0.348	81	81	82	82	82	0.55	81.6	3	A/81/3
Deviations:		2	0.344	0.345	0.344	0.0006	0.344	82	82	82	81	83	0.71	82.0	3	A/82/3
Gasket product specimen. The lateral dimensions of all specimens were not enough to attain the minimum 12.0 mm from any edge as per ASTM D2240.		3	0.343	0.342	0.343	0.0006	0.343	82	82	83	84	83	0.84	82.8	3	A/82/3
		4	0.342	0.342	0.342	0.0000	0.342	83	82	83	83	83	0.45	82.8	3	A/82/3
		5	0.343	0.344	0.342	0.0010	0.343	81	83	81	82	82	0.84	81.8	3	A/81/3
		6	0.343	0.343	0.344	0.0006	0.343	81	81	81	82	83	0.89	81.6	3	A/81/3
		7	0.344	0.345	0.344	0.0006	0.344	83	82	83	83	84	0.71	83.0	3	A/83/3
Durometer Details		8	0.341	0.340	0.340	0.0006	0.340	81	81	82	83	82	0.84	81.8	3	A/81/3
Manufacturer:	Gnehm Härteprüfer	9	0.350	0.349	0.348	0.0010	0.349	83	82	83	82	83	0.55	82.6	3	A/82/3
Type:	Shore A	10	0.345	0.345	0.344	0.0006	0.345	82	82	83	82	83	0.55	82.4	3	A/82/3
Serial Number:	24088	11	0.347	0.347	0.347	0.0000	0.347	83	82	81	83	82	0.84	82.2	3	A/82/3
Date of last calibration:	31-Dec-16	12	0.342	0.343	0.342	0.0006	0.342	82	81	81	81	80	0.71	81.0	3	A/81/3
Calibration due date:	31-Dec-17	13	0.344	0.344	0.345	0.0006	0.344	82	80	82	82	82	0.89	81.6	3	A/81/3
Means of testing:	Handheld	14	0.346	0.345	0.345	0.0006	0.345	83	81	81	82	81	0.89	81.6	3	A/81/3
Test method:	ASTM D2240	15	0.345	0.344	0.344	0.0006	0.344	83	83	83	83	84	0.45	83.2	3	A/83/3
Test pieces details		16	0.344	0.343	0.345	0.0010	0.344	82	82	83	83	82	0.55	82.4	3	A/82/3
No of pcs plied :	1	17	0.348	0.349	0.347	0.0014	0.348	83	82	83	82	83	0.55	82.6	3	A/82/3
Vulcanization date:	Unknown	18	0.342	0.343	0.343	0.0006	0.343	83	82	83	82	83	0.55	82.6	3	A/82/3
Material tested:	Elastomer	19	0.342	0.342	0.342	0.0000	0.342	81	82	81	83	82	0.84	81.8	3	A/81/3
Origin:	CP Edmonton Shop	20	0.344	0.342	0.343	0.0010	0.343	83	83	81	83	82	0.89	82.4	3	A/82/3
Full description:		21	0.343	0.344	0.343	0.0006	0.343	82	82	81	81	80	0.84	81.2	3	A/81/3
Standard gasket geomtry, AAR Specification M602 dimensions allowing more than 6.00 mm of measurement point radius (ASTM D2240 requirement). The gasket was placed on a flat surface as shown below; the arrow marks a measurement point example: 		22	0.350	0.350	0.349	0.0006	0.350	84	82	82	82	82	0.89	82.4	3	A/82/3
		23	0.345	0.345	0.345	0.0000	0.345	83	82	81	82	81	0.84	81.8	3	A/81/3
		24	0.347	0.347	0.347	0.0000	0.347	83	83	83	83	84	0.45	83.2	3	A/83/3
		25	0.342	0.342	0.343	0.0006	0.342	82	82	83	83	82	0.55	82.4	3	A/82/3
		26	0.344	0.345	0.344	0.0006	0.344	83	82	84	82	83	0.84	82.8	3	A/82/3
		27	0.345	0.345	0.344	0.0006	0.345	82	80	82	82	82	0.89	81.6	3	A/81/3
		28	0.344	0.344	0.343	0.0006	0.344	83	81	81	82	81	0.89	81.6	3	A/81/3
		29	0.343	0.345	0.344	0.0010	0.344	83	83	83	83	84	0.45	83.2	3	A/83/3
		30	0.349	0.347	0.348	0.0010	0.348	82	82	83	83	82	0.55	82.4	3	A/82/3

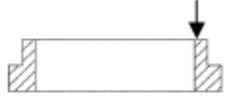


Airbrake Elastomeric Gasket - Durometer Hardness Report																
Test Details			Test results													
Date of Test:	20-Jun-17	Sample	Thickness [in] - ASTM D3767					Hardness [Shore A]						Time [s]	Reading	
Relative Humidity [%]:	50	ID No	h <sub>1</sub>	h <sub>2</sub>	h <sub>3</sub>	σ <sub>s</sub>	MEDIAN	H <sub>1</sub>	H <sub>2</sub>	H <sub>3</sub>	H <sub>4</sub>	H <sub>5</sub>	σ <sub>s</sub>	μ <sub>s</sub>	t	
Test Temperature [°C]:	-40	1	0.348	0.348	0.347	0.0006	0.348	92	93	94	94	93	0.84	93.2	3	A/93/3
Deviations:		2	0.344	0.345	0.344	0.0006	0.344	94	93	93	93	95	0.89	93.6	3	A/93/3
Gasket product specimen. The lateral dimensions of all specimens were not enough to attain the minimum 12.0 mm from any edge as per ASTM D2240.		3	0.343	0.342	0.343	0.0006	0.343	94	94	94	96	95	0.89	94.6	3	A/94/3
		4	0.342	0.342	0.342	0.0000	0.342	94	94	94	94	93	0.45	93.8	3	A/93/3
		5	0.343	0.344	0.342	0.0010	0.343	93	94	92	94	94	0.89	93.4	3	A/93/3
		6	0.343	0.343	0.344	0.0006	0.343	93	93	93	93	94	0.45	93.2	3	A/93/3
		7	0.344	0.345	0.344	0.0006	0.344	95	93	95	94	95	0.89	94.4	3	A/94/3
Durometer Details		8	0.341	0.340	0.340	0.0006	0.340	92	93	94	94	94	0.89	93.4	3	A/93/3
Manufacturer:	Gnehm Härteprüfer	9	0.350	0.349	0.348	0.0010	0.349	94	93	95	93	94	0.84	93.8	3	A/93/3
Type:	Shore A	10	0.345	0.345	0.344	0.0006	0.345	94	94	95	93	95	0.84	94.2	3	A/94/3
Serial Number:	24088	11	0.347	0.347	0.347	0.0000	0.347	95	94	93	94	94	0.71	94.0	3	A/94/3
Date of last calibration:	31-Dec-16	12	0.342	0.343	0.342	0.0006	0.342	94	92	93	93	92	0.84	92.8	3	A/92/3
Calibration due date:	31-Dec-17	13	0.344	0.344	0.345	0.0006	0.344	93	93	94	93	94	0.55	93.4	3	A/93/3
Means of testing:	Handheld	14	0.346	0.345	0.345	0.0006	0.345	95	94	93	94	94	0.71	94.0	3	A/94/3
Test method:	ASTM D2240	15	0.345	0.344	0.344	0.0006	0.344	95	94	95	94	95	0.55	94.6	3	A/94/3
Test pieces details		16	0.344	0.343	0.345	0.0010	0.344	94	93	94	95	94	0.71	94.0	3	A/94/3
No of pcs plied :	1	17	0.348	0.349	0.347	0.0014	0.348	94	94	95	94	95	0.55	94.4	3	A/94/3
Vulcanization date:	Unknown	18	0.342	0.343	0.343	0.0006	0.343	95	94	94	94	95	0.55	94.4	3	A/94/3
Material tested:	Elastomer	19	0.342	0.342	0.342	0.0000	0.342	92	94	93	94	94	0.89	93.4	3	A/93/3
Origin:	CP Edmonton Shop	20	0.344	0.342	0.343	0.0010	0.343	94	94	93	94	94	0.45	93.8	3	A/93/3
Full description:		21	0.343	0.344	0.343	0.0006	0.343	93	93	92	92	91	0.84	92.2	3	A/92/3
Standard gasket geomtry, AAR Specification M602 dimensions allowing more than 6.00 mm of measurement point radius (ASTM D2240 requirement). The gasket was placed on a flat surface as shown below; the arrow marks a measurement point example: 		22	0.350	0.350	0.349	0.0006	0.350	95	94	94	94	94	0.45	94.2	3	A/94/3
		23	0.345	0.345	0.345	0.0000	0.345	95	94	94	93	93	0.84	93.8	3	A/93/3
		24	0.347	0.347	0.347	0.0000	0.347	94	95	94	94	96	0.89	94.6	3	A/94/3
		25	0.342	0.342	0.343	0.0006	0.342	93	93	94	95	93	0.89	93.6	3	A/93/3
		26	0.344	0.345	0.344	0.0006	0.344	95	93	95	94	95	0.89	94.4	3	A/94/3
		27	0.345	0.345	0.344	0.0006	0.345	93	92	94	94	94	0.89	93.4	3	A/93/3
		28	0.344	0.344	0.343	0.0006	0.344	95	93	94	94	93	0.84	93.8	3	A/93/3
		29	0.343	0.345	0.344	0.0010	0.344	94	95	94	95	95	0.55	94.6	3	A/94/3
		30	0.349	0.347	0.348	0.0010	0.348	94	93	95	94	94	0.71	94.0	3	A/94/3

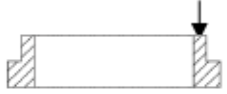
Airbrake Elastomeric Gasket - Durometer Hardness Report																
Test Details			Test results													
Date of Test:	20-Jun-17	Sample	Thickness [in] - ASTM D3767					Hardness [Shore A]						Time [s]	Reading	
Relative Humidity [%]:	50	ID No	h <sub>1</sub>	h <sub>2</sub>	h <sub>3</sub>	σ <sub>s</sub>	MEDIAN	H <sub>1</sub>	H <sub>2</sub>	H <sub>3</sub>	H <sub>4</sub>	H <sub>5</sub>	σ <sub>s</sub>	μ <sub>s</sub>	t	
Test Temperature [°C]:	23	1	0.330	0.328	0.332	0.0020	0.330	80	80	80	79	80	0.45	79.8	3	A/79/3
Deviations:		2	0.330	0.331	0.332	0.0010	0.331	81	80	81	80	80	0.55	80.4	3	A/80/3
Gasket product specimen. The lateral dimensions of all specimens were not enough to attain the minimum 12.0 mm from any edge as per ASTM D2240.		3	0.331	0.333	0.329	0.0020	0.331	80	79	79	80	80	0.55	79.6	3	A/79/3
		4	0.330	0.331	0.333	0.0015	0.331	79	80	80	80	79	0.55	79.6	3	A/79/3
		5	0.329	0.328	0.332	0.0021	0.329	80	80	79	80	80	0.45	79.8	3	A/79/3
		6	0.330	0.331	0.329	0.0010	0.330	80	80	80	80	79	0.45	79.8	3	A/79/3
		7	0.330	0.329	0.333	0.0021	0.330	81	80	80	80	81	0.55	80.4	3	A/80/3
Durometer Details		8	0.328	0.331	0.331	0.0017	0.331	80	80	80	81	80	0.45	80.2	3	A/80/3
Manufacturer:	Gnehm Härteprüfer	9	0.330	0.334	0.335	0.0026	0.334	80	80	80	81	80	0.45	80.2	3	A/80/3
Type:	Shore A	10	0.330	0.327	0.330	0.0017	0.330	79	80	80	80	80	0.45	79.8	3	A/79/3
Serial Number:	24088	11	0.326	0.332	0.330	0.0031	0.330	80	80	79	80	80	0.45	79.8	3	A/79/3
Date of last calibration:	31-Dec-16	12	0.330	0.329	0.329	0.0006	0.329	80	80	80	80	78	0.89	79.6	3	A/79/3
Calibration due date:	31-Dec-17	13	0.330	0.330	0.331	0.0006	0.330	80	80	80	79	80	0.45	79.8	3	A/79/3
Means of testing:	Handheld	14	0.318	0.325	0.320	0.0036	0.320	78	80	79	80	80	0.89	79.4	3	A/79/3
Test method:	ASTM D2240	15	0.326	0.331	0.329	0.0025	0.329	79	80	80	80	80	0.45	79.8	3	A/79/3
Test pieces details		16	0.326	0.329	0.332	0.0030	0.329	79	79	79	78	79	0.45	78.8	3	A/78/3
No of pcs plied :	1	17	0.331	0.328	0.330	0.0015	0.330	80	79	80	79	79	0.55	79.4	3	A/79/3
Vulcanization date:	01-Jun-17	18	0.325	0.326	0.325	0.0006	0.325	79	78	78	79	79	0.55	78.6	3	A/78/3
Material tested:	EPDM	19	0.331	0.328	0.331	0.0017	0.331	78	79	79	79	78	0.55	78.6	3	A/78/3
Origin:	GEMMA plastics	20	0.331	0.332	0.332	0.0006	0.332	79	79	78	79	79	0.45	78.8	3	A/78/3
Full description:		21	0.331	0.332	0.328	0.0021	0.331	79	79	79	79	78	0.45	78.8	3	A/78/3
Simplified Standard gasket geometry, dimensions allowed more than 6.00 mm of measurement point radius (ASTM D2240 requirement). The gasket was placed on a flat surface as shown below; the arrow marks a measurement point example: 		22	0.329	0.332	0.334	0.0025	0.332	80	79	79	79	80	0.55	79.4	3	A/79/3
		23	0.330	0.327	0.331	0.0021	0.330	79	79	79	80	79	0.45	79.2	3	A/79/3
		24	0.330	0.331	0.328	0.0015	0.330	79	79	79	80	79	0.45	79.2	3	A/79/3
		25	0.331	0.330	0.334	0.0021	0.331	78	79	79	79	79	0.45	78.8	3	A/78/3
		26	0.327	0.332	0.331	0.0026	0.331	79	79	78	79	79	0.45	78.8	3	A/78/3
		27	0.329	0.334	0.335	0.0032	0.334	79	79	79	79	77	0.89	78.6	3	A/78/3
		28	0.331	0.326	0.329	0.0025	0.329	79	79	79	78	79	0.45	78.8	3	A/78/3
		29	0.325	0.333	0.330	0.0040	0.330	77	79	78	79	79	0.89	78.4	3	A/78/3
		30	0.331	0.330	0.329	0.0010	0.330	78	79	79	79	79	0.45	78.8	3	A/78/3



Airbrake Elastomeric Gasket - Durometer Hardness Report																
Test Details			Test results													
Date of Test:	20-Jun-17	Sample	Thickness [in] - ASTM D3767					Hardness [Shore A]						Time [s]	Reading	
Relative Humidity [%]:	50	ID No	h <sub>1</sub>	h <sub>2</sub>	h <sub>3</sub>	σ <sub>s</sub>	MEDIAN	H <sub>1</sub>	H <sub>2</sub>	H <sub>3</sub>	H <sub>4</sub>	H <sub>5</sub>	σ <sub>s</sub>	μ <sub>s</sub>	t	Reading
Test Temperature [°C]:	-40	1	0.330	0.328	0.332	0.0020	0.330	95	95	95	94	94	0.55	94.6	3	A/94/3
Deviations:		2	0.330	0.331	0.332	0.0010	0.331	95	94	96	95	95	0.71	95.0	3	A/95/3
Gasket product specimen. The lateral dimensions of all specimens were not enough to attain the minimum 12.0 mm from any edge as per ASTM D2240.		3	0.331	0.333	0.329	0.0020	0.331	95	93	94	94	95	0.84	94.2	3	A/94/3
		4	0.330	0.331	0.333	0.0015	0.331	94	95	94	95	94	0.55	94.4	3	A/94/3
		5	0.329	0.328	0.332	0.0021	0.329	94	95	94	94	94	0.45	94.2	3	A/94/3
		6	0.330	0.331	0.329	0.0010	0.330	95	95	94	95	93	0.89	94.4	3	A/94/3
		7	0.330	0.329	0.333	0.0021	0.330	96	94	95	95	95	0.71	95.0	3	A/95/3
Durometer Details		8	0.328	0.331	0.331	0.0017	0.331	95	94	94	96	95	0.84	94.8	3	A/94/3
Manufacturer:	Gnehm Härteprüfer	9	0.330	0.334	0.335	0.0026	0.334	95	95	95	96	94	0.71	95.0	3	A/95/3
Type:	Shore A	10	0.330	0.327	0.330	0.0017	0.330	94	94	95	95	95	0.55	94.6	3	A/94/3
Serial Number:	24088	11	0.326	0.332	0.330	0.0031	0.330	95	95	94	94	95	0.55	94.6	3	A/94/3
Date of last calibration:	31-Dec-16	12	0.330	0.329	0.329	0.0006	0.329	95	95	94	94	94	0.55	94.4	3	A/94/3
Calibration due date:	31-Dec-17	13	0.330	0.330	0.331	0.0006	0.330	94	95	95	93	94	0.84	94.2	3	A/94/3
Means of testing:	Handheld	14	0.318	0.325	0.320	0.0036	0.320	94	94	94	95	95	0.55	94.4	3	A/94/3
Test method:	ASTM D2240	15	0.326	0.331	0.329	0.0025	0.329	93	94	94	94	94	0.45	93.8	3	A/93/3
Test pieces details		16	0.326	0.329	0.332	0.0030	0.329	94	93	94	92	93	0.84	93.2	3	A/93/3
No of pcs plied :	1	17	0.331	0.328	0.330	0.0015	0.330	95	93	94	94	94	0.71	94.0	3	A/94/3
Vulcanization date:	01-Jun-17	18	0.325	0.326	0.325	0.0006	0.325	94	93	93	94	94	0.55	93.6	3	A/93/3
Material tested:	EPDM	19	0.331	0.328	0.331	0.0017	0.331	92	93	94	94	93	0.84	93.2	3	A/93/3
Origin:	GEMMA plastics	20	0.331	0.332	0.332	0.0006	0.332	93	94	93	93	93	0.45	93.2	3	A/93/3
Full description:		21	0.331	0.332	0.328	0.0021	0.331	94	93	94	93	93	0.55	93.4	3	A/93/3
Simplified Standard gasket geometry, dimensions allowed more than 6.00 mm of measurement point radius (ASTM D2240 requirement). The gasket was placed on a flat surface as shown below; the arrow marks a measurement point example: 		22	0.329	0.332	0.334	0.0025	0.332	95	93	94	94	94	0.71	94.0	3	A/94/3
		23	0.330	0.327	0.331	0.0021	0.330	94	93	94	94	94	0.45	93.8	3	A/93/3
		24	0.330	0.331	0.328	0.0015	0.330	94	93	93	95	94	0.84	93.8	3	A/93/3
		25	0.331	0.330	0.334	0.0021	0.331	92	93	93	94	93	0.71	93.0	3	A/93/3
		26	0.327	0.332	0.331	0.0026	0.331	94	93	93	93	94	0.55	93.4	3	A/93/3
		27	0.329	0.334	0.335	0.0032	0.334	94	93	93	94	93	0.55	93.4	3	A/93/3
		28	0.331	0.326	0.329	0.0025	0.329	94	94	93	92	93	0.84	93.2	3	A/93/3
		29	0.325	0.333	0.330	0.0040	0.330	92	94	93	94	94	0.89	93.4	3	A/93/3
		30	0.331	0.330	0.329	0.0010	0.330	92	93	94	93	93	0.71	93.0	3	A/93/3

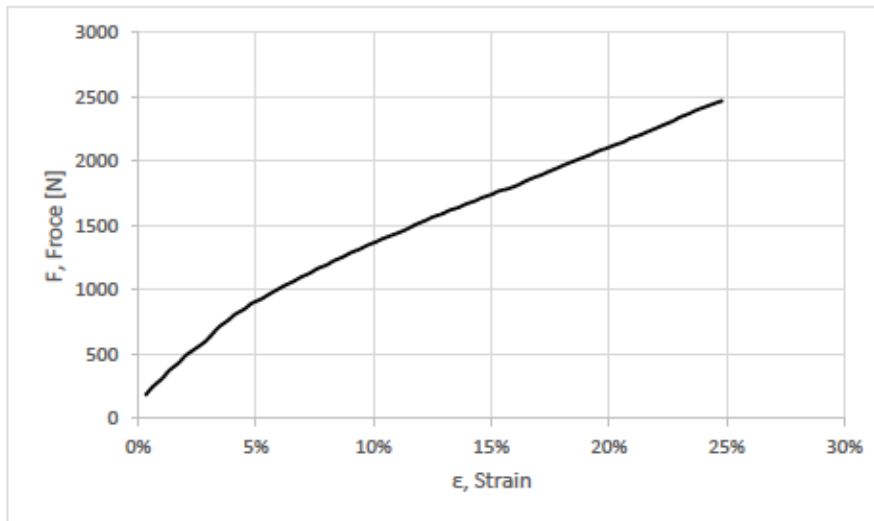
Airbrake Elastomeric Gasket - Durometer Hardness Report																
Test Details			Test results													
Date of Test:	20-Jun-17	Sample	Thickness [in] - ASTM D3767					Hardness [Shore A]						Time [s]	Reading	
Relative Humidity [%]:	50	ID No	h <sub>1</sub>	h <sub>2</sub>	h <sub>3</sub>	σ <sub>s</sub>	MEDIAN	H <sub>1</sub>	H <sub>2</sub>	H <sub>3</sub>	H <sub>4</sub>	H <sub>5</sub>	σ <sub>s</sub>	μ <sub>s</sub>	t	
Test Temperature [°C]:	23	1	0.307	0.301	0.314	0.0065	0.307	74	73	73	73	73	0.45	73.2	3	A/73/3
Deviations:		2	0.306	0.310	0.311	0.0026	0.310	75	74	75	74	74	0.55	74.4	3	A/74/3
Gasket product specimen. The lateral dimensions of all specimens were not enough to attain the minimum 12.0 mm from any edge as per ASTM D2240.		3	0.305	0.307	0.312	0.0036	0.307	74	74	74	74	75	0.45	74.2	3	A/74/3
		4	0.311	0.308	0.310	0.0015	0.310	73	74	74	73	73	0.55	73.4	3	A/73/3
		5	0.311	0.308	0.312	0.0021	0.311	74	74	75	74	74	0.45	74.2	3	A/74/3
		6	0.306	0.307	0.311	0.0026	0.307	74	74	75	74	73	0.71	74.0	3	A/74/3
		7	0.311	0.314	0.309	0.0025	0.311	74	73	74	73	73	0.55	73.4	3	A/73/3
Durometer Details		8	0.315	0.318	0.322	0.0035	0.318	75	73	74	73	74	0.84	73.8	3	A/73/3
Manufacturer:	Gnehm Härteprüfer	9	0.307	0.308	0.308	0.0006	0.308	74	75	74	73	74	0.71	74.0	3	A/74/3
Type:	Shore A	10	0.310	0.308	0.310	0.0012	0.310	74	75	75	74	74	0.55	74.4	3	A/74/3
Serial Number:	24088	11	0.311	0.310	0.309	0.0010	0.310	74	74	74	73	74	0.45	73.8	3	A/73/3
Date of last calibration:	31-Dec-16	12	0.313	0.311	0.308	0.0025	0.311	74	74	75	74	74	0.45	74.2	3	A/74/3
Calibration due date:	31-Dec-17	13	0.311	0.312	0.313	0.0010	0.312	73	72	72	73	74	0.84	72.8	3	A/72/3
Means of testing:	Handheld	14	0.310	0.307	0.308	0.0015	0.308	71	71	72	70	70	0.84	70.8	3	A/70/3
Test method:	ASTM D2240	15	0.308	0.311	0.312	0.0021	0.311	73	73	73	73	74	0.45	73.2	3	A/73/3
Test pieces details		16	0.310	0.311	0.312	0.0010	0.311	71	72	73	73	73	0.89	72.4	3	A/72/3
No of pcs plied :	1	17	0.306	0.300	0.314	0.0070	0.306	74	74	73	73	72	0.84	73.2	3	A/73/3
Vulcanization date:	01-Jun-17	18	0.307	0.310	0.310	0.0017	0.310	74	73	73	73	73	0.45	73.2	3	A/73/3
Material tested:	Chloroprene (CR)	19	0.304	0.306	0.313	0.0047	0.306	73	71	71	72	71	0.89	71.6	3	A/71/3
Origin:	GEMMA plastics	20	0.310	0.307	0.309	0.0015	0.309	72	72	72	71	71	0.55	71.6	3	A/71/3
Full description:		21	0.312	0.308	0.312	0.0023	0.312	71	72	73	73	73	0.89	72.4	3	A/72/3
Simplified Standard gasket geometry, dimensions allowed more than 6.00 mm of measurement point radius (ASTM D2240 requirement). The gasket was placed on a flat surface as shown below; the arrow marks a measurement point example: 		22	0.305	0.306	0.312	0.0038	0.306	74	74	75	74	73	0.71	74.0	3	A/74/3
		23	0.311	0.314	0.309	0.0025	0.311	73	73	73	75	74	0.89	73.6	3	A/73/3
		24	0.316	0.319	0.321	0.0025	0.319	74	73	72	72	73	0.84	72.8	3	A/72/3
		25	0.307	0.307	0.307	0.0000	0.307	70	71	71	72	70	0.84	70.8	3	A/70/3
		26	0.311	0.307	0.310	0.0021	0.310	72	73	73	73	72	0.55	72.6	3	A/72/3
		27	0.310	0.311	0.310	0.0006	0.310	73	71	72	73	73	0.89	72.4	3	A/72/3
		28	0.314	0.310	0.308	0.0031	0.310	75	74	74	73	73	0.84	73.8	3	A/73/3
		29	0.312	0.313	0.312	0.0006	0.312	75	74	73	74	74	0.71	74.0	3	A/74/3
		30	0.312	0.311	0.313	0.0010	0.312	72	73	71	71	72	0.84	71.8	3	A/71/3



Airbrake Elastomeric Gasket - Durometer Hardness Report																
Test Details			Test results													
Date of Test:	20-Jun-17	Sample	Thickness [in] - ASTM D3767					Hardness [Shore A]						Time [s]	Reading	
Relative Humidity [%]:	50	ID No	h <sub>1</sub>	h <sub>2</sub>	h <sub>3</sub>	σ <sub>s</sub>	MEDIAN	H <sub>1</sub>	H <sub>2</sub>	H <sub>3</sub>	H <sub>4</sub>	H <sub>5</sub>	σ <sub>s</sub>	μ <sub>s</sub>	t	Reading
Test Temperature [°C]:	-40	1	0.307	0.301	0.314	0.0065	0.307	85	84	85	84	83	0.84	84.2	3	A/84/3
Deviations:		2	0.306	0.310	0.311	0.0026	0.310	85	84	85	84	83	0.84	84.2	3	A/84/3
Gasket product specimen. The lateral dimensions of all specimens were not enough to attain the minimum 12.0 mm from any edge as per ASTM D2240.		3	0.305	0.307	0.312	0.0036	0.307	84	84	83	84	85	0.71	84.0	3	A/84/3
		4	0.311	0.308	0.310	0.0015	0.310	84	84	83	83	82	0.84	83.2	3	A/83/3
		5	0.311	0.308	0.312	0.0021	0.311	84	84	84	84	82	0.89	83.6	3	A/83/3
		6	0.306	0.307	0.311	0.0026	0.307	83	84	85	83	83	0.89	83.6	3	A/83/3
		7	0.311	0.314	0.309	0.0025	0.311	83	83	83	82	82	0.55	82.6	3	A/82/3
Durometer Details		8	0.315	0.318	0.322	0.0035	0.318	84	82	83	82	83	0.84	82.8	3	A/82/3
Manufacturer:	Gnehm Härteprüfer	9	0.307	0.308	0.308	0.0006	0.308	84	84	84	83	84	0.45	83.8	3	A/83/3
Type:	Shore A	10	0.310	0.308	0.310	0.0012	0.310	84	84	84	83	84	0.45	83.8	3	A/83/3
Serial Number:	24088	11	0.311	0.310	0.309	0.0010	0.310	84	84	83	82	83	0.84	83.2	3	A/83/3
Date of last calibration:	31-Dec-16	12	0.313	0.311	0.308	0.0025	0.311	83	84	85	84	84	0.71	84.0	3	A/84/3
Calibration due date:	31-Dec-17	13	0.311	0.312	0.313	0.0010	0.312	82	81	81	82	83	0.84	81.8	3	A/81/3
Means of testing:	Handheld	14	0.310	0.307	0.308	0.0015	0.308	81	81	82	80	80	0.84	80.8	3	A/80/3
Test method:	ASTM D2240	15	0.308	0.311	0.312	0.0021	0.311	83	84	83	82	83	0.71	83.0	3	A/83/3
Test pieces details		16	0.310	0.311	0.312	0.0010	0.311	81	83	82	83	83	0.89	82.4	3	A/82/3
No of pcs plied :	1	17	0.306	0.300	0.314	0.0070	0.306	83	84	82	83	82	0.84	82.8	3	A/82/3
Vulcanization date:	01-Jun-17	18	0.307	0.310	0.310	0.0017	0.310	83	83	84	84	83	0.55	83.4	3	A/83/3
Material tested:	Chloroprene (CR)	19	0.304	0.306	0.313	0.0047	0.306	82	81	81	82	80	0.84	81.2	3	A/81/3
Origin:	GEMMA plastics	20	0.310	0.307	0.309	0.0015	0.309	82	81	81	80	81	0.71	81.0	3	A/81/3
Full description:		21	0.312	0.308	0.312	0.0023	0.312	81	82	83	83	83	0.89	82.4	3	A/82/3
Simplified Standard gasket geometry, dimensions allowed more than 6.00 mm of measurement point radius (ASTM D2240 requirement). The gasket was placed on a flat surface as shown below; the arrow marks a measurement point example: 		22	0.305	0.306	0.312	0.0038	0.306	84	84	84	83	82	0.89	83.4	3	A/83/3
		23	0.311	0.314	0.309	0.0025	0.311	85	84	84	85	83	0.84	84.2	3	A/84/3
		24	0.316	0.319	0.321	0.0025	0.319	84	82	82	82	82	0.89	82.4	3	A/82/3
		25	0.307	0.307	0.307	0.0000	0.307	80	80	81	81	80	0.55	80.4	3	A/80/3
		26	0.311	0.307	0.310	0.0021	0.310	82	83	84	83	82	0.84	82.8	3	A/82/3
		27	0.310	0.311	0.310	0.0006	0.310	83	82	82	82	82	0.45	82.2	3	A/82/3
		28	0.314	0.310	0.308	0.0031	0.310	85	83	84	83	83	0.89	83.6	3	A/83/3
		29	0.312	0.313	0.312	0.0006	0.312	84	83	82	84	83	0.84	83.2	3	A/83/3
		30	0.312	0.311	0.313	0.0010	0.312	82	82	81	80	81	0.84	81.2	3	A/81/3

Data	Acquisition	Time:	102.428	Sec	23-Jun-17	11:35:42	AM
Axial Load	Axial Stroke	Time	Strain	Axial Load	Original thickness $h_0$ [mm]	$\Delta L$ @ $\epsilon \approx 25\%$ [mm]	
N	mm	Sec	$\epsilon$	N, no sign	4.758	-1.190	
-179.056	-0.014	0.203	0.003	179.056	$F_{N@25\%} = S_{c@25\%}$ [N]		
-241.825	-0.030	0.303	0.006	241.825	2467		
-306.285	-0.047	0.403	0.010	306.285			
-368.347	-0.063	0.503	0.013	368.347			
-427.375	-0.080	0.603	0.017	427.375			
-485.479	-0.097	0.703	0.020	485.479			
-537.052	-0.113	0.803	0.024	537.052			
-589.708	-0.131	0.903	0.028	589.708			
-644.961	-0.146	1.002	0.031	644.961			
-704.744	-0.164	1.102	0.034	704.744			
-759.274	-0.180	1.202	0.038	759.274			
-805.630	-0.197	1.302	0.041	805.630			
-847.284	-0.214	1.402	0.045	847.284			
-890.288	-0.230	1.502	0.048	890.288			
-923.813	-0.246	1.602	0.052	923.813			
-967.757	-0.264	1.702	0.056	967.757			
-998.263	-0.280	1.802	0.059	998.263			
-1029.268	-0.296	1.902	0.062	1029.268			
-1063.733	-0.313	2.002	0.066	1063.733			
-1094.780	-0.329	2.102	0.069	1094.780			
-1128.176	-0.347	2.202	0.073	1128.176			
-1161.265	-0.364	2.302	0.076	1161.265			
-1190.995	-0.380	2.402	0.080	1190.995			
-1222.648	-0.396	2.501	0.083	1222.648			
-1253.740	-0.413	2.601	0.087	1253.740			
-1283.902	-0.430	2.701	0.090	1283.902			
-1313.173	-0.448	2.801	0.094	1313.173			
-1340.886	-0.463	2.901	0.097	1340.886			
-1370.590	-0.480	3.001	0.101	1370.590			
-1396.053	-0.496	3.101	0.104	1396.053			
-1423.609	-0.514	3.201	0.108	1423.609			
-1451.726	-0.531	3.301	0.112	1451.726			
-1477.605	-0.547	3.401	0.115	1477.605			
-1506.293	-0.564	3.501	0.118	1506.293			
-1536.703	-0.580	3.601	0.122	1536.703			
-1563.107	-0.596	3.701	0.125	1563.107			
-1587.091	-0.612	3.801	0.129	1587.091			
-1613.834	-0.630	3.901	0.132	1613.834			
-1637.152	-0.646	4.000	0.136	1637.152			
-1662.735	-0.663	4.100	0.139	1662.735			
-1687.961	-0.680	4.200	0.143	1687.961			
-1713.873	-0.697	4.300	0.146	1713.873			
-1737.898	-0.712	4.400	0.150	1737.898			
-1764.364	-0.729	4.500	0.153	1764.364			
-1782.655	-0.746	4.600	0.157	1782.655			
-1809.903	-0.764	4.700	0.161	1809.903			
-1838.068	-0.779	4.800	0.164	1838.068			

-1862.922	-0.795	4.900	0.167	1862.922
-1888.975	-0.813	5.000	0.171	1888.975
-1914.047	-0.828	5.100	0.174	1914.047
-1944.483	-0.846	5.200	0.178	1944.483
-1969.196	-0.863	5.300	0.181	1969.196
-1998.382	-0.879	5.400	0.185	1998.382
-2019.492	-0.896	5.500	0.188	2019.492
-2047.440	-0.913	5.599	0.192	2047.440
-2073.883	-0.929	5.699	0.195	2073.883
-2099.069	-0.946	5.799	0.199	2099.069
-2121.182	-0.963	5.899	0.202	2121.182
-2146.302	-0.979	5.999	0.206	2146.302
-2175.114	-0.996	6.099	0.209	2175.114
-2200.477	-1.012	6.199	0.213	2200.477
-2223.902	-1.027	6.299	0.216	2223.902
-2254.417	-1.046	6.399	0.220	2254.417
-2278.681	-1.062	6.499	0.223	2278.681
-2308.923	-1.080	6.599	0.227	2308.923
-2338.913	-1.096	6.699	0.230	2338.913
-2368.061	-1.113	6.799	0.234	2368.061
-2393.906	-1.129	6.899	0.237	2393.906
-2421.424	-1.145	6.999	0.241	2421.424
-2441.782	-1.162	7.098	0.244	2441.782
-2466.522	-1.180	7.198	0.248	2466.522

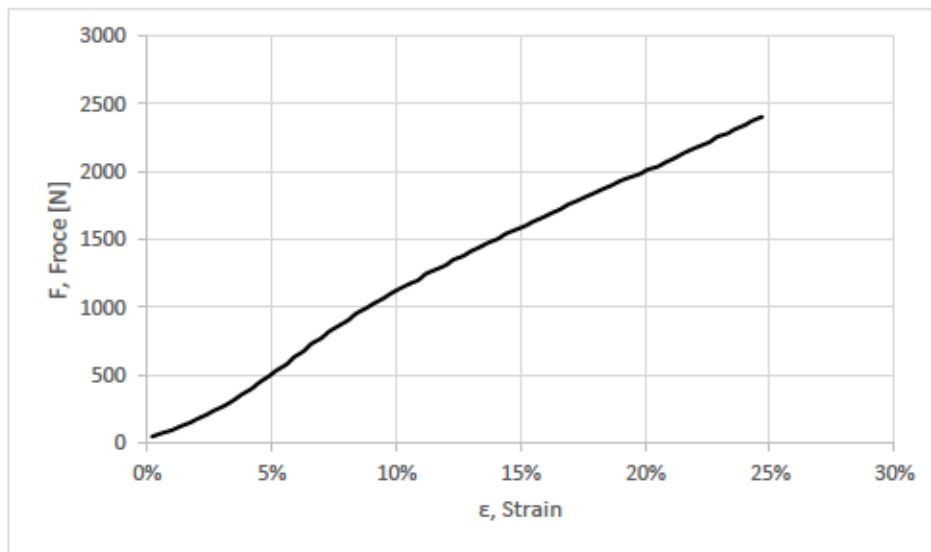


Data Acquisition Time: 77.088 Sec 23-Jun-17 2:32:47 PM

Axial Load	Axial Stroke	Time	Strain	Axial Load	Original thickness ho [mm]	$\Delta L$ @ $\epsilon \approx 25\%$ [mm]
N	mm	Sec	$\epsilon$	N, no sign	4.699	-1.175
-44.251	-0.011	0.142	0.002	44.251	FN@25% = Sc@25% [N]	
-69.958	-0.029	0.242	0.006	69.958	2403	
-91.596	-0.045	0.342	0.010	91.596		
-116.783	-0.063	0.442	0.013	116.783		
-145.222	-0.079	0.542	0.017	145.222		
-172.938	-0.096	0.642	0.020	172.938		
-206.860	-0.112	0.742	0.024	206.860		
-237.169	-0.129	0.842	0.027	237.169		
-271.155	-0.146	0.942	0.031	271.155		
-314.985	-0.163	1.042	0.035	314.985		
-354.135	-0.179	1.142	0.038	354.135		
-397.557	-0.196	1.242	0.042	397.557		
-441.767	-0.212	1.341	0.045	441.767		
-490.746	-0.229	1.441	0.049	490.746		
-531.603	-0.245	1.541	0.052	531.603		
-577.131	-0.262	1.641	0.056	577.131		
-628.783	-0.278	1.741	0.059	628.783		
-676.350	-0.295	1.841	0.063	676.350		
-728.565	-0.312	1.941	0.066	728.565		
-770.141	-0.329	2.041	0.070	770.141		
-817.498	-0.345	2.141	0.073	817.498		
-861.607	-0.362	2.241	0.077	861.607		
-905.955	-0.379	2.341	0.081	905.955		
-951.862	-0.395	2.441	0.084	951.862		
-991.503	-0.412	2.541	0.088	991.503		
-1025.165	-0.428	2.641	0.091	1025.165		
-1064.746	-0.447	2.741	0.095	1064.746		
-1100.319	-0.462	2.840	0.098	1100.319		
-1140.180	-0.479	2.940	0.102	1140.180		
-1175.863	-0.497	3.040	0.106	1175.863		
-1199.664	-0.513	3.140	0.109	1199.664		
-1244.307	-0.528	3.240	0.112	1244.307		
-1276.718	-0.546	3.340	0.116	1276.718		
-1309.094	-0.562	3.440	0.120	1309.094		
-1347.992	-0.578	3.540	0.123	1347.992		
-1376.984	-0.595	3.640	0.127	1376.984		
-1410.220	-0.613	3.740	0.130	1410.220		
-1444.936	-0.628	3.840	0.134	1444.936		
-1473.933	-0.645	3.940	0.137	1473.933		
-1503.763	-0.662	4.040	0.141	1503.763		
-1539.230	-0.678	4.140	0.144	1539.230		
-1569.253	-0.695	4.240	0.148	1569.253		
-1599.293	-0.712	4.340	0.152	1599.293		
-1629.124	-0.729	4.439	0.155	1629.124		



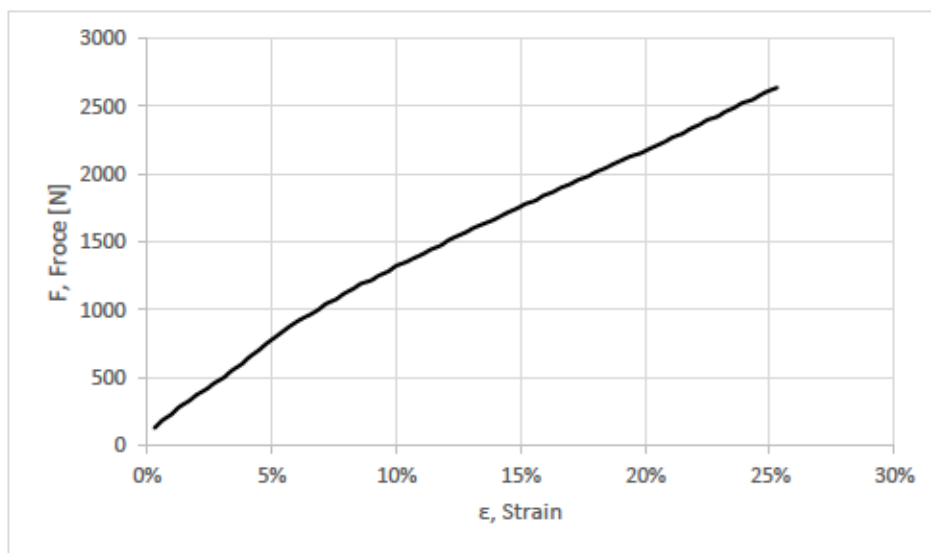
-1661.462	-0.746	4.539	0.159	1661.462
-1688.660	-0.762	4.639	0.162	1688.660
-1721.509	-0.779	4.739	0.166	1721.509
-1754.276	-0.795	4.839	0.169	1754.276
-1785.852	-0.813	4.939	0.173	1785.852
-1811.712	-0.829	5.039	0.176	1811.712
-1843.863	-0.845	5.139	0.180	1843.863
-1869.599	-0.861	5.239	0.183	1869.599
-1901.133	-0.878	5.339	0.187	1901.133
-1929.678	-0.895	5.439	0.190	1929.678
-1957.339	-0.911	5.539	0.194	1957.339
-1982.421	-0.929	5.639	0.198	1982.421
-2012.998	-0.945	5.739	0.201	2012.998
-2035.302	-0.961	5.839	0.205	2035.302
-2065.138	-0.979	5.938	0.208	2065.138
-2099.366	-0.995	6.038	0.212	2099.366
-2130.114	-1.011	6.138	0.215	2130.114
-2164.363	-1.028	6.238	0.219	2164.363
-2187.312	-1.044	6.338	0.222	2187.312
-2217.863	-1.061	6.438	0.226	2217.863
-2255.000	-1.078	6.538	0.229	2255.000
-2279.272	-1.095	6.638	0.233	2279.272
-2310.496	-1.111	6.738	0.236	2310.496
-2341.465	-1.128	6.838	0.240	2341.465
-2373.094	-1.144	6.938	0.243	2373.094
-2402.878	-1.161	7.038	0.247	2402.878



Data Acquisition Time: 102.428 Sec 23-Jun-17 10:21:49 AM

Axial Load	Axial Stroke	Time	Strain	Axial Load	Original thickness ho [mm]	$\Delta L$ @ $\epsilon \approx 25\%$ [mm]
N	mm	Sec	$\epsilon$	N, no sign	4.792	-1.198
-124.785	-0.015	0.170	0.003	124.785	FN@25% = Sc@25% [N]	
-179.447	-0.031	0.270	0.006	179.447	2607	
-228.779	-0.047	0.370	0.010	228.779		
-280.936	-0.063	0.470	0.013	280.936		
-327.106	-0.081	0.570	0.017	327.106		
-370.609	-0.098	0.670	0.020	370.609		
-413.767	-0.114	0.770	0.024	413.767		
-455.989	-0.129	0.869	0.027	455.989		
-500.216	-0.147	0.969	0.031	500.216		
-548.305	-0.163	1.069	0.034	548.305		
-596.735	-0.181	1.169	0.038	596.735		
-646.874	-0.198	1.269	0.041	646.874		
-701.309	-0.214	1.369	0.045	701.309		
-748.190	-0.229	1.469	0.048	748.190		
-802.278	-0.247	1.569	0.052	802.278		
-844.020	-0.264	1.669	0.055	844.020		
-884.131	-0.280	1.769	0.058	884.131		
-929.817	-0.297	1.869	0.062	929.817		
-966.723	-0.314	1.969	0.066	966.723		
-1000.786	-0.330	2.069	0.069	1000.786		
-1042.625	-0.347	2.169	0.072	1042.625		
-1076.033	-0.363	2.269	0.076	1076.033		
-1115.098	-0.380	2.368	0.079	1115.098		
-1154.713	-0.397	2.468	0.083	1154.713		
-1190.588	-0.413	2.568	0.086	1190.588		
-1214.495	-0.431	2.668	0.090	1214.495		
-1248.679	-0.447	2.768	0.093	1248.679		
-1281.960	-0.463	2.868	0.097	1281.960		
-1320.591	-0.480	2.968	0.100	1320.591		
-1349.556	-0.497	3.068	0.104	1349.556		
-1376.790	-0.513	3.168	0.107	1376.790		
-1410.842	-0.530	3.268	0.111	1410.842		
-1441.841	-0.548	3.368	0.114	1441.841		
-1472.501	-0.564	3.468	0.118	1472.501		
-1509.846	-0.580	3.568	0.121	1509.846		
-1536.613	-0.597	3.668	0.124	1536.613		
-1569.009	-0.613	3.768	0.128	1569.009		
-1599.889	-0.630	3.868	0.131	1599.889		
-1630.388	-0.646	3.967	0.135	1630.388		
-1659.598	-0.664	4.067	0.139	1659.598		
-1688.103	-0.679	4.167	0.142	1688.103		
-1716.087	-0.697	4.267	0.145	1716.087		
-1748.929	-0.712	4.367	0.149	1748.929		
-1778.446	-0.729	4.467	0.152	1778.446		

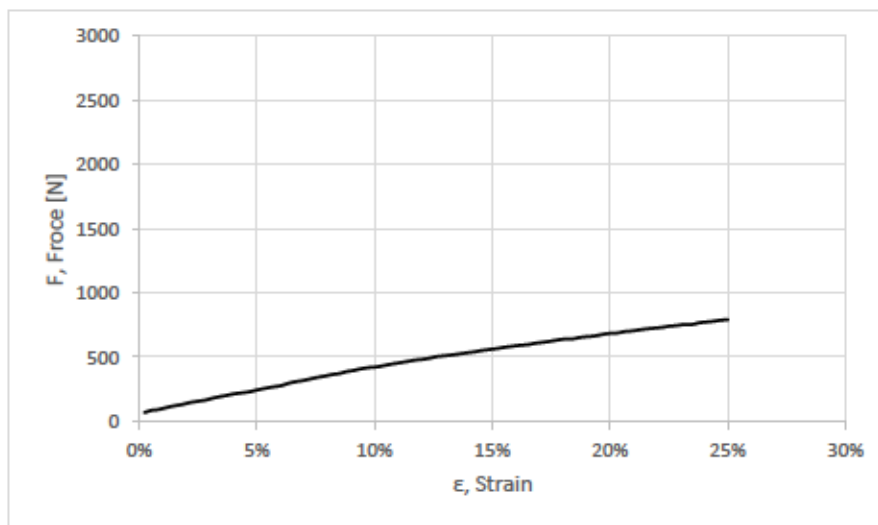
-1803.396	-0.747	4.567	0.156	1803.396
-1837.549	-0.762	4.667	0.159	1837.549
-1866.229	-0.780	4.767	0.163	1866.229
-1895.851	-0.797	4.867	0.166	1895.851
-1924.817	-0.813	4.967	0.170	1924.817
-1954.229	-0.830	5.067	0.173	1954.229
-1981.136	-0.847	5.167	0.177	1981.136
-2011.547	-0.864	5.267	0.180	2011.547
-2042.088	-0.880	5.367	0.184	2042.088
-2069.944	-0.897	5.466	0.187	2069.944
-2095.110	-0.913	5.566	0.190	2095.110
-2128.038	-0.930	5.666	0.194	2128.038
-2151.095	-0.948	5.766	0.198	2151.095
-2177.892	-0.963	5.866	0.201	2177.892
-2203.436	-0.979	5.966	0.204	2203.436
-2237.243	-0.996	6.066	0.208	2237.243
-2269.143	-1.013	6.166	0.211	2269.143
-2297.063	-1.030	6.266	0.215	2297.063
-2330.551	-1.046	6.366	0.218	2330.551
-2364.562	-1.063	6.466	0.222	2364.562
-2397.509	-1.079	6.566	0.225	2397.509
-2421.949	-1.098	6.666	0.229	2421.949
-2455.929	-1.113	6.766	0.232	2455.929
-2490.054	-1.129	6.866	0.236	2490.054
-2522.582	-1.147	6.965	0.239	2522.582
-2546.323	-1.163	7.065	0.243	2546.323
-2578.597	-1.179	7.165	0.246	2578.597
-2607.129	-1.195	7.265	0.249	2607.129
-2635.623	-1.213	7.365	0.253	2635.623



Data	Acquisition	Time: 102.428	Sec	24-Jun-17	11:35:42	AM
Axial Load	Axial Stroke	Time	Strain	Axial Load	Original thickness h <sub>0</sub> [mm]	$\Delta L$ @ $\epsilon \approx 25\%$ [mm]
N	mm	Sec	$\epsilon$	N, no sign	5.232	-1.308
-68.206	-0.012	0.155	0.002	68.206	$F_{N@25\%} = S_{c@25\%}$ [N]	
-84.986	-0.028	0.255	0.005	84.986	790	
-91.420	-0.044	0.355	0.008	91.420		
-109.666	-0.061	0.455	0.012	109.666		
-121.416	-0.077	0.555	0.015	121.416		
-130.301	-0.094	0.655	0.018	130.301		
-144.094	-0.111	0.755	0.021	144.094		
-153.945	-0.128	0.855	0.024	153.945		
-165.004	-0.145	0.955	0.028	165.004		
-179.774	-0.160	1.055	0.031	179.774		
-191.345	-0.177	1.154	0.034	191.345		
-201.566	-0.194	1.254	0.037	201.566		
-213.258	-0.211	1.354	0.040	213.258		
-222.432	-0.228	1.454	0.044	222.432		
-230.849	-0.245	1.554	0.047	230.849		
-243.726	-0.262	1.654	0.050	243.726		
-255.380	-0.277	1.754	0.053	255.380		
-265.547	-0.294	1.854	0.056	265.547		
-277.068	-0.312	1.954	0.060	277.068		
-294.366	-0.327	2.054	0.063	294.366		
-307.019	-0.343	2.154	0.066	307.019		
-315.904	-0.361	2.254	0.069	315.904		
-327.218	-0.377	2.354	0.072	327.218		
-340.002	-0.394	2.454	0.075	340.002		
-353.178	-0.411	2.554	0.079	353.178		
-364.530	-0.427	2.653	0.082	364.530		
-372.272	-0.444	2.753	0.085	372.272		
-386.937	-0.461	2.853	0.088	386.937		
-395.778	-0.479	2.953	0.091	395.778		
-408.495	-0.493	3.053	0.094	408.495		
-419.253	-0.511	3.153	0.098	419.253		
-423.740	-0.527	3.253	0.101	423.740		
-434.217	-0.544	3.353	0.104	434.217		
-444.844	-0.561	3.453	0.107	444.844		
-457.063	-0.578	3.553	0.111	457.063		
-462.998	-0.594	3.653	0.113	462.998		
-475.991	-0.611	3.753	0.117	475.991		
-481.764	-0.627	3.853	0.120	481.764		
-490.360	-0.644	3.953	0.123	490.360		
-502.756	-0.662	4.053	0.126	502.756		
-509.083	-0.677	4.153	0.129	509.083		
-516.921	-0.696	4.252	0.133	516.921		
-524.780	-0.711	4.352	0.136	524.780		
-532.804	-0.727	4.452	0.139	532.804		
-542.435	-0.746	4.552	0.143	542.435		
-550.057	-0.761	4.652	0.145	550.057		
-559.696	-0.777	4.752	0.149	559.696		

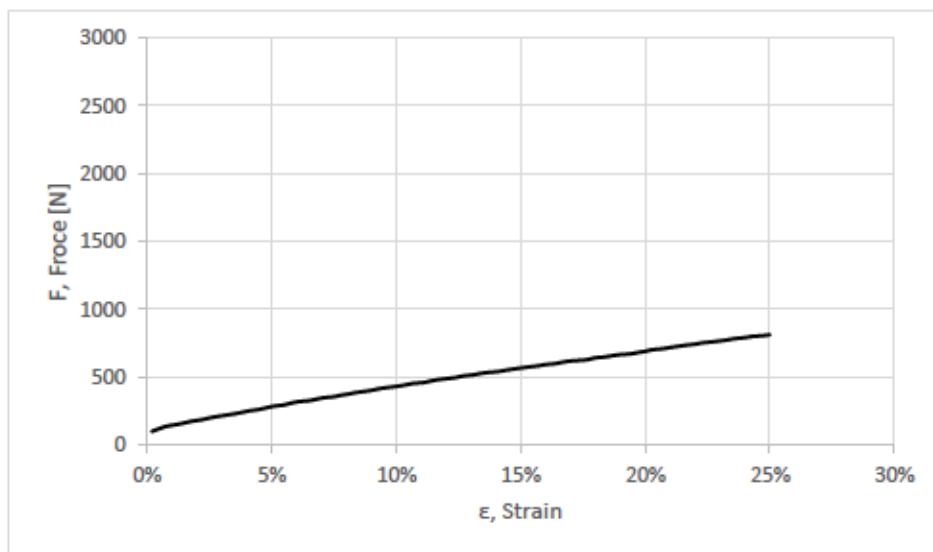


-566.730	-0.795	4.852	0.152	566.730
-576.152	-0.810	4.952	0.155	576.152
-583.070	-0.828	5.052	0.158	583.070
-590.108	-0.844	5.152	0.161	590.108
-596.799	-0.861	5.252	0.165	596.799
-606.932	-0.878	5.352	0.168	606.932
-613.803	-0.894	5.452	0.171	613.803
-621.173	-0.911	5.552	0.174	621.173
-630.957	-0.926	5.652	0.177	630.957
-638.796	-0.944	5.751	0.180	638.796
-641.497	-0.961	5.851	0.184	641.497
-651.941	-0.977	5.951	0.187	651.941
-658.591	-0.995	6.051	0.190	658.591
-663.125	-1.011	6.151	0.193	663.125
-673.307	-1.027	6.251	0.196	673.307
-682.900	-1.043	6.351	0.199	682.900
-687.430	-1.061	6.451	0.203	687.430
-697.924	-1.078	6.551	0.206	697.924
-702.860	-1.093	6.651	0.209	702.860
-710.556	-1.110	6.751	0.212	710.556
-718.225	-1.127	6.851	0.215	718.225
-725.670	-1.145	6.951	0.219	725.670
-730.766	-1.161	7.051	0.222	730.766
-740.075	-1.177	7.151	0.225	740.075
-744.920	-1.194	7.250	0.228	744.920
-752.397	-1.211	7.350	0.231	752.397
-754.708	-1.229	7.450	0.235	754.708
-767.093	-1.244	7.550	0.238	767.093
-772.826	-1.261	7.650	0.241	772.826
-778.813	-1.277	7.750	0.244	778.813
-786.672	-1.294	7.850	0.247	786.672
-790.500	-1.309	7.950	0.250	790.500



Data	Acquisition Time:	77.088 Sec	24-Jun-17		2:32:47 PM	
Axial Load	Axial Stroke	Time	Strain	Axial Load	Original thickness ho [mm]	ΔL @ ε≈25% [mm]
N	mm	Sec	ε	N, no sign	5.038	-1.259
-96.391	-0.008	0.128	0.002	96.391	Fn@25% = Sc@25% [N]	
-117.067	-0.025	0.228	0.005	117.067	809	
-135.053	-0.042	0.328	0.008	135.053		
-147.597	-0.058	0.428	0.012	147.597		
-159.032	-0.075	0.528	0.015	159.032		
-171.694	-0.092	0.627	0.018	171.694		
-182.867	-0.109	0.727	0.022	182.867		
-195.326	-0.125	0.827	0.025	195.326		
-205.900	-0.143	0.927	0.028	205.900		
-214.740	-0.158	1.027	0.031	214.740		
-226.026	-0.175	1.127	0.035	226.026		
-236.474	-0.191	1.227	0.038	236.474		
-248.142	-0.209	1.327	0.041	248.142		
-258.806	-0.225	1.427	0.045	258.806		
-271.102	-0.242	1.527	0.048	271.102		
-282.749	-0.258	1.627	0.051	282.749		
-291.925	-0.275	1.727	0.055	291.925		
-305.927	-0.292	1.827	0.058	305.927		
-316.362	-0.308	1.927	0.061	316.362		
-323.368	-0.325	2.027	0.065	323.368		
-334.015	-0.341	2.126	0.068	334.015		
-345.010	-0.358	2.226	0.071	345.010		
-352.366	-0.376	2.326	0.075	352.366		
-363.969	-0.392	2.426	0.078	363.969		
-372.557	-0.409	2.526	0.081	372.557		
-383.455	-0.425	2.626	0.084	383.455		
-393.185	-0.441	2.726	0.088	393.185		
-402.639	-0.459	2.826	0.091	402.639		
-414.000	-0.475	2.926	0.094	414.000		
-423.538	-0.492	3.026	0.098	423.538		
-430.697	-0.508	3.126	0.101	430.697		
-440.116	-0.524	3.226	0.104	440.116		
-450.795	-0.541	3.326	0.107	450.795		
-456.835	-0.559	3.426	0.111	456.835		
-468.507	-0.575	3.526	0.114	468.507		
-478.460	-0.592	3.625	0.117	478.460		
-487.213	-0.609	3.725	0.121	487.213		
-493.875	-0.625	3.825	0.124	493.875		
-505.557	-0.641	3.925	0.127	505.557		
-513.617	-0.658	4.025	0.131	513.617		
-524.115	-0.675	4.125	0.134	524.115		
-531.382	-0.692	4.225	0.137	531.382		
-537.894	-0.709	4.325	0.141	537.894		
-547.547	-0.724	4.425	0.144	547.547		

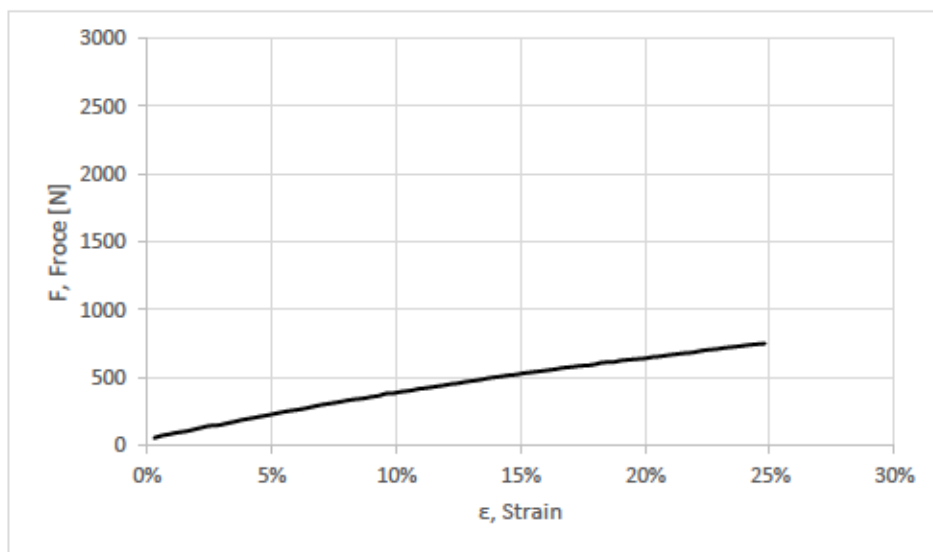
-556.201	-0.741	4.525	0.147	556.201
-566.478	-0.759	4.625	0.151	566.478
-573.615	-0.775	4.725	0.154	573.615
-579.939	-0.791	4.825	0.157	579.939
-589.566	-0.808	4.925	0.160	589.566
-596.742	-0.825	5.025	0.164	596.742
-607.505	-0.842	5.125	0.167	607.505
-615.897	-0.858	5.224	0.170	615.897
-621.062	-0.875	5.324	0.174	621.062
-626.364	-0.892	5.424	0.177	626.364
-639.284	-0.909	5.524	0.180	639.284
-646.327	-0.925	5.624	0.184	646.327
-655.682	-0.941	5.724	0.187	655.682
-662.823	-0.958	5.824	0.190	662.823
-668.305	-0.975	5.924	0.194	668.305
-677.932	-0.991	6.024	0.197	677.932
-687.151	-1.008	6.124	0.200	687.151
-699.200	-1.024	6.224	0.203	699.200
-706.312	-1.041	6.324	0.207	706.312
-715.317	-1.059	6.424	0.210	715.317
-723.565	-1.075	6.524	0.213	723.565
-733.976	-1.092	6.624	0.217	733.976
-739.640	-1.108	6.723	0.220	739.640
-749.793	-1.125	6.823	0.223	749.793
-757.173	-1.141	6.923	0.227	757.173
-763.883	-1.159	7.023	0.230	763.883
-771.429	-1.175	7.123	0.233	771.429
-780.864	-1.191	7.223	0.236	780.864
-788.207	-1.208	7.323	0.240	788.207
-797.138	-1.226	7.423	0.243	797.138
-802.583	-1.242	7.523	0.247	802.583
-808.888	-1.258	7.623	0.250	808.888



Data	Acquisition	Time:	102.4279	Sec	24-Jun-17	10:21:49	AM
Axial Load	Axial Stroke	Time	Strain	Axial Load	Original thickness ho [mm]	$\Delta L$ @ $\epsilon \approx 25\%$ [mm]	
N	mm	Sec	$\epsilon$	N, no sign	5.165	-1.291	
-52.203	-0.014	0.157	0.003	52.203	Fn@25% = Sc@25% [N]		
-69.220	-0.031	0.257	0.006	69.220	748		
-79.414	-0.048	0.357	0.009	79.414			
-90.742	-0.064	0.457	0.012	90.742			
-101.944	-0.081	0.557	0.016	101.944			
-114.881	-0.097	0.657	0.019	114.881			
-128.087	-0.114	0.757	0.022	128.087			
-140.904	-0.131	0.856	0.025	140.904			
-146.706	-0.147	0.956	0.029	146.706			
-159.068	-0.165	1.056	0.032	159.068			
-170.849	-0.180	1.156	0.035	170.849			
-184.415	-0.197	1.256	0.038	184.415			
-197.317	-0.215	1.356	0.042	197.317			
-208.098	-0.230	1.456	0.045	208.098			
-217.976	-0.248	1.556	0.048	217.976			
-229.162	-0.264	1.656	0.051	229.162			
-240.845	-0.281	1.756	0.054	240.845			
-250.719	-0.297	1.856	0.057	250.719			
-261.296	-0.315	1.956	0.061	261.296			
-271.574	-0.331	2.056	0.064	271.574			
-284.072	-0.347	2.156	0.067	284.072			
-295.928	-0.364	2.256	0.070	295.928			
-307.555	-0.380	2.355	0.074	307.555			
-316.056	-0.397	2.455	0.077	316.056			
-327.036	-0.414	2.555	0.080	327.036			
-335.742	-0.430	2.655	0.083	335.742			
-343.924	-0.448	2.755	0.087	343.924			
-354.524	-0.463	2.855	0.090	354.524			
-362.897	-0.482	2.955	0.093	362.897			
-379.268	-0.498	3.055	0.096	379.268			
-382.188	-0.513	3.155	0.099	382.188			
-392.364	-0.529	3.255	0.102	392.364			
-401.611	-0.548	3.355	0.106	401.611			
-413.692	-0.564	3.455	0.109	413.692			
-420.148	-0.581	3.555	0.112	420.148			
-431.051	-0.597	3.655	0.116	431.051			
-439.132	-0.613	3.755	0.119	439.132			
-449.061	-0.630	3.854	0.122	449.061			
-455.432	-0.647	3.954	0.125	455.432			
-465.877	-0.663	4.054	0.128	465.877			
-476.034	-0.681	4.154	0.132	476.034			
-485.263	-0.696	4.254	0.135	485.263			
-495.670	-0.714	4.354	0.138	495.670			
-504.905	-0.731	4.454	0.142	504.905			



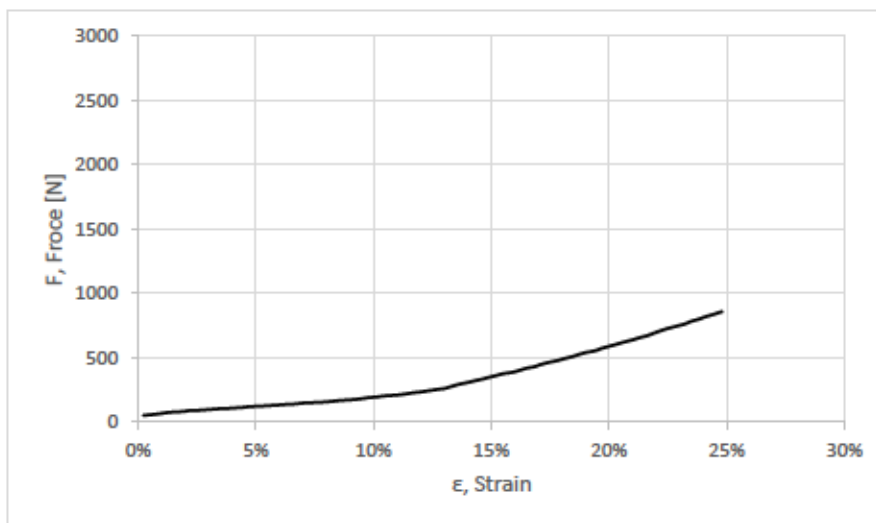
-513.314	-0.747	4.554	0.145	513.314
-518.595	-0.763	4.654	0.148	518.595
-528.612	-0.780	4.754	0.151	528.612
-535.399	-0.797	4.854	0.154	535.399
-544.286	-0.814	4.954	0.158	544.286
-551.287	-0.829	5.054	0.161	551.287
-558.890	-0.847	5.154	0.164	558.890
-568.772	-0.864	5.254	0.167	568.772
-576.416	-0.881	5.354	0.171	576.416
-583.441	-0.896	5.453	0.174	583.441
-586.721	-0.913	5.553	0.177	586.721
-595.403	-0.931	5.653	0.180	595.403
-608.532	-0.947	5.753	0.183	608.532
-610.507	-0.964	5.853	0.187	610.507
-621.782	-0.980	5.953	0.190	621.782
-627.758	-0.996	6.053	0.193	627.758
-632.492	-1.014	6.153	0.196	632.492
-638.702	-1.031	6.253	0.200	638.702
-648.569	-1.048	6.353	0.203	648.569
-653.294	-1.063	6.453	0.206	653.294
-661.907	-1.081	6.553	0.209	661.907
-668.444	-1.097	6.653	0.212	668.444
-675.652	-1.113	6.753	0.215	675.652
-681.836	-1.130	6.853	0.219	681.836
-692.840	-1.147	6.952	0.222	692.840
-701.186	-1.163	7.052	0.225	701.186
-708.256	-1.180	7.152	0.229	708.256
-716.750	-1.197	7.252	0.232	716.750
-722.379	-1.213	7.352	0.235	722.379
-728.654	-1.229	7.452	0.238	728.654
-736.115	-1.247	7.552	0.241	736.115
-743.632	-1.263	7.652	0.245	743.632
-748.182	-1.280	7.752	0.248	748.182





Data	Acquisition	Time: 102.428	Sec	22-Jun-17	12:37:53	PM
Axial Load	Axial Stroke	Time	Strain	Axial Load	Original thickness $h_0$ [mm]	$\Delta L$ @ $\epsilon \approx 25\%$ [mm]
N	mm	Sec	$\epsilon$	N, no sign	5.232	-1.308
-45.461	-0.013	0.204	0.002	45.461	$F_{N@25\%} = S_{c@25\%}$ [N]	
-52.737	-0.030	0.304	0.006	52.737	854	
-59.108	-0.047	0.404	0.009	59.108		
-67.464	-0.064	0.504	0.012	67.464		
-72.211	-0.080	0.604	0.015	72.211		
-76.340	-0.097	0.704	0.019	76.340		
-84.342	-0.114	0.804	0.022	84.342		
-85.090	-0.130	0.904	0.025	85.090		
-88.858	-0.146	1.004	0.028	88.858		
-94.602	-0.165	1.104	0.032	94.602		
-98.430	-0.181	1.204	0.035	98.430		
-100.203	-0.197	1.304	0.038	100.203		
-104.061	-0.213	1.404	0.041	104.061		
-107.568	-0.230	1.504	0.044	107.568		
-113.846	-0.246	1.604	0.047	113.846		
-116.590	-0.264	1.703	0.050	116.590		
-120.279	-0.280	1.803	0.054	120.279		
-124.042	-0.298	1.903	0.057	124.042		
-127.562	-0.313	2.003	0.060	127.562		
-131.741	-0.330	2.103	0.063	131.741		
-134.256	-0.347	2.203	0.066	134.256		
-142.122	-0.364	2.303	0.070	142.122		
-144.582	-0.380	2.403	0.073	144.582		
-147.321	-0.397	2.503	0.076	147.321		
-150.267	-0.413	2.603	0.079	150.267		
-155.083	-0.431	2.703	0.082	155.083		
-160.932	-0.447	2.803	0.085	160.932		
-166.131	-0.464	2.903	0.089	166.131		
-170.165	-0.481	3.003	0.092	170.165		
-176.635	-0.496	3.103	0.095	176.635		
-184.778	-0.514	3.202	0.098	184.778		
-189.014	-0.529	3.302	0.101	189.014		
-196.436	-0.547	3.402	0.104	196.436		
-202.018	-0.564	3.502	0.108	202.018		
-206.494	-0.579	3.602	0.111	206.494		
-214.219	-0.598	3.702	0.114	214.219		
-222.801	-0.613	3.802	0.117	222.801		
-228.598	-0.630	3.902	0.120	228.598		
-236.902	-0.646	4.002	0.123	236.902		
-248.130	-0.662	4.102	0.127	248.130		
-255.302	-0.680	4.202	0.130	255.302		
-271.180	-0.697	4.302	0.133	271.180		
-287.145	-0.714	4.402	0.136	287.145		
-302.723	-0.730	4.502	0.140	302.723		
-315.909	-0.746	4.602	0.143	315.909		
-328.024	-0.763	4.701	0.146	328.024		
-342.774	-0.779	4.801	0.149	342.774		

-356.208	-0.796	4.901	0.152	356.208
-370.677	-0.813	5.001	0.155	370.677
-381.897	-0.830	5.101	0.159	381.897
-397.095	-0.846	5.201	0.162	397.095
-413.575	-0.863	5.301	0.165	413.575
-423.869	-0.881	5.401	0.168	423.869
-442.163	-0.897	5.501	0.171	442.163
-456.768	-0.912	5.601	0.174	456.768
-472.808	-0.930	5.701	0.178	472.808
-488.135	-0.946	5.801	0.181	488.135
-501.908	-0.964	5.901	0.184	501.908
-519.117	-0.980	6.001	0.187	519.117
-535.015	-0.996	6.101	0.190	535.015
-549.192	-1.013	6.201	0.194	549.192
-568.547	-1.030	6.300	0.197	568.547
-583.750	-1.045	6.400	0.200	583.750
-599.017	-1.062	6.500	0.203	599.017
-614.875	-1.079	6.600	0.206	614.875
-633.985	-1.096	6.700	0.210	633.985
-650.807	-1.112	6.800	0.213	650.807
-665.612	-1.130	6.900	0.216	665.612
-685.644	-1.146	7.000	0.219	685.644
-705.628	-1.164	7.100	0.222	705.628
-723.015	-1.179	7.200	0.225	723.015
-741.931	-1.196	7.300	0.229	741.931
-756.785	-1.212	7.400	0.232	756.785
-778.838	-1.229	7.500	0.235	778.838
-793.799	-1.246	7.600	0.238	793.799
-813.912	-1.263	7.700	0.241	813.912
-835.690	-1.279	7.799	0.245	835.690
-853.769	-1.296	7.899	0.248	853.769

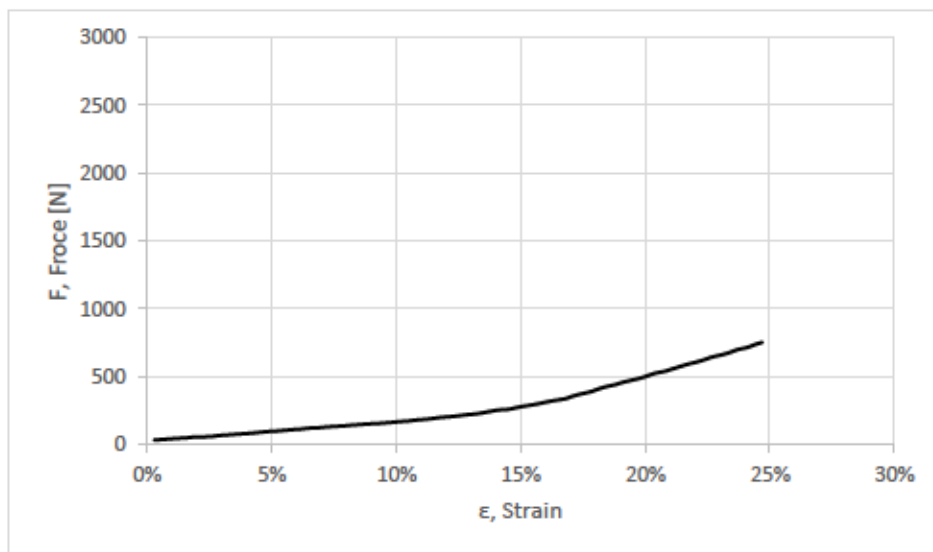




Data Acquisition Time: 77.088 Sec 22-Jun-17 2:28:29 PM

Axial Load	Axial Stroke	Time	Strain	Axial Load	Original thickness ho [mm]	$\Delta L$ @ $\epsilon \approx 25\%$ [mm]
N	mm	Sec	$\epsilon$	N, no sign	5.038	-1.259
-30.032	-0.013	0.126	0.003	30.032	FN@25% = Sc@25% [N]	
-33.346	-0.029	0.226	0.006	33.346	750	
-37.632	-0.047	0.326	0.009	37.632		
-41.655	-0.062	0.426	0.012	41.655		
-45.999	-0.079	0.526	0.016	45.999		
-51.850	-0.095	0.626	0.019	51.850		
-52.584	-0.112	0.726	0.022	52.584		
-55.993	-0.129	0.826	0.026	55.993		
-62.826	-0.146	0.926	0.029	62.826		
-66.822	-0.162	1.026	0.032	66.822		
-72.223	-0.179	1.125	0.036	72.223		
-76.319	-0.195	1.225	0.039	76.319		
-80.225	-0.212	1.325	0.042	80.225		
-85.684	-0.228	1.425	0.045	85.684		
-92.757	-0.246	1.525	0.049	92.757		
-95.625	-0.261	1.625	0.052	95.625		
-100.702	-0.279	1.725	0.055	100.702		
-106.854	-0.296	1.825	0.059	106.854		
-110.734	-0.313	1.925	0.062	110.734		
-117.031	-0.329	2.025	0.065	117.031		
-120.512	-0.345	2.125	0.069	120.512		
-125.661	-0.364	2.225	0.072	125.661		
-129.472	-0.380	2.325	0.075	129.472		
-133.814	-0.396	2.425	0.079	133.814		
-139.179	-0.413	2.525	0.082	139.179		
-142.828	-0.429	2.625	0.085	142.828		
-148.546	-0.446	2.724	0.089	148.546		
-150.583	-0.463	2.824	0.092	150.583		
-154.998	-0.480	2.924	0.095	154.998		
-159.390	-0.495	3.024	0.098	159.390		
-166.210	-0.512	3.124	0.102	166.210		
-169.968	-0.529	3.224	0.105	169.968		
-176.961	-0.546	3.324	0.108	176.961		
-182.923	-0.562	3.424	0.112	182.923		
-189.185	-0.579	3.524	0.115	189.185		
-196.464	-0.596	3.624	0.118	196.464		
-202.187	-0.613	3.724	0.122	202.187		
-208.150	-0.630	3.824	0.125	208.150		
-215.328	-0.646	3.924	0.128	215.328		
-222.308	-0.663	4.024	0.132	222.308		
-230.844	-0.679	4.124	0.135	230.844		
-241.293	-0.697	4.223	0.138	241.293		
-250.544	-0.712	4.323	0.141	250.544		
-255.669	-0.729	4.423	0.145	255.669		

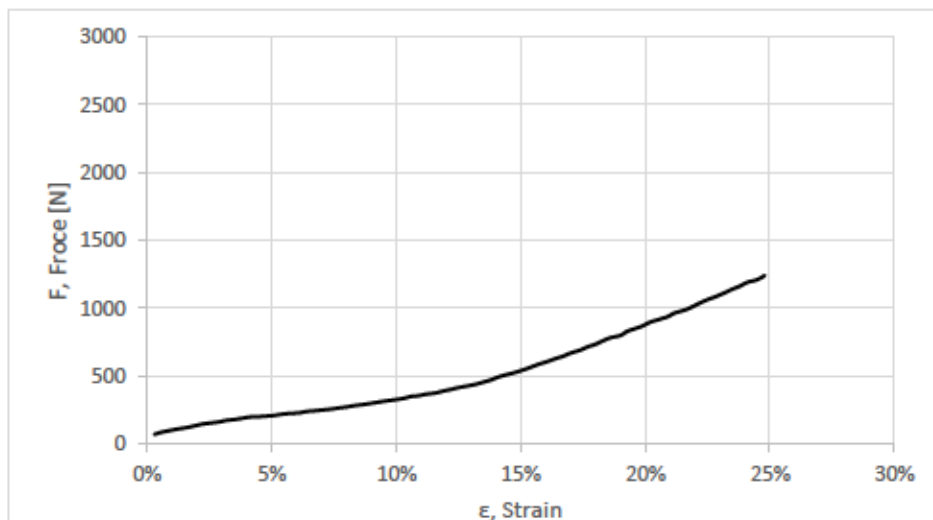
-267.086	-0.745	4.523	0.148	267.086
-277.866	-0.762	4.623	0.151	277.866
-289.872	-0.779	4.723	0.155	289.872
-300.558	-0.796	4.823	0.158	300.558
-312.290	-0.813	4.923	0.161	312.290
-322.175	-0.829	5.023	0.164	322.175
-334.594	-0.845	5.123	0.168	334.594
-353.199	-0.862	5.223	0.171	353.199
-368.268	-0.879	5.323	0.174	368.268
-385.078	-0.896	5.423	0.178	385.078
-404.466	-0.912	5.523	0.181	404.466
-421.541	-0.928	5.623	0.184	421.541
-438.093	-0.945	5.722	0.188	438.093
-454.729	-0.962	5.822	0.191	454.729
-468.097	-0.978	5.922	0.194	468.097
-485.710	-0.996	6.022	0.198	485.710
-503.253	-1.013	6.122	0.201	503.253
-521.770	-1.029	6.222	0.204	521.770
-536.970	-1.046	6.322	0.208	536.970
-554.042	-1.062	6.422	0.211	554.042
-571.326	-1.079	6.522	0.214	571.326
-588.120	-1.095	6.622	0.217	588.120
-606.539	-1.112	6.722	0.221	606.539
-623.464	-1.129	6.822	0.224	623.464
-642.130	-1.145	6.922	0.227	642.130
-659.198	-1.163	7.022	0.231	659.198
-675.446	-1.178	7.122	0.234	675.446
-695.378	-1.194	7.222	0.237	695.378
-712.518	-1.212	7.321	0.241	712.518
-732.519	-1.229	7.421	0.244	732.519
-750.402	-1.245	7.521	0.247	750.402



Data Acquisition Time: 102.428 Sec 22-Jun-17 12:32:29 PM

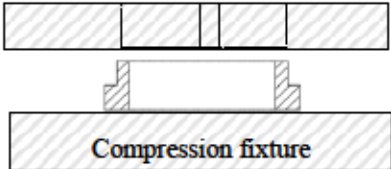
Axial Load	Axial Stroke	Time	Strain	Axial Load	Original thickness ho [mm]	$\Delta L$ @ $\epsilon \approx 25\%$ [mm]
N	mm	Sec	$\epsilon$	N, no sign	5.165	-1.291
-67.145	-0.014	0.130	0.003	67.145	FN@25% = Sc@25% [N]	
-83.577	-0.030	0.230	0.006	83.577	1238	
-94.791	-0.047	0.330	0.009	94.791		
-105.741	-0.064	0.430	0.012	105.741		
-117.605	-0.080	0.530	0.016	117.605		
-129.430	-0.097	0.630	0.019	129.430		
-142.314	-0.114	0.729	0.022	142.314		
-149.731	-0.131	0.829	0.025	149.731		
-159.095	-0.148	0.929	0.029	159.095		
-170.581	-0.164	1.029	0.032	170.581		
-176.396	-0.181	1.129	0.035	176.396		
-185.057	-0.197	1.229	0.038	185.057		
-194.480	-0.214	1.329	0.041	194.480		
-197.922	-0.230	1.429	0.045	197.922		
-201.941	-0.248	1.529	0.048	201.941		
-206.460	-0.264	1.629	0.051	206.460		
-215.307	-0.280	1.729	0.054	215.307		
-220.924	-0.296	1.829	0.057	220.924		
-225.718	-0.313	1.929	0.061	225.718		
-235.776	-0.331	2.029	0.064	235.776		
-240.709	-0.347	2.129	0.067	240.709		
-246.219	-0.364	2.229	0.070	246.219		
-253.731	-0.380	2.328	0.074	253.731		
-261.891	-0.397	2.428	0.077	261.891		
-268.936	-0.414	2.528	0.080	268.936		
-278.546	-0.430	2.628	0.083	278.546		
-287.746	-0.447	2.728	0.087	287.746		
-296.165	-0.463	2.828	0.090	296.165		
-305.121	-0.481	2.928	0.093	305.121		
-313.852	-0.497	3.028	0.096	313.852		
-321.078	-0.514	3.128	0.099	321.078		
-332.521	-0.530	3.228	0.103	332.521		
-346.535	-0.546	3.328	0.106	346.535		
-352.298	-0.563	3.428	0.109	352.298		
-363.056	-0.580	3.528	0.112	363.056		
-372.700	-0.597	3.628	0.116	372.700		
-386.818	-0.614	3.728	0.119	386.818		
-398.180	-0.630	3.827	0.122	398.180		
-411.679	-0.647	3.927	0.125	411.679		
-425.339	-0.664	4.027	0.129	425.339		
-436.662	-0.679	4.127	0.132	436.662		
-451.925	-0.697	4.227	0.135	451.925		
-468.022	-0.713	4.327	0.138	468.022		
-489.549	-0.730	4.427	0.141	489.549		

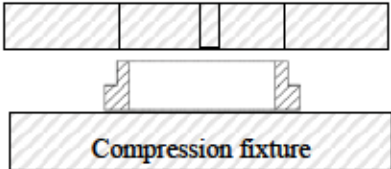
-505.675	-0.746	4.527	0.144	505.675
-524.622	-0.763	4.627	0.148	524.622
-542.203	-0.780	4.727	0.151	542.203
-561.660	-0.797	4.827	0.154	561.660
-582.453	-0.813	4.927	0.157	582.453
-605.807	-0.829	5.027	0.161	605.807
-625.793	-0.847	5.127	0.164	625.793
-643.001	-0.863	5.227	0.167	643.001
-666.011	-0.879	5.326	0.170	666.011
-689.076	-0.896	5.426	0.174	689.076
-712.878	-0.913	5.526	0.177	712.878
-731.254	-0.930	5.626	0.180	731.254
-756.404	-0.946	5.726	0.183	756.404
-779.443	-0.963	5.826	0.186	779.443
-796.401	-0.981	5.926	0.190	796.401
-828.610	-0.996	6.026	0.193	828.610
-846.886	-1.013	6.126	0.196	846.886
-866.866	-1.029	6.226	0.199	866.866
-893.999	-1.045	6.326	0.202	893.999
-917.121	-1.063	6.426	0.206	917.121
-934.939	-1.079	6.526	0.209	934.939
-962.726	-1.096	6.626	0.212	962.726
-984.432	-1.114	6.726	0.216	984.432
-1008.108	-1.129	6.826	0.219	1008.108
-1035.682	-1.146	6.925	0.222	1035.682
-1060.301	-1.163	7.025	0.225	1060.301
-1080.275	-1.180	7.125	0.228	1080.275
-1111.772	-1.196	7.225	0.232	1111.772
-1137.899	-1.213	7.325	0.235	1137.899
-1159.689	-1.230	7.425	0.238	1159.689
-1187.854	-1.246	7.525	0.241	1187.854
-1208.002	-1.263	7.625	0.245	1208.002
-1238.362	-1.280	7.725	0.248	1238.362

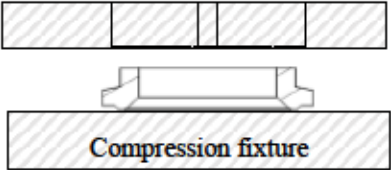







Airbrake Elastomeric Gasket - Compression Stress-Strain Properties Report			
Sample details		Test method	
Origin:	GEMMA Plastics	Reference:	ISO 7743
Compound details:	EPDM with fume silica	Test procedure:	Method D
Cure details:	100 °C	Type of test piece used:	Product (Air brake gasket)
Method of preparation:	Moulded	Test details	
<p>Full description:</p> <p>Simplified geometry gasket. The gasket was placed on the lubricated compression fixture lower section's flat surface, and the upper section had a channel to let the air out during compression:</p> 		Date of Test:	23-Jun-17
		Test Temperature [°C]:	23
		Relative humidity [%]:	50
		Laboratory temperature [°C]:	20
		Conditioning temperature [°C]:	20
		Conditioning time [hr]:	24
		Type of lubrication:	Silicone oil
		No.of test pieces used:	One per test (3 total)
		Deviations:	
		Non to report	
Test results			
Test piece ID	Original thickness h <sub>0</sub> [mm]	ΔL @ ε≈25% [mm]	F <sub>N@25%</sub> = S <sub>c@25%</sub> [N]
14	4.699	-1.175	2403
22	4.758	-1.190	2467
23	4.792	-1.198	2607
MEDIAN, S <sub>c</sub> :	4.758	-1.190	2467
STD DEV, σ <sub>s</sub> :	0.047	0.012	105

Airbrake Elastomeric Gasket - Compression Stress-Strain Properties Report			
Sample details		Test method	
Origin:	GEMMA Plastics	Reference:	ISO 7743
Compound details:	CR with fume silica	Test procedure:	Method D
Cure details:	100 °C	Type of test piece used:	Product (Air brake gasket)
Method of preparation:	Moulded	Test details	
Full description:		Date of Test:	24-Jun-17
<p>Simplified geometry gasket. The gasket was placed on the lubricated compression fixture lower section's flat surface, and the upper section had a channel to let the air out during compression:</p> 		Test Temperature [°C]:	23
		Relative humidity [%]:	50
		Laboratory temperature [°C]:	20
		Conditioning temperature [°C]:	20
		Conditioning time [hr]:	24
		Type of lubrication:	Silicone oil
		No.of test pieces used:	One per test (3 total)
		Deviations:	
		Non to report	
Test results			
Test piece ID	Original thickness h <sub>0</sub> [mm]	ΔL @ ε≈25% [mm]	F <sub>N@25%</sub> = S <sub>c@25%</sub> [N]
11	4.123	-1.031	790
14	4.132	-1.033	809
28	4.208	-1.052	748
MEDIAN, S <sub>c</sub> :	4.132	-1.033	790
STD DEV, σ <sub>s</sub> :	0.047	0.012	31


Airbrake Elastomeric Gasket - Compression Stress-Strain Properties Report			
Sample details		Test method	
Origin:	CP Warehouse	Reference:	ISO 7743
Compound details:	New York proprietary	Test procedure:	Method D
Cure details:	New York proprietary	Type of test piece used:	Product (Air brake gasket)
Method of preparation:	Moulded	Test details	
<b>Full description:</b> Standard AAR geometry gasket. The gasket was placed on the lubricated compression fixture lower section's flat surface, and the upper section had a channel to let the air out during compression: 		Date of Test:	22-Jun-17
		Test Temperature [°C]:	23
		Relative humidity [%]:	50
		Laboratory temperature [°C]:	20
		Conditioning temperature [°C]:	20
		Conditioning time [hr]:	24
		Type of lubrication:	Silicone oil
		No. of test pieces used:	One per test (3 total)
		Deviations:	Non to report
Test results			
Test piece ID	Original thickness $h_0$ [mm]	$\Delta L$ @ $\epsilon \approx 25\%$ [mm]	$F_N@25\% = S_c@25\%$ [N]
18	5.232	-1.308	854
28	5.165	-1.291	1238
10	5.038	-1.259	750
MEDIAN, $S_c$ :	5.165	-1.291	854
STD DEV, $\sigma_s$ :	0.099	0.025	257




**Airbrake Elastomeric Gasket - Effect of Liquids / Chemical Compatibility Report**

Test method		Test results																												
Reference:	ASTM D471	Immersion liquid used:								CRC Antifreeze				Exposure period dates:				Jul 1 to Jul 4			Exposure temp. [°C]:		23±2	Exposure period [hr]:			70			
Sample details		Sample	Original Hardness before immersion [Shore A]							Hardness after immersion [Shore A]							Hardness Change	Mass before [gr]			STD [gr]	Avg [gr]	Mass after [gr]			STD [gr]	Avg [gr]	Mass Change [%]		
Origin:	CP Warehouse	ID No	H <sub>01</sub>	H <sub>02</sub>	H <sub>03</sub>	H <sub>04</sub>	H <sub>05</sub>	μ <sub>0</sub>	σ <sub>0</sub>	H <sub>11</sub>	H <sub>12</sub>	H <sub>13</sub>	H <sub>14</sub>	H <sub>15</sub>	μ <sub>1</sub>	σ <sub>1</sub>	ΔH	M1 <sub>1</sub>	M1 <sub>2</sub>	M1 <sub>3</sub>	σM <sub>1</sub>	μM <sub>1</sub>	M2 <sub>1</sub>	M2 <sub>2</sub>	M2 <sub>3</sub>	σM <sub>2</sub>	μM <sub>2</sub>	ΔM		
Method of preparation:	Moulded	3	82	82	83	84	83	82.8	0.84	83	83	83	83	84	83.2	0.45	0.40	7.753	7.754	7.753	0.001	7.753	7.751	7.751	7.751	0.000	7.751	-0.03%		
Type of test piece used:	NYAB proprietary	7	83	82	83	83	84	83.0	0.71	84	82	84	83	83	83.2	0.84	0.20	7.841	7.840	7.841	0.001	7.841	7.834	7.834	7.835	0.001	7.834	-0.08%		
Full description:		24	83	83	83	83	84	83.2	0.45	84	84	83	83	84	83.6	0.55	0.40	7.782	7.782	7.783	0.001	7.782	7.778	7.779	7.778	0.001	7.778	-0.05%		
Standard gasket geometry																	Avg	0.33											Avg	-0.05%
		Immersion liquid used:								CRC Antifreeze				Exposure period dates:				Jul 1 to Jul 4			Exposure temp. [°C]:		50±2	Exposure period [hr]:			70			
Vulcanization details		Sample	Original Hardness before immersion [Shore A]							Hardness after immersion [Shore A]							Hardness Change	Mass before [gr]			STD [gr]	Avg [gr]	Mass after [gr]			STD [gr]	Avg [gr]	Mass Change [%]		
ID No		H <sub>01</sub>	H <sub>02</sub>	H <sub>03</sub>	H <sub>04</sub>	H <sub>05</sub>	μ <sub>0</sub>	σ <sub>0</sub>	H <sub>11</sub>	H <sub>12</sub>	H <sub>13</sub>	H <sub>14</sub>	H <sub>15</sub>	μ <sub>1</sub>	σ <sub>1</sub>	ΔH	M1 <sub>1</sub>	M1 <sub>2</sub>	M1 <sub>3</sub>	σM <sub>1</sub>	μM <sub>1</sub>	M2 <sub>1</sub>	M2 <sub>2</sub>	M2 <sub>3</sub>	σM <sub>2</sub>	μM <sub>2</sub>	ΔM			
Duration [hr]:	6	25	82	82	83	83	82	82.4	0.55	84	84	84	85	84	84.2	0.45	1.80	7.781	7.781	7.779	0.001	7.780	7.771	7.772	7.771	0.001	7.771	-0.12%		
Temperature [°C]:	120	15	83	83	83	83	84	83.2	0.45	84	84	83	84	85	84.0	0.71	0.80	7.788	7.788	7.787	0.001	7.788	7.777	7.777	7.776	0.001	7.777	-0.14%		
Date of vulcanization:	20-Jun-17	27	82	80	82	82	82	81.6	0.89	84	83	84	83	83	83.4	0.55	1.80	7.791	7.790	7.791	0.001	7.791	7.780	7.780	7.781	0.001	7.780	-0.13%		
Test details																	Avg	1.47											Avg	-0.13%
Date of test:	01-Jul-17																													
Test room temp. [°C]:	23	Immersion liquid used:								Kleen-flo Antifreeze				Exposure period dates:				Jul 1 to Jul 4			Exposure temp. [°C]:		23±2	Exposure period [hr]:			70			
Hardness test method:	ASTM D2240	Sample	Original Hardness before immersion [Shore A]							Hardness after immersion [Shore A]							Hardness Change	Mass before [gr]			STD [gr]	Avg [gr]	Mass after [gr]			STD [gr]	Avg [gr]	Mass Change [%]		
Statement of condition after exposure:		ID No	H <sub>01</sub>	H <sub>02</sub>	H <sub>03</sub>	H <sub>04</sub>	H <sub>05</sub>	μ <sub>0</sub>	σ <sub>0</sub>	H <sub>11</sub>	H <sub>12</sub>	H <sub>13</sub>	H <sub>14</sub>	H <sub>15</sub>	μ <sub>1</sub>	σ <sub>1</sub>	ΔH	M1 <sub>1</sub>	M1 <sub>2</sub>	M1 <sub>3</sub>	σM <sub>1</sub>	μM <sub>1</sub>	M2 <sub>1</sub>	M2 <sub>2</sub>	M2 <sub>3</sub>	σM <sub>2</sub>	μM <sub>2</sub>	ΔM		
No distinctive damage was perceived. A slight whitening was perceived on all surfaces after immersion.		13	82	80	82	82	82	81.6	0.89	84	84	84	84	86	84.4	0.89	2.80	7.735	7.735	7.735	0.000	7.735	7.721	7.720	7.720	0.001	7.720	-0.19%		
		19	81	82	81	83	82	81.8	0.84	84	85	84	85	83	84.2	0.84	2.40	7.781	7.781	7.782	0.001	7.781	7.770	7.770	7.768	0.001	7.769	-0.15%		
		8	81	81	82	83	82	81.8	0.84	83	84	84	84	85	84	0.71	2.20	7.862	7.864	7.864	0.001	7.863	7.854	7.854	7.854	0.000	7.854	-0.12%		
														Avg	2.47											Avg	-0.15%			
		Immersion liquid used:								Kleen-flo Antifreeze				Exposure period dates:				Jul 1 to Jul 4			Exposure temp. [°C]:		50±2	Exposure period [hr]:			70			
Deviations:		Sample	Original Hardness before immersion [Shore A]							Hardness after immersion [Shore A]							Hardness Change	Mass before [gr]			STD [gr]	Avg [gr]	Mass after [gr]			STD [gr]	Avg [gr]	Mass Change [%]		
ID No		H <sub>01</sub>	H <sub>02</sub>	H <sub>03</sub>	H <sub>04</sub>	H <sub>05</sub>	μ <sub>0</sub>	σ <sub>0</sub>	H <sub>11</sub>	H <sub>12</sub>	H <sub>13</sub>	H <sub>14</sub>	H <sub>15</sub>	μ <sub>1</sub>	σ <sub>1</sub>	ΔH	M1 <sub>1</sub>	M1 <sub>2</sub>	M1 <sub>3</sub>	σM <sub>1</sub>	μM <sub>1</sub>	M2 <sub>1</sub>	M2 <sub>2</sub>	M2 <sub>3</sub>	σM <sub>2</sub>	μM <sub>2</sub>	ΔM			
Use of finished product geometry (gasket, instead of standard one (coupon, dumbbell, etc.). 200 ml of test liquid used		30	82	82	83	83	82	82.4	0.55	86	85	86	85	87	85.8	0.84	3.40	7.872	7.873	7.873	0.001	7.873	7.818	7.818	7.818	0.000	7.818	-0.69%		
		10	82	82	83	82	83	82.4	0.55	87	86	86	87	86	86.4	0.55	4.00	7.880	7.880	7.879	0.001	7.880	7.828	7.828	7.827	0.001	7.828	-0.66%		
		5	81	83	81	82	82	81.8	0.84	86	85	87	87	87	86.4	0.89	4.60	7.829	7.829	7.830	0.001	7.829	7.789	7.787	7.789	0.001	7.788	-0.53%		
														Avg	4.00											Avg	-0.63%			

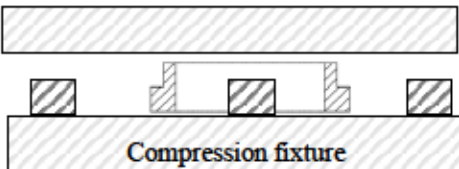
# Airbrake Elastomeric Gasket - Effect of Liquids / Chemical Compatibility Report

Test method		Test results																												
Reference:	ASTM D471	Immersion liquid used:								CRC Antifreeze				Exposure period dates:				Jul 8 to Jul 11				Exposure temp. [°C]:		23±2	Exposure period [hr]:			70		
Sample details		Sample	Original Hardness before immersion [Shore A]							Hardness after immersion [Shore A]							Hardness Change	Mass before [gr]			STD [gr]	Avg [gr]	Mass after [gr]			STD [gr]	Avg [gr]	Mass Change [%]		
Origin:	GEMMA Plastics	ID No	H <sub>01</sub>	H <sub>02</sub>	H <sub>03</sub>	H <sub>04</sub>	H <sub>05</sub>	μ <sub>0</sub>	σ <sub>0</sub>	H <sub>11</sub>	H <sub>12</sub>	H <sub>13</sub>	H <sub>14</sub>	H <sub>15</sub>	μ <sub>1</sub>	σ <sub>1</sub>	ΔH	M1 <sub>1</sub>	M1 <sub>2</sub>	M1 <sub>3</sub>	σM <sub>1</sub>	μM <sub>1</sub>	M2 <sub>1</sub>	M2 <sub>2</sub>	M2 <sub>3</sub>	σM <sub>2</sub>	μM <sub>2</sub>	ΔM		
Method of preparation:	Moulded	19	78	79	79	79	78	78.6	0.55	81	82	83	82	83	82.2	0.84	3.60	6.363	6.364	6.364	0.001	6.364	6.349	6.349	6.349	0.000	6.349	-0.23%		
Type of test piece used:	EPDM	23	79	79	79	80	79	79.2	0.45	82	81	82	81	82	81.6	0.55	2.40	6.373	6.374	6.374	0.001	6.374	6.361	6.361	6.361	0.000	6.361	-0.20%		
Full description:		21	79	79	79	79	78	78.8	0.45	82	82	82	83	82	82.2	0.45	3.40	6.362	6.362	6.363	0.001	6.362	6.353	6.353	6.353	0.000	6.353	-0.15%		
Simplified gasket geometry																	Avg	3.13											Avg	-0.19%
		Immersion liquid used:								CRC Antifreeze				Exposure period dates:				Jul 8 to Jul 11				Exposure temp. [°C]:		50±2	Exposure period [hr]:			70		
Vulcanization details		Sample	Original Hardness before immersion [Shore A]							Hardness after immersion [Shore A]							Hardness Change	Mass before [gr]			STD [gr]	Avg [gr]	Mass after [gr]			STD [gr]	Avg [gr]	Mass Change [%]		
Duration [hr]:	6	6	80	80	80	80	79	79.8	0.45	81	82	83	82	83	82.2	0.84	2.40	6.315	6.315	6.316	0.001	6.315	6.256	6.256	6.256	0.000	6.256	-0.94%		
Temperature [°C]:	120	22	80	79	79	79	80	79.4	0.55	81	82	82	83	82	82.0	0.71	2.60	6.418	6.419	6.419	0.001	6.419	6.343	6.343	6.343	0.000	6.343	-1.18%		
Date of vulcanization:	20-Jun-17	2	81	80	81	80	80	80.4	0.55	82	84	82	82	82	82.4	0.89	2.00	6.365	6.366	6.366	0.001	6.366	6.308	6.308	6.308	0.000	6.308	-0.91%		
Test details																	Avg	2.33											Avg	-1.01%
Date of test:	08-Jul-17																													
Test room temp. [°C]:	23	Immersion liquid used:								Kleen-flo Antifreeze				Exposure period dates:				Jul 8 to Jul 11				Exposure temp. [°C]:		23±2	Exposure period [hr]:			70		
Hardness test method:	ASTM D2240	Sample	Original Hardness before immersion [Shore A]							Hardness after immersion [Shore A]							Hardness Change	Mass before [gr]			STD [gr]	Avg [gr]	Mass after [gr]			STD [gr]	Avg [gr]	Mass Change [%]		
Statement of condition after exposure:		ID No	H <sub>01</sub>	H <sub>02</sub>	H <sub>03</sub>	H <sub>04</sub>	H <sub>05</sub>	μ <sub>0</sub>	σ <sub>0</sub>	H <sub>11</sub>	H <sub>12</sub>	H <sub>13</sub>	H <sub>14</sub>	H <sub>15</sub>	μ <sub>1</sub>	σ <sub>1</sub>	ΔH	M1 <sub>1</sub>	M1 <sub>2</sub>	M1 <sub>3</sub>	σM <sub>1</sub>	μM <sub>1</sub>	M2 <sub>1</sub>	M2 <sub>2</sub>	M2 <sub>3</sub>	σM <sub>2</sub>	μM <sub>2</sub>	ΔM		
No distinctive damage was perceived. A slight whitening was perceived on all surfaces after immersion.		25	78	79	79	79	79	78.8	0.45	84	84	83	84	84	83.8	0.45	5.00	6.291	6.291	6.292	0.001	6.291	6.258	6.258	6.258	0.000	6.258	-0.53%		
		15	79	80	80	80	80	79.8	0.45	84	85	84	85	84	84.4	0.55	4.60	6.303	6.304	6.304	0.001	6.304	6.273	6.273	6.273	0.000	6.273	-0.49%		
		27	79	79	79	79	77	78.6	0.89	84	84	84	86	85	84.6	0.89	6.00	6.353	6.353	6.354	0.001	6.353	6.321	6.321	6.321	0.000	6.321	-0.51%		
																	Avg	5.20											Avg	-0.51%
		Immersion liquid used:								Kleen-flo Antifreeze				Exposure period dates:				Jul 8 to Jul 11				Exposure temp. [°C]:		50±2	Exposure period [hr]:			70		
Deviations:		Sample	Original Hardness before immersion [Shore A]							Hardness after immersion [Shore A]							Hardness Change	Mass before [gr]			STD [gr]	Avg [gr]	Mass after [gr]			STD [gr]	Avg [gr]	Mass Change [%]		
Use of finished product geometry (gasket, instead of standard one (coupon, dumbbell, etc.). 200 ml of test liquid used		ID No	H <sub>01</sub>	H <sub>02</sub>	H <sub>03</sub>	H <sub>04</sub>	H <sub>05</sub>	μ <sub>0</sub>	σ <sub>0</sub>	H <sub>11</sub>	H <sub>12</sub>	H <sub>13</sub>	H <sub>14</sub>	H <sub>15</sub>	μ <sub>1</sub>	σ <sub>1</sub>	ΔH	M1 <sub>1</sub>	M1 <sub>2</sub>	M1 <sub>3</sub>	σM <sub>1</sub>	μM <sub>1</sub>	M2 <sub>1</sub>	M2 <sub>2</sub>	M2 <sub>3</sub>	σM <sub>2</sub>	μM <sub>2</sub>	ΔM		
		1	80	80	80	79	80	79.8	0.45	86	85	86	85	86	85.6	0.55	5.80	6.465	6.466	6.466	0.001	6.466	6.346	6.346	6.346	0.000	6.346	-1.85%		
		7	81	80	80	80	81	80.4	0.55	86	85	85	86	86	85.6	0.55	5.20	6.434	6.434	6.434	0.000	6.434	6.319	6.319	6.319	0.000	6.319	-1.79%		
		17	80	79	80	79	79	79.4	0.55	86	85	87	86	86	86.0	0.71	6.60	6.347	6.348	6.348	0.001	6.348	6.236	6.236	6.236	0.000	6.236	-1.76%		
																	Avg	5.87											Avg	-1.80%

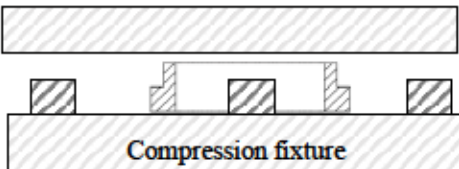
**Airbrake Elastomeric Gasket - Effect of Liquids / Chemical Compatibility Report**

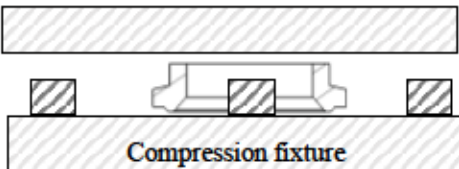
Test method		Test results																												
Reference:	ASTM D471	Immersion liquid used:								CRC Antifreeze				Exposure period dates:				Jul 12 to Jul 15			Exposure temp. [°C]:		23±2	Exposure period [hr]:			70			
Sample details		Sample	Original Hardness before immersion [Shore A]							Hardness after immersion [Shore A]							Hardness Change	Mass before [gr]			STD [gr]	Avg [gr]	Mass after [gr]			STD [gr]	Avg [gr]	Mass Change [%]		
Origin:	GEMMA Plastics	ID No	H <sub>01</sub>	H <sub>02</sub>	H <sub>03</sub>	H <sub>04</sub>	H <sub>05</sub>	μ <sub>0</sub>	σ <sub>0</sub>	H <sub>11</sub>	H <sub>12</sub>	H <sub>13</sub>	H <sub>14</sub>	H <sub>15</sub>	μ <sub>1</sub>	σ <sub>1</sub>	ΔH	M1 <sub>1</sub>	M1 <sub>2</sub>	M1 <sub>3</sub>	σM <sub>1</sub>	μM <sub>1</sub>	M2 <sub>1</sub>	M2 <sub>2</sub>	M2 <sub>3</sub>	σM <sub>2</sub>	μM <sub>2</sub>	ΔM		
Method of preparation:	Moulded	4	73	74	74	73	73	73.4	0.55	77	75	75	75	75	75.4	0.89	2.00	6.138	6.138	6.138	0.000	6.138	6.102	6.102	6.102	0.000	6.102	-0.59%		
Type of test piece used:	CR+fumed silica	29	75	74	73	74	74	74.0	0.71	75	75	76	75	76	75.4	0.55	1.40	6.137	6.137	6.138	0.001	6.137	6.100	6.100	6.100	0.000	6.100	-0.61%		
Full description:		17	74	74	73	73	72	73.2	0.84	76	75	74	75	76	75.2	0.84	2.00	6.136	6.136	6.136	0.000	6.136	6.098	6.098	6.098	0.000	6.098	-0.62%		
Simplified gasket geometry																	Avg	1.80											Avg	-0.60%
		Immersion liquid used:								CRC Antifreeze				Exposure period dates:				Jul 12 to Jul 15			Exposure temp. [°C]:		50±2	Exposure period [hr]:			70			
Vulcanization details		Sample	Original Hardness before immersion [Shore A]							Hardness after immersion [Shore A]							Hardness Change	Mass before [gr]			STD [gr]	Avg [gr]	Mass after [gr]			STD [gr]	Avg [gr]	Mass Change [%]		
ID No		H <sub>01</sub>	H <sub>02</sub>	H <sub>03</sub>	H <sub>04</sub>	H <sub>05</sub>	μ <sub>0</sub>	σ <sub>0</sub>	H <sub>11</sub>	H <sub>12</sub>	H <sub>13</sub>	H <sub>14</sub>	H <sub>15</sub>	μ <sub>1</sub>	σ <sub>1</sub>	ΔH	M1 <sub>1</sub>	M1 <sub>2</sub>	M1 <sub>3</sub>	σM <sub>1</sub>	μM <sub>1</sub>	M2 <sub>1</sub>	M2 <sub>2</sub>	M2 <sub>3</sub>	σM <sub>2</sub>	μM <sub>2</sub>	ΔM			
Duration [hr]:	6	27	73	71	72	73	73	72.4	0.89	78	77	77	77	76	77.0	0.71	4.60	6.107	6.107	6.107	0.000	6.107	5.989	5.989	5.989	0.000	5.989	-1.93%		
Temperature [°C]:	120	1	74	73	73	73	73	73.2	0.45	76	76	76	75	76	75.8	0.45	2.60	6.132	6.132	6.132	0.000	6.132	6.007	6.007	6.007	0.000	6.007	-2.04%		
Date of vulcanization:	20-Jun-17	7	74	73	74	73	73	73.4	0.55	77	76	76	76	77	76.4	0.55	3.00	6.217	6.217	6.217	0.000	6.217	6.088	6.088	6.088	0.000	6.088	-2.07%		
Test details																	Avg	3.40											Avg	-2.02%
Date of test:	12-Jul-17																													
Test room temp. [°C]:	23	Immersion liquid used:								Kleen-flo Antifreeze				Exposure period dates:				Jul 12 to Jul 15			Exposure temp. [°C]:		23±2	Exposure period [hr]:			70			
Hardness test method:	ASTM D2240	Sample	Original Hardness before immersion [Shore A]							Hardness after immersion [Shore A]							Hardness Change	Mass before [gr]			STD [gr]	Avg [gr]	Mass after [gr]			STD [gr]	Avg [gr]	Mass Change [%]		
Statement of condition after exposure:		ID No	H <sub>01</sub>	H <sub>02</sub>	H <sub>03</sub>	H <sub>04</sub>	H <sub>05</sub>	μ <sub>0</sub>	σ <sub>0</sub>	H <sub>11</sub>	H <sub>12</sub>	H <sub>13</sub>	H <sub>14</sub>	H <sub>15</sub>	μ <sub>1</sub>	σ <sub>1</sub>	ΔH	M1 <sub>1</sub>	M1 <sub>2</sub>	M1 <sub>3</sub>	σM <sub>1</sub>	μM <sub>1</sub>	M2 <sub>1</sub>	M2 <sub>2</sub>	M2 <sub>3</sub>	σM <sub>2</sub>	μM <sub>2</sub>	ΔM		
No distinctive damage was perceived. A slight whitening was perceived on all surfaces after immersion.		11	74	74	74	73	74	73.8	0.45	75	76	77	77	76	76.2	0.84	2.40	6.165	6.165	6.165	0.000	6.165	6.098	6.098	6.098	0.000	6.098	-1.09%		
		30	72	73	71	71	72	71.8	0.84	77	76	77	76	77	76.6	0.55	4.80	6.135	6.135	6.135	0.000	6.135	6.070	6.070	6.070	0.000	6.070	-1.06%		
		24	74	73	72	72	73	72.8	0.84	77	76	76	77	78	76.8	0.84	4.00	6.131	6.132	6.132	0.001	6.132	6.067	6.067	6.067	0.000	6.067	-1.05%		
														Avg	3.73											Avg	-1.07%			
		Immersion liquid used:								Kleen-flo Antifreeze				Exposure period dates:				Jul 12 to Jul 15			Exposure temp. [°C]:		50±2	Exposure period [hr]:			70			
Deviations:		Sample	Original Hardness before immersion [Shore A]							Hardness after immersion [Shore A]							Hardness Change	Mass before [gr]			STD [gr]	Avg [gr]	Mass after [gr]			STD [gr]	Avg [gr]	Mass Change [%]		
ID No		H <sub>01</sub>	H <sub>02</sub>	H <sub>03</sub>	H <sub>04</sub>	H <sub>05</sub>	μ <sub>0</sub>	σ <sub>0</sub>	H <sub>11</sub>	H <sub>12</sub>	H <sub>13</sub>	H <sub>14</sub>	H <sub>15</sub>	μ <sub>1</sub>	σ <sub>1</sub>	ΔH	M1 <sub>1</sub>	M1 <sub>2</sub>	M1 <sub>3</sub>	σM <sub>1</sub>	μM <sub>1</sub>	M2 <sub>1</sub>	M2 <sub>2</sub>	M2 <sub>3</sub>	σM <sub>2</sub>	μM <sub>2</sub>	ΔM			
Use of finished product geometry (gasket), instead of standard one (coupon, dumbbell, etc.). 200 ml of test liquid used		9	74	75	74	73	74	74.0	0.71	78	78	77	76	77	77.2	0.84	3.20	6.090	6.090	6.090	0.000	6.090	5.962	5.962	5.962	0.000	5.962	-2.10%		
		3	74	74	74	74	75	74.2	0.45	78	77	79	77	78	77.8	0.84	3.60	6.142	6.142	6.142	0.000	6.142	6.010	6.010	6.010	0.000	6.010	-2.15%		
		29	75	74	73	74	74	74.0	0.71	78	77	78	78	77	77.6	0.55	3.60	6.119	6.119	6.119	0.000	6.119	5.991	5.991	5.991	0.000	5.991	-2.09%		
														Avg	3.47											Avg	-2.11%			





Airbrake Elastomeric Gasket - Compression Set at Low Temperature			
Sample details		Test method	
Origin:	GEMMA Plastics	Reference:	ISO 815-2
Compound details:	CR with fume silica	Test method used:	Method 1
Cure details:	100 °C	Type of test piece used:	Gasket - not laminated
Method of preparation:	Moulded	Type of lubrication:	Silicone oil
Full description:		Tested separately or as set?	Separately
<p>Simplified gasket geometry. The gasket was placed on the lubricated compression fixture lower section's flat surface, along with three dowel pins, and then compressed with three c-clamps, up to the allowable pins height:</p>  <p>Compression fixture</p>		Test details	
		Laboratory temperature [°C]:	23
		Conditioning temperature [°C]:	-40
		Conditioning time [hr]:	1
		Recovery time t [min]:	30±3
		Duration of test [hr]:	4
		Test Temperature [°C]:	-40
		Compression used:	3 C-clamps and vice
		Deviations or procedures not specified:	
		Reduced time to 4 hr in cool bath (dry ice + methanol)	
Test results			
No of test pieces used:	One per test (3 total)	Date of test:	25-Jul-17
Test piece ID	12	2	29
h <sub>0</sub> : Initial thickness [in]:	0.315	0.318	0.322
h <sub>s</sub> : Spacer thickness [in]:	0.255	0.257	0.256
h <sub>1</sub> : Thickness after t [in]:	0.311	0.310	0.313
Compression Set [CS]:	7%	8%	3%
CS Standard Deviation, σ <sub>cs</sub> :	2.55%		
CS MEDIAN:	7%		




Airbrake Elastomeric Gasket - Compression Set at Low Temperature			
Sample details		Test method	
Origin:	GEMMA Plastics	Reference:	ISO 815-2
Compound details:	EPDM	Test method used:	Method 1
Cure details:	100 °C	Type of test piece used:	Gasket - not laminated
Method of preparation:	Moulded	Type of lubrication:	Silicone oil
Full description:		Tested separately or as set?	Separately
<p>Simplified gasket geometry. The gasket was placed on the lubricated compression fixture lower section's flat surface, along with three dowel pins, and then compressed with three c-clamps, up to the allowable pins height:</p>  <p>Compression fixture</p>		Test details	
		Laboratory temperature [°C]:	23
		Conditioning temperature [°C]:	-40
		Conditioning time [hr]:	1
		Recovery time t [min]:	30±3
		Duration of test [hr]:	4
		Test Temperature [°C]:	-40
		Compression used:	3 C-clamps and vice
		Deviations or procedures not specified:	
		Reduced time to 4 hr in cool bath (dry ice + methanol)	
Test results			
No of test pieces used:	One per test (3 total)	Date of test:	25-Jul-17
Test piece ID	8	19	30
h <sub>0</sub> : Initial thickness [in]:	0.329	0.334	0.332
h <sub>s</sub> : Spacer thickness [in]:	0.256	0.257	0.256
h <sub>1</sub> : Thickness after t [in]:	0.311	0.310	0.312
Compression Set [CS]:	25%	26%	23%
CS Standard Deviation, σ <sub>cs</sub> :	1.37%		
CS MEDIAN:	25%		

Airbrake Elastomeric Gasket - Compression Set at Low Temperature			
Sample details		Test method	
Origin:	CP Warehouse	Reference:	ISO 815-2
Compound details:	NYAB proprietary	Test method used:	Method 1
Cure details:	NYAB proprietary	Type of test piece used:	Gasket - not laminated
Method of preparation:	Moulded	Type of lubrication:	Silicone oil
Full description:		Tested separately or as set?	Separately
<p>Standard gasket geometry, AAR Specification M602 dimensions. The gasket was placed on the lubricated compression fixture lower section's flat surface, along with three dowel pins, and then compressed with three c-clamps, up to the allowable pins height:</p>  <p>Compression fixture</p>		Test details	
		Laboratory temperature [°C]:	23
		Conditioning temperature [°C]:	-40
		Conditioning time [hr]:	1
		Recovery time t [min]:	30±3
		Duration of test [hr]:	4
		Test Temperature [°C]:	-40
		Compression used:	3 C-clamps and vice
		Deviations or procedures not specified:	
		Reduced time to 4 hr in cool bath (dry ice + methanol)	
Test results			
No of test pieces used:	One per test (3 total)	Date of test:	25-Jul-17
Test piece ID	6	27	3
h <sub>0</sub> : Initial thickness [in]:	0.382	0.380	0.381
h <sub>s</sub> : Spacer thickness [in]:	0.254	0.259	0.256
h <sub>1</sub> : Thickness after t [in]:	0.322	0.326	0.319
Compression Set [CS]:	47%	44%	49%
CS Standard Deviation, σ <sub>cs</sub> :	2.74%		
CS MEDIAN:	47%		

Shore A Durometer Nominal Values		Sample	Shore A Hardness	Dimensionless Hardness	Dimensionless Young's Modulus	Calculated Young's Modulus	Calculated Compression Modulus	Calculated Compression Modulus
MI		ID	H	H	Y	E <sub>1</sub> [MPa]	E <sub>c1</sub> [MPa]	E <sub>c2</sub> [MPa]
F <sub>0</sub> [N]	13.64	1	81.6	0.816	65.93	13.77	14.94	5.59
p <sub>0</sub> [m]	0.55	2	82.0	0.820	67.69	14.14	15.34	5.64
r [m]	0.0025	3	82.8	0.828	71.48	14.93	16.20	5.74
Sample details		4	82.8	0.828	71.48	14.93	16.20	5.74
Origin:	GEMMA Plastics	5	81.8	0.818	66.80	13.95	15.14	5.61
Compound details:	CR with fume silica	6	81.6	0.816	65.93	13.77	14.94	5.59
Method of preparation:	Moulded	7	83.0	0.830	72.48	15.14	16.42	5.77
Full description:		8	81.8	0.818	66.80	13.95	15.14	5.61
Simplified gasket geometry		9	82.6	0.826	70.50	14.72	15.97	5.72
		10	82.4	0.824	69.54	14.52	15.76	5.69
		11	82.2	0.822	68.61	14.33	15.54	5.66
Calculation results		12	81.0	0.810	63.41	13.24	14.37	5.51
Avg outer radius, R [m]	0.019	13	81.6	0.816	65.93	13.77	14.94	5.59
Avg inner radius, r [m]	0.015	14	81.6	0.816	65.93	13.77	14.94	5.59
Avg Cross Sectional Area, A <sub>0</sub> [m <sup>2</sup> ]	0.000428	15	83.2	0.832	73.50	15.35	16.65	5.80
Median original thickness h <sub>0</sub> [m]	0.010	16	82.4	0.824	69.54	14.52	15.76	5.69
Avg Shape Factor, SF	0.206	17	82.6	0.826	70.50	14.72	15.97	5.72
Median Normal Force, F <sub>N@25%</sub> [N]	854	18	82.6	0.826	70.50	14.72	15.97	5.72
Secant Modulus, S <sub>M@25%</sub> [MPa]	1.996	19	81.8	0.818	66.80	13.95	15.14	5.61
Experimental Comp. Mod., E <sub>cexp</sub> [MPa]	7.99	20	82.4	0.824	69.54	14.52	15.76	5.69
Avg Calculated Young's Mod, E <sub>c1</sub> [MPa]	15.58	21	81.2	0.812	64.23	13.42	14.55	5.53
Avg Calculated Young's Mod, E <sub>c2</sub> [MPa]	5.67	22	82.4	0.824	69.54	14.52	15.76	5.69
Percent Error E <sub>cexp</sub> VS E <sub>c1</sub>	49%	23	81.8	0.818	66.80	13.95	15.14	5.61
Percent Error E <sub>cexp</sub> VS E <sub>c2</sub>	41%	24	83.2	0.832	73.50	15.35	16.65	5.80
Percent Error E <sub>c1</sub> VS E <sub>c2</sub>	64%	25	82.4	0.824	69.54	14.52	15.76	5.69
Observations:		26	82.8	0.828	71.48	14.93	16.20	5.74
For the shape factor, the loaded area was considered the gasket ring cross sectional area, and the unloaded areas were considered the inner and outer radial areas of the gasket.		27	81.6	0.816	65.93	13.77	14.94	5.59
		28	81.6	0.816	65.93	13.77	14.94	5.59
		29	83.2	0.832	73.50	15.35	16.65	5.80
		30	82.4	0.824	69.54	14.52	15.76	5.69

Shore A Durometer Nominal Values		Sample	Shore A Hardness	Dimensionless Hardness	Dimensionless Young's Modulus	Calculated Young's Modulus	Calculated Compression Modulus	Calculated Compression Modulus
MI		ID	H	H	Y	E <sub>1</sub> [MPa]	E <sub>c1</sub> [MPa]	E <sub>c2</sub> [MPa]
F <sub>0</sub> [N]	13.64	1	79.8	0.798	58.84	12.29	16.57	7.88
p <sub>0</sub> [m]	0.55	2	80.4	0.804	61.05	12.75	17.20	7.99
r [m]	0.0025	3	79.6	0.796	58.12	12.14	16.37	7.84
Sample details		4	79.6	0.796	58.12	12.14	16.37	7.84
Origin:	GEMMA Plastics	5	79.8	0.798	58.84	12.29	16.57	7.88
Compound details:	CR with fume silica	6	79.8	0.798	58.84	12.29	16.57	7.88
Method of preparation:	Moulded	7	80.4	0.804	61.05	12.75	17.20	7.99
Full description:		8	80.2	0.802	60.30	12.59	16.99	7.95
Simplified gasket geometry		9	80.2	0.802	60.30	12.59	16.99	7.95
		10	79.8	0.798	58.84	12.29	16.57	7.88
		11	79.8	0.798	58.84	12.29	16.57	7.88
Calculation results		12	79.6	0.796	58.12	12.14	16.37	7.84
Avg outer radius, R [m]	0.023	13	79.8	0.798	58.84	12.29	16.57	7.88
Avg inner radius, r [m]	0.016	14	79.4	0.794	57.43	11.99	16.18	7.80
Avg Cross Sectional Area, A <sub>0</sub> [m <sup>2</sup> ]	0.000855	15	79.8	0.798	58.84	12.29	16.57	7.88
Median original thickness h <sub>0</sub> [m]	0.008	16	78.8	0.788	55.42	11.57	15.61	7.69
Avg Shape Factor, SF	0.418	17	79.4	0.794	57.43	11.99	16.18	7.80
Median Normal Force, F <sub>N@25%</sub> [N]	2467	18	78.6	0.786	54.77	11.44	15.43	7.65
Secant Modulus, S <sub>M@25%</sub> [MPa]	2.885	19	78.6	0.786	54.77	11.44	15.43	7.65
Experimental Comp. Mod., E <sub>cexp</sub> [MPa]	11.54	20	78.8	0.788	55.42	11.57	15.61	7.69
Avg Calculated Young's Mod, E <sub>c1</sub> [MPa]	16.16	21	78.8	0.788	55.42	11.57	15.61	7.69
Avg Calculated Young's Mod, E <sub>c2</sub> [MPa]	7.80	22	79.4	0.794	57.43	11.99	16.18	7.80
Percent Error E <sub>cexp</sub> VS E <sub>c1</sub>	29%	23	79.2	0.792	56.74	11.85	15.98	7.76
Percent Error E <sub>cexp</sub> VS E <sub>c2</sub>	48%	24	79.2	0.792	56.74	11.85	15.98	7.76
Percent Error E <sub>c1</sub> VS E <sub>c2</sub>	52%	25	78.8	0.788	55.42	11.57	15.61	7.69
Observations:		26	78.8	0.788	55.42	11.57	15.61	7.69
For the shape factor, the loaded area was considered the gasket ring cross sectional area, and the unloaded areas were considered the inner and outer radial areas of the gasket.		27	78.6	0.786	54.77	11.44	15.43	7.65
		28	78.8	0.788	55.42	11.57	15.61	7.69
		29	78.4	0.784	54.14	11.31	15.25	7.62
		30	78.8	0.788	55.42	11.57	15.61	7.69



Shore A Durometer Nominal Values		Sample	Shore A Hardness	Dimensionless Hardness	Dimensionless Young's Modulus	Calculated Young's Modulus	Calculated Compression Modulus	Calculated Compression Modulus
MI		ID	H	H	Y	E <sub>1</sub> [MPa]	E <sub>c1</sub> [MPa]	E <sub>c2</sub> [MPa]
F <sub>0</sub> [N]	13.64	1	73.2	0.732	40.99	8.56	11.86	6.92
p <sub>0</sub> [m]	0.55	2	74.4	0.744	43.55	9.10	12.60	7.14
r [m]	0.0025	3	74.2	0.742	43.10	9.00	12.47	7.11
Sample details		4	73.4	0.734	41.40	8.65	11.98	6.96
Origin:	GEMMA Plastics	5	74.2	0.742	43.10	9.00	12.47	7.11
Compound details:	CR with fume silica	6	74.0	0.740	42.67	8.91	12.34	7.07
Method of preparation:	Moulded	7	73.4	0.734	41.40	8.65	11.98	6.96
Full description:		8	73.8	0.738	42.24	8.82	12.22	7.03
Simplified gasket geometry		9	74.0	0.740	42.67	8.91	12.34	7.07
		10	74.4	0.744	43.55	9.10	12.60	7.14
		11	73.8	0.738	42.24	8.82	12.22	7.03
Calculation results		12	74.2	0.742	43.10	9.00	12.47	7.11
Avg outer radius, R [m]	0.023	13	72.8	0.728	40.18	8.39	11.63	6.85
Avg inner radius, r [m]	0.016	14	70.8	0.708	36.50	7.62	10.56	6.50
Avg Cross Sectional Area, A <sub>0</sub> [m <sup>2</sup> ]	0.000872	15	73.2	0.732	40.99	8.56	11.86	6.92
Median original thickness h <sub>0</sub> [m]	0.008	16	72.4	0.724	39.40	8.23	11.40	6.78
Avg Shape Factor, SF	0.439	17	73.2	0.732	40.99	8.56	11.86	6.92
Median Normal Force, F <sub>N@25%</sub> [N]	790	18	73.2	0.732	40.99	8.56	11.86	6.92
Secant Modulus, S <sub>M@25%</sub> [MPa]	0.907	19	71.6	0.716	37.91	7.92	10.97	6.64
Experimental Comp. Mod., E <sub>cexp</sub> [MPa]	3.63	20	71.6	0.716	37.91	7.92	10.97	6.64
Avg Calculated Young's Mod, E <sub>c1</sub> [MPa]	11.84	21	72.4	0.724	39.40	8.23	11.40	6.78
Avg Calculated Young's Mod, E <sub>c2</sub> [MPa]	6.91	22	74.0	0.740	42.67	8.91	12.34	7.07
Percent Error E <sub>cexp</sub> VS E <sub>c1</sub>	69%	23	73.6	0.736	41.81	8.73	12.10	7.00
Percent Error E <sub>cexp</sub> VS E <sub>c2</sub>	48%	24	72.8	0.728	40.18	8.39	11.63	6.85
Percent Error E <sub>c1</sub> VS E <sub>c2</sub>	42%	25	70.8	0.708	36.50	7.62	10.56	6.50
Observations:		26	72.6	0.726	39.79	8.31	11.51	6.82
For the shape factor, the loaded area was considered the gasket ring cross sectional area, and the unloaded areas were considered the inner and outer radial areas of the gasket.		27	72.4	0.724	39.40	8.23	11.40	6.78
		28	73.8	0.738	42.24	8.82	12.22	7.03
		29	74.0	0.740	42.67	8.91	12.34	7.07
		30	71.8	0.718	38.27	7.99	11.07	6.68